UNIVERSITY OF THE
WITWATERSRAND,
JOHANNESBURG

The Use of Photochemical Reactions and Bio-based Starting Materials for the Synthesis of Nitrogen and Oxygen Heterocycles

Songeziwe Ntsimango

Supervised by C B de Koning, M L Bode and K J Ngwira

A thesis submitted to the Faculty of Science, University of the Witwatersrand, in fulfilment of the requirements of the Doctor of Philosophy

Declaration

I declare that the work presented in this thesis was carried out exclusively by myself under the supervision of Prof Charles B. de Koning, Prof Moira L. Bode and Dr Kennedy J. Ngwira. It is being submitted for the degree of Doctor of Philosophy at the University of the Witwatersrand, Johannesburg. It has not been submitted before for any degree or any examination in any other University.

Songeziwe Ntsimango

22 September 2021

Abstract

The work detailed in this thesis can be broadly divided into two parts. The first part was concerned with investigating the scope and limitation of a novel light-mediated C–N aromatic ring-forming reaction from methoxy-containing biaryl aromatic oximes.

Previously in our laboratories at Wits University, in an attempted synthesis of phenanthroviridone, an advanced biaryl intermediate 3-methoxy-5-methyl-2-(1,4,5-trimethoxynaphthalen-2-yl)benzaldehyde *O*-phenyloxime when exposed to UV irradiation yielded 1,10,12-trimethoxy-8-methylbenzo[*c*]phenanthridine, together with 3-methoxy-5-methyl-2-(1,4,5-trimethoxynaphthalen-2-yl)benzonitrile, instead of the desired natural product phenanthroviridone. This fortuitous synthesis of a phenanthridine nucleus is thought to arise from homolysis of the weak N–O bond from the *O*-phenyloxime intermediate, generating iminyl radicals. The putative iminyl radical then undergoes intramolecular cyclization, forging a C–N bond with concomitant expulsion of the *ortho*-methoxy group, furnishing the phenanthridine nucleus.

This serendipitous discovery allowed for the construction of the biologically important phenanthridine framework using UV irradiation. For the first part of this PhD we set out to investigate the substrate scope and limitations and to determine if this reaction could be applied generally. As a consequence, simple biaryl intermediates carrying an oxime ester group *ortho* to the biaryl axis were synthesised. In addition, the second aryl ring (the accepting ring) of the said intermediates had varying degrees of substitution and positioning of methoxy groups. However, in all cases, the substrates had to possess at least one methoxy group also *ortho* to the biaryl axis. The substrates were then irradiated under similar conditions as in the reaction described above and the products were analysed using NMR spectroscopy, FTIR and HRMS. It was demonstrated that the reaction prefers electron-rich accepting rings as irradiation of 2',4',5'-trimethoxy-

[1,1'-biphenyl]-2-carbaldehyde *O*-acetyl oxime gave 2,3-dimethoxyphenanthridine in 74% yield. On the other hand, irradiation of 2'-methoxy-[1,1'-biphenyl]-2-carbaldehyde *O*-acetyl oxime yielded 2'-methoxy-[1,1'-biphenyl]-2-carbonitrile exclusively. The reaction is also sensitive to the positioning of the methoxys groups on the accepting ring. A case in point is the irradiation of the *ortho* 2',3'-dimethoxy-[1,1'-biphenyl]-2-carbaldehyde *O*-acetyl oxime which gave 4-methoxyphenanthridine, while irradiation of the *meta* 2',4'-dimethoxy-[1,1'-biphenyl]-2-carbaldehyde *O*-acetyl oxime furnished 2',4'-dimethoxy-[1,1'-biphenyl]-2-carbonitrile with no 3-methoxyphenanthridine produced. The corresponding nitrile side product resulting from the elimination of acetic acid was produced in all cases.

This novel photo-mediated methodology was successfully extended to the synthesis of the naturally occurring phenanthridine – trisphaeridine, albeit, overall in moderate yield. The synthesis of trisphaeridine was achieved through the photo cyclization of 6-(2,4,5-trimethoxyphenyl)benzo[*d*][1,3]dioxole-5-carbaldehyde *O*-acetyl oxime which gave 2,3-dimethoxy-[1,3]dioxolo[4,5-*j*]phenanthridine. This step was followed by the removal of the methoxy groups *via* the [1,3]dioxolo[4,5-*j*]phenanthridine-2,3-dione that was reduced to the desired trisphaeridine by the action of zinc in acetic acid. In turn 6-(2,4,5-trimethoxyphenyl)benzo[*d*][1,3]dioxole-5-carbaldehyde *O*-acetyl oxime was synthesized from the Suzuki coupling reaction between 1-bromo-2,4,5-trimethoxybenzene and(6-formylbenzo[*d*][1,3]dioxol-5-yl)boronic acid furnishing 6-(2,4,5-trimethoxyphenyl)benzo[*d*][1,3]dioxole-5-carbaldehyde. Subsequent oxime formation of the resultant aldehyde with hydroxylamine hydrochloride and esterification with acetyl chloride formed 6-(2,4,5-trimethoxyphenyl)benzo[*d*][1,3]dioxole-5-carbaldehyde *O*-acetyl oxime.

The second part of this PhD thesis details the synthesis of cardol- and cardanol-based oxa-heterocyclic compounds. The aim was to use well-established reactions to generate compounds that are known to absorb UV light, with the atoms coming exclusively from bio-renewable resources. As a consequence, coumarin derivatives were synthesized from the reaction between naturally-occurring malic acid and cardanol or cardol in the

presence of catalytic amounts of sulfuric acid. For example, reaction between cardol and malic acid gave 7-hydroxy-5-pentadecyl-2*H*-chromen-2-one. Further elaboration of the 7-hydroxy-5-pentadecyl-2*H*-chromen-2-one gave tricyclic annellated coumarin derivatives, such as 5-pentadecylpyrano[2,3-*f*]chromene-2,8-dione, 4-pentadecyl-7H-furo[3,2-*g*]chromen-7-one and 5-pentadecyl-2H-furo[2,3-*h*]chromen-2-one.

Finally, a concise synthesis of cardol-derived tetrahydrocannabinol (THC) derivative ((6a*R*,10a*R*)-6,6,9-trimethyl-3-pentadecyl-6a,7,8,10a-tetrahydro-6*H*-benzo[*c*]chromen-1-ol) is also described. This synthesis was achieved through Lewis-acid mediated union between 5-pentadecylbenzene-1,3-diol and (1*S*,5*R*,6*R*)-2,7,7-trimethylbicyclo[3.1.1]hept-2-en-6-ol in dichloromethane.

List of abbreviations

AcCl	acetyl chloride
AcOH	acetic acid
BQ	benzoquinone
CAN	ceric ammonium nitrate
CBD	cannabidiol
CNSL	cashew nut shell liquid
DBU	1,8-diazabicyclo[5.4.0]undec-7-ene
DMAP	4-dimethylaminopyridine
DME	1,2-dimethoxyethane
DMF	*N*,*N*-dimethylformamide
DMSO	dimethyl sulfoxide
EtOAc	ethyl acetate
HOMO	highest occupied molecular orbital
HRMS	high resolution mass spectrometry
hν	photon of light
IC	internal conversion
ISC	intersystem crossing
LAH	lithium aluminum hydride
LEDs	light-emitting diodes
LUMO	lowest unoccupied molecular orbital

MAP	4-methoxyacetophenone
MeCN	acetonitrile
MeOH	methanol
MsOH	methanesulfonic acid
NBS	*N*-bromosuccinimide
NMR	nuclear magnetic resonance
PhCl	chlorobenzene
PDT	photodynamic therapy
PhMe	toluene
PPA	polyphosphoric acid
p-TsCl	*para*-tosyl chloride
Pyr	pyridine
S_0	ground state
S_1, S_2, S_3…	singlet excited states
SOMO	singly occupied molecular orbitals
T_1	triplet state
*t*BuOH	*tert*-butyl alcohol
TMS	trimethylsilane
THC	tetrahydrocannabinol
THF	tetrahydrofuran
TLC	thin layer chromatography
UV	Ultraviolet

Acknowledgements

I wishes to take this opportunity to express my sincere appreciation to my supervisors Prof Charles de Koning, Prof Moira Bode and Dr Kennedy Ngwira, without whose guidance this work would not have been realized. Charles thank you so much for the immense patience you practiced during my tenure as your student. Your role stretched far beyond your call as a supervisor. Moira thank you for your insightful suggestions and your high standard of research. Ken thanks for the constant encouragement and friendly conversations.

To the staff members of the Organic Group at Wits, Prof Amanda Rousseau, Prof Dean Brady, Dr Memory Zimwandeyi and Ms Kamokgelo Butsi.

A special debt of gratitude is to Prof Joseph Michael whose help and counsel, always generously and unstintingly given, made the burden of conducting research and lecturing bearable.

The constant association with the past and present postgraduate members of the Organic group has been most pleasurable. Special mention goes to Fatema Jagot who had enormous influence during the course of this work. Thank you for everything Fa.

A very big thanks to Prof Dr Till Opatz (Johannes-Gutenberg-Universität Mainz, Germany) who opened his laboratories and for the memorable chemistry discussions we had. Appreciation is also extended to the postgraduate members of that group.

I would also like to thank my family, Mr Wilson Ntsimango, Lihleli, Okuhle, Hlumisa, Siphenathi, Siyathemba and Buhle for their unfailing support. Thank you to my friends, Luthando Kapoyi, Dr Sunday Ogunlaja, Dr Kagiso Mosia, and Zakhele Skhosana.

Finally, I would like to thank the LORD for guiding me and placing me in the midst of the wonderful people that helped me during the course of my studies.

Table of Contents

Abstract……...iii

List of Abbreviations……...vi

Acknowledgments……viii

Table of Contents……ix

Chapter 1……1

1.1 General Introduction……..1

Part I – Investigations on the Usefulness of Photo-generated Nitrogen-centered Radicals: Synthesis of the Phenanthridines …….....5

Chapter 2……6

2.1 Introduction……..6

2.2 Photochemistry……6

2.3 Photochemistry in chemical synthesis……...9

2.3.1 Infancy Era (1886–1914)……10

2.3.2 Mechanistic Era (1921–1945)……12

2.3.2.1 Norrish Type I pathway……12

2.3.2.2 Norrish Type II pathway……...14

2.3.2.3 Miscellaneous reactions……...15

2.3.3 Theoretical Era (1950-1970s)……..16

2.3.4 Modern Era (1980s-present)……20

2.4 Radicals……...23

2.4.1 *N*-centred radicals……24

2.4.1.1 Aminyl radicals……25

2.4.1.2 Amidyl radical……..26

2.4.1.3 Iminyl radicals……..29

2.5 Phenanthridines……...30
2.5.1 Synthesis of phenanthridines……...32
2.5.1.1 Construction ring A……..…….....……...33
2.5.1.2 Construction of rings B and C..…….....34
2.5.1.3 Construction of ring B……39
2.5.1.4 Construction of ring B through C1'–C10' bond……..41
2.5.1.5 Construction of ring B through C6–C6' bond…….44
2.5.1.6 Construction of ring B through C6–N5 bond……..47
2.5.1.7 Construction of ring B through C4'–N5 bond…….48
2.6 Aims and objectives……52
Chapter 3……..54
3.1 Results and discussion…….54
3.1.1 Pre-functionalization of methoxybenzenes…….54
3.1.2 Suzuki-coupling reactions……...56
3.1.3 Attempted conversion of Suzuki adducts to oxime ethers……58
3.1.4 Conversion of Suzuki adducts to oxime esters…….62
3.1.5 Photochemical induced ring closure……64
3.1.6 Synthesis of trisphaeridine……..67
3.1.7 Conclusions……73
Part II – The Synthesis of UV Absorbing Oxygen Containing-Heterocyclic Compounds from Cashew Nut Shell Liquid…….74
Chapter 4……..75
4.1 Introduction……75
4.2 Bio-based aromatic starting materials……78
4.2.1 Cashew nut shell liquid (CNSL) as a bio-renewable resource…….79
4.3 The synthesis of value-added products from cardanol……79
4.3.1 Alkene centered reactions……80

4.3.2 Nuclear reactions of cardanol……..83
4.3.2.1 Synthesis of benzofurans from cardanol……...83
4.3.2.2 Synthesis of benzoxathiines from cardanol……..85
4.3.2.3 Synthesis of benzoxazines from cardanol…….86
4.3.2.4 Synthesis of coumarins from cardanol……..87
4.3.2.5 Synthesis of UV absorbers from CNSL-based compounds……..88
4.4 Aims of the study…….90
4.5 Results and discussion…….91
4.5.1 Attempted synthesis of fluorescein……..91
4.5.2 Synthesis of coumarins and annellated coumarins derivatives……92
4.6 Conclusions…….98
Chapter 5……..99
5.1 Introduction…….99
5.2 Structural features of THC…….101
5.3 Biosynthesis of THC…….101
5.4 Total syntheses of THC…….102
5.5 Aims and objectives……..104
5.6 Results and discussion……...104
5.6.1 Retrosynthetic analysis of cardol derived THC…….104
5.6.2 Attempted condensation between cardol and verbenol……..105
5.6.3 Condensation of cardol and (+)-*cis*-chrysanthenol……106
5.7 Conclusions……...108
Chapter 6……110
General conclusions and future outlook…….109
6.1 Synthesis of phenanthridines…….109
6.1.1 Future work……...111
6.2 Synthesis of coumarins and annellated coumarins derivatives……..112

6.2.1 Future work……...113
6.3 Synthesis of cardol derived Δ^9– *trans*–tetrahydrocannabinol……113
6.3.1 Future work……...114
Experimental……116
7.1 General experimental procedures……..116
7.2 Synthesis of the Phenanthridines……...117
7.2.1 Preparation of halogenated methoxybenzenes……...117
7.2.2 General Procedure for Suzuki-Miyaura Cross Coupling reactions……120
7.2.3 Attempted synthesis of oxime ethers…….126
7.2.4 Oxime formation general procedure……..127
7.2.5 UV cyclisation of oxime ester derivatives general procedure……134
7.3 Synthesis of coumarins and annellated coumarins derivatives……..142
7.4 Synthesis of cardol derived Δ^9–trans–tetrahydrocannabinol…….147
References…….....150
Appendices……166
Synthesis of the phenanthridines……166
Synthesis of coumarins and annellated coumarins derivatives……...205

Chapter 1

1.1 General introduction

Organic synthesis has achieved monumental feats since its inception, from Friedrich Wöhler's synthesis of urea (1820)[1] to the Kishi synthesis of palytoxin (1989),[2-3] the synthetic targets have increased both in size and complexity. These ever more complicated syntheses are mirrored by the development of sophisticated synthetic methodologies and exotic reagents. However, the synthetic community has paid little attention to the environmental impact of such endeavours. It is only in the past two decades that concerns about the pending depletions of the petrochemical starting materials and the waste generated from organic reactions has been highlighted. Surprisingly, a blueprint of environmentally friendly chemistry (Green Chemistry) was proposed and demonstrated by Giacomo Ciamician in 1908.[4] It took more than a century for chemists to warm up to his ideas. Following the Rio Declaration on Environment and Development from The United Nations Conference on Environment and Development in 1992,[5] Anastas and Warner proposed the twelve principles of Green Chemistry.[6] These principles are not to be regarded as the *panacea* of all environmental ills, rather they are to be taken as guidelines to avoiding the health and environmental impacts of chemical production, and also point to areas of potential development through the design of novel green technologies.

The principles address concepts such as atom economy as introduced by Barry Trost in 1991.[7] Atom economy deals with the conversion efficiency of a process. The aim is to design a process that maximizes the amount of raw material that ends up in the product.[7] Methyleneation (14 g/mol) with methyltriphenylphosphonium bromide **1** (365 g/mol) expelling more than 278 g/mol from triphenylphosphine oxide **2** (shown in Scheme 1) is a good example of a non-atom economical reaction. However, albeit

rare, atom economical reactions existed even in the primordial annals of organic synthesis as exemplified by the Robinson (1917) synthesis of tropinone **3** (Scheme 2(a)).[8] Interestingly, this synthesis utilizes succinaldehyde **4**, methanamine **5** and acetonedicarboxylic acid **6,** highly functionalized starting materials that can be derived from bio-renewable resources. In his seminal and in subsequent publications, Trost makes a close connection between atom economy and catalysis, transition-metal catalysis in particular.[7, 9] It comes as no surprise that catalysis makes one of the principles.[6] Metal complexes added in catalytic amounts can improve atom efficiency of a reaction by lowering the activation energy of the reagents and allow their subsequent union without the catalyst being changed. Catalytic processes also permit short reaction time, reduce reaction temperature and, significantly, waste produced.[10] The palladium cross coupling reactions are a testament to the usefulness of catalysis as evidenced by their application in forging new C–C bonds both in industry and academia. The success of this area of chemistry was recognized by the Nobel Prize awarded to Richard Heck, Ei-ichi Negishi and Akira Suzuki in 2010.

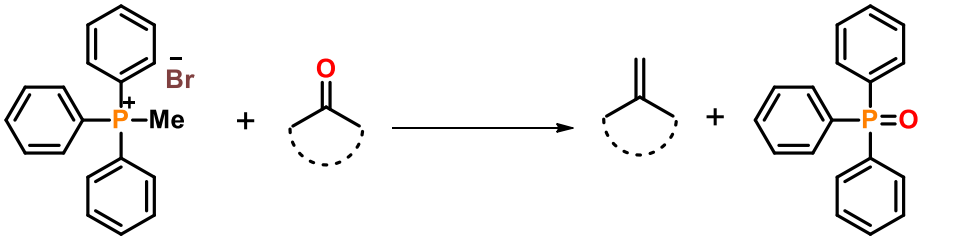

Scheme 1. Methylation through the Wittig reaction

Another important principle is the replacement of fossil resource based chemical processes with renewable material feedstocks and energy sources. Currently, an overwhelmingly high number of raw materials employed in chemical processes are derived from the depleting, CO_2-liberating and chemically not so diverse fossil resources.[11] Often brute force is used to install the missing functionalities as exemplified by the Willstätter (1901) tropinone **3** synthesis,[12] where in the transformation **7** → **8**, the bromide **7** is treated with sulfuric acid in a sealed vessel at 200 °C (!) yielding β-tropine **8** (Scheme 2(b)). It is instructive to point out that all of

the more than fifteen steps in this synthesis were functional group manipulations. This synthesis is in stark contrast with the one step Robinson synthesis of the same tropinone (Scheme 2(a)) that utilizes bio-renewable derived starting materials.

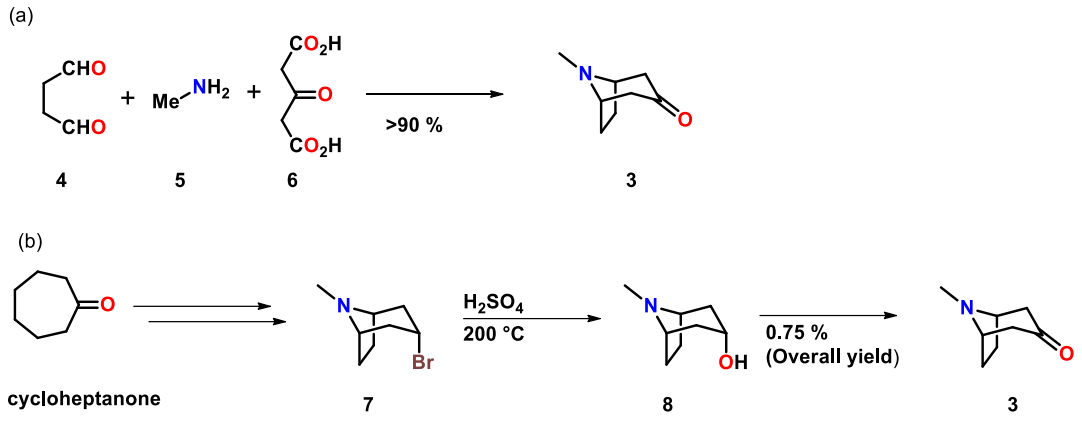

Scheme 2. Synthesis of tropinone by (a) Robinson and (b) Willstätter

Replacing fossil resource based processes with alternative resources presents an attractive option. A feasible substitute, however, should not compete with food production, must be CO_2-neutral, and should be renewable and sustainable.[13] Although some platform compounds have been obtained from lignocellulose – the inedible plant biomass,[14-17] extracting aromatic compounds remains a challenge.[18] Cashew nut shell liquid (CNSL) provides an alluring opportunity. CNSL is a by-product of the cashew nut processing industry whose principal constituents are a mixture of non-isoprenoic phenolic compounds such as cardanol **9**, cardol 1**0**, anacardic acid **11** and 2-methyl cardol **12** (Figure 1b).[19] Stemming from our continued interest in the synthesis of value-added products from bio-renewable feedstocks,[20] this work will focus on the use of cardanol and cardol as starting materials in the synthesis of functional molecules. Another attractive prospect is the development of strategies that employ clean and sustainable energy resources together with catalysis in the synthesis of important organic frameworks, such as azacyclic compounds. Therefore, also addressed in this thesis is the development of novel methodology for the synthesis of phenanthridines (Figure 1a). The key to the successes of the strategy lies with the utilization of palladium catalysed Suzuki-coupling reactions to assemble the carbon backbone,

followed by functional group manipulations that will provide the requisite intermediate, which under photochemical conditions should yield phenanthridines.

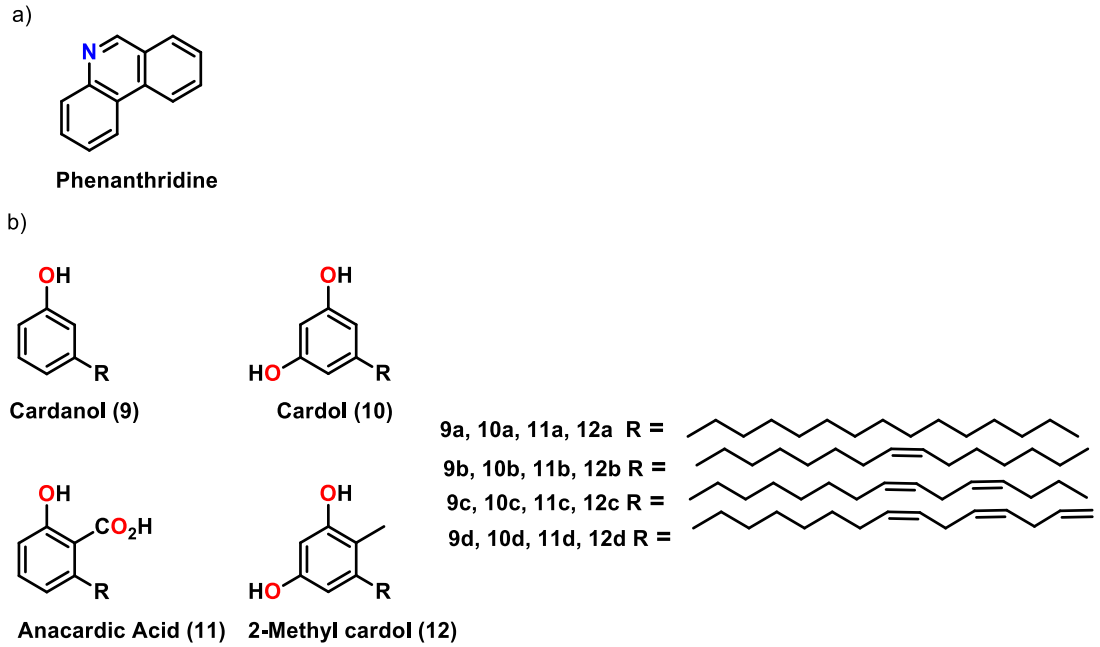

Fig 1. a) The structure of phenanthridine; b) the main constituents of cashew nut shell liquid

This thesis is broadly divided into two parts. Part I focuses on the method-orientated synthesis of phenanthridines from nitrogen-centred radical precursors, using light as a reagent. Target-orientated synthesis of functional molecules from renewable starting materials is the subject of part II. Part I is covered in Chapters 2 and 3. Chapters 4-5 constitute part II that deals with the use of bio-renewable starting materials in the synthesis of functional molecules. Each chapter details biological relevance of the targeted scaffold, and the important methods involved in their syntheses are presented. Following the introduction, the execution of the synthesis is discussed. In the conclusion subsection, the main findings are summarized in a concise manner. Chapter 6 will entail overall conclusions of the whole thesis and future outlook.

Part I

Investigations and the Usefulness of Photo-generated Nitrogen-centred Radicals: Synthesis of the Phenanthridines

Chapter 2

2.1 Introduction

Nitrogen-containing frameworks are ubiquitous in molecules that are essential for our very survival and comfort. Due to their heightened demand, numerous synthetic methods to access these privileged structures have been devised over the past decades. Most of these methods are able to deliver the desired compounds in high yields, however, not without the accompanying undesired side products – courtesy of stoichiometric amounts of auxiliary reagents that are often required for the success of these transformations. Copious amounts of other reagents may also be necessary to deliver clean products. The waste generated in these endeavours requires monetary incentive to get rid of and this often ends up in the environment. This realization poses a challenge on modern synthetic organic chemists to develop efficient transformations that are not only high yielding but that also require sustainable energy sources and minimal auxiliary reagents, thus minimizing waste generation. Photochemistry holds great promise in addressing the sustainability, environmental and financial challenges that riddle traditional thermal organic chemistry manifolds.

2.2 Photochemistry

Photochemistry is the study of light driven chemical reactions of atoms or molecules. In a photochemical reaction the reactant is electronically excited through absorption of a photon of light (*hν*), resulting in the promotion of a ground state (S_0) electron from the highest occupied molecular orbital (HOMO) to the lowest unoccupied molecular orbital (LUMO) or to higher orbitals. As a consequence, the electronic configuration of the electronically excited molecule changes. However, the electron spin remains unchanged, as spin inversion during excitation is forbidden by quantum mechanics. Depending on the energy of the photon absorbed, an array of singlet excited states (S_1, S_2, S_3…) differing in energies can be attained. However, within a few picoseconds, all

higher lying excited states relax to the lowest excited energy state, S_1. Once attaining S_1 excited state, an excited molecule can return to S_0 through radiative or non-radiative pathways. Radiative pathways involve transitioning to the ground state by emitting a photon of light in a process called fluorescence, while non-radiative transition returns to S_0 through the loss of energy as heat (internal conversion, IC). An excited molecule (S_1) can also proceed to a triplet state (T_1) *via* spin-forbidden process, also a non-radiative transition known as intersystem crossing (ISC). The transition from S_0 to T_1 is accompanied by spin inversion resulting in a molecule with two unpaired electrons with the same spin. T_1 can then transition to S_0 *via* radiative decay known as phosphorescence, or *via* non-radiative decay. The possible pathways an excited molecule can undergo are summarized in the Jablonsky diagram in Figure 2 below.

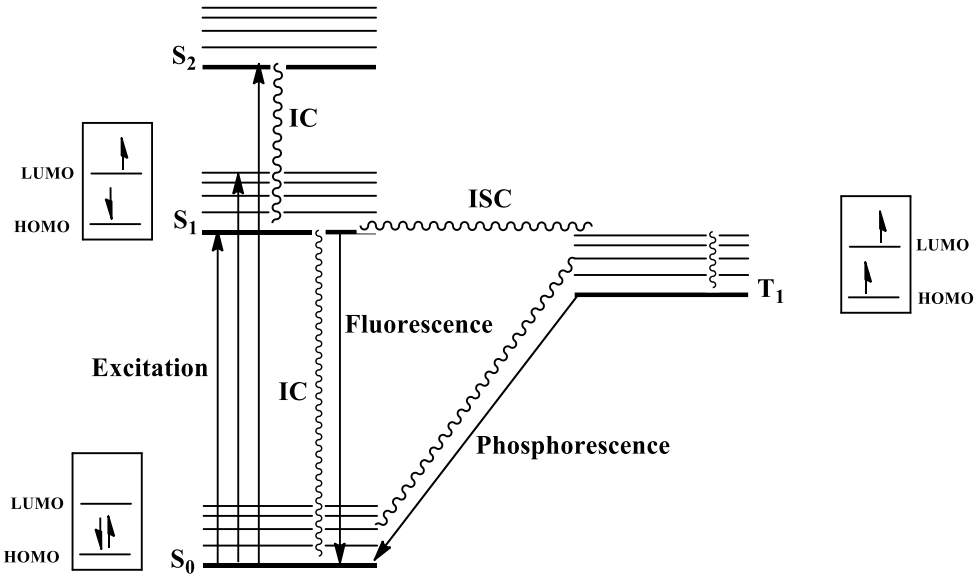

Fig 2. Jablonski diagram depicting possible pathways an excited molecule can undergo. The arrows represent radiative pathways, the non-radiative pathways are represented by the wavy lines.

The S_1 and T_1 excited states are the most relevant states in photochemistry. It is noteworthy to point out that both the S_1 and T_1 possess low-energy singly occupied molecular orbitals (SOMO), rendering them stronger oxidants than ground state species.[21] Conversely, the excited states are also strong reductants due to the high-

energy SOMO they possess.[21] This peculiar combination renders photoexcited molecules prone to single electron transfer (SET) processes under a redox-neutral environment - a feature that cannot be achieved through other synthetic strategies.

Photochemical transformations are carried out in the 170 – 700 nm range. This region of the electromagnetic spectrum is subdivided phenomenologically into five sub bands: vacuum-ultraviolet (VUV, 100 – 200 nm), UV-C (200 – 280 nm), UV-B (280 – 315 nm), UV-A (315 – 380 nm), and visible (Vis - light, 380 – 780 nm).[22] The UV region represents the high energy end of the range and most organic molecules are able to absorb a photon of light corresponding to this region. Thus photochemical reactions in the UV region can take place without the addition of a photosensitizer.[23] When visible light emitting sources are used to drive a reaction, it may be necessary to use photosensitizers for a reaction to take place since most organic molecules do not absorb in the visible region of the electromagnetic spectrum.

Photochemistry possesses a number of advantages such as that the use of light represents an ecologically clean, highly specific and renewable source of energy, thus making light a green "reagent". Photochemical methods are generally executed at ambient temperatures, therefore, they offer less aggressive conditions in chemical synthesis as compared to their thermal counterparts. Often, substrates that are participating in photochemical reactions do not require any protecting groups. As a consequence, photochemical reactions have been be used to considerably shorten synthetic steps as compared to thermal manifolds (*vide infra*). This makes photochemical reactions more desirable and may be the key to economically feasible synthesis of products that are not easily obtained. Most importantly, because antibonding orbitals are occupied in the excited state, photochemical reactions can achieve many reactions that are not possible *via* thermal reactions.

Photochemical technologies have enjoyed increased attention from both academia and the chemical industry. It is apparent that they will become major areas of research and development in the future. This is largely influenced by the depletion of fossil resources

and the ever increasing need for renewable and clean sources of energy and basic chemicals.

2.3 Photochemistry in chemical synthesis

Photochemistry finds its root in natural phenomena such as photosynthesis, Vitamin D synthesis and bleaching, to name a few. Such natural processes have inspired generations of chemists for centuries and are seen as the pinnacle of sustainability. For example, chemists have been puzzled about nature's ability to use radiation energy from the sun to drive some chemical reactions. It followed naturally that some chemists started to investigate the effects of light in organic molecules. As a consequence, a myriad of preparative organic chemistry reactions that can be classified into more than 550 reaction types have been developed through the years.[24] These photochemical reactions started appearing in the literature in the early 19th century and have continued to grow especially in what I have termed "Modern Era" (more on this later). The sheer size of the photochemistry literature renders the herculean task of a thorough review of this field in a small section of a PhD thesis impossible. Therefore, omissions of important literature references are inevitable. Our focus is on the important contributions that drove the development of the field, culminating in photo-induced C–N forming reactions. The literature is presented from a historical and developmental viewpoint, focusing on the big players in the field and their contributions. Examples from recent literature that demonstrate the utility of some of classical photochemical reactions will also be presented.

The development of organic photochemistry can be divided into four "eras" characterized by the research focus of that particular era. For the purposes of this review, I have named them as the "Infancy, Mechanistic, Theoretical and Modern Era". The Infancy Era is characterised by serendipitous discoveries and the first systematic studies on photochemistry. The Mechanistic Era represents the period between the First and Second World Wars (WWI and WWII) and is characterised by slow progress but with the first mechanistic studies. The Theoretical Era is characterised by the influx of spectroscopists and physical organic chemists into the field and the subsequent

investigations of the photophysical and theoretical underpinnings of photochemical reactions. Most of the terminology we use today to describe photochemical processes come from this era. And finally, the Modern Era that is characterised by invention of novel and re-invention of classical photochemical reactions using low frequency light sources such as light-emitting diodes (LEDs), the application of photochemistry to obtain challenging heteroatom radicals, and the broader application of photochemical reactions in complex organic synthesis.

2.3.1 Infancy Era (1886–1914)

The earliest examples of photochemical reactions were dominated by carbonyl compounds, a consequence of their favourable photochemical and photophysical properties. Some of these reactions include oxidations and reductions, fragmentations, auto-oxidations, rearrangements, polymerizations, and condensations. It must be noted that most of these reactions were the product of a very fruitful collaboration between Giacomo Ciamician and Paul Silber,[25] who were the first researchers to perform systematic studies in photochemistry. For example, their selective oxidation of alcohols to aldehydes was impressive, even by today's standards.[26-29] The potential of this oxidation was demonstrated in the conversion of erythrol **13** to erythrose **14** in the presence of benzoquinone and sunlight (Scheme 3)[26] This oxidation is accompanied by the reduction of benzoquinone **15** to hydroquinone **16** and therefore, has also been viewed as a reduction reaction. Besides the obvious merit of the reaction with regards to selectivity, it also avoids using stoichiometric, harsh and sometimes toxic oxidizing reagents often employed in traditional organic synthesis. This photochemical oxidation is complementary to the mild enzymatic oxidations as described by Roger Sheldon and others.[30] George Hammond utilized the reduction side of this reaction to prove the triplet state of ketones (*vide infra*).

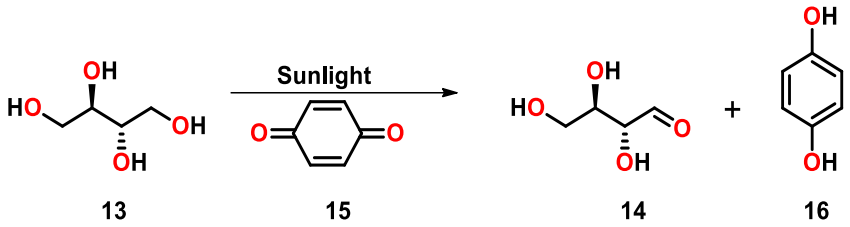

Scheme 3. The oxidation of erythrol to erythrose and the simultaneous reduction of benzoquinone to hydroquinone under photochemical conditions.

Another equally impressive feat achieved by this duo was the photochemical C–H activation/C–C cross coupling (using modern terminology) of alcohols and ketones, in the absence of additional reagents.[31] For example, irradiation of benzophenone **17** and benzyl alcohol **18** gave diol **19** as the sole product (Scheme 4).[31] This reaction works best with aromatic ketones and benzylic alcohols like **18** due to the stabilized radical intermediates. A similar cross coupling reaction was observed in aliphatic ketones and alcohols, albeit, with homo coupling products, thus limiting its practical application in synthesis. This reaction was known as a condensation reaction, as most C–C forming reactions were called at the time.

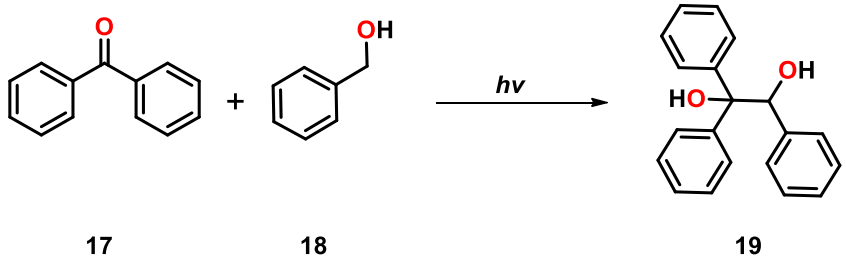

Scheme 4. Photo-induced cross coupling of aromatic ketones and alcohols.

Other transformations such as photo-induced halogenations, cycloadditions, *cis-trans* isomerization of alkenes and photochemistry of diazo and diazonium compounds were discovered during this period.[32-33] Despite the achievements made during this time, little attention was paid to the mechanism of these reactions.

2.3.2 Mechanistic Era (1921–1945)

Sadly, the collaboration between Ciamician and Silber was one of the casualties of the First World War,[25] and so was the progress in photochemistry, which was greatly hindered and remained so well beyond the Second World War! However, not all was lost, for it was during this period; between the world wars that some of the seminal discoveries in photochemistry were made. For example, it was during this time that Ronald Norrish came onto the photochemistry scene. The exploits of Norrish on photochemistry overlapped with Ciamician's and Silber's earlier work on the photochemistry of ketones and aldehydes. However, the thrust of his program was not directed towards the preparative aspects of photochemistry, but rather on the mechanistic underpinnings of such reactions. Thus, Norrish and co-workers exposed various ketones and aldehydes to photochemical conditions and the products were analysed.[34] They discovered that photo-excited ketones and aldehydes react in one of two pathways aptly termed *Norrish Type I* and *Norrish Type II*. In these processes, photo-excitation of aliphatic ketones or aldehydes results in the singlet state (**S_1**) that undergoes ISC to triplet state (**T_1**).[35]

2.3.2.1 Norrish Type I pathway

When the *Norrish Type I* is in operation (Scheme 5), the triplet state results in the C–C scission between the carbonyl carbon and the α-carbon, yielding a diradical **20** that can suffer one of three fates. The diradical **20** can recombine giving the starting material **SM**. Alternatively, the diradical **20** can rapidly dissociate to carbon monoxide and alkyl diradical **21**, followed by radical combination, forging a new C–C bond (like in **22**). The overall reaction is a decarbonylation reaction. Finally, **20** can disproportionate either through the abstraction of the hydrogen alpha to the acyl group yielding a ketene **23** or through the abstraction of the hydrogen beta to the alkyl radical yielding an aldehyde and an alkene **24**. *Norrish Type I* processes dominate in 5 to 7 membered cyclic aliphatic ketones and also in short-chain acyclic ketones and aldehydes.[34, 36-37]

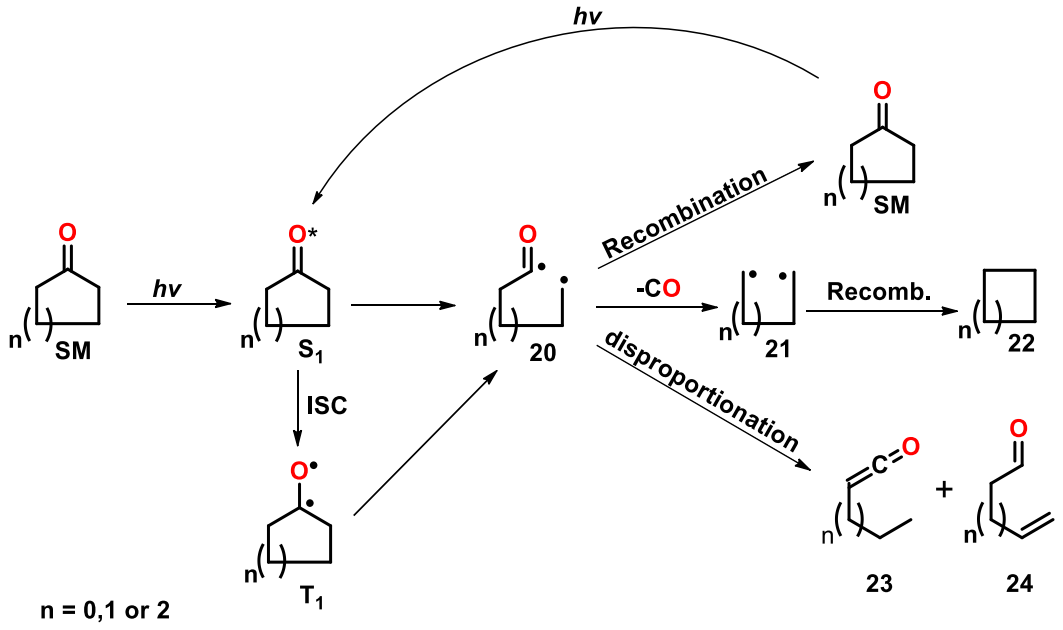

Scheme 5. General schematic representation of *Norrish Type I* processes using cycloalkanones as an example.

The utility of this reaction type in synthetic organic chemistry is limited in scope due to the number of competing reactions. However, *Norrish Type I* has been utilized in specific substrates poised to participate in one of the possible pathways. For example, Deslongchamps and co-workers effectively employed *Norrish Type I* in their 1978 synthesis of triquinacene **25**[38] from Thiele's acid **26** in 6 steps (Scheme 6). Thiele's acid **26** was converted to diketone **27** under acidic conditions through the Schmidt reaction. Their earlier synthetic strategy of triquinacene **25** necessitated a protection operation for one of the carbonyl groups of **27**.[38-39] However, in their photochemical strategy such protection operation was rendered obsolete, and, compounded with the ease of generating the key intermediate **28** by photochemical means, the synthetic steps were reduced significantly.[38] Thus, irradiation of diketone **27** with 450 W Hanovia medium pressure Hg in Pyrex resulted in the rupture of the strained norbornanone carbonyl group furnishing aldehyde **28** in 95% yield,[40] and subsequent transformations led to triquinacene **25**. *Norrish Type I* reaction has also been used to access structurally

complex and challenging organic molecules such as dodecahedrane,[41] and [4,5]Coronane[42] by other groups with varying success.

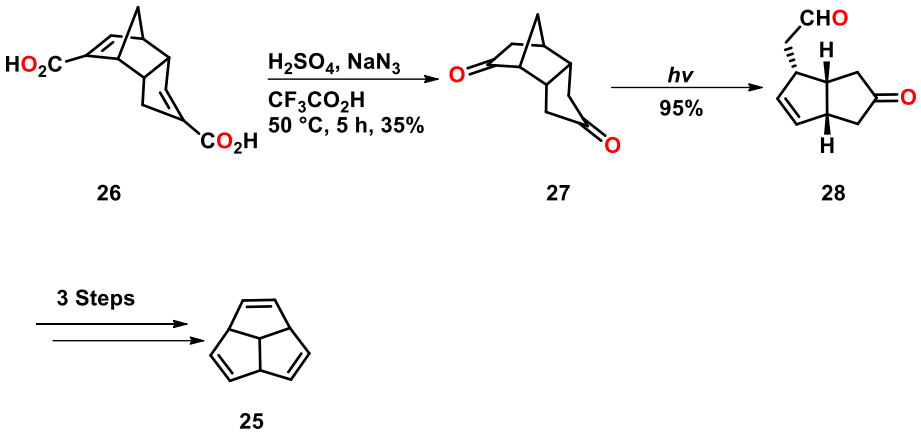

Scheme 6. Deslongchamps' utilization of *Norrish Type I* reaction on the total synthesis of triquinacene.

2.3.2.2 Norrish Type II pathway

In the *Norrish Type II*, a photo-excited ketone or aldehyde **SM** in triplet state $\mathbf{T_1}$ *via* singlet state $\mathbf{S_1}$ and ISC,[34] can also endure a γ-hydrogen abstraction resulting in a 1,4-diradical **29** (Scheme 7). The 1,4-diradical **29** may subsequently suffer either a fragmentation reaction, forming an enol **30** and an alkene **31**, or an intramolecular radical recombination forging a substituted cyclobutanol **32**. The reaction has been utilized in total synthesis by workers such as Leo A. Paquette (1986) in his total synthesis of punctatin A[43] and Phil Baran in his 2013 total synthesis of ouabageni.[44]

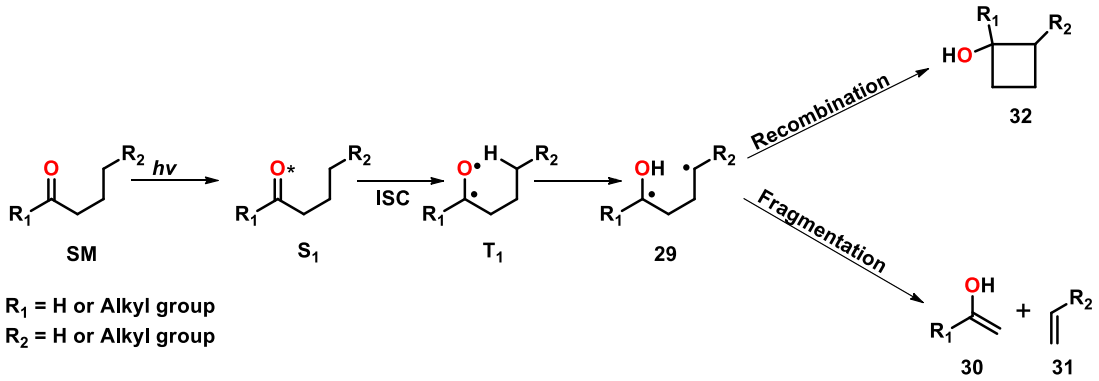

Scheme 7. General schematic representation of *Norrish Type II* processes.

2.3.2.3 Miscellaneous photochemical reactions during the Mechanistic Era

Other contributions during this period were the diastereoselective oxidation of alkenes with singlet oxygen in the presence of a sensitizer, affording allylic hydroperoxides. The Schenck reaction, as it is known, closely resembles the enzymatic hydroperoxidations that are implicated in the biosysnthesis of various natural products.[45] Günther Schenck and Karl Ziegler (1944) employed this reaction in their synthesis of ascaridol **33** from α-terpinene **34** and molecular oxygen, using chlorophyll (**sen**) extracted from the leaves of spinach as a photosensitizer (Scheme 8).[46] Under these conditions, chlorophyll (**sen**) is photo-excited through the absorption of a photon leading to **sen*** that participates in energy transfer reaction with triplet oxygen ($^3O_2$) generating singlet oxygen ($^1O_2$) and the subsequent Diels-Alder reaction between $^1O_2$ and α-terpinene. This process is thought to mimic the biosynthesis of ascaridole[47] and was adopted for industrial production of ascaridole in Germany.[48] Schenck's work in photochemistry forms the theoretical basis for photodynamic therapy (PDT).[49-50] The work of Schenck is not only held in high regard for its PDT theoretical prestige, but also for its prowess in the synthetic organic chemistry arena.[51-52] Other discoveries in photochemistry that were made during this era are beautifully reviewed in the book "*Chemical Photocatalysis*".[32]

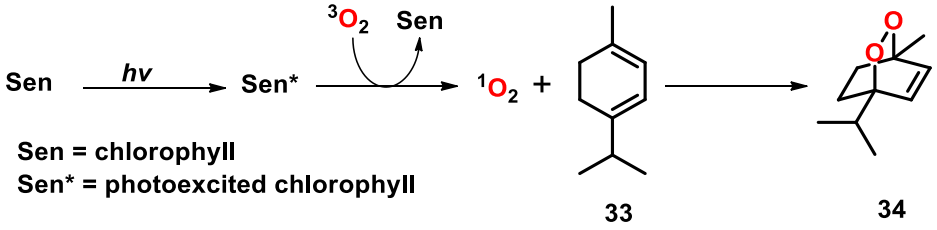

Scheme 8. The Günther Schenck and Karl Ziegler (1944) synthesis of ascaridol from α-terpinene and molecular oxygen using chlorophyll as photosensitizer.

Up to this point, most notable contributions in photochemistry were made in mainland Europe and Britain. However, after WWII some of the major contributions in the field came from the other side of the Atlantic, in the United States (US).

2.3.3 Theoretical Era (1950-1970s)

The period after WWII into the 1970s is marked by advances in both invention of novel synthetic tools and molecular electronic theory and its application in reaction mechanisms, fostering the synthesis of complex molecules, with some of the towering figures such as RB Woodward, Gilbert Stork, and others at the forefront. These were mirrored by advances in qualitative and quantitative techniques such as crystallography, spectrometry and spectroscopy that made it possible to detect even the most transient of intermediates. The ground was fertile for the application of such techniques to solve the theoretical challenges that plagued photochemistry at the time. As a result, this field was dominated by physical organic chemists and spectroscopists.

According to Westheimer; "*Only two great schools of physical-organic chemistry have thrived: that of Sir Christopher Ingold at University College, London, and that of Paul Bartlett at Harvard.*"[53]

While the school of Ingold focused on ionic reactions such as electrophilic substitution reactions, most co-workers of Bartlett focused on photochemistry, hence most of the landmark discoveries in photochemistry were made in the US. Photochemistry was never a research focus of Bartlett, he only used it as a means to an end in his singlet oxygen oxidations.[54] Despite this, a number of Bartlett's co-workers became leaders in photochemistry.

One such figure was George S. Hammond (1921–2005). Hammond (1959) provided experimental proof for the highly reactive triplet state that was only theorised upon at the time. [55] To achieve this, he used the Ciamician photopinacolization of ketones in the presence of an alcohol (Scheme 9). Hammond and co-workers irradiated benzophenone **17** at 366 nm and showed that it undergoes n→π* transition giving a singlet state **17a** that is followed by ISC to triplet state **17b**, a transition first postulated

by Robert Mulliken at the University of Chicago (1935).[56] The triplet state then participates in fast hydrogen abstraction with benzhydrol **35** forming *C*–centred radicals, followed by radical coupling furnishing benzpinacol **36**. Hammond took the studies on the triplet state a bit further; he showed that energy can be directly transferred from a triplet state molecule to a ground state molecule (quenching). Quenching made it possible to generate triplet states of molecules that are otherwise difficult through direct irradiation since singlet states may be the dominant mode of excitation in certain molecules. This direct energy transfer is the basis for photocatalysis, and most photo-induced natural phenomena like photosynthesis where chlorophyll is a sensitizer (photocatalyst), and also in the *cis-trans* isomerizations of alkenes. While Hammond in California focused on reactions and quenching of relatively simple aliphatic and aromatic ketones, as well as stilbene isomerizations and its application in synthesis, Howard Zimmerman at the University of Wisconsin-Madison concentrated on rationalizing unusually complex rearrangements of unsaturated cyclic ketones and bicyclic alkenes.

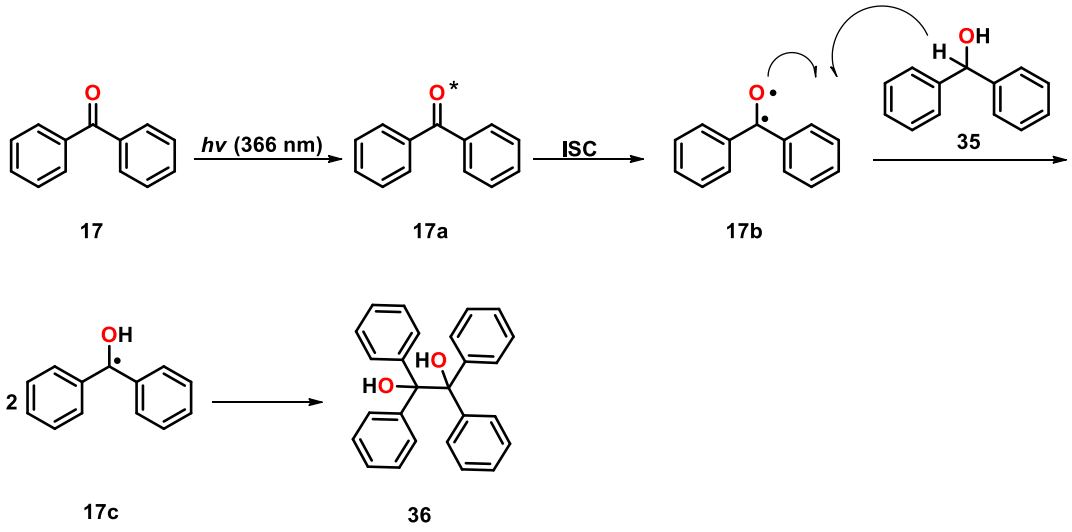

Scheme 9. Hammond's photosynthesis of benzpinacol, the experimental proof of the triplet state in ketones.

Zimmerman – using his knowledge of quantum mechanics and synthetic chemistry, solved one of the enduring and complicated photochemical transformations at the time

– the photochemical rearrangement of α-santonin **37** to lumisantonin **38**. Lumisantonin **38** was first isolated by George Büchi (MIT)[57] and others[58] as an intermediate in the rearrangement of santonin **37** to photosantonic acid **39**, one of the earliest organic photochemical transformations reported in literature (Scheme 10a).[32-33] The structure of lumisantonin **38** was elucidated by Derek Barton (1958).[58] The photorearrangement of α-santonin **37** to lumisantonin **38** is accompanied by the inversion of stereochemistry at C–10; the C–4 methyl group migrates to C–1 and the C–3 carbonyl group migrates to C–2. Perhaps the most striking feature of this transformation is the formation of the hexasubstituted cyclopropane structural motif that bears three contiguous stereogenic quaternary carbons in a single step! This feat is unmatched by traditional thermal chemistry to date. To explain these bond reorganizations, Zimmerman and co-workers applied Kasha's rules to establish the electronic configuration of the excited state and subsequently applied the "arrow pushing" notions that were well established for ground state reactions to reach the product. Using this approach, Zimmerman rationalized that upon irradiation, the carbonyl group of the 2,5-cyclohexadienone moiety of α-santonin **37** undergoes n→π* transition attaining triplet state (Scheme 10b).[56] The resulting diradical **37a** is poised to partake in β-β bond formation due to the large bond order between the β carbons (C–1 and C–5) of the 2,5-cyclohexadienone moiety as revealed by the Hückle computations.[59] Thus, **37a** forms **37b** followed by ISC transition revealing the zwitterion **37c** which then participates in a 1,3-alkyl shift to lumisantonin **38**. Zimmerman also demonstrated that this transformation is not limited to α-santonin **37** or bicyclic 2,5-cyclohexadienones, but simple dienones can also undergo analogous photorearrangements. This was elegantly achieved with 4,4-diphenylcyclohexadienone[59] which was shown to undergo photorearrangements similar to those observed for α-santonin **37**.[60] 4,4-Diphenylcyclohexenone (with one double bond missing) was also investigated and shown to undergo a different but equally impressive photo-induced rearrangement.[61]

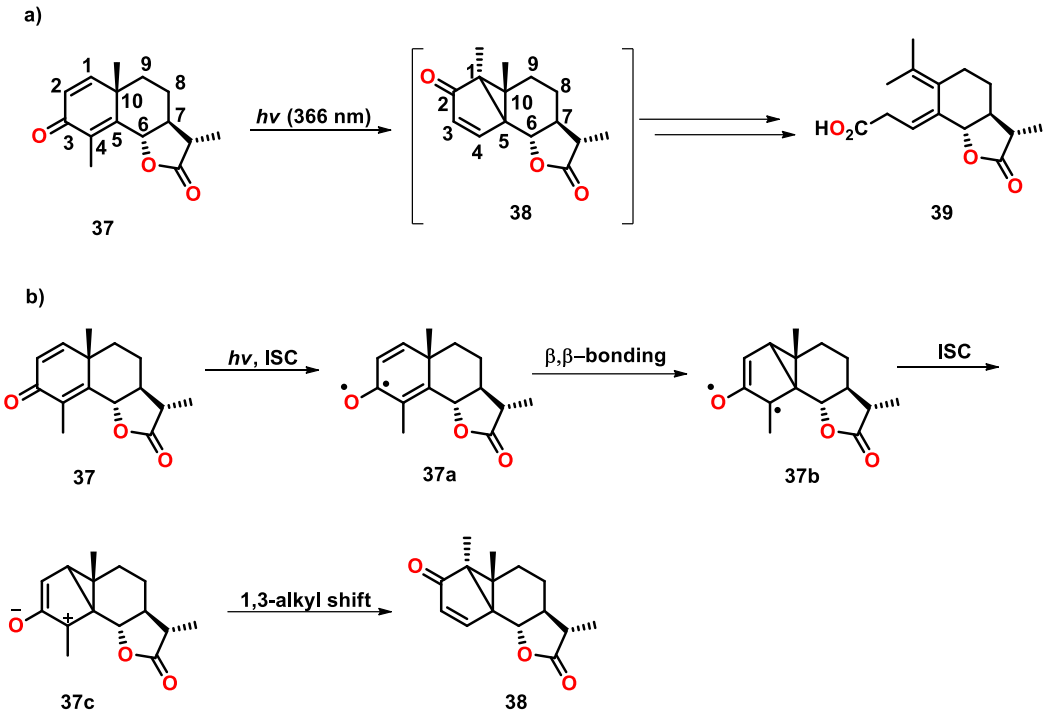

Scheme 10. a) The photochemical rearrangement of α-santonin to photosantonic acid via the intermediary of lumisantonin, b) photochemical rearrangement of α-santonin to lumisantonin as described by Zimmerman and co-workers.

As a natural extension of his exploits on 2,5-dienones, Zimmerman investigated photo reactions of 1,4-dienes (similar to the dienones he investigated, but without the carbonyl group). He soon discovered that photo-excited 1,4-dienes underwent π→π* transition resulting in triplet and singlet states that underwent di-π methane reaction also known as the Zimmerman rearrangement, giving a variety of products depending on the substrate and the conditions employed. For example Zimmerman and Grunewald demonstrated that a triplet-sensitized barrelene (bicyclo[2.2.2]octa-2,5,7-triene) **40** rearranges to semibullvalene **41**, while when barrelene **40** is irradiated in the absence of a sensitizer it rearranges to semibullvalene **41** and (1*Z*,3*Z*,5*Z*,7*Z*)-cycloocta-1,3,5,7-tetraene **42** (Scheme 11). The aforementioned transformations were rationalized by the Zimmerman group.[60] The photochemical community benefited from the exploits of Zimmerman which resulted in what is known as the Zimmerman paradigm. This paradigm constitutes four steps; (i) photo-excitation, (ii) electronic

rearrangements of the excited substrate, (iii) relaxation to ground state and, (iv) the subsequent rearrangements to the final products.

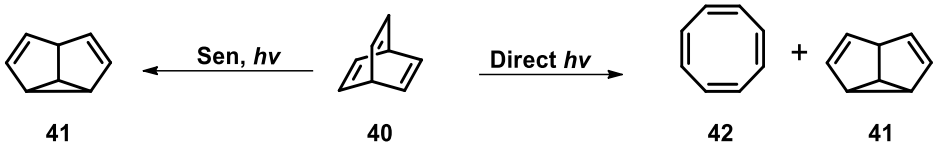

Scheme 11. Rearrangement of barrelene under different photochemical conditions.

Other important contributions in photochemistry in this period came from synthetic organic chemistry luminaries such as George H. Büchi,[62] who showed that the then unknown product of the photochemical reaction between alkenes and carbonyl compounds reported by Paternò is an oxetane that results from the [2 + 2] cycloaddition between the alkene and the carbonyl carbon. Most of the photochemical lexicon that we use today came from the contributions of Micheal Kasha at the University of Florida.

It is important to note that photochemistry was not confined within the borders of the United States. Other prominent figures in this field also included workers in Europe such as Günther O. Schenck (University of Göttingen, Germany and later Paris and Britain), Albert Weller (University of Göttingen), George Porter (University of Sheffield UK), Egbert Havinga (Leiden University, The Netherlands), Sir Derek H.R. Barton (various universities in the UK, France and the US) and others.

This period saw increased interest in the field of photochemistry, as exemplified by numerous discoveries both in industry and academia between the late 1950s to the late 1970s. Much of the photochemical body of work produced from this era was organized by V. Ramamurthy and Nicholas Turro and presented in 28 reviews that appeared in a *Chemical Reviews* thematic issue.[63]

2.3.4 Modern era (1980s-present)

Despite its promise as a powerful synthesis tool, photochemistry largely remained underutilised due to the inherent radical nature of photochemical reactions and the

perception that radical reactions cannot be controlled and lack selectivity. However, advances in solar cells research, the development of LEDs and increasing insight into the governing factors in radical processes, such as radical propagation, radical polarities and bond dissociation energies (BDEs), coupled with increased interest in heteroatom centred radicals, ushered in the Modern Era of photochemistry.

Before the Theoretical Era, photochemical transformations were seen as random and unpredictable with no practical applications in organic synthesis. However by the end of this Era, chemists could predict the outcome of a number of photochemical reactions with confidence. Synthetic organic chemists recognised the potential of photochemical manifolds in producing complexity in a single operation from simple and easily accessible substrates. Therefore, photochemical reactions soon found application in the synthesis of complex natural products by prominent synthetic organic chemists throughout the world. Certain classes of photochemical reactions such as photo-induced cycloadditions have enjoyed heightened attention as a powerful tool in total synthesis. A case in point is the utilization of [3 + 2] intramolecular arene−alkene cycloaddition of the dialkylanisole **43** in the concise total synthesis of α-Cedrene **44** by Paul Wender (Scheme 12).[64] The starting dialkylanisole **43** was obtained from the reaction of ketone **45** and chloro-anisole **46** under reducing conditions and the subsequent photo-cycloaddition gave adducts **47** and **48**. Adducts **47** and **48** were converged into a single product **49** through bromination and radical debromination. Ketone **49** was subjected to Wolff−Kischner reduction yielding α-Cedrene **44**. Perhaps the real potential of this reaction were the syntheses of structurally diverse sesquiterpenes starting from appropriately substituted arynes and alkenes. The literature on arene−alkene cycloaddition was the subject of a review by Richard Remy and Christian G. Bochet.[65]

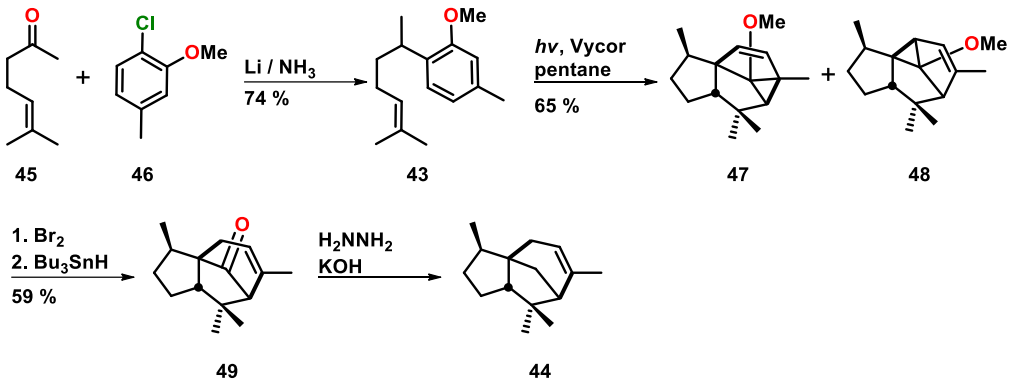

Scheme 12. Wender utilization of photoinduced [3 + 2] total synthesis of intramolecular arene−alkene cycloaddition in the total synthesis of α-Cedrene.

Morden photochemistry has benefited immensely from research efforts aimed at harnessing solar energy using polypyridyl-transition-metal photocatalysts such as $Ru(bpy)_3^{2+}$ and related complexes.[66] Stemming from their favourable photochemical and photophysical properties, these complexes have been used as photocatalysts to convert water and carbon dioxide into fuel, and also to directly convert solar energy to electrical current. Tehshik Yoon (University of Wisconsin–Madison) and David MacMillan (Princeton University) capitalized on the success of polypyridyl-transition-metal complexes and independently demonstrated that these complexes can catalyse both inter- and intramolecular [2 + 2] cycloadditions of enones in the presence of visible light sources such as LEDs and store-bought fluorescent light bulbs.[66-67] This strategy relies on the ability of metal complexes to partake in single-electron transfer (SET) reactions with organic substrates upon photo-excitation with visible light. Therefore, such reactions are collectively known as photoredox reactions. Photoredox processes are not only confined to metal-based photocatalysts, organic chromophores have also been utilized principally in visible light manifolds.[68] These processes are by no means limited to [2 + 2] cycloadditions of enones, but include myriad other reactions such as functional group interconversions, oxidative couplings, and reductive couplings, to name a few. Photoredox reactions and their applications in the synthetic organic context have been the subject of numerous reviews.[69]

2.4 Radicals

Photochemical reactions are unique in their ability to generate open-shell reactive intermediates (radicals) from stable closed-shell precursors in the complete absence of toxic reagents and under the mild irradiation conditions. Therefore, photochemical strategies are fundamentally free-radical in nature, and thus it is imperative to know a thing or two about radical strategies and their application in organic synthesis. It must be noted that the term 'radicals' has changed its meaning in the organic chemistry literature.[70] This term is used throughout this thesis to mean open-shell reactive intermediates, and has the same meaning as 'free-radicals'.

As has already been pointed out, radical mechanisms dominate photochemical transformations. Today, invoking radical intermediates to rationalize reaction mechanisms can be taken for granted, but this was not always the case. Radical intermediates were alluded to in organic chemistry during its infancy. However, most reactions that were thought to undergo free-radical mechanism were proven to be ionic, therefore, radicals were only theorised upon with no evidence in sight, and thus their existence was highly contested. Radicals remained elusive and eventually succumbed to their ionic counterparts whose evidence was stronger at the time. Consequently, radicals remained whimsical assertions only lingering in the minds of unorthodox and seemingly backward thinking chemists. In retrospect, the fleeting nature of most radical intermediates, compounded by the lack of the appropriate tools to detect such species were the main contributing factors to this misunderstanding. The definitive proof of the existence of radicals was presented by Moses Gomberg in 1900 when he encountered the persistent triphenylmethyl radical **50** in his attempted synthesis of hexaphenylethane **51** through the Wurtz coupling of triphenylmethyl chloride **52,** in the presence of silver or zinc metal powder (Scheme 13).[71] The controversy that transpired following his famous "*Triphenylmethyl, ein Fall von dreiwerthigem Kohlenstoff*" makes for an exciting read for those with interest in the history of chemistry.[70] It took another decade for the chemical community to accept the existence

of radicals and it would take almost a century for their application in the synthesis of complex organic compounds.

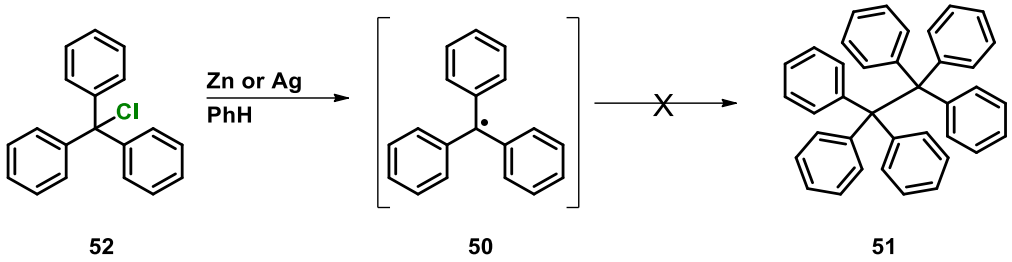

Scheme 13. The Gomberg synthesis of the persistent triphenylmethyl radical in his attempt at the synthesis of hexaphenylethane from triphenylmethyl chloride.

For a very long time, radical reactions were believed to be messy, and uncontrollable. This belief hindered progress and utilization of radical strategies in synthetic organic chemistry. However, systematic studies of radical reactions did not only prove that they can be controlled, but also that they can be more selective than polar reactions.

2.4.1 Nitrogen-centred radicals

Most radical reactions involve carbon-centred radicals; heteroatom radicals only gained interest in recent years. Of particular interest are nitrogen-centred radicals due to their potential to furnish the C–N bond that is prevalent in many bioactive compounds. Traditionally, the C–N bond is formed through metal mediated coupling reactions such as the copper-catalysed Ullman and Goldberg reactions, or Pd-catalyzed Buchwald−Hartwig amination or amidation.[72] However, these reactions require pre-functionalized substrates and elevated temperatures. These disadvantages open an opportunity for the development of novel strategies for forging the C–N bond. Nitrogen-centred radicals present an alluring possibility for the construction of C–N bonds.

N-centred radicals can be generated through indirect means, *via* the addition of a preformed radical to an unsaturated nitrogen-containing group such as azide, hydrazone, oxime, imine or nitrile. A more general strategy to *N*-centred radicals

involves homolytic cleavage of a weak N–X bond, where X can be a halogen (except fluorine), a nitrogen-, oxygen-, or sulfur-containing group.

2.4.1.1 Aminyl radicals

The earliest example of an *N*-centred radical can be traced back to the von Hofmann (1878) indolizidine **53** synthesis from *N*-bromo-2-propylpiperidine **54** (Scheme 14), in what later became known as the Hofmann–Löffler–Freytag (HLF) reaction. Upon heating or irradiation in the presence of a strong acid, the N–Br bond of *N*-bromo-2-propylpiperidine **54** is presumed to undergo homolytic scission, fashioning the highly electrophilic ammonium radical **55** that suffers a fast intramolecular 1,5 hydrogen atom transfer (HAT). Subsequent trapping of the resulting *C*-centred radical **56** with a Br radical yields δ-bromo amine **57**, which participates in ionic cyclization upon basic work-up, providing indolizidine **54**. The preferential δ-hydrogen abstraction in the transformation **55**→**56** has been attributed to a six-membered transition state **55a**, which favours the chair-type conformation (Figure 3).[73] Conceptually, the reaction is related to the Barton reaction.[74] The HLF reaction can be viewed as one of the earliest examples of remote C–H functionalization. In the absence of δ-hydrogen atoms, the aminyl radical can add to electron-rich unsaturated compounds such as alkenes and alkynes.

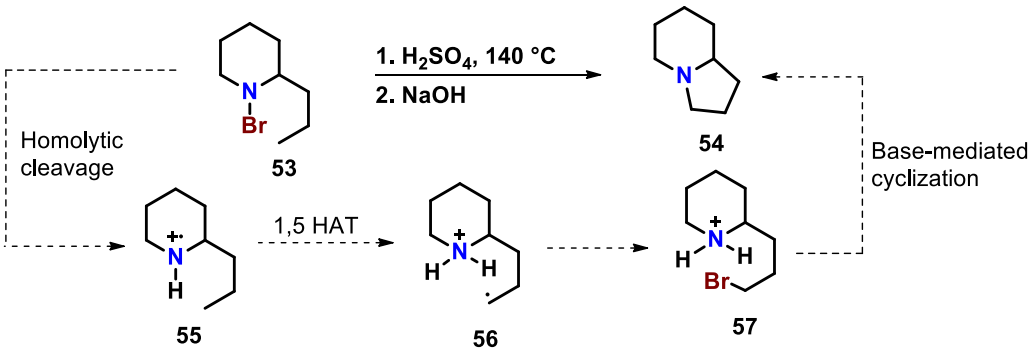

Scheme 14. Mechanism of the 1878 von Hofmann indolizidine synthesis.

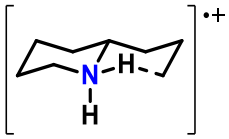

55a

Fig 3. The transition state of the 1,5 hydrogen atom transfer in the Hofmann–Löffler–Freytag reaction.

The synthetic utility of this reaction in synthetic organic chemistry was later realized by Karl Löffler and co-workers (1909) in their classical synthesis of nicotine **58** from *N*-bromo-*N*-methyl-4-phenylbutan-1-amine **59**.[75] Aminyl radicals have also been applied in the synthesis of steroid hormone precursors and other compounds, however the scope of this reaction remains limited due to the harsh conditions employed and the instability of the resulting aminyl radicals.

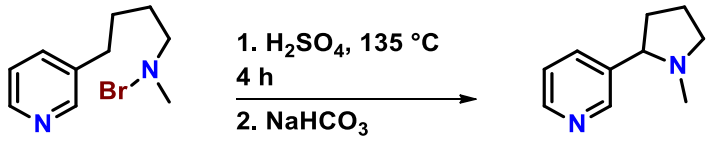

59 **58**

Scheme 15. The Löffler synthesis of nicotine.

2.4.1.2 Amidyl Radical

Appending electron-withdrawing functionalities such as a carbonyl or sulfone group on the nitrogen atom stabilizes the resulting amidyl radical. As a consequence of their relative stability, amidyl radicals can be prepared with ease from different precursors at neutral pH and ambient temperature, thus widening the substrate scope of the HLF reaction. Ernesto Suárez and co-workers demonstrated that the requisite, often unstable *N*-haloamide precursors **60** can be generated *in situ* from the stable amide starting materials **61**.[76] Homolytic cleavage of *N*-haloamides **60** through thermal or photochemical means generates amidyl radicals **62** that give the HLF adducts **63** upon treatment with base (Scheme 16a). The Suárez (1989) photochemical transannulation of lactam **64** to oxoindolizidine **65** in the presence of $PhI(OAc)_2$ and iodine in 82%

yield in a single chemical operation stands as testament to the superiority of this approach (Scheme 16b).[77]

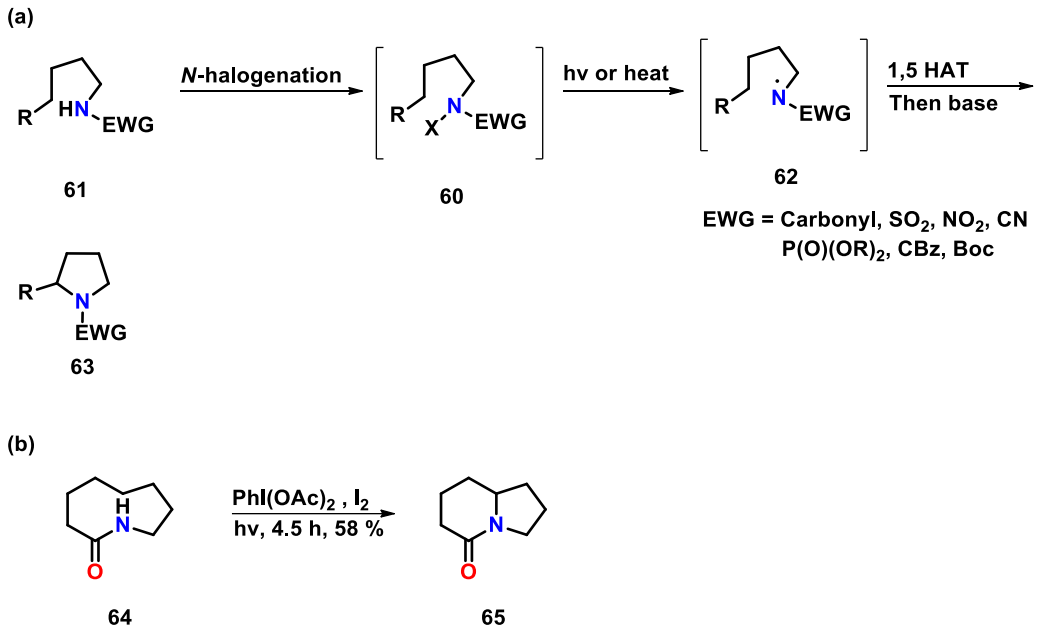

Scheme 16. The Suárez modification of the Hofmann–Löffler–Freytag reaction (a) the general representation and (b) synthesis of oxoindolizidine.

Not surprisingly, this strategy has been tactfully incorporated in numerous multistep synthesis campaigns such as the Phil Baran (2008) 1,3-diol **66** synthesis from alcohol **67** *via* carbamate **68** which was converted to *N*-bromocarbamate **69** followed by 1,5 HAT and the subsequent bromination yielding alkyl bromide **70** (Scheme 17).[78] Ag_2CO_3-promoted cyclization of **70** gives iminocarbonate **71** exclusively, with no formation of cyclic carbamate **72** that could potentially result from nucleophilic substitution *via* the nitrogen atom of the carbamate group of **70**, instead of the desired oxygen nucleophilic attack. Acetic acid and K_2CO_3 hydrolysis provides 1,3-diol **66**.

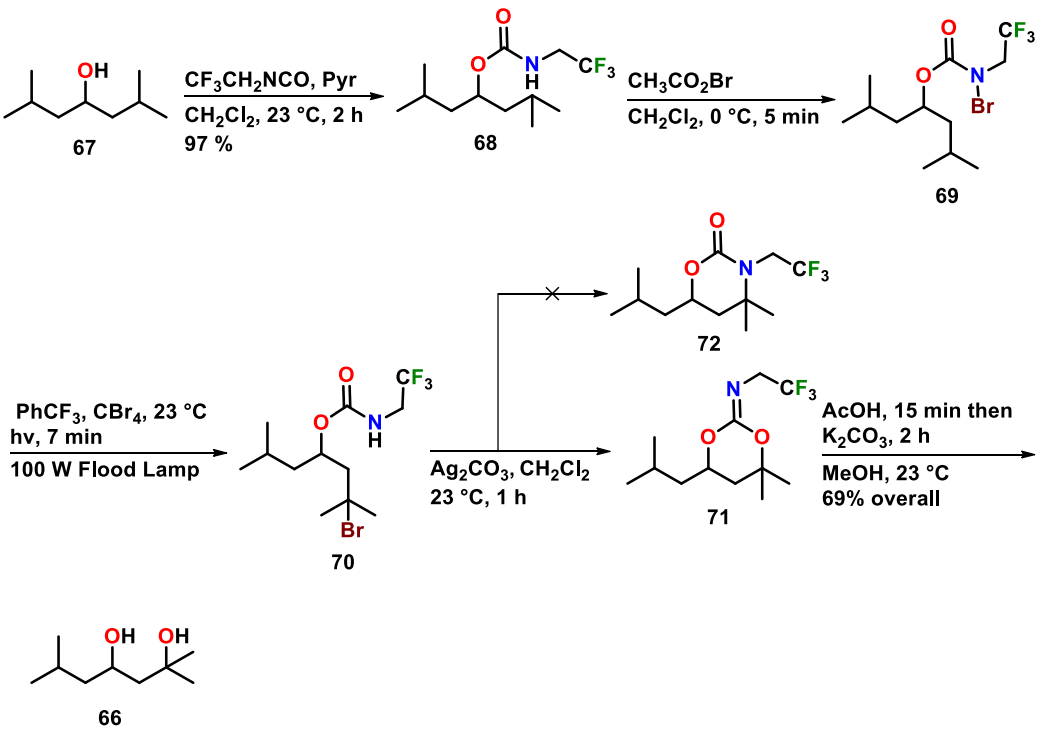

Scheme 17. The Baran 1,3-diol synthesis employing the modified Hofmann–Löffler–Freytag reaction as key step.

Recently, the groups of Robert Knowles (Princeton University),[79] Tomislav Rovis (Columbia University),[80] Sherry Chemler (University at Buffalo),[81] and others have demonstrated that amidyl radicals can be generated directly from both amides and sulphonamides without *N*-prefunctionalization of the starting precursors. Taking advantage of these developments, Corey Stephenson and co-workers developed a visible light-mediated polypyridyl-iridium photocatalyzed amidyl radical (**72**) cyclization/dearomatization cascade strategy to assemble 1,4-cyclohexadiene-fused sultams **73** starting from γ,δ-unsaturated *N*-arylsulfonyl enamides **74** (Scheme 18).[82]

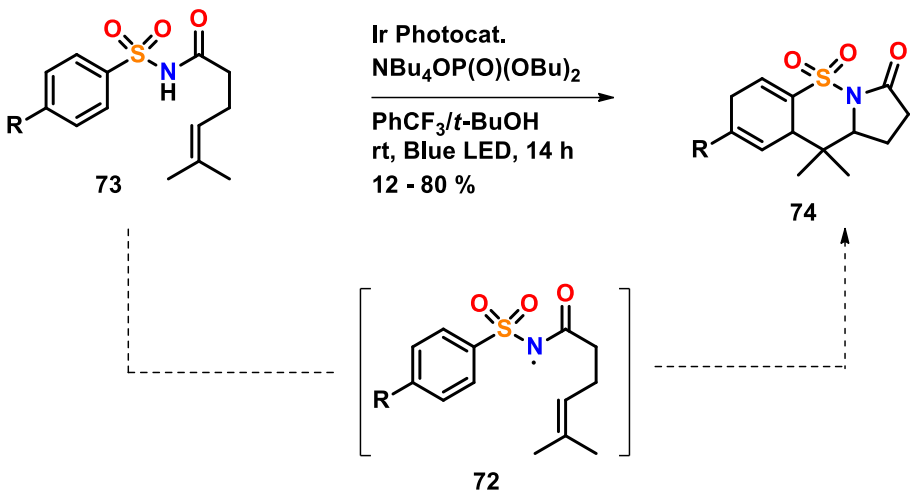

Scheme 18. Synthesis of 1,4-cyclohexadiene-fused sultams through the visible light-mediated polypyridyl-iridium photocatalyzed amidyl radical (**72**) cyclization/dearomatization cascade reaction.

2.4.1.3 Iminyl radicals

The Hofmann–Löffler–Freytag reaction is a powerful tool for constructing aliphatic *N*-heterocyclic compounds. The synthesis of Aza-arenes through HLF may require additional oxidation steps. The ability of the iminyl radicals to forge Ar–N bonds through radical addition and the subsequent aromatization offer a direct route to access *N*-heterocyclic aromatic compounds. Iminyl radicals were also shown to participate in fast cyclization reactions with unsaturated functional groups, and were slow towards hydrogen atom transfer reactions.[83] These favourable kinetics also render iminyl radicals useful candidates for cyclization transformations in the synthesis of aliphatic *N*-heterocyclic compounds.

A convenient method for synthesizing iminyl radicals involves photo-induced homolysis of unsaturated nitrogen-containing functional groups of the form C=N–X (where X is O, S, N or a halogen). The precursors of the general formula C=N–O–C are the most popular choice due to their ease of preparation and their long shelf lifetime. The weak N–O bond (53 kcal/mol) compared to the C–O (68 kcal/mol) and C=N (147 kcal/mol) means upon photolysis or heating, the N–O bond should fragment first

yielding iminyl radicals. Strategies that involve iminyl radical intermediate cyclization provide a succinct route to *N*-heterocyclic compounds of varying ring sizes.

Different aspects of iminyl radicals have been the subject of numerous reviews. Zard published an extensive review on the methodology development for generation of *N*-centred radicals, including the iminyl radical and the following trapping reactions in the period ranging from 1968 to 2007.[84] The synthetic utility of these methods are also covered in the same review. The mechanistic aspects of iminyl radical chemistry including characterization of the intermediates are discussed in comprehensive reviews by Walton.[83, 85] The development of visible light-mediated transition-metal photoredox iminyl radical cyclization reactions and their utility in the synthesis of aza-heterocyclic compounds is the subject of a perspective by Kärkäs.[72] The application of cyclization reactions of iminyl radical chemistry in the construction of polycyclic azacompounds of varying ring sizes was the subject of a recent review by Castle.[86]

2.5 Phenanthridines

Advances in iminyl radical chemistry and their largely unexplored potential in synthetic organic chemistry presents an opportunity for the utilization of these species in the synthesis of important classes of *N*-heterocyclic compounds such as phenanthridines. Phenanthridines have captivated the imagination of synthetic chemists and biologists alike since the 1960s due to their favourable biological activities. The fluorescent nucleic acid stain ethidium bromide (homidium bromide) **74a** (Figure 4) belongs to the phenanthridine family. Due to its efficient DNA binding ability, it is used in agarose gel electrophoresis to determine the presence of DNA or the lack thereof. Ethidium bromide **74a** intercalates kinetoplastid DNA, changing the conformation to Z-DNA that is lethal to trypanosomes, thus it has been used to treat trypanosomiasis in cattle. Propidium iodide **74b** (Figure 4), another member of this family, is also a DNA intercalator used as a cell viability probe.

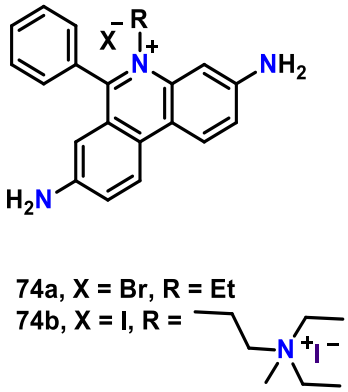

Fig 4. DNA intercalating synthetic phenanthridines that are used as fluorescent stains.

Phenanthridines are not limited to synthetic compounds. The phenanthridine nucleus is present in more than 100 natural products isolated from five plant families that include *Rutaceae, Fumariaceae, Paxpaveraceae, Caprifoliaceae,* and *Meliaceae*.[87] For example, oxyavicine, a naturally occurring benzo[*c*]phenanthridine isolated from the root and fruits of plants belonging to the *Rutaceae* family is used to treat ophthalmic disorders.[87] Oxynitidine **75**, also isolated from the *Rutaceae* family of plants, shows activity against hepatitis B virus.[87] Other members of naturally occurring benzo[*c*]phenanthridines such as sanguinarine **76,** and the simplest naturally occurring phenanthridine, trisphaeridine **77,** have been shown to inhibit DNA topoisomerase I, making them potential anti-tumour candidates.[88] Sanguinarine **76** was also shown to inhibit human telomeric G-quadruplex DNA, making it a potentially selective anti-cancer agent, since telomerase is overexpressed in 80−85% of cancer cells but is missing in normal cells.[89] Several other phenanthridine natural products, including trisphaeridine **77** and decarine **78**, show anti-parasitic activity. Some of the naturally occurring phenanthridines are shown in Figure 5 below.

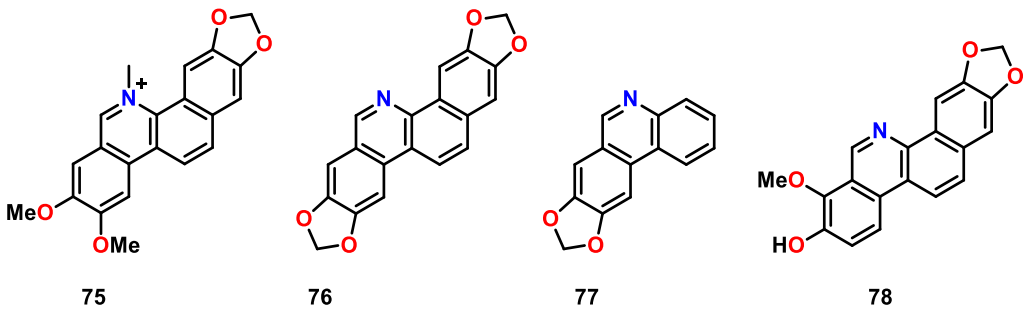

75 76 77 78

Fig 5. Some examples of biologically active naturally occurring phenanthridines.

2.5.1 Synthesis of phenanthridines

Stemming from their attractive biological applications, phenanthridines have inspired synthetic organic chemists to develop numerous synthetic methods to access this privileged scaffold. The phenanthridine skeleton can be viewed as a benzo[*d*]quinoline, giving an angular tricyclic heteroaromatic compound with two benzene rings at the periphery of the central pyridine moiety (Figure 6). There are different numbering systems for phenanthridines; the numbering system adopted here is depicted in Figure 6. For convenience, we have assigned the "quinoline" benzene ring as **A**, the central pyridine ring as **B** and the benzo moiety as **C**. This discussion will be limited to strategies that deliver phenanthridines through cyclization means, therefore, facile modification of tricyclic compounds to phenanthridines such as ring expansion of *N*-methylated carbazoles, fluorenone derivatives and reduction of phenanthridones will be omitted.[90]

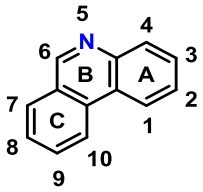

Fig 6. The phenanthridine skeleton and the numbering system adopted throughout the ensuing discussion.

2.5.1.1 Construction of ring A

Phenanthridines can conceptually arise from either inter- or intra-molecular [2π + 2π + 2π] carbocyclization reactions of suitably functionalized isoquinolines (Scheme 19). This approach constitutes the least explored route to phenanthridines. Indeed, the publication by Kundu and co-workers represents the only report exploring this route to benzo[*a*]phenanthridines **79** (Scheme 20).[91] Thus, the Kundu group developed a multicomponent/tandem strategy to benzo[*a*]phenanthridines **79** starting from 2-bromobenzaldehydes **80**, $tBuNH_2$ **81** and various 1,3-diynes **82** that underwent annulation yielding a mixture of geometric isomers of alkynylisoquinolines (**83a** and **83b**) upon exposure to catalytic amounts of $Pd(PPh_3)_4$ in the presence of LiCl under basic conditions (yields 50-70%) as depicted in Scheme 20. Subsequent Au^+/Ag^+ alkynyl activation of **83a** facilitated 6-*endo*-dig carbocyclization, furnishing ring A of the phenanthridine scaffold, revealing benzo[*a*]phenanthridines **79** in yields between 60-72% (Scheme 20). The $AuClCPh_3$ catalyst is believed to activate the alkynyl moiety of **83a** rendering it electrophilic and therefore suffers nucleophilic attack from the aryl group appended on the isoquinoline, yielding benzo[*a*]phenanthridines **79**. This reaction is limited to substrates that do not contain halogens. In the case of halogenated alkynylisoquinolines **83a**, iodine monochloride (ICI) was used as an alternative alkynyl activating reagent leading to the desired 6-*endo*-dig cyclization, furnishing 4-iodo-benzo[*a*]phenanthridines **79**. As pointed out above, this approach remains underutilized in the synthesis of phenanthridines. Even though the reaction steps in the sequence are high yielding, the use of expensive reagents, regioselectivity issues and limited substrate scope limits the utility of this approach in synthesis.

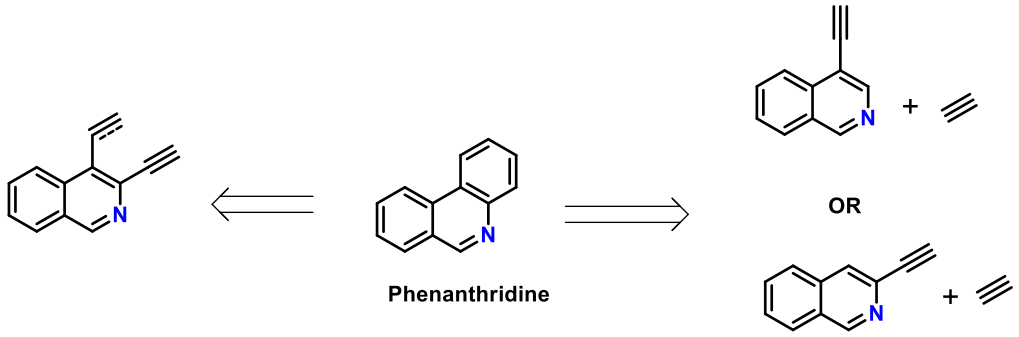

Scheme 19. Conceptual synthesis of the phenanthridine core through the construction of ring **A** *via* inter- and intra-molecular carbocyclizations.

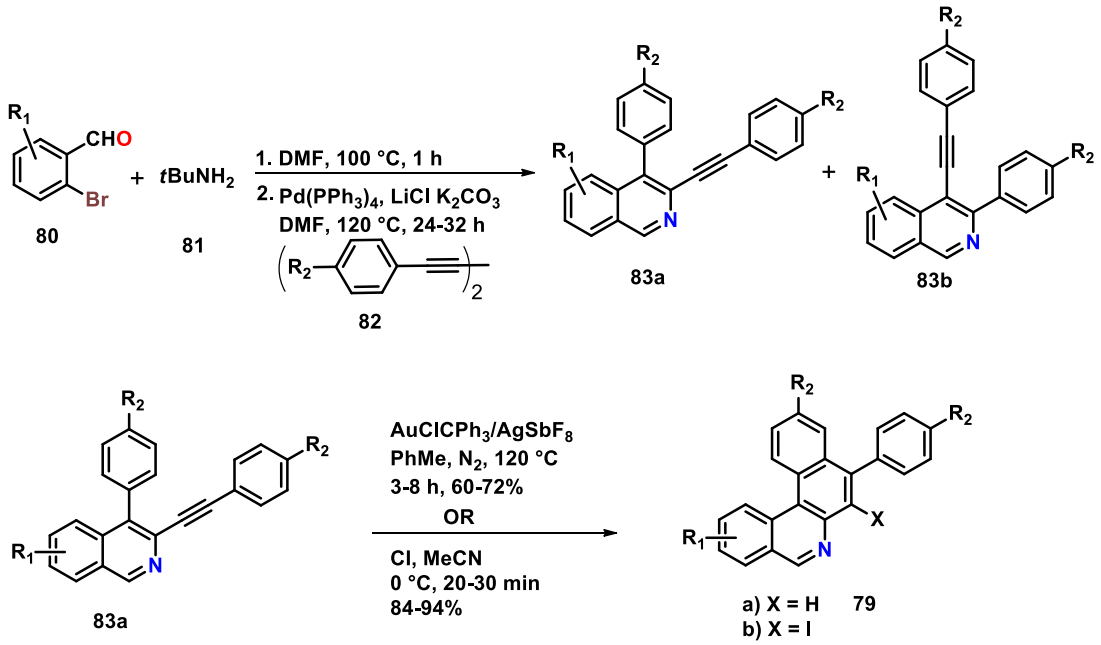

Scheme 20. The synthesis of benzo[*a*]phenanthridines through the construction of ring A of phenanthridines.

2.5.1.2 Construction of rings B and C

Various cycloaddition reactions have been utilized to either sequentially or simultaneously form rings **B** and **C** of the phenanthridine nucleus. In most cases, cycloadditions lead to dihydrophenanthridine intermediates that have all the atoms of

the phenanthridine framework in place. The final oxidation step to yield fully aromatized phenanthridines may be unnecessary since dihydrophenanthridine intermediates frequently undergo spontaneous oxidation to phenanthridines. A case in point is the Chattopadhyay phenanthridine **84** synthesis from 2-vinylanilines **85** through the aza-Claisen rearrangement, ring-closing enyne metathesis and Diels–Alder reaction sequence (Scheme 21).[92] This approach is unique in its utilization of three sequential atom-economic reactions. The requisite *E*-2-vinylanilines **85** were obtained from allylation of Boc-protected anilines **86** to Boc-protected allylaminoarenes **87**, followed by acidic Boc deprotection to allylaminoarenes **88**. The ensuing Lewis acid-catalysed aza-Claisen rearrangement and the concurrent isomerisation in the presence of superstoichiometric $BF_3 \cdot OEt_2$ of allylaminoarenes **88** furnished the desired *E*-2-vinylanilines **85** in good yields (59-80 %). Sequential *N*-tosylation and *N*-alkylation of *E*-2-vinylanilines **85** with propargyl bromide fashioned the enyne derivatives **89** that are predisposed to partake in a ring-closing enyne metathesis reaction. Indeed, exposure of enyne derivatives **89** to the Grubbs' 2nd generation catalyst resulted in the formation of vinyl-dihydroquinolines **90**, thus installing ring **B** of the phenanthridine. Intermolecular Diels-Alder reaction of vinyl-dihydroquinolines **90** with dimethyl- or diethyl-acetylenedicarboxylate furnishes ring **C** yielding the expected reduced phenanthridine **91**. Base-mediated removal of the tosyl group proceeded with concomitant aromatization giving fully aromatized phenanthridine **84**. This sequential construction of rings **B** and **C** coupled with the two protection and deprotection operations and the use of expensive reagents diminishes the advantage of using atom economic reactions.

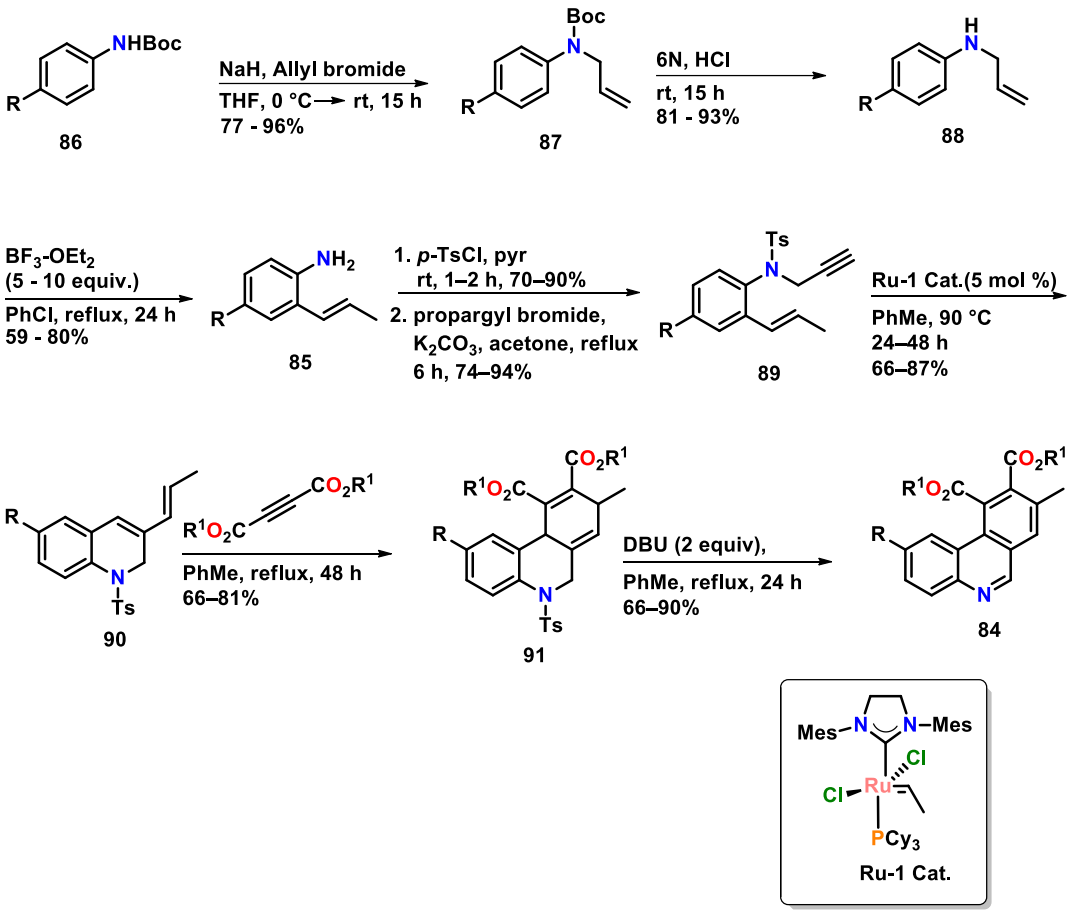

Scheme 21. Synthesis of phenanthridines through the aza-Claisen rearrangement, ring-closing enyne metathesis and a Diels–Alder reaction sequence.

Simultaneous construction of both rings **B** and **C** in a tandem fashion can reduce waste generated and enhance the overall yields. The validity of such tandem construction of rings **B** and **C** was demonstrated by Read and Gundersen who achieved the synthesis of phenanthridines **92** through the microwave-mediated intramolecular Diels-Alder reaction of allylaminofurylarenes **93** (Scheme 22).[93] The presence of a catalytic amount of aqueous HCl solution proves crucial in driving the reaction to dihydrophenanthridines **94**, the absence of which leads to the incomplete reaction giving the DA-adducts **95**. Read and Gundersen also observed that dihydrophenanthridines **94** underwent aromatization to phenanthridines during workup

or column chromatography, an observation also made earlier by Chattopadhyay and co-workers.[92-93]

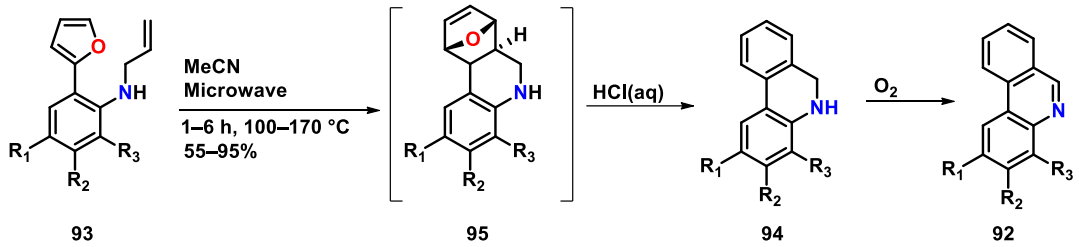

Scheme 22. Synthesis of phenanthridines through the simultaneous construction of rings **B** and **C** using Diels-Alder reaction.

Cycloaddition reactions to phenanthridines are not limited to the Diels-Alder reaction. A striking alkyne trimerization reaction reported by Li and co-workers serves as an example.[94] In their report, Li and co-workers demonstrated that the union between fluoro-alkynylimines **96** and electron-rich alkynes **97** revealed 6-substituted phenanthridines **98a** in a formal [2 + 2 + 2] cycloaddition facilitated by the Wilkinson's catalyst (Scheme 23). The reaction was shown to give the desired 6-trifluoromethyl phenanthridines **98** starting from appropriately substituted trifluoromethyl-alkynylimines **96a**. When the trifluoromethyl group was substituted with bromodifluoromethyl to make alkynylimines **96b**, polycyclic heterocyclic arenes **99** were obtained alongside the desired 6-bromodifluoromethyl phenanthridines **98b**. The polycyclic side products are believed to form through rhodium-catalysed C-H functionalization by way of oxidative addition of Rh on the preformed phenanthridine **98b** forming intermediate **I**. This then undergoes C-H functionalization forming rhodocycle **II** that suffer reductive elimination revealing polycyclic arenes **99**.[94] The experimental evidence to support this excessively ornate mechanism is eerily missing. A far more humble mechanism can be invoked to explain the formation of this side product. It is conceivable that a Friedel-Crafts-type alkylation mechanism is in operation in this reaction owing to the low-lying C–F σ* orbitals coupled with the ever

weaker C–Br bond, both a consequence of the geminal difluoro effect. As a result, the carbon of the bromodifluoromethyl group is susceptible to nucleophilic attack even from a mild nucleophile like a phenyl group.

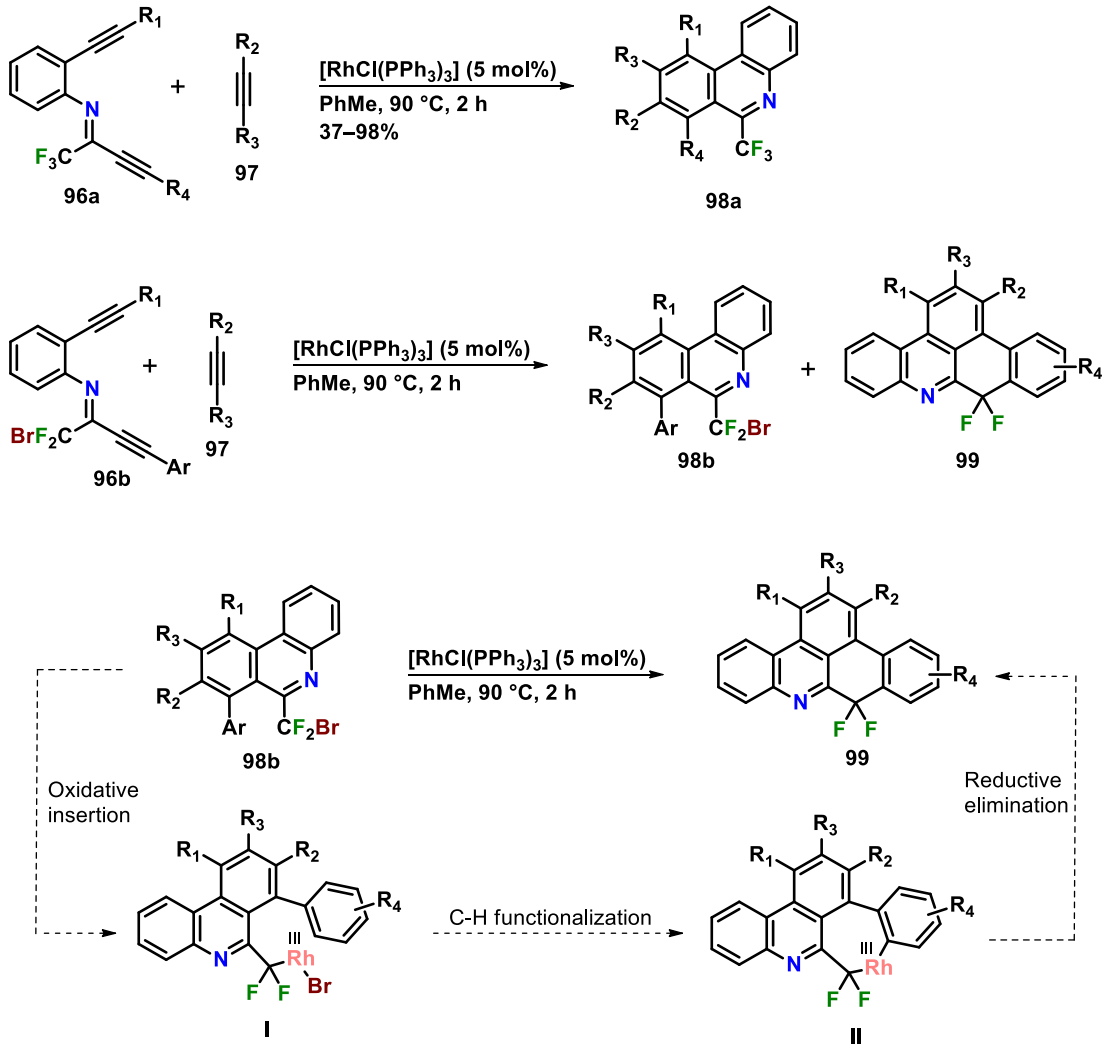

Scheme 23. Rhodium-catalysed alkyne [2 + 2 + 2] cycloaddition reaction.

As elegant as the cycloaddition approaches to phenanthridines may be, they suffer from excessive number of steps and harsh reactions conditions that are required in the construction of the requisite precursors that participate in the key cycloaddition reactions. Different R_1, R_2, R_3 and R_4 groups may also led to a number of different

products, which might prove to be inseparable. Another undesirable common feature of these reactions is the use of expensive and sometimes toxic platinum group metals.

2.5.1.3 Construction of ring B

A strategically diverse route to phenanthridines involves intramolecular cyclization of biaryl precursors that are endowed with suitable substituents, allowing for the construction of the pyridine ring **B**. The success of this strategy relies on the abundance of mild coupling reactions that can form C–C bonds, forging biaryl axes often in the presence of sensitive functional groups, thus considerably shortening synthetic routes and improving "greenness" of these syntheses.

Coupling reactions

Since the first reported laboratory C–C formation by Kolbe in his 1845 classical synthesis of acetic acid, C–C bond-formation continues to transform and shape organic synthesis as a whole. In the intervening years, equally impressive C–C bond-forming transformations made their appearance in the chemical literature. Grignard-, Aldol-, and Wittig-type reactions, together with pericyclic reactions, such as the Diels-Alder reaction are but a few examples of methods that have enabled our ability to conveniently construct C–C bonds of complex molecular frameworks.

The second part of the 20th century witnessed the emergence of a mild and selective class of carbon-carbon forming reactions that rely on transition-metal catalysis. These reactions are capable of forging C–C bonds between or within substrates endowed with sensitive functionalities, providing new opportunities for synthetic organic chemists to assemble complex molecular frameworks. In organic chemistry, the term coupling reactions is given to a variety of homogeneous metal-catalyzed reactions (metal-free and organo-catalytic variants have also been reported), where an organometallic compound of the type R–M (nucleophile) reacts with an alkyl halide or pseudo halide (R'–X, electrophile), forming R–R'. The metal (M) on the nucleophilic partner can

either be a transition-metal such as Zn (Negishi coupling) and Sn (Stille coupling) or a main group element for example Si (Hiyama–Denmark coupling), B (Suzuki coupling), and many other related couplings.

The coupling chemistry arsenal also comprises heteroatom couplings as reflected in the classical copper-catalyzed Ulmann reaction and the modern palladium-catalyzed Buchwald-Hartwig amination reaction. Coupling reactions can be classified as being either homocoupling, where the reacting partners are identical, or heterocoupling, where the reacting partners are different. The latter are also known as cross-coupling reactions and are the most useful type both in academia and the chemical industry.

Palladium catalysis dominates the cross-coupling reaction arena, and it can be argued that the Suzuki coupling reaction stands at the pinnacle of palladium-catalyzed reactions. This is due in part to the relative ease of the synthesis, low toxicity and the stability of the requisite boronic acids. These advantages compounded with the relatively low catalytic loadings and low toxicity of most palladium complexes means the Suzuki coupling reaction can be used in green synthesis. It is no surprise then that the Suzuki coupling reaction has been incorporated in various processes to access the biaryl intermediates that are required in the synthesis of phenanthridines *via* the construction of ring **B**. Some of these methods, including others that do not incorporate the Suzuki coupling reaction, will be discussed below.

There are three possible retrosynthetic bond disconnections on ring **B** from intermediates possessing a biaryl axis, namely C6–C6', C6–N5 and C4'–N5 bond scissions, provided rings **A** and **C** are kept intact. A C1'–C10' bond formation between *N*-benzylideneaniline is another possible mode of constructing ring **B** of phenanthridines. These are shown in Scheme 24 below. In the forward sense, the bond construction can be achieved both by polar or radical reaction means. Both these reaction manifolds will be discussed.

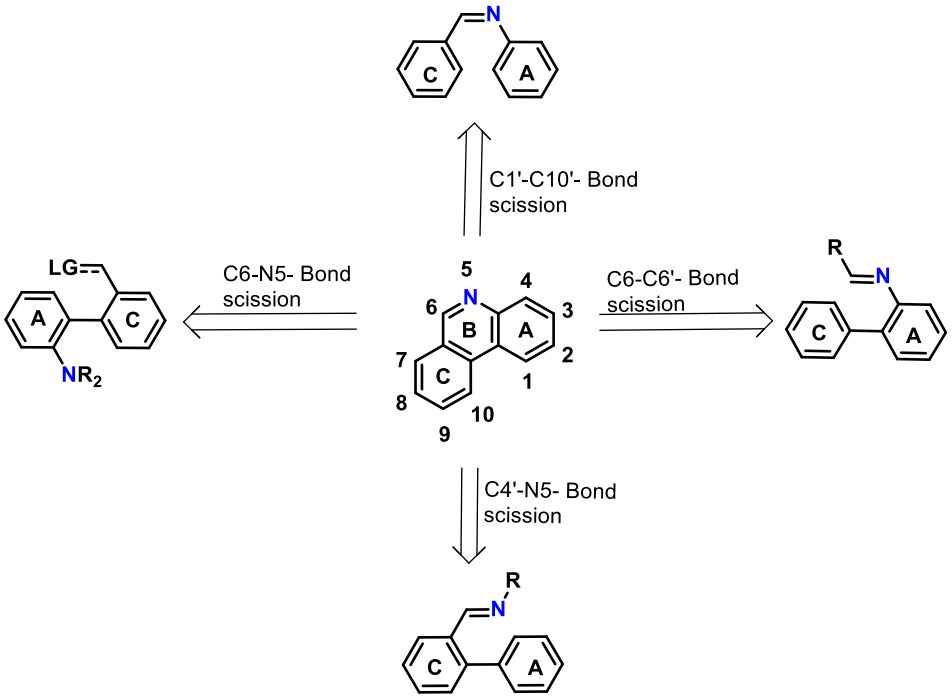

Scheme 24. Possible retrosynthetic scissions on ring **B** of phenanthridines.

*2.5.1.4 Construction of ring **B** through C1'–C10' bond*

The quintessential method for the synthesis of phenanthridines involves pyrolysis of *N*-benzylideneaniline **100** – a condensation product of benzaldehyde and aniline, forging the C1'–C10' bond. This method was disclosed by Pictet and Ankersmit (1891), claiming the first ever synthesis of phenanthridines.[95] This approach is reflected in modern syntheses, for example Batra and colleagues reported on the synthesis of phenanthridines **101** from the union of anthranilic acid derivatives **102** and 2-bromobenzaldehydes **103** *via* the intermediary of *N*-benzylideneanilines **101** that suffer Pd-Cu catalyzed C-H functionalization yielding phenanthridine-4-carboxylic acids **102** (Scheme 25).[96] Some methods involve *t*BuOK-mediated C-H arylation of conveniently substituted *N*-benzylaniline and Pd-catalysed intramolecular cyclization of biaryl imidoyl-selenides,[97] to name just a few.

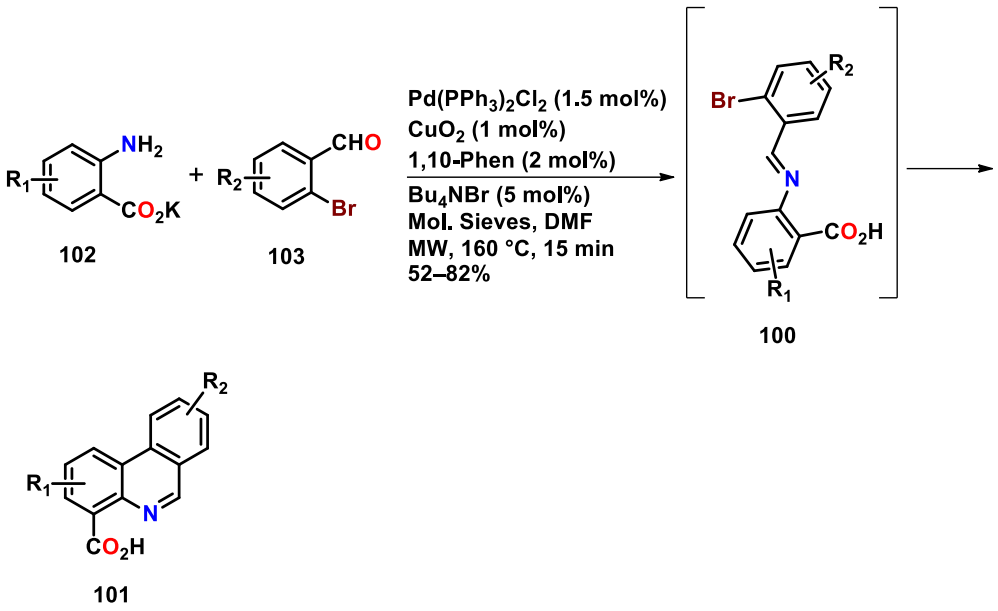

Scheme 25. Synthesis of phenanthridines through ring closure of *N*-benzylideneaniline *via* a C1'– C10' bond-formation.

C1'–C10' bond construction of the phenanthridine nucleus has also been accessed from conveniently functionalized precursors through *C*-centred radical cyclization reactions forging the middle pyridine ring **B** of phenanthridines. Using this strategy, Katritzky and co-workers synthesized 6-arylphenanthridines **104** from diaryl(benzotriazol-1-yl)methanes **105** *via* intramolecular radical cyclization of *C*-centred *N*-benzylideneaniline radical **106** (Scheme 26).[98] Radical **106** was generated from **105** through deprotonation of the methine proton using *n*BuLi, generating a benzotriazole-stabilized carbanion **107** that underwent oxidation upon treatment with copper iodide, forming methine radical **108**. Concomitant loss of nitrogen gas gave radical **106**. This reaction suffers from low yield, regioselectivity issues associated with the key cyclization step, and the preparation of the diaryl(benzotriazol-1-yl)methanes **105** precursors is problematic.

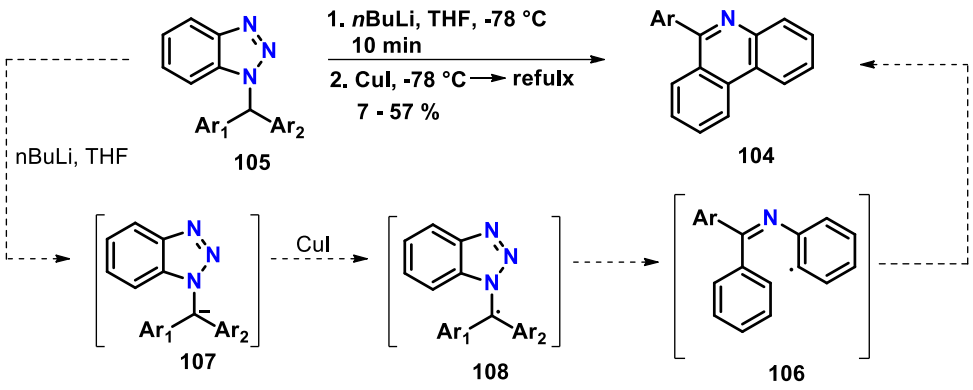

Scheme 26. *C*-centred radical mediated synthesis of 6-arylphenanthridines

The groups of Leardini and Bowman demonstrated that *N*-benzylideneaniline radical **106** can be obtained directly from *N*-benzylideneaniline **109** in the presence of peroxide radical initiators in benzene or chlorobenzene (Scheme 27).[97, 99] Under these conditions, *N*-benzylideneaniline radical **106** participates in the expected intramolecular cyclization giving 6-substituted phenathridines **104**. So far, this approach has found limited utilization in organic synthesis, possibly due to the lack of a practical synthesis of the starting materials and the use of hazardous reagents.

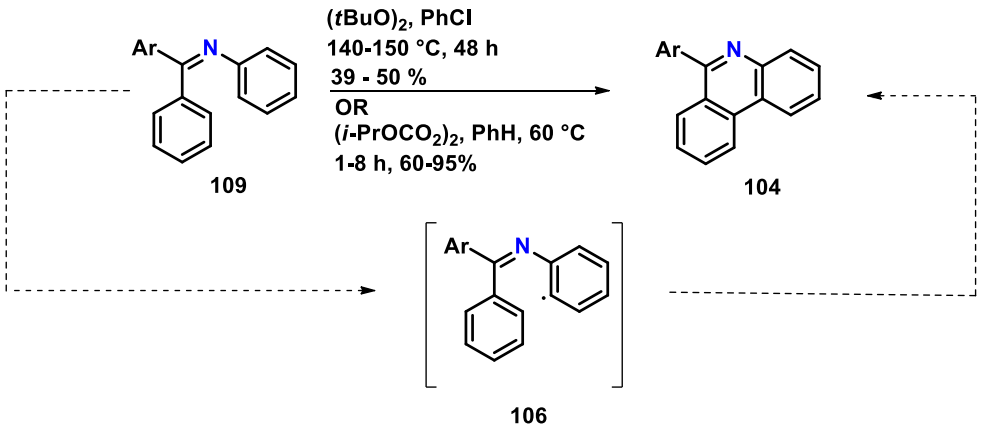

Scheme 27. Direct generation of *N*-benzylideneaniline radical and the subsequent cyclization in the synthesis of phenanthridines

In general, the methods that rely on C1'–C10' bond formation are low yielding, and they have a limited substrate scope, owing to the harsh conditions that are often

employed. Therefore, other methods for the construction of ring **B** of phenanthridines have been investigated.

*2.5.1.5 Construction of ring **B** through C6–C6' bond*

The synthesis of phenanthridines through the construction of ring **B** by way of C6–C6' bond formation presents an alternative route to C1'–C10' bond formation. At present, all the methods that forge C6–C6' bond of the central pyridine ring give 6-substituted phenanthridines. As an example, the classical synthesis of phenanthridine derivatives **110** by Pictet and Hubert involves the dehydrative cyclization of acyl-*O*-aminobiphenyls **111** on heating at 250 – 300 °C in the presence of zinc chloride in what is known as the Pictet–Hubert reaction (Scheme 28).[100] Due to the drastic conditions employed in the Pictet–Hubert reaction, the reaction is not tolerant of various functional groups often encountered in organic synthesis. The reactions also suffer from side-product formation and low yields. Morgan and Walls improved the substrate of the reaction to some extent by boiling acyl-*O*-aminobiphenyls **111** in nitrobenzene in the presence of $POCl_3$ giving phenanthridines **110** in good yields (61–80 %) (Scheme 26).[101] The Morgan–Walls modification has been used by other groups[102-103] to synthesize phenanthridines bearing functional groups that can withstand these harsh conditions.

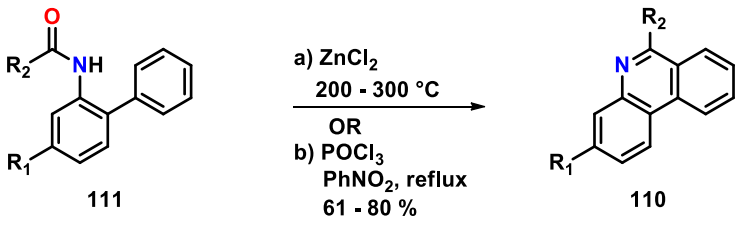

Scheme 28. The condensation of acyl-*O*-aminobiphenyls to phenanthridines a) Pictet and Hubert reaction conditions, b) Morgan and Walls reaction conditions.

The C6–C6' bond can also be formed through homolytic aromatic substitution (HAS) of 2-isocyanobiphenyls **112** with various radicals. Fundamentally, the HAS methods follow a similar mechanism where an *in situ* generated radical undergoes

intermolecular addition to the radical accepting isocyano group of 2-isocyanobiphenyls **112** giving imidoyl radicals **113.** These radicals subsequently suffer an intramolecular cyclization with the pendant arene leading to the delocalised radical intermediate **114**. A single electron transfer (SET) event by an oxidant gives cation **115**, followed by de-protonation and re-aromatization revealing 6-substituted phenanthridines **105** (Scheme 29).

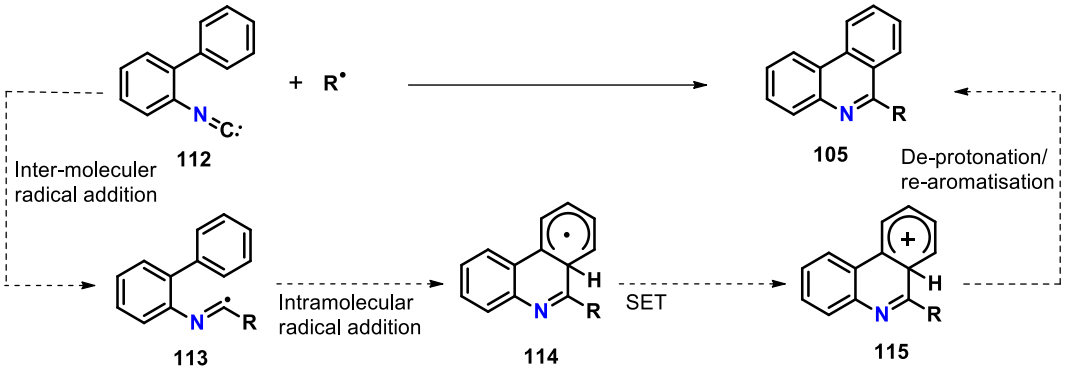

Scheme 29. General mechanism for the formation of phenanthridines through the imidoyl radical.

This approach was first demonstrated by Chatani and co-workers where 2-isocyanobiphenyls **112** were reacted with aryl or alkyl boronic acids **116** in the presence of $Mn(acac)_3$ (3.0 equiv.) in toluene at 80 °C giving 6-substituted phenanthridines **105,** with yields ranging between 49– 84% (Scheme 30).[104] The reaction proceeds through the expected *C*-centred radical formation upon the exposure of boronic acids **116** to $Mn(acac)_3$ which then adds to the isocyano group following the mechanistic steps discussed above giving phenanthridines **105**. The superstoichiometric amount of $Mn(acac)_3$ is crucial for the completion of the reaction since it acts as an oxidant in the final oxidative re-aromatization step. Yu and co-workers disclosed a similar route to 6-substituted phenanthridines **105** where the radical was generated *via* photochemical means from alkyl bromides.[105]

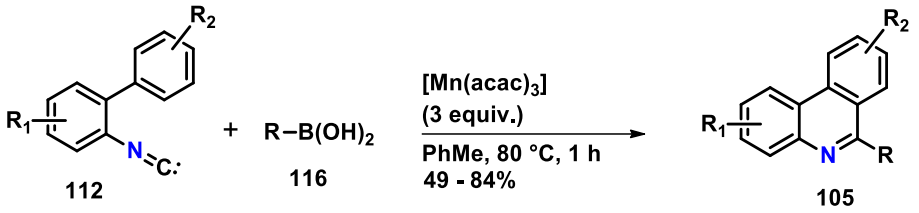

Scheme 30. An example of the synthesis of phenanthridines from 2-isocyanobiphenyls.

This approach was adopted by Zhou and co-workers where hypervalent iodine-mediated *in situ* generated electrophilic trifluoromethyl radical was shown to partake in radical addition to 2-isocyanobiphenyls **112** inducing HAS akin to that reported by Chatani (Scheme 29).[106] The mild generation of trifluoromethyl radical from $TMSCF_3$ (4 equiv) and $PhI(OAc)_2$ (2.1 equiv) in NMP and the subsequent union with 2-isocyanobiphenyls **112** to give 6-trifluoromethyl phenanthridines **98** is worth noting. A similar electrophilic trifluoromethylation/radical cyclization was independently disclosed by Studer and co-workers employing the popular Togni reagent as both the source of trifluoromethyl radical and an oxidizing reagent (Scheme 31).[107] This reaction was done in 1,2-dioxane as solvent and best yields were obtained when Bu_4NI was employed as an initiator, however $FeCl_2$ also gave decent yields. Studer also showed that alkyl and aryl acyl radicals can add to isocyanobiphenyls yielding 6-aroylated phenanthridines.[108] In retrospect, the acyl radicals can be generated from various initiators and *t*BuOOH as an oxidant; best yields were obtained when catalytic amounts of $FeCl_3$ were used. The synthesis of phenanthridines through C6–C'6 bond formation is by no means limited to *C*-centred radicals. The lab of Studer also reported on the synthesis of 6-phosphorylated phenanthridines through *P*-centred radical addition to 2-isocyanobiphenyls.[109]

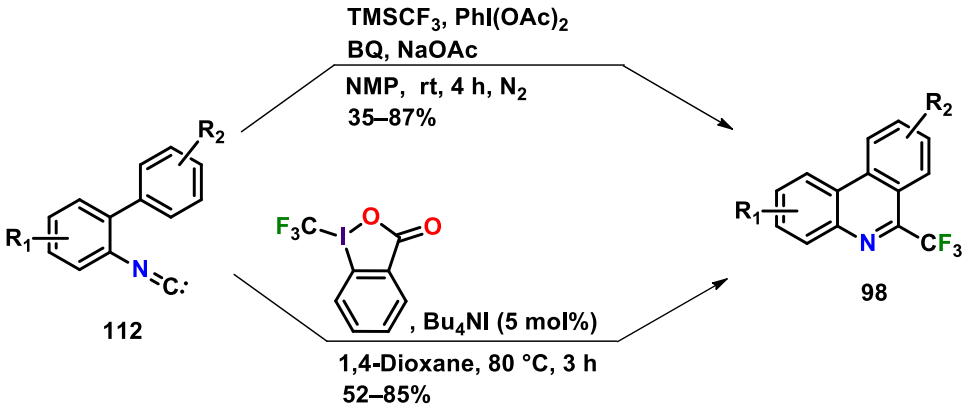

Scheme 31. Synthesis of 6-substituted phenanthridines through electrophilic trifluoromethylation/radical cyclization sequence.

Besides the obvious limitation of this approach to 6-substituted phenanthridines, these methods also suffer from regioselectivity issues.

*2.5.1.6 Construction of ring **B** through C6–N5 bond*

The phenanthridine framework has also been accessed through C6–N5 bond formation through cyclization of the biaryl compounds of the type represented by **117** (Scheme 32). This approach has gained popularity in recent years as a result of the emergence of mild metal catalysed coupling reactions that can form a biaryl axis, joining rings **A** and **C.** Metal catalysed cross-couplings of unprotected anilines can be complicated by the propensity of this group to irreversibly bind to the metal catalyst rendering them ineffective. Thus, the **Y** group on **117** type substrates often exists as a masked amine in the form of a nitro group; in such cases the C6–N5 bond is forged through reductive cyclization. A concise method to phenanthridines involves masking the amino group as a carbamate; this allows tandem construction of C1'–C10' through coupling reactions giving **117** type molecules that spontaneously cyclize to phenanthridines. This method was first disclosed by Suzuki and co-workers [110] and was further explored by researchers such as Victor Snieckus [111] and others.[112]

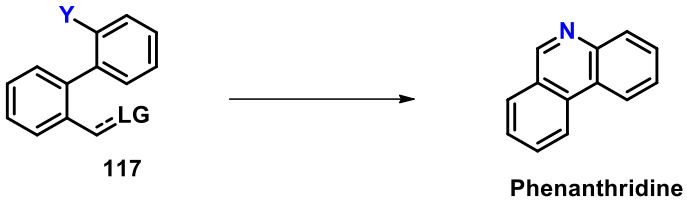

Scheme 32. General scheme for the synthesis of phenanthridines from biaryls through the formation of C6–N5 bond

This is a versatile way to access phenanthridines in good to excellent yields, including the challenging phenanthridines that are not substituted at position six. However, it is limited to substrates with good leaving **Y** groups, such as carbonyl groups, for the final condensation reaction.

*2.5.1.7 Construction of ring **B** through C4'–N5 bond*

It comes as no surprise that the formation of the C4'–N5 bond of phenanthridines takes advantage of the easily accessible *ortho*-functionalized biaryl precursors through coupling reactions. Thus, cyclization reactions of such *ortho*-functionalized biaryls presents an attractive way of synthesizing phenanthridines. These cyclization reactions can take the form of anionic or radical ring-closing manifolds. The former relies on Grignard additions on *ortho*-cyanobiphenyls **118** resulting in the iminyl metal species **119**, followed by the intramolecular nucleophilic aromatic substitution event, furnishing 6-substituted phenanthridines **105** (Scheme 33). This approach was utilized by Vedsø and Begtru in their expedient synthesis of 6-substituted phenanthridines **105** through organometallic addition/cyclization reactions of *ortho*-cyanobiphenyls **118**.[113] In the same vein, Chiba and colleagues disclosed a similar but milder aerobic one-pot two-step cyclization of *ortho*-cyanobiphenyls **118.**[114] Grignard addition is followed by the actual copper-catalyzed cyclization event that forms the C–N bond unveiling phenanthridine **105**.

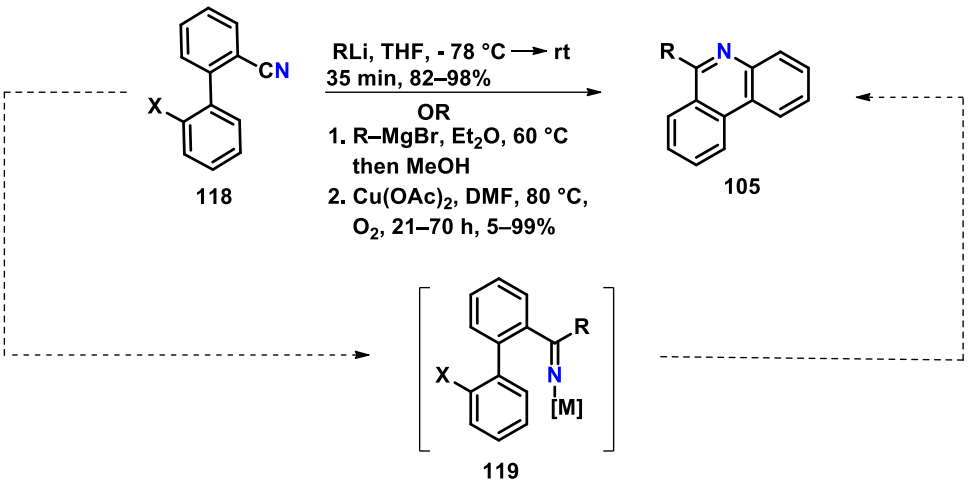

Scheme 33. Synthesis of 6-substituted phenanthridines through anionic cyclization of *ortho*-cyanobiphenyls.

Deb and Yoshikai reported what appears to be an inverse electron demand version of the above reaction. In their synthesis, Deb and Yoshikai exposed 2-biaryl-*O*-acetyl oximes **120** to catalytic amounts of $Fe(acac)_3$ in acetic acid at 80 °C giving 6-substituted phenanthridines **105** (Scheme 34).[115] This method is limited to 2-biarylketoxime esters ($R_1 \neq H$), as 2-biarylaldoxime esters ($R_1 = H$) give *ortho*-cyanobiphenyls (nitriles) exclusively through the elimination of acetic acid. The method also failed to give the desired phenanthridines when ring **C** bears methoxy groups at the *para*- and *ortho*-positions. This observation, coupled with labelling and radical quenching studies, compelled the authors to speculate that $Fe(acac)_3$ activates the acetoxy group, followed by an electrophilic attack on the nucleophilic aryl group, forging the C–N bond in an intramolecular Friedel–Crafts type fashion.

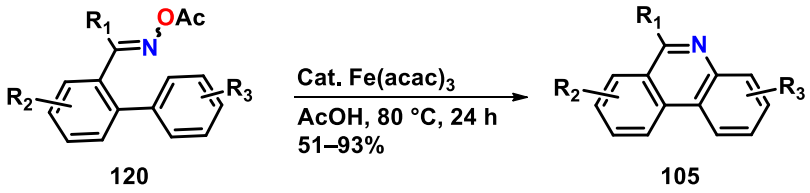

Scheme 34. Synthesis of phenanthridines from 2-biaryl-*O*-acetyl oximes.

The inability of the above protocol to give phenanthridines from *para*- or *ortho*-methoxy substituted 2-biaryl-*O*-acetyl oximes **120** is in stark contrast to the reports by the groups of Rodrıguez and Walton who achieved intramolecular cyclization of 2-biaryl-*O*-acetyl oximes **120** to phenanthridines **105** through photochemical means (Scheme 35).[85, 116] Mechanistic studies of the photochemically-induced intramolecular cyclization of 2-biaryl-*O*-acetyl oximes **120** as carried out by Walton and colleagues revealed that a radical mechanism is in operation in this process, with the iminyl radical **121** as an intermediate.[83, 85] Thus, exposure of 2-biaryl-*O*-acetyl oximes **120** results in the homolytic cleavage of the weak N–O bond, producing iminyl radical **121** and an acyloxyl type radical. The latter rapidly decarboxylates releasing a *C*-centred radical (**R**·) and CO_2; while in the C–N bond-forming event, iminyl radical **121** is intercepted by an aromatic acceptor, cyclizing in a 6-endo-trig mode forming cyclohexadienyl radical **114**. It is conceivable that cyclohexadienyl radical **114** can be converted to cyclohexadienes in the presence of suitable H-donors. This mode of reactivity of the cyclohexadienyl radicals **114** has rarely been explored. A disproportionation reaction between the cyclohexadienyl radicals **114** and *C*-centred radicals (**R**·) giving cyclohexadienyl cation **115** is the prevailing path. Cyclohexadienyl cation **115** rapidly deprotonates furnishing the fully aromatized phenanthridine **105**.

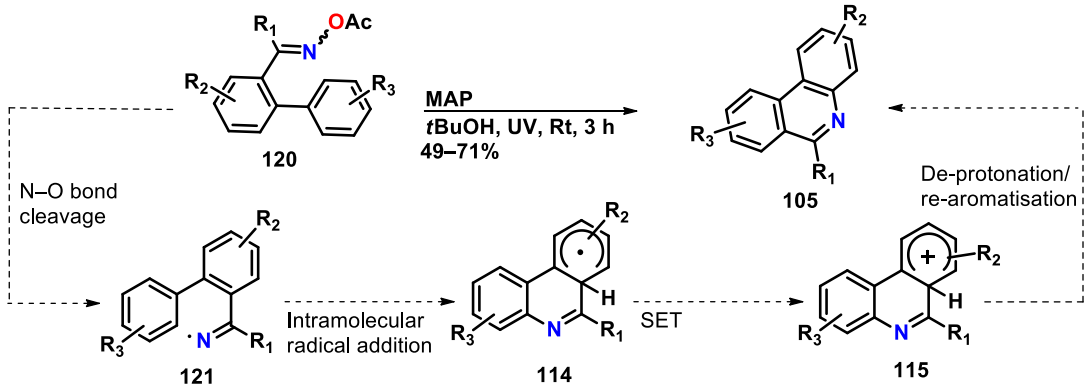

Scheme 35. Photochemical cyclization of 2-biaryl-*O*-acetyl oximes to phenanthridines and the intermediates that are formed during the course of the reactions.

Inspired by the work of Rodrıguez and Walton,[85, 116] our group sought to employ their protocol in the attempt to synthesize phenanthroviridone **122** from oxime **123** through intermediate **124** (Scheme 36).[117] To this end, oxime **123** was synthesized and exposed to the conditions of Rodriguez.[116] Surprisingly, the reaction yielded phenanthridine **125** alongside nitrile **126**. It was speculated that oxime **123** undergoes homolytic cleavage of the weak N–O bond, as expected, giving iminyl radical **127** (Scheme 37).[117] At this stage, iminyl radical **127** participates in an unexpected *ipso* attack on the *ortho*-methoxy group appended on the accepting aryl moiety giving cyclohexadienyl radical **128**, instead of the anticipated attack of the H-bonded *ortho*-position of the accepting aryl group. To the best of our knowledge, this mode of reactivity is unprecedented in the literature. Presumably, cyclohexadienyl radical **128** then partakes in SET yielding cyclohexadienyl cations **129** followed by the expulsion of the methoxy gourp, liberating phenanthridine **125**.

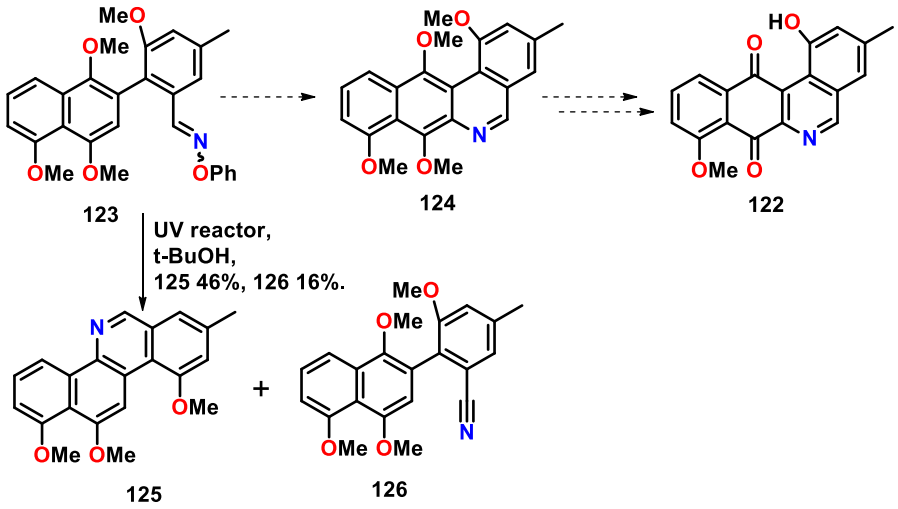

Scheme 36. Previous unexpected synthesis of the phenanthridine framework.

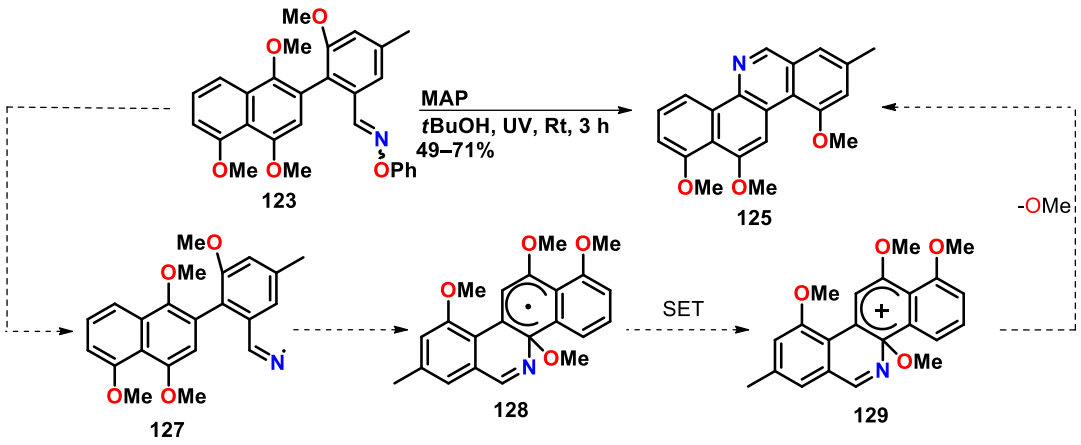

Scheme 37. Proposed mechanism for the formation of phenanthridine **125**.

Besides its environmental and green appeal, this reaction can potentially solve the regioselectivity challenge often encountered in similar reactions when applied to substrates with an unsymmetrically substituted accepting aryl group. With this in mind, there are questions that arose from this reaction. Is the reaction specific to this particular substrate? Can the reaction be applied to simpler substrates to generate simple phenanthridines? Does the position of the methoxy group on the accepting aromatic ring (ring **A** in phenanthridines) play any role? And most importantly, can it be applied in the context of total synthesis?

2.6 Aims and objective

Therefore, one objective of this PhD project was to establish the substrate scope and limitations of this reaction. Another question to consider was the utility of this reaction in the total synthesis context.

With regard to the substrate scope and limitations question, were planned to synthesize various methoxy-substituted 2-biaryl-*O*-acetyl oximes **130** according to Scheme 38. Of particular interest was to synthesize substrates that contain a methoxy group in the *ortho*-position to the biaryl axis, and vary the number and position of additional methoxy groups in other positions. It was envisaged that exposing such substrates to the photochemical conditions as reported from our laboratories by Ngwira *et al* may give phenanthridines **131**, thus establishing the scope of the reaction.

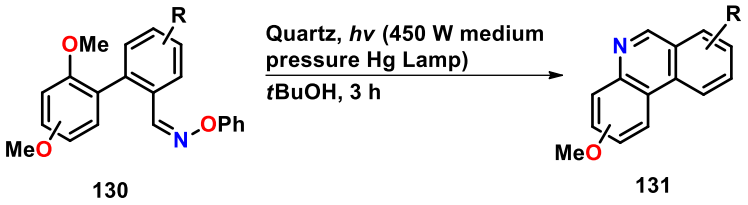

130 131

Scheme 38. Proposed substrates to understand the scope and limitation of the reaction.

To answer the question regarding the utility of this reaction in the context of total synthesis, the synthesis of trisphaeridine **77** was carried out. Trisphaeridine **77** – a naturally occurring phenanthridine is an alluring target, not only due to its structure but also for its interesting pharmacological activity since it exhibits antitumour activity.[118]

Chapter 3

3.1 Results and Discussion

With the objective of assembling methoxy-substituted biaryl oximes **130** in mind, we followed the route published by de Koning and co-workers,[117] where phenanthridines 131 could be accessed from oxime ether intermediates , which in turn could be obtained from biaryl aldehydes **132** (Scheme 39). In a forward sense, it was anticipated that treatment of biaryl aldehydes **132** with *O*-phenylhydroxylamine hydrochloride would furnish biaryl oxime ethers **130** that could then be exposed to photochemical conditions to generate phenanthridines **131**. Biaryl aldehydes **132** can be derived from methoxybenzenes **133** and (2-formylphenyl)boronic acid **134** *via* the Suzuki coupling reaction.

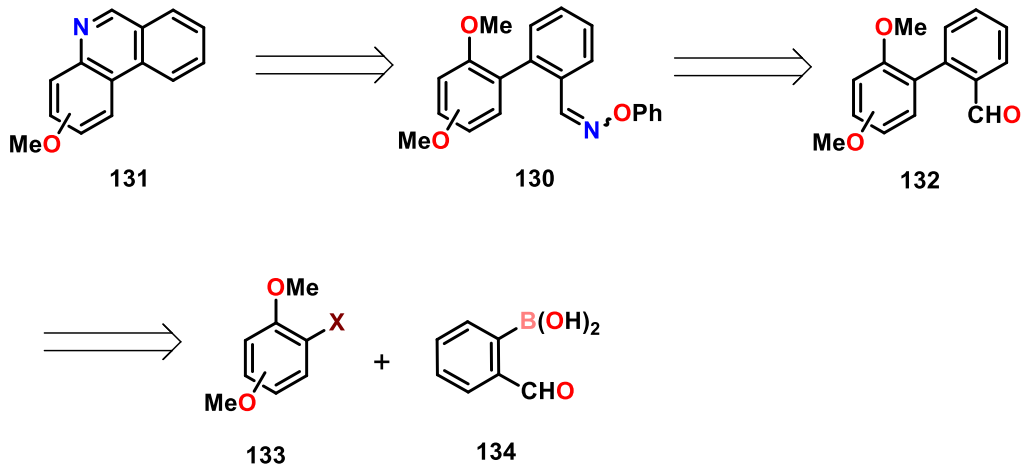

Scheme 39. Retrosynthetic analysis to phenanthridines

3.1.1 Pre-functionalization of methoxybenzenes

As alluded to in Scheme 39 above, our synthetic strategy was to stitch halogenated methoxybenzene derivatives of the type **133** with the boronic acid **134** exploiting the highly reliable Suzuki coupling reaction, securing the carbon backbone of the substrates. Functional group manipulations should in turn forge the coveted biaryl

oximes **130**, ready to be evaluated for their ability to cyclize under photochemical conditions to phenanthridines **131**.

Therefore, our synthesis began with pre-functionalization of methoxybenzenes (Scheme 40) in preparation for the ensuing Suzuki coupling reaction. Thus, 1,2,4-trimethoxybenzene **135a**, 1,3,5-trimethoxybenzene **135b** and 1,3-dimethoxybenzene **135c** were brominated following literature protocols. The brominations were uneventful, yielding brominated methoxybenzenes (**133a-c**) in excellent yields. Following a reliable literature procedure, directed *ortho* lithiation of 1,2-dimethoxybenzene **135d** with *n*BuLi and the subsequent metal-halogen exchange with electrophilic iodine gave 1-iodo-2,3-dimethoxybenzene **133d** in 83% yield, a slightly lower yield than the literature value of 90%.[119] An attempt at direct bromination of 1,4-dimethoxybenzene **135e** gave the desired 1-bromo-2,5-dimethoxybenzene **133e** together with the starting 1,4-dimethoxybenzene **135e** that proved challenging to separate. Increasing reaction times and the amount of NBS yielded the same result. The bromination was also attempted with molecular bromine both in the absence and presence of iron as catalyst and the reaction gave complex mixtures. Discouraged, we decided to synthesize 1-bromo-2,5-dimethoxybenzene **133e** from 4-methoxyphenol **136** in two steps through 2-bromo-4-methoxyphenol **137**. Indeed, treatment of 4-methoxyphenol **136** with NBS in MeCN, followed by *O*-alkylation of the resulting 2-bromo-4-methoxyphenol **137** with dimethylsulfate in acetone in the presence of K_2CO_3 gave 1-bromo-2,5-dimethoxybenzene **133e** (92% overall yield) as shown in Scheme 40. 1-Bromo-2-methoxybenzene **133f** was obtained from Sigma-Aldrich.

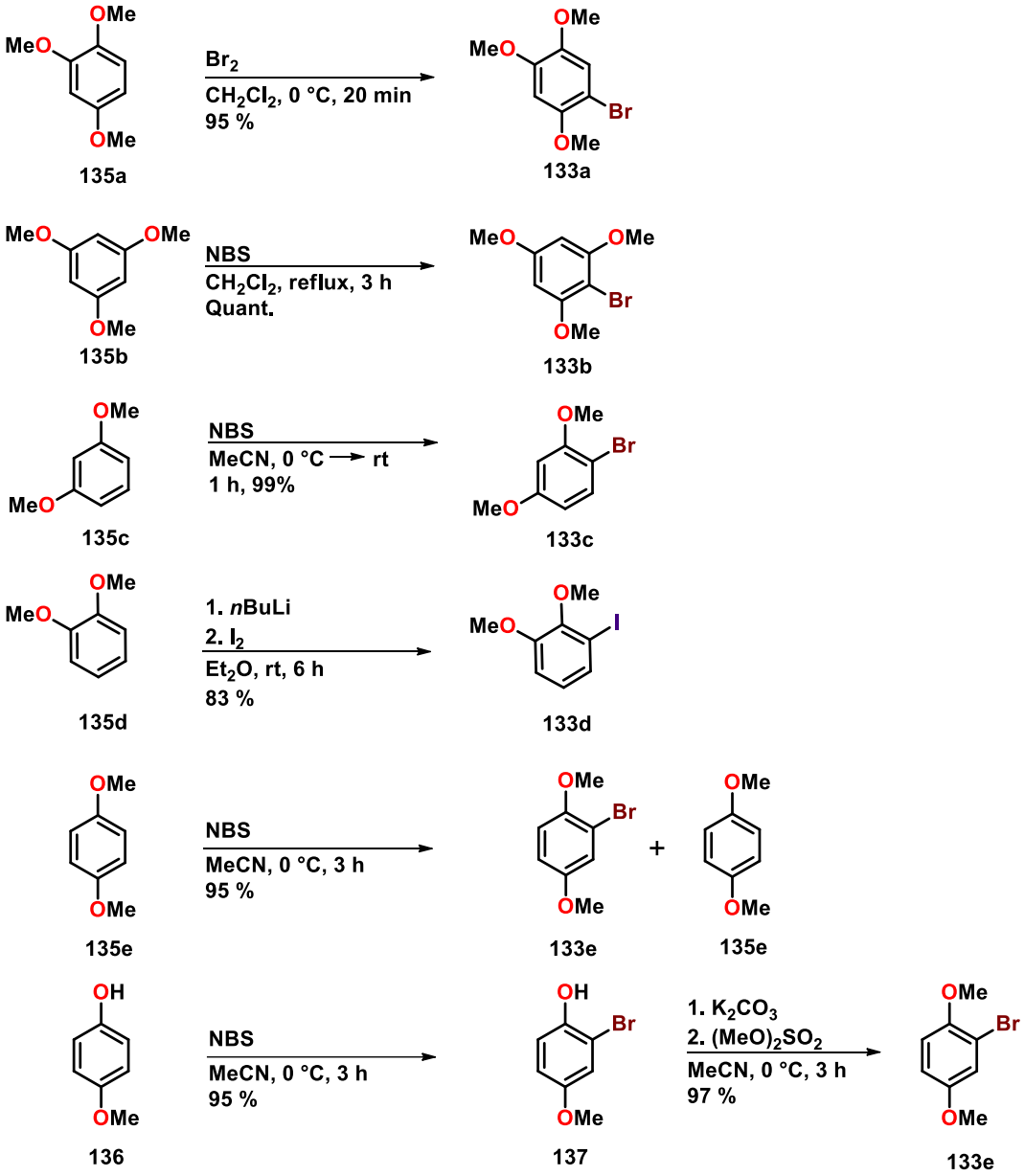

Scheme 40. Pre-functionalization of methoxybenzenes.

3.1.2 Suzuki-coupling reactions

At this point the stage was set for the union between halogenated methoxybenzenes **133a-f** and the commercially available (2-formylphenyl)boronic acid **134** to fashion biaryl aldehydes **132a-f**. This transformation was achieved *via* Suzuki-Miyaura coupling reaction, a convenient tool for furnishing the biaryl axis in the presence of

freshly prepared $Pd(PPh_3)_4$ as the catalyst and Na_2CO_3 as the base as depicted in Figure 7. This coupling operation has been used successfully in numerous synthetic endeavours in our group, thus it was performed with ease – the benefit of transferred skills that I am grateful for. Therefore, Suzuki-Miyaura coupling gave the planned biaryl aldehydes **132a-f** in mediocre to good yields (39–68%) after purification with column chromatography. The low yield for **132b** could be attributed to steric hindrance from the two methoxy groups *ortho* to the bromine involved in the cross coupling. The yield for **132b** could in principle have been improved using conditions developed by Suzuki suitable for highly congested couplings. However, this effort was not undertaken owing to the sufficient amounts obtained of this substrate. The ^{1}H NMR spectra of biaryl aldehydes **132a-f** showed the diagnostic aldehyde chemical shift (δ 9.80 – 9.69 ppm) from (2-formylphenyl)boronic acid **134** and the upfield chemical shift of the methoxy groups (δ 3.39 – 3.96 ppm) as contributed by halogenated methoxybenzenes **133a-f**. The above-mentioned chemical shifts were accompanied by the expected number of aromatic protons, six for **132a**, and eight for **132f** and so on, pronouncing the success of the operation. These results were complemented by ^{13}C NMR spectra, where the carbonyl carbon of the aldehyde functionality was observed at chemical shifts of 193.1 – 192.2 ppm and the methoxy carbon peaks at 55.2 – 56.0 ppm. The mass of the previously unknown Suzuki adducts *viz* **132a** and **132b** were measured with HRMS and both gave 273.1127 corresponding to $[M + H]^+$ since these compounds are isomers.

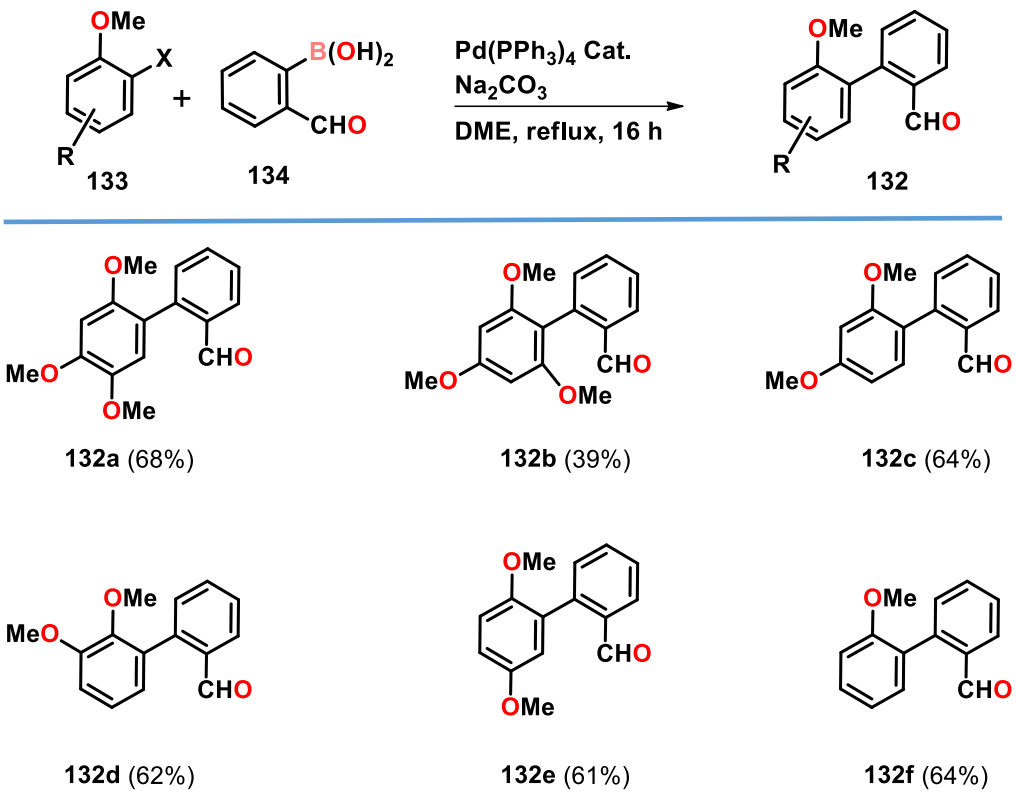

Fig 7. Examples and yields for the Suzuki reaction.

3.1.3 Attempted conversion of Suzuki adducts to oxime ethers.

A priori, oximation between stoichiometric amounts of Suzuki adducts **132a-f** and *O*-phenylhydroxylamine hydrochloride **138** could secure oxime ether intermediates **130** that are required for the pivotal photochemical intramolecular cyclization step, leading to phenanthridines **131**. Our interest in **138** as a condensation partner to **132a-f** was provoked by the realization that oximes **130** could be formed in a single synthetic operation and the foreknowledge that these oximes possess the weakest N–O bond (33–37 kcal.mol^{-1}), a property we imagined would be useful in the intended photo-induced cyclization. The observed low dissociation energy of oxime ethers has been attributed to the resonance stabilized phenoxyl radical that results from the N–O bond cleavage. Additionally, the acidic nature of the phenol side product renders purification of basic

phenanthridines relatively easy. Therefore, biaryl aldehyde **132a** was subjected to oximation by condensation with *O*-phenylhydroxylamine hydrochloride **138** in anhydrous pyridine under argon at ambient temperature for 18 h (Scheme 41). The product was purified utilizing silica gel column chromatography.

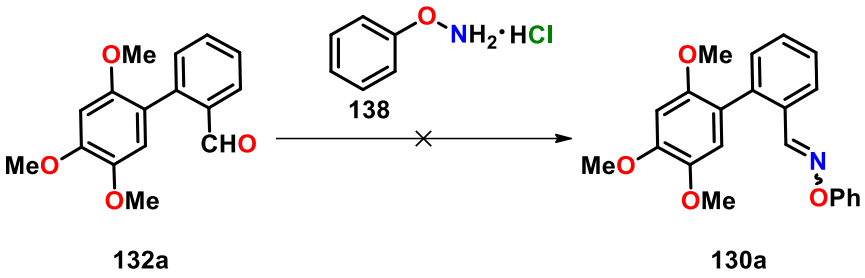

Scheme 41. Attempted synthesis of bisaryloxime ether **130a** in alkaline medium.

To our displeasure, ^{1}H NMR spectroscopic analyses of the product lacked the diagnostic deshielded aldoximine singlet peak usually appearing above 8.0 ppm and the five aromatic protons from the phenoxyl fragment. This was accompanied by the disappearance of the aldehyde peak at 9.80 ppm and ^{13}C NMR spectroscopy also confirmed this disappearance of the aldehydic carbonyl carbon at 192.8 ppm. These observations suggest that a reaction between the reagents ensued, however, at this point the identity of the resulting product was unclear. The ^{1}H NMR spectrum had six aromatic protons and three methoxy groups and the ^{13}C NMR spectrum had 15 carbon peaks. Having ruled out oxime ether **130a** as the product formed, it is also conceivable that oxime ether **130a** did indeed form, albeit transiently, then suffered subsequent N–O bond cleavage giving iminyl radical intermediate **139** (owing to the low dissociation energy of these species) that then cyclized furnishing the final phenanthridine **131a** (Scheme 42). This possibility was quickly dispelled from the observation that there were three methoxy groups in the ^{1}H NMR spectrum as opposed to the two methoxy groups that would have been expected for phenanthridine **131a**. This then opened two other possibilities. In principle the putative iminyl radical **139** can cyclize in the 'normal' mode through attack on C–1 furnishing phenanthridine **140** (Scheme 42). Upon cursory inspection of the NMR data, phenanthridine **140** satisfies the general

features of the observed ^{1}H NMR spectrum, with the exception that the H–6 (phenanthridine numbering) singlet appears upfield instead of being deshielded. Despite the doubts, the HRMS of the product was measured and found to have a mass of 270.1225, corresponding to $[M + H]^{+}$ of the then suspected phenanthridine **140**. This proved to be a diabolically deceptive compound, for examination of its FTIR spectrum revealed the diagnostic nitrile band at 2225.4 cm^{-1}. This realization and a close inspection of the NMR spectra (both ^{1}H and ^{13}C) indeed pointed to nitrile **141a**, an elimination product of oxime ether **130a**. Since nitrile **141a** is a structural isomer of phenanthridine **140**, their calculated masses are identical!

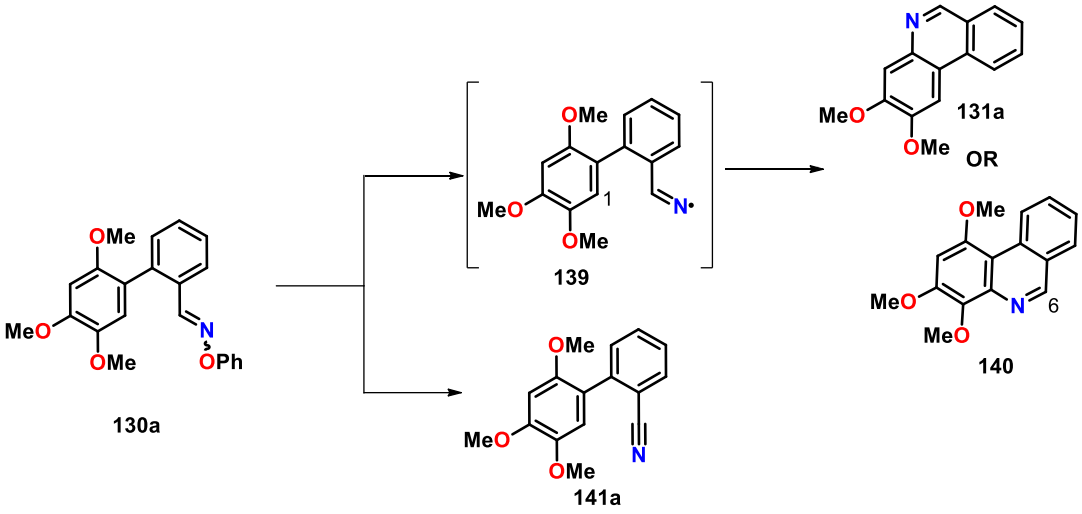

Scheme 42. Possible products that can potentially arise for oxime ether **130a**.

At this point we started to wonder whether this preference for nitrile was specific to the substrate we employed (biaryl aldehyde **132a**). Following the same procedure, oximation of aldehydes **132c**,**e**, was attempted under the same reaction conditions (Scheme 43) with the same outcome; the reaction gave benzonitriles **141c,e** in virtually quantitative yields.

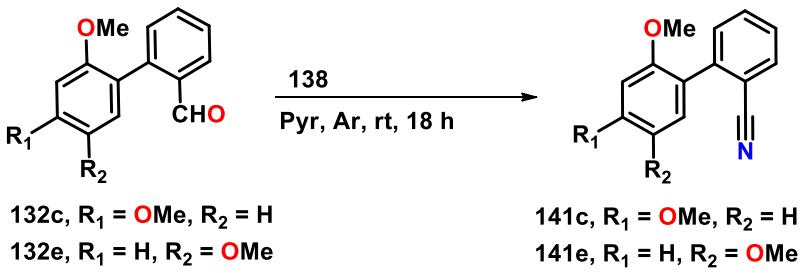

Scheme 43. The outcome of the exposure of some biaryl aldehydes to *O*-phenylhydroxylamine hydrochloride **138** in mild basic conditions.

A quick literature survey revealed a wealth of detailed studies of base-induced elimination reactions of bisaryloxime ethers. In general, this reaction favours substrates decorated with electron-withdrawing groups on the phenoxyl motif. Additionally, the substituents appended on the benzaldoxime moiety exert little influence on the outcome of the reaction, with the exception of *ortho*-nitrobenzaldoxime.[120] This reaction proceeds *via* an E2 mechanism. It is believed that in the transition state **142**, the developing base-induced cleavage of the C_β–H is accompanied by increased carbanionic character on the β-carbon (Figure 8). However, the incipient negative charge cannot be stabilized by the benzaldoxime fragment through resonance due to the C_β–H bond lying orthogonal to the π-orbitals of the benzaldoxime fragment. Thus, the electron density is stabilized by the well-developed triple bond and phenoxyl leaving group.[120]

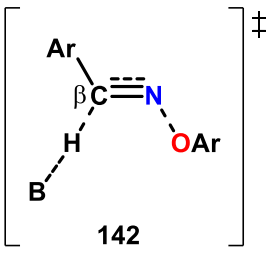

Fig 8. The proposed transition state of the bisaryloxime ether elimination.

It is not clear whether the same mechanism is in operation in our substrates. It must be pointed out that the mechanistic studies on base-induced elimination reactions of

bisaryloxime ethers has been limited to substrates endowed with electron-withdrawing functionalities on either of the aryl fragments. The higher propensity of bisaryloxime ethers with electron-rich substituents to give the elimination products i.e. nitriles and phenols has also been reported by others.[120] The stability of oxime ethers can be influenced by the pH of the media they are prepared in.[120]

Armed with this information, we decided to synthesize oxime ether **130a** under acidic conditions following the report by the group of Sharpless.[120] Thus, to a solution of *O*-phenylhydroxylamine hydrochloride **138** (54 mg, 0.37 mmol, 1.0 equiv) in 1,4-dioxane (5.0 mL) was added biaryl aldehyde **132a** (0.14 g, 0.37 mmol, 1.0 equiv.) and a single drop of 0.5 N HCl and the solution was allowed to stir for 18 h at room temperature. Work-up and purification again gave quantitative amounts of nitrile **141a** (Scheme 44).

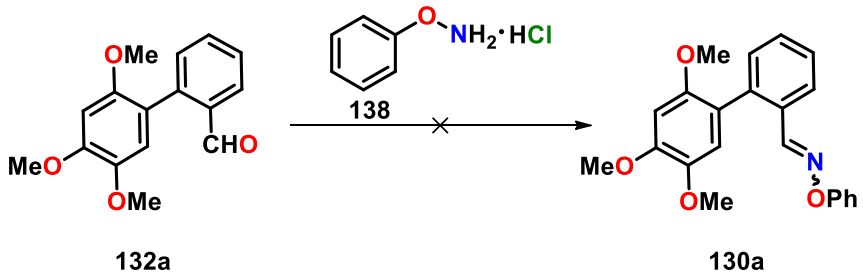

Scheme 44. Attempted synthesis of bisaryloxime ether **130a** under acidic conditions.

3.1.4 Conversion of Suzuki adducts to oxime esters.

Dejected, we turned our focus towards the synthesis of the relatively stable 2-biaryl-*O*-acetyl oximes **143**. The synthesis of oxime esters **143** is depicted in Scheme 45. The projected synthesis of 2-biaryl-*O*-acetyl oximes **143** was approached with some trepidation owing to the heightened propensity of these species to participate in electrocyclic decomposition leading to nitriles. Therefore, biaryl aldehydes **132a-f** were carefully advanced to oximes esters **143a-f** by treatment with hydroxylamine hydrochloride in the presence of sodium acetate for 2 h in methanol at room temperature. The resulting oximes were used in the next step without further purification. Therefore, the oximes were exposed to acetyl chloride in the presence of triethylamine giving mixtures of *E*/*Z* 2-biaryl-*O*-acetyl oximes **143a-f** in combined

yields between 70-79% yields from biaryl aldehydes **132a-f**. The disappearance of the characteristic aldehyde signal between 10-9.5 ppm of **132a-f** was accompanied by the appearance of an upfield imine chemical shift (relative to the expected aldehyde chemical shift) at 8.56-8.37 ppm and the acyl peak at 1.5-1.3 ppm confirmed the successful synthesis of 2-biaryl-*O*-acetyl oximes **143a-f**. The ^{1}H NMR spectroscopic results were complemented by ^{13}C NMR spectroscopy. The diagnostic carbon shifts corresponding to the carbonyl, aldoxime and methoxy groups were observed at ranges 169.3-168.8, 155.8-155.2 and 19.7-19.6 ppm, respectively. The HRMS of the substrates corresponded to $[M + Na]^{+}$, for example the mass of oxime **143e** was 322.1048 m/z. Decomposition to nitriles was common to all the substrates; this decomposition was more pronounced for the trimethoxy substrates, which only gave the nitriles (270.1120 m/z) with no observable oxime ester masses. The presence of the methoxycarbonyl group on substrates **143a-f** was confirmed by FTIR where bands that correspond to this group were observed at 1604.1-1778.8 cm^{-1} (C=O) and 1312.6-1365.0 cm^{-1} (N–O stretch). The band for the C=N bond was masked by the C=O stretch.

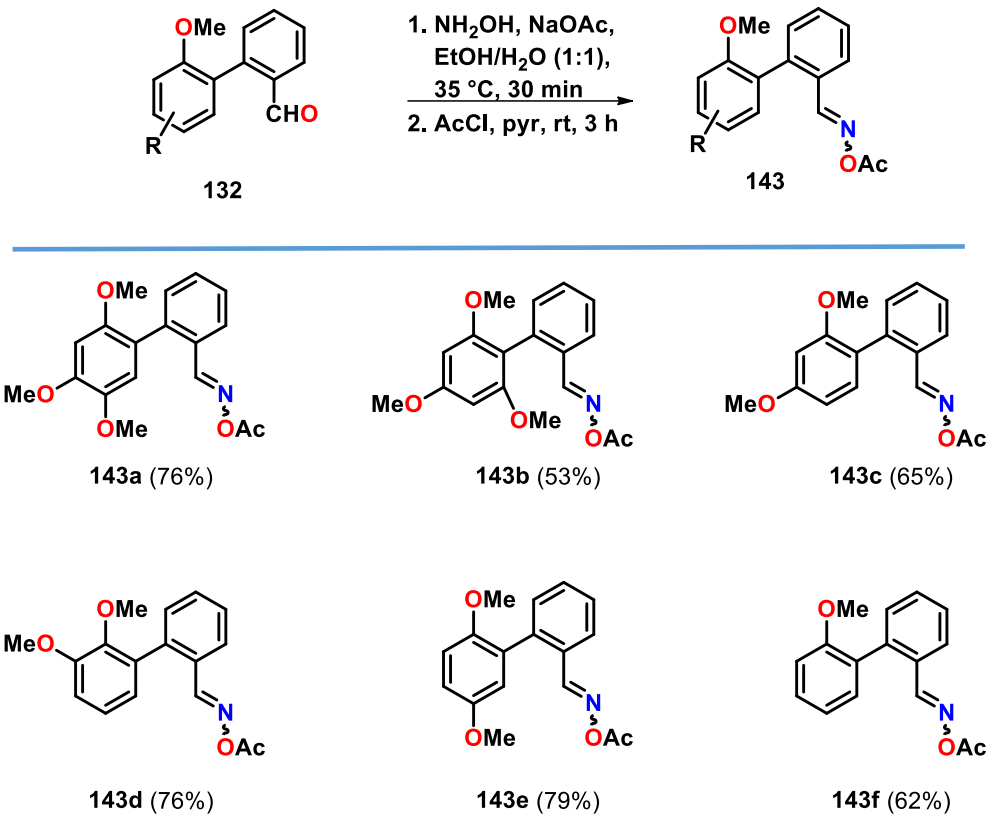

Scheme 45. Conversion of biaryl aldehydes to oxime esters.

3.5 Photochemical induced ring closure

Confident that we had the oximes at hand, the stage was set for the key photochemical-induced cyclization. Since 2-biaryl-*O*-acetyl oximes **143a-f** were employed in the reaction, special attention was paid to the solvent choice. It is well established that *O*-acetyl oximes dimerise through non-bonding interactions and these dimers are prone to participate in electrocyclic decomposition to nitriles. Therefore, *t*BuOH has been used as a polar protic solvent that can disrupt the non-bonding interactions between oxime molecules.[83, 85] Thus, 2-biaryl-*O*-acetyl oximes **143a-f** were dissolved in *t*BuOH (0.05 M) in an immersion-well photochemical reactor equipped with a quartz jacket with running water (for cooling) and the resulting solution was degassed with argon for 15 min (Table 1). Then a 450 W medium pressure Hg lamp was placed inside the quartz jacket and the reaction was allowed to run for 3 h under argon. Upon completion (from TLC evidence) the products were purified with column chromatography without

any work up. The reactions were clean, only two spots were observed by TLC. In many cases, to obtain a pure compound it was necessary to purify the products using preparative-layer chromatography.

The scope of the photochemical induced cyclization reaction with respect to the pendant methoxy groups on the accepting aryl group is summarized in Table 1. In all cases, the nitrile product resulting from the *prima facie* competing electrocyclic decomposition were observed. In general, the reaction prefers electron-rich acceptors as the highest yield of 74% was obtained from the trisubstituted substrate **143a**, forging phenanthridine **131a**, alongside appreciable amounts of nitrile **141a** (yield = 12%). Moreover, steric effects proved deleterious to the reaction, as illustrated by the low yield of phenanthridine **131b** (28%) from irradiation of sterically congested oxime **143b**, notwithstanding that the starting material is a trisubstituted benzene. The view that this transformation favours electron-rich substrates holds with remarkable fidelity when considering the observation that mono-substituted oxime **143f** yielded nitrile **141f** exclusively in 69% yield. On the other hand *ortho*- and *para*-substituted substrates **143d** and **143e** gave considerable yields of phenanthridines **131d** and **131e**, respectively. On the contrary, the *meta*-substituted oxime ester **143c** yielded nitrile **141e** exclusively in 81% yield. Phenanthridine **131c** that would have formed from substrate **143c** was not detected. The latter case points to the importance of not only the number of methoxy groups, but also on its position, suggesting resonance stabilization of the presumed cyclohexadienyl radical and/or cation intermediates (Scheme 37).

Curiously, phenanthridines **131d** and **131e** were previously obtained from a single substrate that underwent a non-regioselective cyclization, further attesting to the superiority of our method as far as regioselectivity is concerned.[121]

Table 1. Photo-induced cyclization of biaryl oxime esters

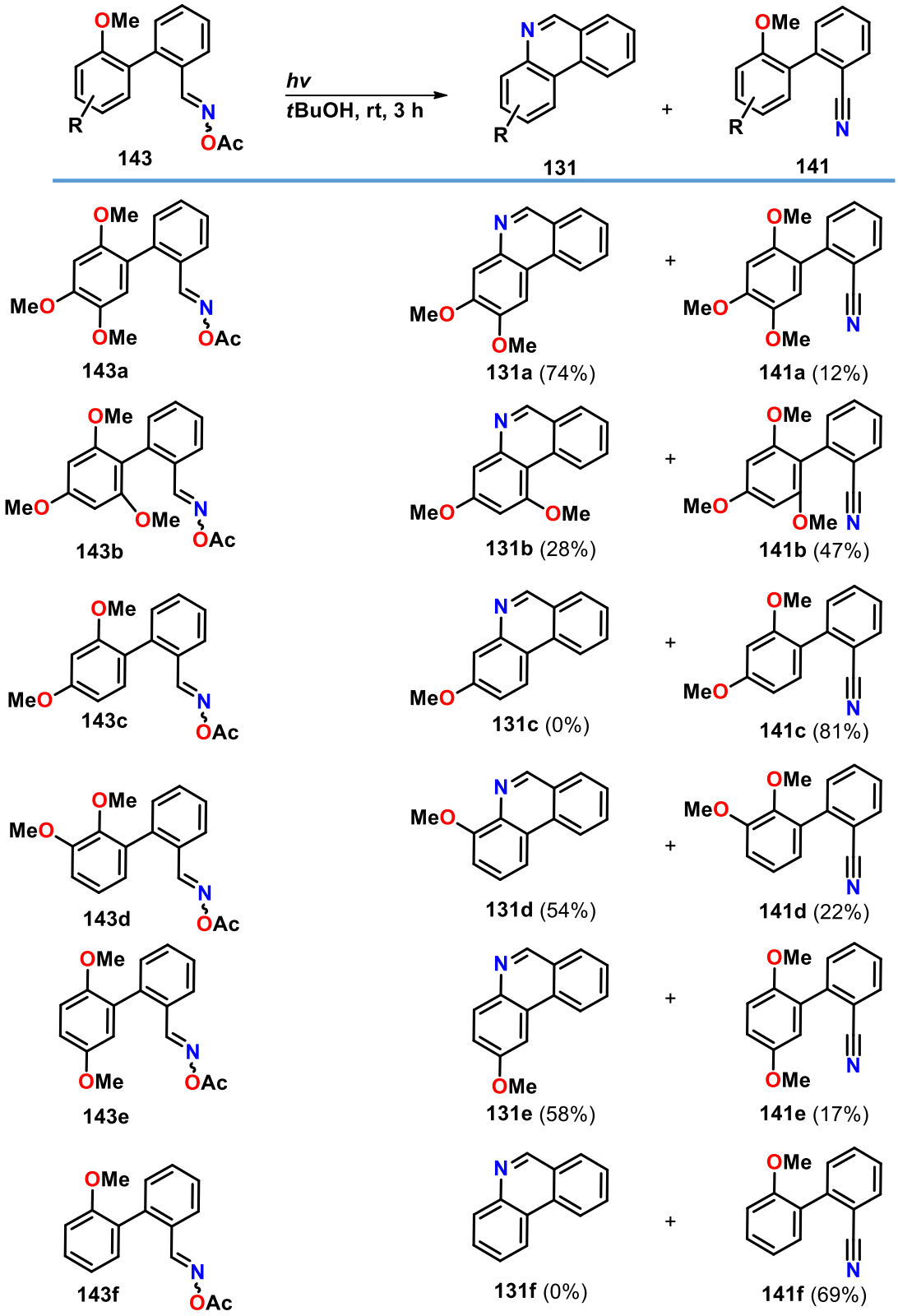

3.1.6 Synthesis of trisphaeridine

Gratified with the results obtained, we sought to leverage this photochemical cyclization in an attempt to synthesize the naturally occurring phenanthridine, trisphaeridine **77** (Scheme 46). We envisaged trisphaeridine **77** could arise from nickel-catalyzed reductive demethoxylation of phenanthridine **144** in the presence of a hydride source as reported by Martin and co-workers.[122] The setup of the projected demethoxylation is no trivial task and the manoeuvre was particularly risky when considering that the nickel catalyst could potentially insert to the C–O bond of 1,2-methylenedioxy group. However, the lessons that could be learnt from this endeavour proved too much of a temptation to ignore! It is easy to see that **144** could in turn be furnished by photochemical cyclization of oxime ester **145** which could be assembled by way of Suzuki coupling of **133e** and phenylboronic acid **146**, forming aldehyde **147** followed by the formation of the oxime.

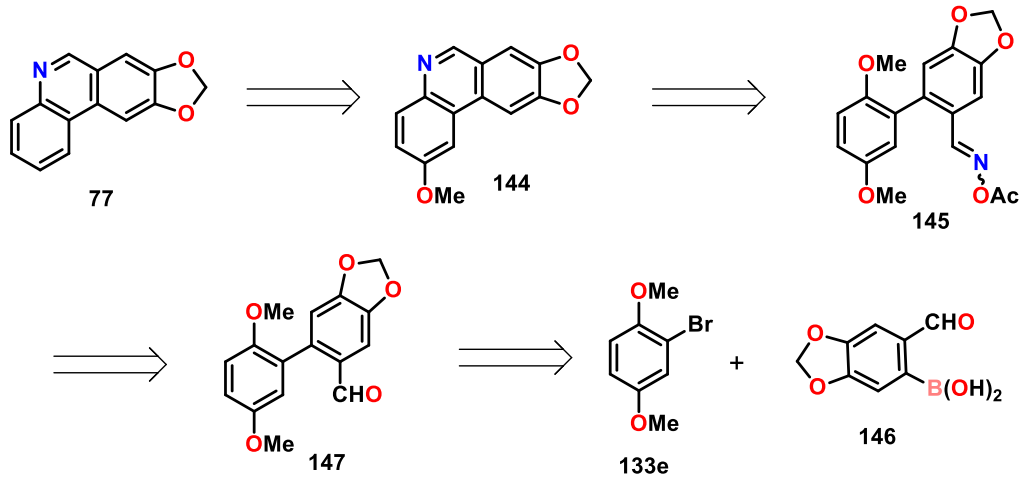

Scheme 46. Projected synthesis of trisphaeridine **77**.

The Suzuki coupling operation between bromobenzene **133e** and phenylboronic acid **146** proceeded smoothly affording the expected biaryl aldehyde **147** as a white solid in 68% yield (Scheme 47). As is characteristic in organic synthesis, our joy was short-lived as the ensuing oximation gave nitrile **148** and no oxime ester **145** was detected (from ^{1}H NMR spectroscopy). This result came as a surprise as oxime **145** closely

resembles **143e** (Scheme 45), with the 1,2-methylenedioxy structural motif appended on the phenylboronic acid half as the only exception.

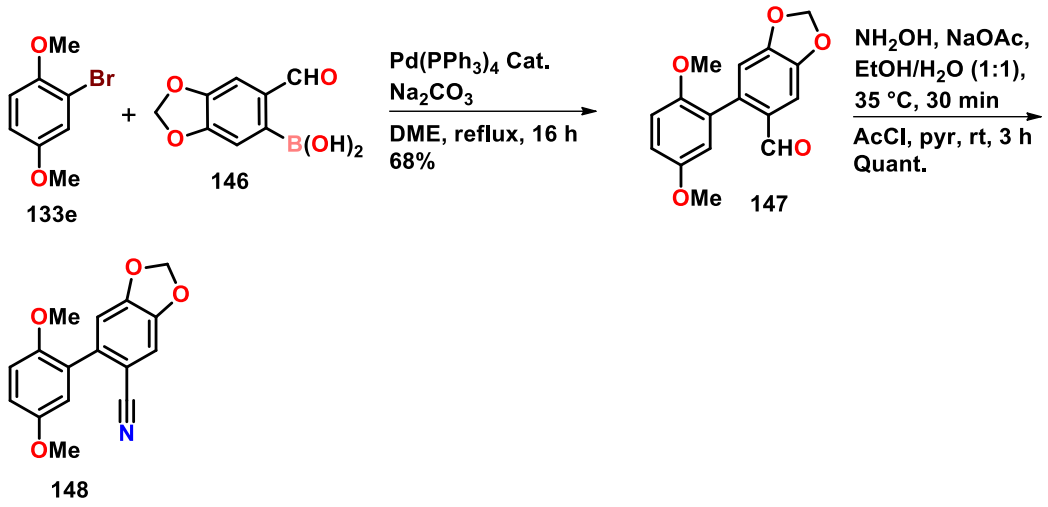

Scheme 47. Attempted synthesis of oxime ester **145**.

This observation presented an occasion to investigate the influence that the substituents on the formyl-phenyl fragment have on the oxime-forming reaction. As such, aldehyde substrates **149a** and **149b** were prepared from the union of commercially available 2-formyl-phenylboronic acids **150a** and **150b** and bromobenzene **133a** (Scheme 48). Compound **150a** was chosen because it carries an electron donating group, a methoxy in position 5, while **150b** has an electron withdrawing group, a chlorine in the same position. We were drawn to **133a** since the best phenanthridine yield was obtained for oxime ester **130a** (Table 1) – a substrate harbouring the trimethoxybenzene fragment from **133a**. The synthesis followed the general route adopted for the synthesis of oxime esters **130a-f**. Therefore, bromobenzene **133a** was coupled with boronic acids **150a** or **150b** yielding biaryl aldehydes **149a** and **149b**, respectively, as disclosed in Scheme 48. The following oxime formation from aldehyde **149b** gave nitrile **151b** despite isolating and purifying the intermediary oxime **152b**. On the contrary, the oxime ester **151a** generated from aldehyde **149a** proved stable when dried and kept at ambient temperature for months, however, it showed significant isomerization and slight

decomposition in chloroform in just a few hours (see NMR spectroscopic data in Figure 9).

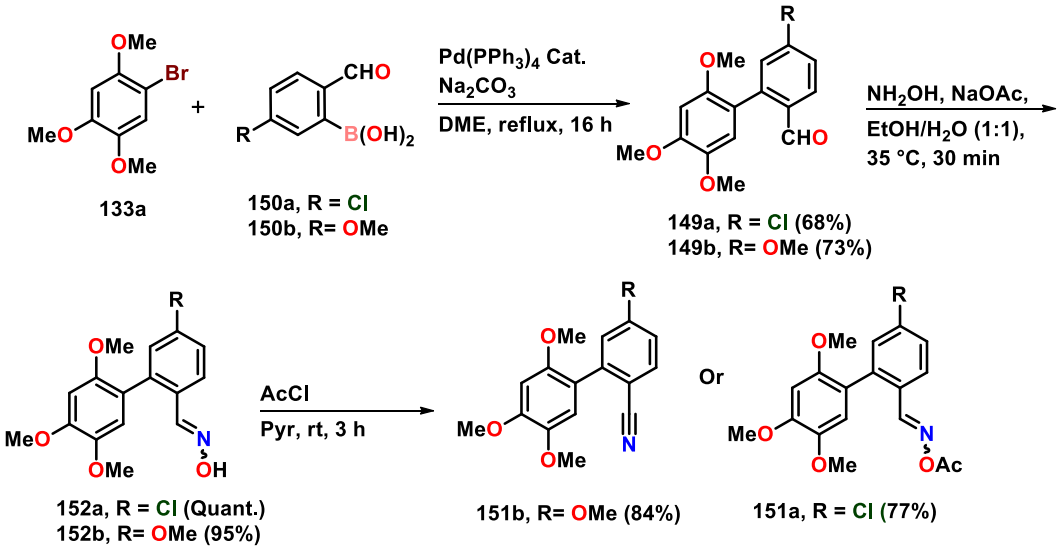

Scheme 48. Studies directed towards assessing effects of substituents on the formyl-phenyl fragment on oxime formation.

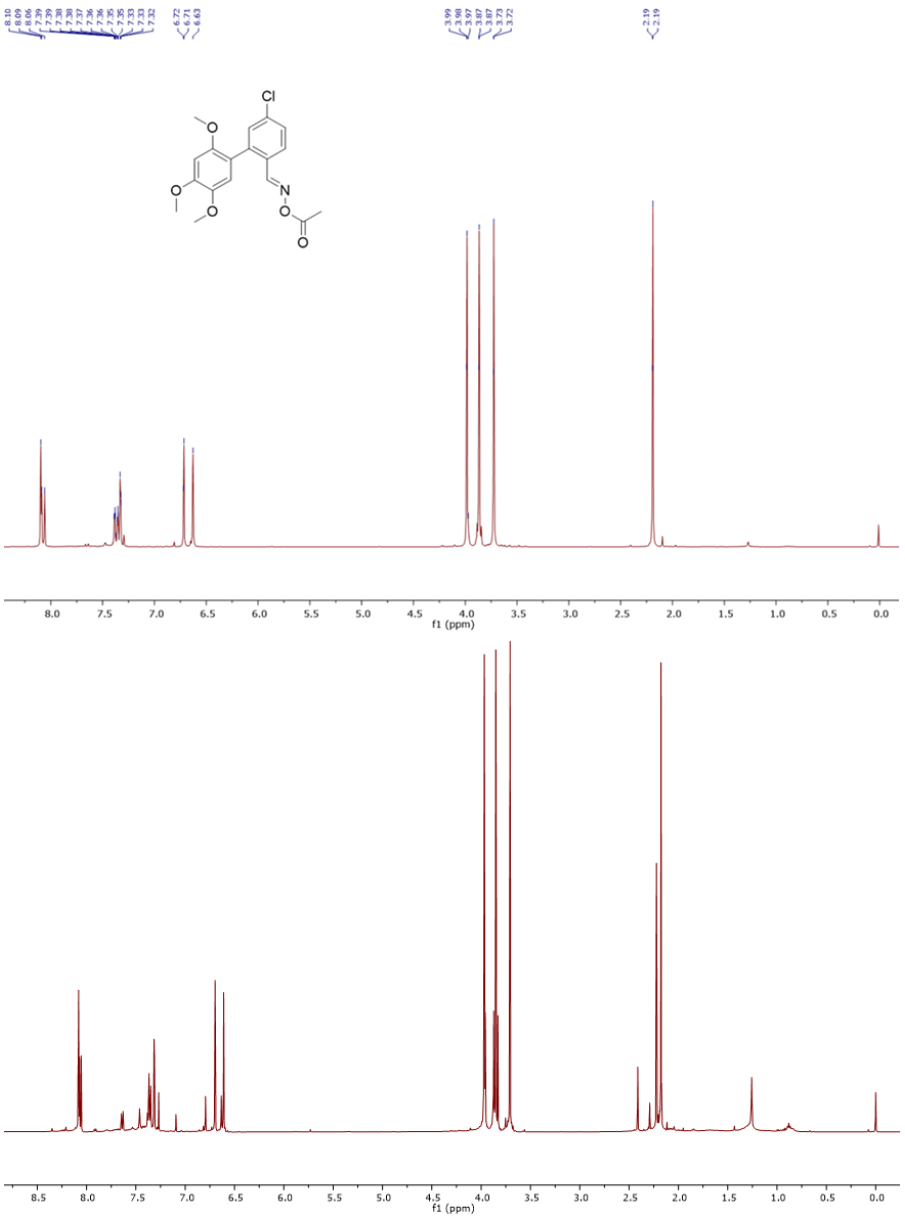

Fig 9. A) ^{1}H NMR spectrum of the freshly prepared sample of oxime ester **151a**, B) ^{1}H NMR spectrum of the same sample showing decomposition when run after about 12 hours.

The observation that the chlorine substituted substrate **151a** was stable appear to contradict the reports that nitro group (also an electron-withdrawing functionality) facilitates the decomposition of oxime esters to nitriles. Further investigation is needed.

Undeterred by the mixed results, it was decided to plough through with the synthesis of trisphaeridine **77** following a similar route to the one proposed in Scheme 46, with

the exception that **133e** was replaced by **133a**. As a consequence, Suzuki coupling between **133a** and phenylboronic acid **146** using the conditions described in Scheme 49 was carried out. Standard work-up and purification with column chromatography gave a cream-coloured solid. ^{1}H NMR spectroscopy of the pure sample showed the aldehyde chemical shift at 9.61 ppm, four aromatic singlets at 7.44, 6.80, 6.79 and 6.61 ppm together with a peak at 6.08 ppm (2H), corresponding to 1,2-methylenedioxy, giving away the identity of the product as aldehyde **153** (yield = 58%). Aldehyde **153** proved to be our *deus ex machina* in many ways. The highly coveted oxime ester was obtained from the treatment of **153** with NH_2OH using ethanol-water solvent mixture in the presence of NaOAc. The resulting oxime **154** was isolated and its identity was confirmed by ^{1}H NMR spectroscopy. The oxime was further elaborated to afford the oxime ester **155** in 74% yield alongside trace amounts of nitrile **156**.

Oxime ester **155** was dissolved in *tert*-butyl alcohol, degassed by bubbling with argon for 30 min and subsequently subjected to photochemical illumination with a 450 W medium pressure Hg lamp for 3 h. Direct column chromatographic purification of the reaction contents without any work-up gave the sought-after phenanthridine **157** in 41% yield, just lower than the 53% yield of the accompanying nitrile **156**. The NMR spectra (^{1}H and ^{13}C) of phenanthridine **157** were identical with the literature report. The choice of **133a** as a coupling partner to phenylboronic acid **146** proved to be useful in the ensuing oxidation and subsequent reduction steps. To complete the synthesis, it was necessary to remove the two methoxy groups. Taking advantage of the *ortho* relationship between the groups in question, we saw fit to convert phenanthridine **157** to *ortho*-benzoquinone **158**, which could be reduced to the targeted trisphaeridine **77** using well-established methods. This improvement avoids the risky, yet tempting nickel-catalyzed demethoxylation. Therefore, phenanthridine **157** was advanced to benzoquinone **158** by means of ceric ammonium nitrate oxidation in acetone and was obtained as a black solid after standard work-up and the removal of volatile materials. Due to concerns with stability and the scale (63 mg) at which the reaction was performed, benzoquinone **158** was taken to the next reduction step fashioning the target

trisphaeridine **77**. Thus, **158** was exposed to zinc and acetic acid, using NaCl as an additive, and trisphaeridine **77** was obtained as a cream solid in 59% over the two steps. The NMR spectroscopic data matched the reported spectra of trisphaeridine **77**. This route accomplished the synthesis of trisphaeridine **77** in five steps with an overall yield of 6.1%. In general, overall yields of trisphaeridine **77** tend to be higher than the one we obtained, owing to the possibility of assembling this compound in cascade C–C and C–N bond forming operations, often employing the venerable Suzuki coupling reaction of appropriate coupling partners. However, our route provides an alternative that utilizes oxime esters.

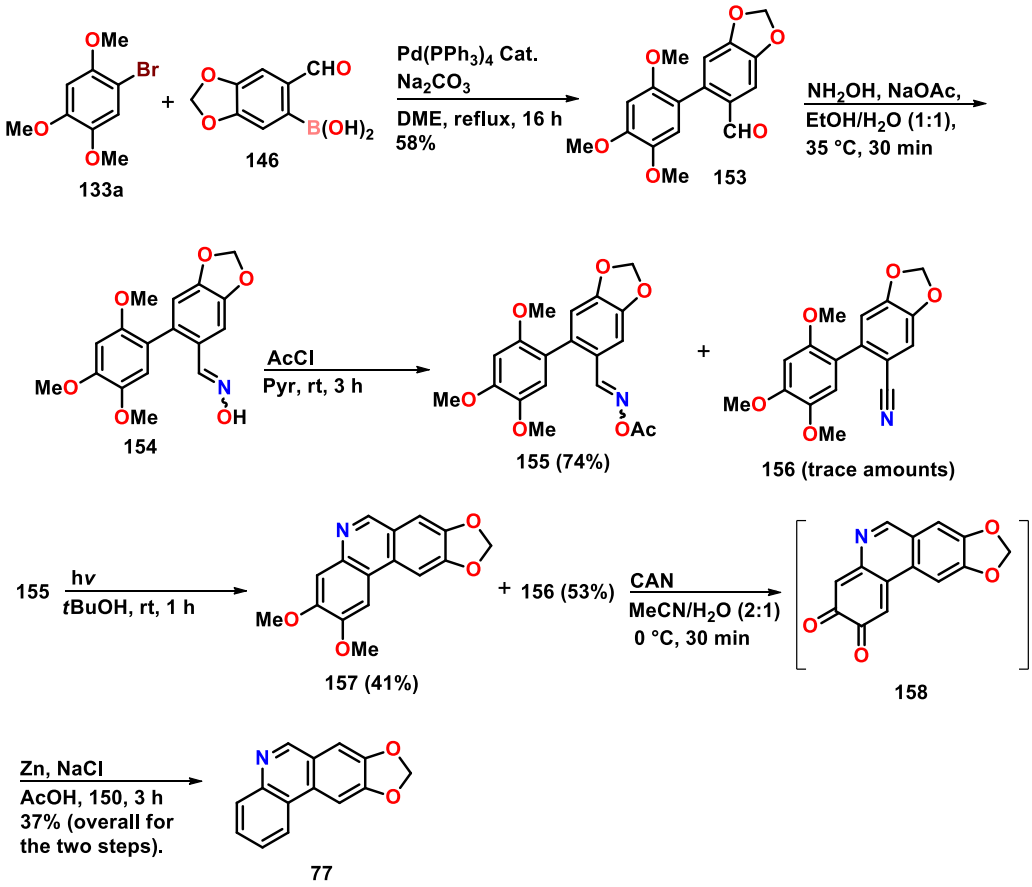

Scheme 49. Total synthesis of trisphaeridine.

3.1.7 Conclusions

At the start of this program, we set out to answer three questions with regard to the photochemical cyclization of *o*-methoxy biaryl oximes to afford phenanthridines as initially disclosed by our group. Firstly, this project was concerned with the generality of the method; we were able to establish that indeed the reaction is not specific to oxime ether **123** (Scheme 37), but can be applied to simpler oxime esters **130a-f**. Also key to the success of these model studies was the use of the Suzuki coupling reaction which proved indispensable in securing the carbon framework of the requisite intermediary biaryl aldehydes. Another memorable highlight is the heightened propensity of the corresponding oxime ethers to eliminate to biaryl nitriles. This behaviour was also witnessed on certain biaryl oxime esters where there are substituents on the 2-formylphenyl fragment.

This work also revealed that the photo-induced cyclization of *ortho*-methoxy biaryl oxime esters to afford phenanthridines prefers electron-rich accepting aryl groups. The substitution pattern was also crucial, preferring *ortho*- and *para*-substituted substrates. The reaction is also sensitive to steric hindrance and provides a possible solution to regioselectivity issues associated with cycloadditions of unsymmetrical accepting aryl moieties.

Finally, this method proved useful in the arena of total synthesis, as exemplified by the synthesis of naturally occurring phenanthridine, trisphaeridine **77**. This was accomplished in five steps in an overall yield of 6.1%.

Part II

The Synthesis of UV Absorbing Oxygen Containing-Heterocyclic Compounds from Cashew Nut Shell Liquid

Chapter 4

4.1 Introduction

The foregoing chapters detailed light-driven chemical reactions as described by our work on the synthesis of phenanthridines from photolysis of 2-biaryl-*O*-acetyl oxime chromophores **143a-f**. Photo-excitation of chromophores does not always lead to chemical change, an excited molecule can transfer its excess energy to an 'acceptor' molecule, returning to the ground state unchanged. Photo-excitation of certain chromophores (sensitizers) in the presence of ground-state triplet molecular oxygen [$^3O_2$ ($^3\Sigma_g$)] can lead to quenching, resulting in two possible singlet excited-states, namely delta [$^1O_2$ ($^1\Delta g$)] and sigma [$^1O_2$ ($^1\Sigma_g$)] (Figure 10).[123] The latter requires higher energy and is often irrelevant in most transformations. On the other hand, the former has been implicated in some areas of enquiry such as photodynamic therapy, photocatalysis, and phototoxic insecticides. This section is concerned with our research on phototoxic insecticides.

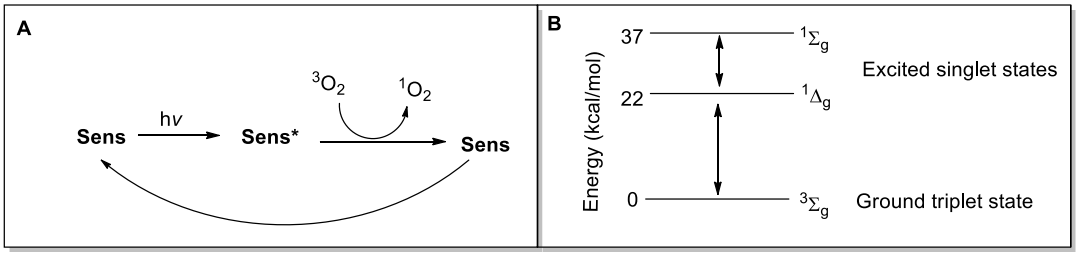

Fig 10. A) Excitation of oxygen ground triplet state to excited singlet state, B) Possible transitions between triplet ground state oxygen and the two possible singlet excited states.[123]

"If you think you are too small to make a difference, try sleeping with a mosquito"- goes a saying often attributed to the Dalai Lama. Although this quote is meant as positive encouragement, it also points to the rocky relationship we share with insects. The animosity we hold against insects is not unfounded as they are responsible for

some of the gravest atrocities that befell humanity since time immemorial. From life-threatening diseases such as malaria (that they gladly share), to the blood meal and the unharmonious songs they sing in our sleep! Insects still continue to be unwelcome guests in our spaces. These abuses are not only confined to kingdom Animalia, but also extend to plants, thus imposing a threat to food security.[124]

Over the years there have been efforts to fight against the scourge of insects mainly through the use of chemical agents colloquially known as insecticides. Environmental ills caused by most of the insecticides available on the market have been well documented.[125] Therefore, considerable efforts have been made to design and synthesize insecticides that can incite novel activity against insects.[125] One strategy that is being investigated is the use of photo-activated insecticides.[125] This is hardly an innovation as photo-activated secondary metabolites form part of an arsenal of plant weaponry produced as defense against the bane of insects. For example, *Umbelliferae* and *Rutaceae* plant families produce furanocoumarins that can absorb a photon from sunlight leading to the highly reactive excited state that can directly react with biomolecules such as DNA, membrane lipids or proteins of the invading insects with concomitant toxic effects.[126-127] Photo-activated insecticides are not limited to this mode of activity, sunlight-induced photo excitation of polyacetylenes from *Asteraceae* and quinones found on *Guttiferae* can be quenched by $^{3}O_2$ from the atmosphere forming the highly reactive $^{1}O_2$, which then can react with other biomolecules.[127-128]

Surprisingly, scant progress has been made in the development of photo-activated insecticides. Current investigations are focused on known photosensitizers such as methylene blue, α-terthienyl, acridine red, phenothiazine, furanocoumarins and xanthenes.[127] Due to our ongoing studies on the synthesis of light absorbing CNSL-based benzo-heterocyclic compounds (*vide infra*) we were naturally drawn to the challenge of the synthesis of photo-activated insecticides.[20]

At the moment, fossil-based raw materials serve as the source of starting materials in most chemical synthesis endeavours.[11] Individual compounds from fossil resources correspond to the minimum free energy, a consequence of geo- and bio-chemical

processes acting on remains of what was once thriving flora and fauna in bygone eras. It is not surprising then that these low free energy compounds also lack functional group diversity and are often aromatic in nature.

In general, synthetic organic chemistry targets possess higher free energy content than the precursors they are derived from, implying the need for additional work to drive the uphill reactions. Historically, this challenge has been mitigated through periodical and controlled introduction of free energy employing various external energy sources such as electrical, heat or light energy. Chemical energy as stored in the chemical bonds of highly reactive reagents is also used in organic synthesis. For example the hypothetical synthetic processes depicted in Figure 11, shows the conversion of **SM1** to **Pro**.[12] It is worthwhile to note that free energy is introduced gradually through the use of reactive reagents and other external energy sources. The increase in free energy of the intermediates between **SM1** and **Pro** poses a danger of the intermediates taking a *cul-de-sac*, sliding down to a potential well through the formation of undesired low potential energy side products, relinquishing some of the energy to the surrounding environment. Thus, extra caution needs to be practiced in ensuring that the accumulated potential energy in the intermediates is directed towards the desired transformations, a challenging feat that synthetic organic chemists have to contend with.

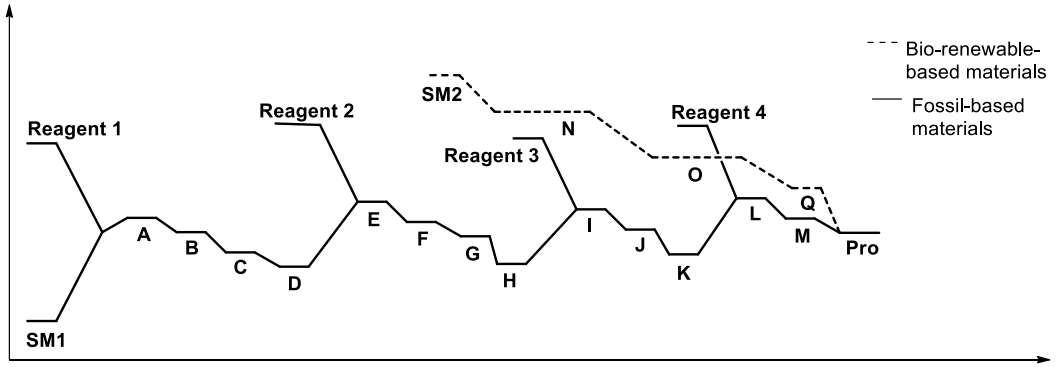

Fig 11. A projected synthesis of **Pro** from hypothetical fossil-based raw material starting material **SM1** or bio-renewable starting material **SM2**.[12]

The idea of using high potential energy raw materials can reverse the thermodynamic situation in the practice of organic synthesis. This approach holds potential to eliminate

or at least greatly reduce the use of highly reactive and sometimes toxic reagents that are crucial in the success of processes that use fossil-based raw materials. Revisiting our hypothetical synthetic route in Figure 11, it can be conceived that **Pro** could also be obtained from **SM2**, a high potential starting material through downhill processes, therefore minimal energy input is required to achieve the synthesis of **Pro**. Raw materials that can potentially achieve the above rather ambitious goals can be obtained from abundant and bio-renewable natural resources like plants. Indeed bio-renewable derived raw materials possess high potential energy as compared to fossil based raw materials. Additionally, they possess functionalities or congeners of functionalities that the target compounds have, thus shortening the number of steps that may be required to install the functional groups that are often missing in petrochemical-based starting materials. A good example of the difference in the number of steps and efficiency between a route that employs fossil-based and bio-renewable-based is the synthesis of tropinone by Robinson and Willstätter.[8, 129] Consequently, the search for novel bio-renewable-based raw materials has been pursued with intense vigour.

4.2 Bio-based aromatic starting materials

An exciting challenge encountered in the search for bio-renewable platform chemicals is a suitable source of aromatic compounds. Aromatic fragments are ubiquitous in compounds that find use in everyday life. As such, intense efforts have been made in trying to sequester aromatic platform compounds from bio-renewable resources. Chief amongst the sources investigated as a potential source for phenolic aromatic compounds is lignin, a component of lignocellulose.[15-17] Lignin is an abundant material and renewable, and this, compounded with its inedibility means it does not compete with food sources. These are attributes that render lignin a potential bio-renewable resource of aromatic compounds. However, obtaining the phenolic compounds from lignin remains a challenge.[16, 18, 130-131] Thus, alternative phenolic bio-renewable raw materials are desirable. To this end, cashew nut shell liquid (CNSL) has been investigated as a potentially renewable feedstock, especially in the context of green chemistry.[132-134]

4.2.1 Cashew nut shell liquid (CNSL) as a bio-renewable resource

CNSL is a non-edible industrial waste product of cashew nut processing. Copious amounts of cashew nut shells are produced annually and it is estimated that 1.2 million tons of CNSL are produced per year.[135-136] This makes CNSL an ideal renewable feedstock owing to its abundance and it is cheap! CNSL constitutes a mixture of phenolic compounds such as cardanol **9**, cardol **10**, anacardic acid **11** and 2-methyl cardol **12** with a pendant C15 chain of varying saturation *meta* to the hydroxyl group (Figure 1). The various components of CNSL are sometimes separated using solvent extraction methods or cold-press, with anacardic acid **11** as the major component.[135] However, an industrial isolation of CNSL components involves distillation of CNSL, a process that leads to decarboxylation of anacardic acid **11** giving technical cashew nut shell liquid (tCNSL), with cardanol **9** as the major component.[135] This has led to the development of cardanol-derived materials and products such as anticorrosive paints, diesel engine fuel alternatives, anti-oxidants, coating, lubricants, diesel engine fuel alternatives, food additives, sodium cardanol sulfate detergent, resins and polymers. However, there are few examples in the literature that involve the transformation of cardanol **9** to small high-valued compounds; there are even fewer examples with cardol as the starting material **10**. The ensuing discussion will be concerned with valorization of cardanol **9** and cardol **10** in the synthesis of small value-added compounds. As such, polymerization reactions and the synthesis of functional molecules for example, the synthesis of cardanol derived porphyrins and fullerene hybrids will be omitted. If the reader is interested in this area, reviews by Vasapollo and collaborators provide further information.[136-137]

4.3 The synthesis of value-added products from cardanol

Cardanol has three reaction sites, namely the alkene functionality found in the unsaturated cardanol analogues, the phenol substituent and the benzene ring (Figure 12). Research efforts have been directed towards utilizing the alkene and the nuclear ring functional groups in an effort to synthesize value-added compounds. The synthesis

of cardanol based value-added molecules through the sole reaction of the phenol group are very rare.[138-139]

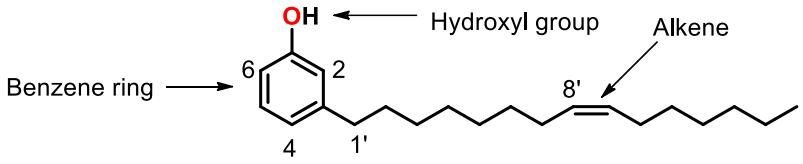

Fig 12. Reactive sites on (Z)-8-cardanol, the major phenolic component of cashew nut shell liquid

4.3.1 Alkene centered reactions

Cole-Hamilton and colleagues reported on the cardanol chain shortening process in their three-step synthesis of a natural tsetse fly attractant, kairomone **159** (Scheme 50).[140] This route takes advantage of the unsaturation at C–8' on the monoene cardanol **9** that makes up 87% of cardanol that is obtained from thermal decarboxylation of anacardic acid **11**. Therefore, monoene cardanol **9b** was subjected to isomerization in the presence of catalytic amounts of $Pd_2(dba)_3$ and the ligand, [bis(ditertiarybutylphosphinomethyl)benzene] (DTBPMB), at 90 °C for over 24 h. These conditions induce double bond migration from its natural position (C–8') to the benzylic position (C–1'), giving isocardanol **160** in 40% yield, alongside other constitutional isomers which were not isolated. The stereochemistry around the newly formed double bond of **160** was not investigated, however, the thermodynamically stable *trans*-isomer was assumed. The mixture of stereo- and constitutional isomers were then subjected to cross-metathesis reaction with *cis*-2-butene aided by the Hoveyda–Grubbs catalyst (**HG-2**) unveiling a mixture of *cis*- and *trans*-3-(prop-2-enyl)phenol **161** in low yield of 11%. Reduction of **161** under standard conditions gave 3-propylphenol **159** in 94% yield.

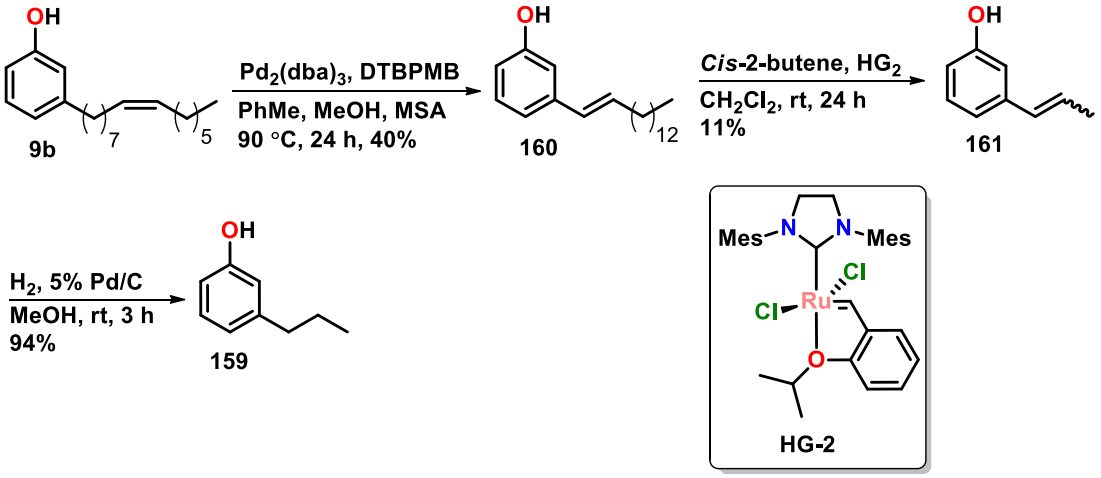

Scheme 50. Cole-Hamilton first generation synthesis of kairomone.

The same group later showed that ethenolysis of CNSL which consists of mainly mono-, bi- and tri-unsaturated anacardic acid with superstoichiometric amounts of ethylene in the presence of phosphine-ligated ruthenium catalyst such as first generation Hoveyda–Grubbs catalyst (**HG-1**) gave a single C–8' monoene anacardic acid derivative **162** (Scheme 51).[141] The reaction was able to deliver C–8' monoene anacardic acid **162** as the main product due to the common feature of all the unsaturated anacardic acid isomers, namely that they all possess a double bond at C–8'. Therefore, ethenolysis shortens the unsaturated side-chain to ω-nonenyl groups. Decarboxylation of the intermediate **162** during purification by distillation furnished 3-(non-8-enyl)phenol **163** quantitatively. Phenol **163** can be converted to 3-vinylphenols **161** through isomerization metathesis. Indeed, this feat was achieved by Cole-Hamilton and co-workers who demonstrated that exposure of phenol **163** to various NHC-ligated ruthenium catalysts in the presence of simple alkenes yields 3-vinylphenols **161**, with catalytic ruthenium (shown below) giving the best optimized yield (77 %), albeit at elevated pressures. This intermediate was recently employed in preparative-scale transformations to a number of natural products like kairomones (3-ethylphenol and 3-propylphenol) **159**, metaraminol, norfenefrine, etilefrine, phenylephrine, and fenoprofen.[142]

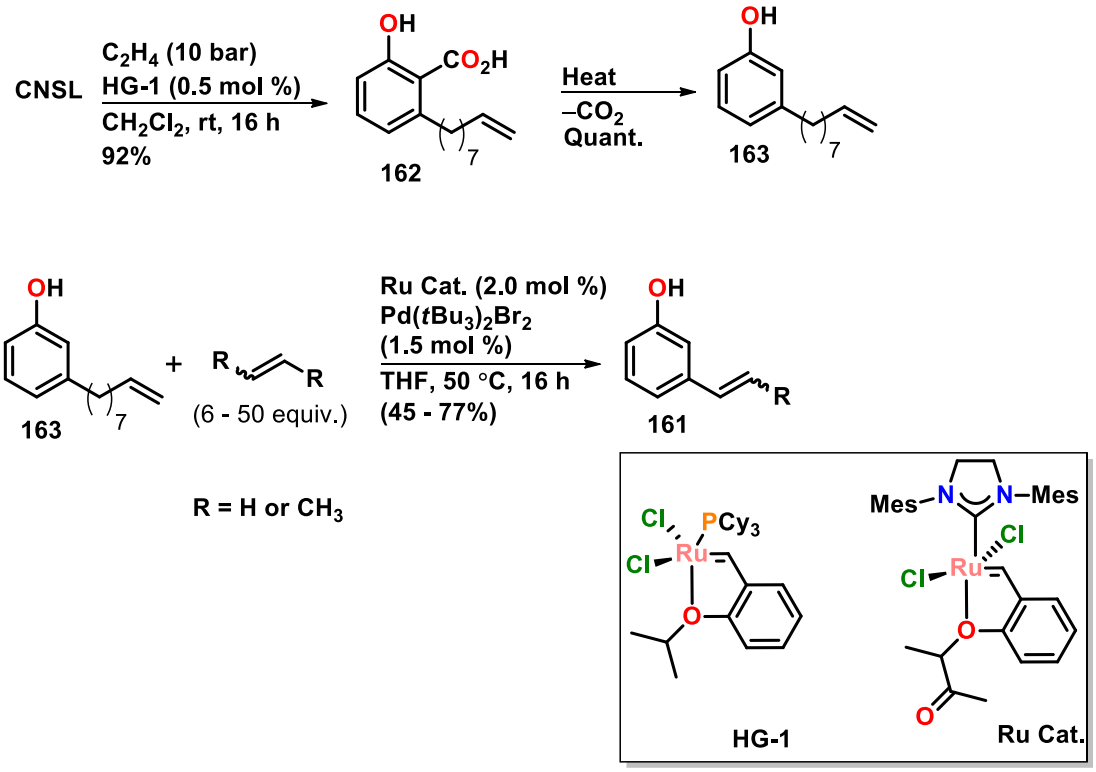

Scheme 51. Cole-Hamilton's improved synthesis of kairomones.

Monoene anacardic acid **162** proved to be an important intermediate in most syntheses of value added small molecules from anacardic acid **11**. For example, **162** was used as a key intermediate by the Gooßen group in their total synthesis of ginkgolic acid **164**, a tyrosinase inhibitor (Scheme 52).[143] To this end, monoene anacardic acid **162** was subjected to hexenolysis with 7.0 equivalents of 1-hexene using 1 mol % of **HG-1** catalyst in methylene chloride at ambient temperature for 6 h yielding acid **165**. Subsequent addition of charcoal, methanol and hydrogen gas at 5 bar of **165** gave the desired ginkgolic acid **164** in 72% from **162**. This process was done at a multigram scale.

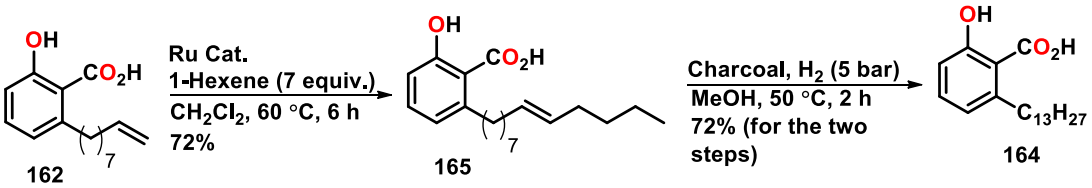

Scheme 52. Anarcadic-based total synthesis of ginkgolic acid.

Promising as they are, alkene centered transformations of cardanol **9** and anacardic acid **11** do not fare well in terms of atom economy as they often involve "chopping off" part of the pendant carbon chain. This situation can be improved if the "chopped" aliphatic carbon chain can be used to make other value added chemicals.

4.3.2 Nuclear aromatic reactions of cardanol

Cardanol **9a-d** is an electron-rich aromatic system, owing to the electron donating functionalities that are appended to the benzene ring. Therefore, it is not surprising that cardanol **9a,b** has been subjected to various classical electrophilic substitution reactions such as alkylation,[136] halogenations,[144] nitration,[145] and sulfonation reactions.[140] Fries and Claisen Rearrangements of preformed *O*-acylated or *O*-alkylated cardanol derivatives have also been disclosed.[20, 146] However, with very few exceptions, these reactions are overwhelmingly non-site specific, with high propensity to produce mixtures of mono-, di- and tri-substituted products that are often very difficult to separate.[144, 147] Even some rearrangement reactions are not exempt from this non-site specificity as they also often give mixtures of *ortho*- and *para*-products.[146]

4.3.2.1 Synthesis of benzofurans from cardanol

This lack of site-selectivity in nuclear functionalization of cardanol **9a,b** could be directly linked to the slow progress made in the synthesis of benzo-fused heterocyclic compounds from **9a,b**. The situation is even worse in synthetic campaigns that seek to incorporate the hydroxyl group as part of the heterocyclic frameworks such as benzofurans, xanthenes, and chromenone, as the synthesis of such scaffolds may require *O*-functionalization of cardanol. A case in point is the synthesis of 2-subtituted benzofuran **166** by Arcadi and co-workers (Scheme 53).[148] Their strategy involved accessing the benzofuran core through sequential Sonogashira alkynylation/cyclisation sequence of dibromo-iodo-cardanol **167**. In turn, iodo-cardanol **167** was synthesized from iodination of dibrominated cardanol **168**, which was retrospectively obtained as one of cardanol bromination products. As pointed out earlier (*vide supra*),

halogenations of cardanol **9a** tend to give mixtures of *para*-, and *ortho*-products together with di- and tri-substituted products. This approach was also adapted by Giancarlo Fabrizi and colleagues in their synthesis of 2,3-disubstituted benzofurans from 2-iodocardanol.[149] However, the group did not disclose the details on the synthesis of 2-iodocardanol. As expected, the overall yields of the above-cited syntheses are low.

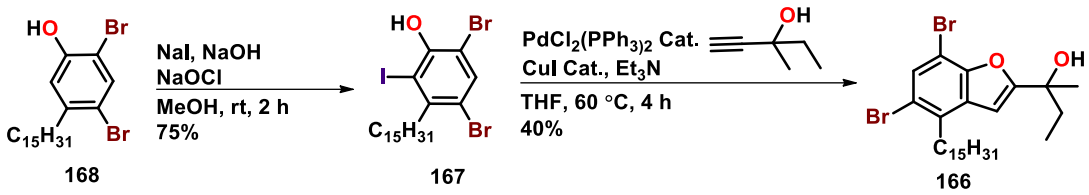

Scheme 53. Synthesis of brominated 2- benzofuran.

It is clear that a more regioselective halogenation processes or other strategies that can selectively functionalize the *O*-position of cardanol are desirable. The Barker synthesis of 2,3-unsubstituted benzofuran **169** from polyphosphoric acid (PPA) induced intramolecular cyclization of cardanol acetaldehyde acetal **170** is instructive (Scheme 54).[150] This strategy takes advantage of the hydroxyl functionality that is already present in cardanol, and therefore sets a precedent for a possible way of achieving *ortho*-selectivity in the synthesis of cardanol-based oxa-heterocyclic compounds. However, two *ortho* products could arise in the case of cardanol **9**. In their report, Barker and co-workers did not report the formation of the isomeric *ortho* product but only benzofuran **169**.

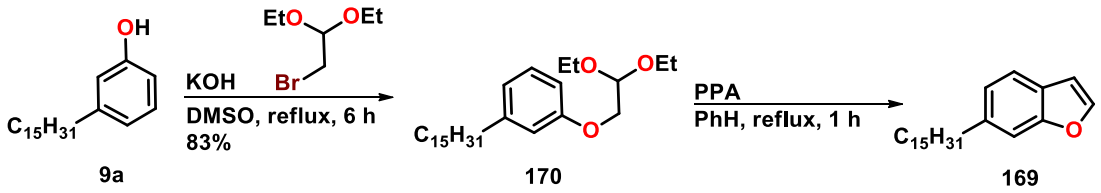

Scheme 54. Synthesis of cardanol derived 2,3-unsubstituted benzofuran.

4.3.2.2 Synthesis of benzoxathiines from cardanol

Sterically encumbered reagents can also be used to discriminate between the *ortho*- and *para*-substitution (phenolic group is used as reference) in favour of substitution on the easily accessible *ortho*-position. Due to the presence of the C15 chain neighbouring the *para*-position. Such an approach was explored by Amorati and colleagues in their synthesis of benzoxathiines **171** *via* inverse-electron-demand hetero-Diels-Alder reaction between the electron-poor *ortho*-thioquinone **172** and electron-rich styrenes **173** (Scheme 55).[151] In return, the *ortho*-thioquinone **172** was obtained through electrophilic substitution of cardanol **9** with bulky phthalimidesulfenyl chloride **174**, yielding the less hindered 2-hydroxy-4-pentadecyl-*N*-thiophenyl phthalimide **175**. Subsequent exposure of phthalimide **175** to Et_3N in dry $CHCl_3$ at 60 °C furnished the transient electron deficient *ortho*-thioquinone **172** that was immediately trapped with electron-rich styrenes **173** forming benzoxathiines **171**. This reaction proceeds with remarkable regioselectivity, only delivering a single 1,4-benzooxathiin product, where the oxygen of the *ortho*-thioquinone **172** is directly linked to the aryl-bearing carbon of the styrene reacting partner. The stereochemical basis supplied as an explanation for the observed regioselectivity in the transformation of **172** to **171** left much to be desired.[152]

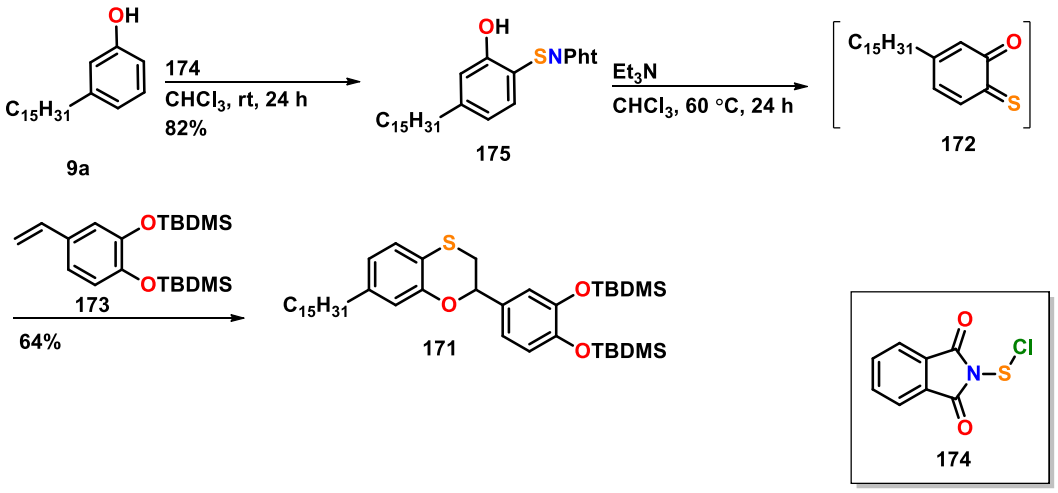

Scheme 55. Synthesis of benzoxathiine from cardanol.

The use of sterically encumbered reagents to incite bias between *ortho*- and *para*-position in the synthesis of heterocyclic compounds from cardanol is rarely employed as a strategy in this area. The reason for this is unclear.

4.3.2.3 Synthesis of benzoxazines from cardanol

Exploiting the phenol substituent still stands as the most profitable and a method of choice when synthesizing cardanol-derived benzo-fused heterocyclic compounds. This strategy is not limited to the intramolecular cyclization of *O*-alkylated cardanol derivatives (*vide supra*). Indeed, this approach is mostly employed in intermolecular processes. The synthesis of benzoxazines **176** from cardanol **9a**, amines **177** and 2 equiv. of formaldehyde **178** in the Betti reaction (Scheme 56) serves as an example.[153] The first mechanistic step of the reaction involves the formation of imine **179** between the amine **177** and 1 equivalent of formaldehyde **178**, followed by nucleophilic attack by the cardanol **9** in a Mannich-type fashion producing α-aminobenzylphenol **180**. A second condensation reaction between α-aminobenzylphenol **180** and formaldehyde **178** yields an iminium intermediate **181** that is electrophilic enough to participate in intramolecular nucleophilic attack from the hydroxylate group yielding benzoxazines **176**.

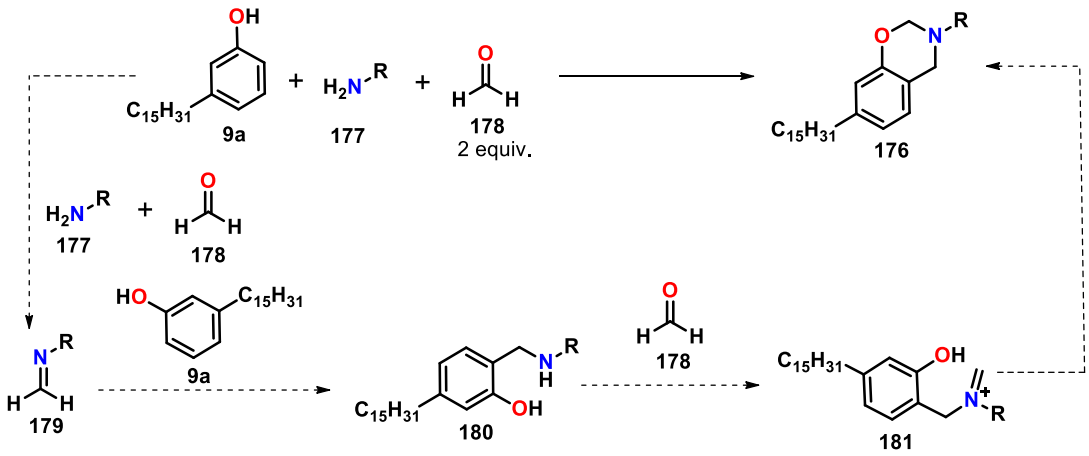

Scheme 56. Synthesis of cardanol derived benzoxazines through the Betti reaction.

At first glance, this method does not reveal its reliance on the hydroxyl group, until we realize that no γ-aminobenzylphenol was isolated from the reaction mixture, which would have resulted from attack at the *para* position. Therefore, the first electrophilic substitution between cardanol **9a** and imine **179** appears to be regioselective. Mechanistic investigations on the Betti reaction revealed that the transition state **I** of the reaction involves hydrogen bonding between the hydroxyl group and the imine yielding the short-lived dienone **182** that re-aromatizes to **180** (Scheme 57).[154] Thus, the hydroxyl group serves two functions, first as an *ortho* director and also to activate the imine functionality.

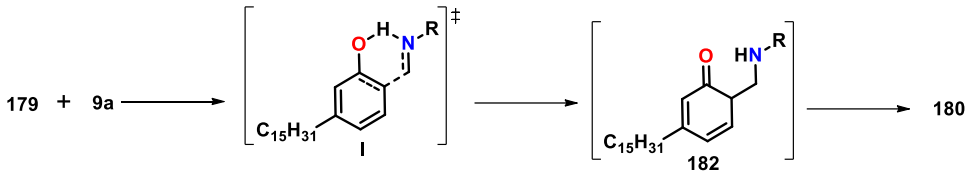

Scheme 57. Proposed transition state of the reaction between imine **179** and cardanol **9**.

4.3.2.4 Synthesis of coumarins from cardanol

Hydrogen bonding is not the only means of exploiting the *ortho* directing ability of the phenol group of cardanol **9a**. Metals such as Mg and Sn have also been used to install a formyl group on position 6 forming *ortho*-formyl cardanol **183**, an intermediate that has been used to fashion various cardanol derived heterocyclic compounds. The Lalitha and Nagarajan cardanol derived coumarins **184** was exemplary (Scheme 58).[155] Their synthesis disclosed Mg-mediated union between cardanol and paraformaldehyde forming *ortho*-formyl cardanol **183** which was subsequently elaborated to cardanol-based pyrene coupled coumarin derivatives **184** that were used as fluorescent probes in cell imaging.

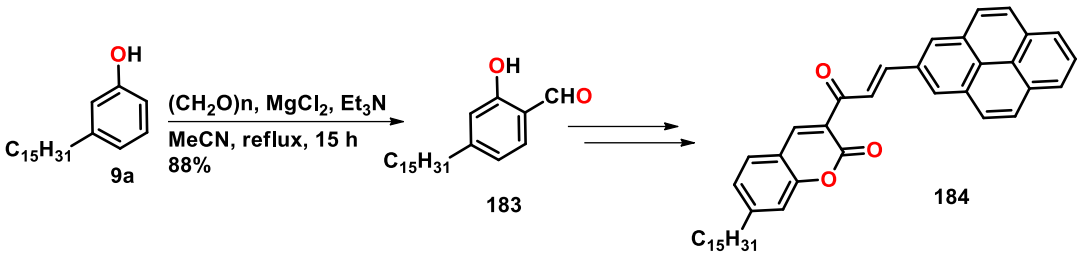

Scheme 58. Synthesis of cardanol **9a** derived coumarins.

4.3.2.5 Synthesis of UV absorbers from CNSL-based compounds

The de Koning group have also utilized bio-renewable resources containing phenolic compounds in the campaign to synthesize UV absorbing compounds from cardanol **9a** and other CNSL phenolic components.[20] Taking advantage of the *ortho*-selectivity of formylation of cardanol **9a** in the presence of $SnCl_4$, 2-formylcardanol **183** was prepared and was used as a key intermediate in the synthesis of various heterocyclic compounds. This work was not only focused on benzo-fused oxa-heterocyclic compounds, as triazines and oxadiazole were also synthesized from 2-formylcardanol **183**, both in two steps. In the arena of benzo-fused oxa-heterocyclic compounds, 3-hydroxyflavone **185** and 1,8-dihydroxyxanthone **186** were synthesized from cardanol **9** (Schemes 59 and 60). The synthesis of 3-hydroxyflavone **185** was achieved through *O*-acylation of cardanol **9a**, subsequent microwave assisted Fries rearrangement of the resultant *O*-acyl cardanol **186** in the presence of $AlCl_3$ yielding hydroxy ketone **187** (Scheme 59). This step appears to proceed with astonishing never-seen-before *ortho*-selectivity yielding only product **187** quantitatively with no *para*-product in sight! Hydroxyketone **187** was then subjected to an aldol condensation reaction with benzaldehyde **188** to furnish chalcone intermediate **189**, which was converted to the desired 3-hydroxyflavone **185** through *in situ* oxidation with hydrogen peroxide. An important feature of 3-hydroxyflavone **185** is the *ortho* relationship between the carbonyl and hydroxyl groups that form an external pseudo-five membered ring through intramolecular hydrogen bonding (Figure 13), a property that is important in

most UV absorbers. It must be noted that all the atoms that make up 3-hydroxyflavone **185** in this synthesis can be derived from bio-renewable starting materials.

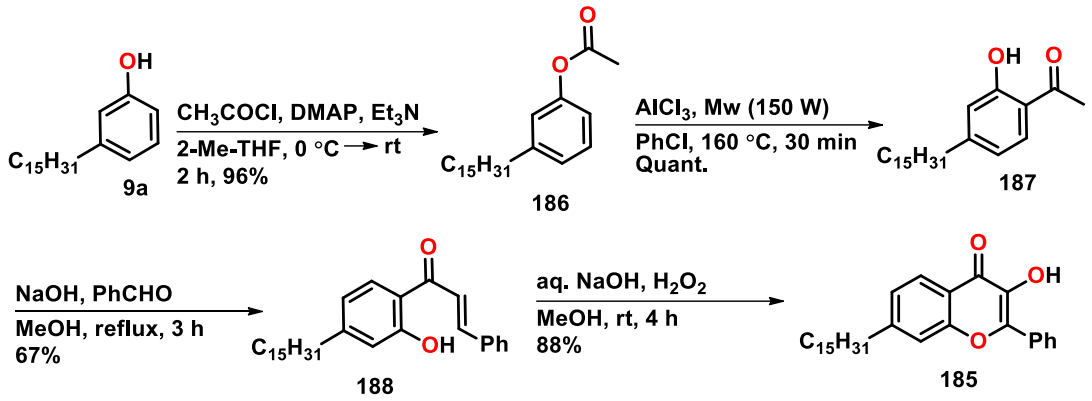

Scheme 59. Synthesis of 3-Hydroxyflavone from cardanol.

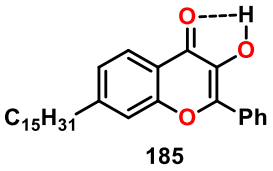

Fig 13. Intramolecular hydrogen bonding in 3-Hydroxyflavone **185**.

In a similar manner, cardanol **9a** was reacted with 2-fluorobenzoyl chloride **189** in the presence of DMAP and Et_3N, using 2-Me-THF as solvent to give phenol ester **190** in quantitative yield. Employing the microwave assisted Fries rearrangement described above proved useful yet again as the desired benzophenone **191** was synthesized in an unprecedented high yield of 84% as the sole product (Scheme 60). Subsequent base-induced cyclization of benzophenone **191** upon treatment with K_2CO_3 in refluxing acetone furnished xanthone **192** in high yield of 86%. Xanthone **192** lacks a hydrogen donating group in positions 1 or 8 of **192** that is crucial in forming intramolecular hydrogen bonding with the hydrogen bond accepting carbonyl group, to render the xanthone **192** a potential UV absorber. This challenge was anticipated in the planning stages of the project and it was agreed that a late-stage electrophilic hydroxylation would be employed to install the requisite hydroxyl group in the final step of the synthesis following a procedure developed by the group of Ackermann.[156] Generally,

in organic synthetic campaigns risky operations such as the late-stage C–H functionalization of **192** are usually carried out early in the synthesis; the final steps are reserved for reliable and well established methods. However, in this case the benefits of installing the hydroxyl group late in the synthesis outweighed the risks. Introducing the hydroxyl group early in the synthesis would require a protection step to mask this reactive functionality and deprotection step at the end of the synthesis. Therefore, it was decided to delay the introduction of this group to the last step. Hence to complete the synthesis xanthone **192** was boiled in TFA/TFAA solvent mixture in the presence of catalytic amounts of [Ru(*p*-cymene)Cl_2]$_2$ and stoichiometric amounts of $K_2S_2O_8$ as oxidant delivering the desired 1,8-dihydroxyxanthone **186** in 64% yield.

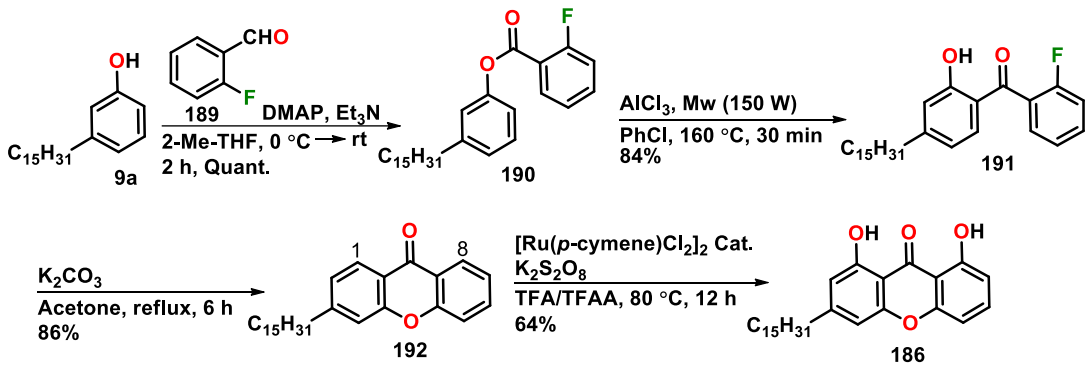

Scheme 60. Synthesis of 1,8-dihydroxyxanthone from cardanol.

These compounds were shown to possess favorable UV absorbing properties and are currently being investigated as possible commercial UV absorbers.[20]

4.4 Aims of the study

Encouraged by these results, and motivated by the moderate progress in photo-activated insecticides, for the purposes of this PhD we were tasked with the synthesis of benzo-fused oxa-heterocyclics from cardanol **9a** and cardol **10a**. The aim was to synthesize known photosensitizers that can possibly be employed as photo-activated insecticides. Here special attention was made to synthesize these scaffolds using bio-renewable starting materials. It was speculated that using cardanol and cardol provides an added advantage. Owing to their hydrophobic C15 side chain, cardanol- and cardol-

based photosensitizers can easily adhere to the hydrophobic surfaces of plant leave. Our attention was attracted by the promising results obtained from xanthenes and furanocoumarins.

4.5 Results and discussion

4.5.1 Attempted synthesis of cardol 9a-based fluorescein derivative

Due to the promising results of xanthenes as potential photo-activated insecticides, it was determined that a cardol-based fluorescein derivative **193** would be a viable target. Fluorescein is a prominent member of the xanthene family known to generate triplet oxygen. It was envisaged that fluorescein **193** could arise from the fusion of two equivalents of cardol **10a** and phthalic anhydride **194** in the presence of an acid catalyst (Scheme 61). Although it was our ambition to synthesize the dyes using bio-renewable starting materials, the proposed route employs phthalic anhydride **194** that is commercially produced from the oxidation of petrochemical starting materials such as naphthalene or *o*-xylene.[157] However, this route could give **193** in a single synthetic operation. Thus, a 10 mL round-bottom flask placed in an oil bath and equipped with a stirrer bar was charged with cardol **10a** (2.0), phthalic anhydride **194** (1.0 equiv.) and concentrated H_2SO_4 (1 mL). The resulting slurry was stirred while gradually increasing the temperature to 190 °C, and once that temperature was reached the reaction was allowed to stir for an additional 30 min. The contents of the flask were poured into crushed ice, forming a precipitate that was recovered through filtration. TLC of the precipitate revealed an abundance of spots all lacking the characteristic fluorescence often visible under UV light for xanthenes. Efforts to separate the spots through column chromatography and recrystallization led to indiscernible NMR spectra – presumably decomposition products. Other attempts such as changing the acid catalyst to $ZnCl_2$ both neat and dissolving the reagents in DMSO in a sealed tube yielded the same discouraging results.

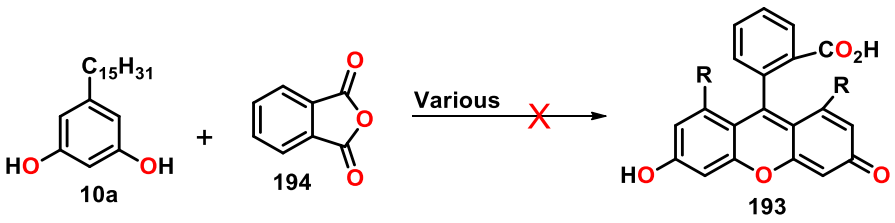

Scheme 61. Attempted synthesis of fluorescein derivative from cardol **10a** and phthalic anhydride.

The failure of cardol **10a** to form **193** could be attributed to steric hindrance imposed by the C15 chains in positions 1 and 8 of the xanthene scaffold. This view is supported by the realization that a similar synthesis of a fluorescein derivative from orcinol, a structurally similar compound to cardol, save for the C15 chain being replaced by a methyl group, gave a mixture of three xanthenes, with the desired fluorescent isomer produced in scant amounts.[158] The other two non-fluorescent xanthenes were produced in higher amounts and were very difficult to separate. This could have been the case in our synthesis considering the pronounced steric congestion of cardol **10a** as compared to orcinol, it makes perfect sense that the proposed fluorescein derivative **193** was not detected. Due to this revelation and the observation that cardanol **9a** and cardol **10a** tend to decompose at temperatures above 120 °C it was decided to abandon any further research on this part of the project.

4.5.2 Synthesis of coumarins and annellated coumarins derivatives

Our attention was then diverted to the synthesis of cardanol **9a** and cardol **10a** derived coumarins **195** and **196**, respectively and annellated coumarins (benzodipyrandione **197** and furanocoumarin **198**). We were interested on coumarins and furanocoumarins because they are produced as photo defensive secondary metabolites by *Citrus* species as protection against herbivorous insects and pathogens.[159] The biosynthesis of coumarins and furanocoumarins was discussed in a recent article by Rodrigues.[160] The most popular route to coumarins involves cyclization reactions of *o*-hydroxy-benzaldehydes employing classical condensation reactions such as the Perkin reaction and Knoevenagel condensation.[161] In our case employing the above-mentioned

reactions would have necessitated a carbonylation step to prepare the requisite formylated cardanol and cardol. As such we decided to adopt the Pechmann reaction since it could give rise to coumarins **195** and **196** in a single synthetic step from acid-catalyzed condensation of phenols (cardanol **9a** and cardol **10a**, respectively) and malic acid **199** (Schemes 62 and 63). Once achieved, coumarin **196** would possess a free hydroxyl group that could be exploited as a handle for further annulation reactions giving benzodipyrandione **197** through a second Pechmann reaction upon treatment with malic acid **199**. On the other hand, alkylation of coumarin **196** with bromoacetaldehyde diethyl acetal **200** to give intermediate **201** followed by acid-induced cyclization should produce furanocoumarin **198**. It was anticipated that the final cyclization steps of the projected syntheses towards benzodipyrandione **197** and furanocoumarin **198** could potentially furnish regioisomers (more on this below). If successful, this diversity oriented syntheses could allow access to both the angular and linear products of both scaffolds, allowing for evaluation of the photo-physical properties.

With the goal of synthesizing coumarin **195**, cardanol **9a** was reacted with malic acid **199** (1.2 equiv.) in the presence of H_2SO_4 as catalyst. The reaction was heated to 100 °C for 3 h (Scheme 62). After quenching with crushed ice and filtration of the precipitate, the pure product was obtained through recrystallization. The ^{1}H NMR spectrum of the sample revealed a doublet at 7.69 ppm that coupled with a proton appearing at an upfield chemical shift of 6.37 ppm. These shifts are characteristic of the pyran ring fragment of coumarins. The rest of the aromatic protons show a classical first order multiplicity of 1,2,4-trisubstituted benzenes with signals at 7.39 (d, J = 7.8), 7.15 (d, J = 1.5) and 7.11 (dd, J = 7.9, 1.6) ppm, betraying the identity of the product as coumarin **195**. Pointing out that coumarin **195** was expected would be a quintessential case of truism since Pechmann condensation of *meta* alkylphenols such as *m*-cresol overwhelmingly favor 7-alkylcoumarins (like **195**)[162-163] against 4-alkylcoumarins which were only detected by GC but have never been isolated.[164] In

our case, GC measurements were not carried out to determine whether the 4-substituted coumarin was formed or not.

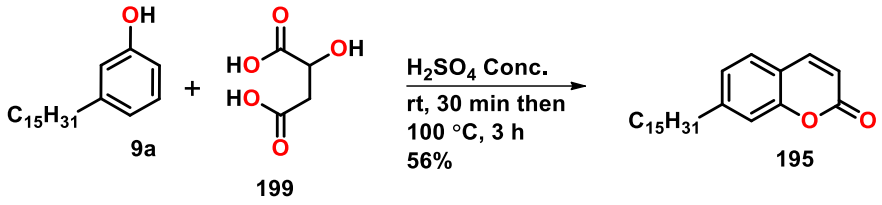

Scheme 62. Synthesis of coumarin from cardanol **9a** *via* Pechmann condensation with malic acid.

Satisfied with the outcome, we set our sights on the synthesis of the annellated coumarins **197** and **198**. As a prelude, umbelliferone derivatives, **196** was synthesized through the condensation of cardol **10a** (1.0 equiv.) with malic acid **199** (1.2 equiv.) as described for cardanol **9a** above (Scheme 63). In theory two possible regioisomers could arise from this reaction, namely substituted coumarins **196a** and **196b**. However, the formation of umbelliferone derivative **196b** has never been achieved this way.[160] Indeed, a single coumarin was obtained and the ^{1}H NMR spectrum of the product was measured. The benzenoid protons appear as singlets at 6.83 and 6.40 ppm. H-3 (coumarin numbering) of the pyran motif appears upfield as a doublet at 6.34 ppm as expected. Coupling to H-3 is H-4 (both have *J* coupling of 9.7 Hz) which has a chemical shift of 8.14 ppm. In comparison with subtituted coumarin **195**, H-4 of umbelliferone derivative **196** appears shifted downfield, the chemical shift of the former is 7.69 ppm. This downfield shift observed for umbelliferone derivative **196** can been attributed to the characteristic *peri*-deshielding effect from the proximal C15 chain, a feature lacking on **195**.[164] This points to umbelliferone derivative **196a** as the regioisomer formed, an anticipated outcome. The aromatic region of the ^{1}H NMR spectrum together with the ^{13}C NMR spectrum of umbelliferone derivative **196a** closely resembles umbelliferone obtained from the condensation between orcinol and malic acid **199**.[164] A FTIR of the sample was measured to further prove the identity of the product and the spectrum showed bands at 3171.5, 2915.0, 2848.8, 1732.3, 1555.5 and 1139.7 cm^{-1} corresponding to OH, C–H stretch, C=O, C=C and C–O, respectively. The HRMS

analysis of the sample gave a mass of 373.2739, correlating remarkably well with the calculated mass of 373.2743 ($[M + H]^+$) for umbelliferone derivative **196a**.

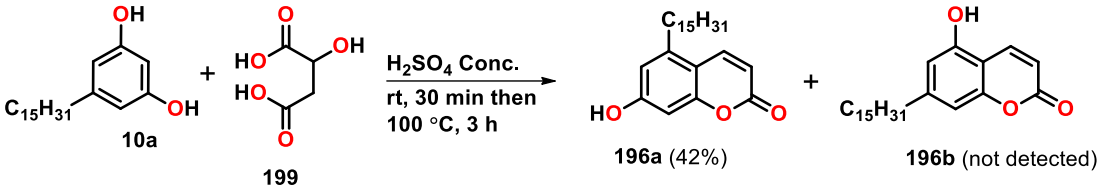

Scheme 63. Synthesis of cardol **10a**-derived umbelliferone derivative through Pechmann reaction.

With umbelliferone derivative **196a** in hand, the stage was set for further annulation reactions to give tricyclic oxa-heterocyclic compounds based on cardanol. Therefore, umbelliferone derivative **196a** was advanced to benzodipyrandione **197** by reacting with malic acid **199** in the presence of H_2SO_4, furnishing another pyran ring in a second Pechmann

condensation (Scheme 64). The reaction mixture was quenched with ice and the product filtered as described for the substituted coumarin **195** (*vide supra*). The NMR spectrum of the crude sample was measured to ascertain whether both possible regioisomers had formed. To our surprise, only the angular benzodipyrandione **197a** isomer was detected by NMR spectroscopy. The assignment of the product as **197a** stems from ^{1}H NMR and ^{13}C NMR spectra and is reinforced by the observation that **197b** is symmetrical therefore H-3 and H-7 should resonate at the same chemical shift and so should H-4 and H-6.[165] However, the inspection of the ^{1}H NMR spectrum reveals five distinct protons, a singlet that can be attributed to the benzenoid H-6 (7.09 ppm), H-3 and H-9 overlap at 6.51-6.47 ppm. On the other hand, H-10 in **197a** resonates at a distinctly higher field than H-4 (8.30 vs. 7.97 ppm, respectively). The ^{1}H NMR spectrum is complemented by the ^{13}C NMR spectrum that shows two non-equivalent carbonyl groups at 159.7 and 159.4 ppm. The mass of the product was measured (with HRMS) to be 425.2691 a.u, matching the calculated $[M + H]^+$ 425.2692 m/z. Reacting cardol **10a** with 2.4 equiv. of malic acid **199** also resulted in

benzodipyrandione **197a** presumably *via* umbelliferone derivative **196a**, albeit, in a slightly low yield of 52%.

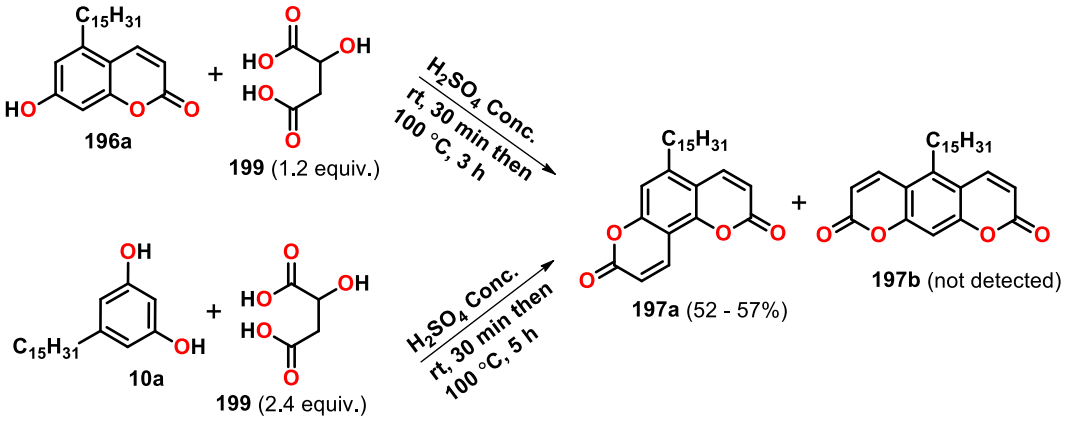

Scheme 64. Benzodipyrandione synthesis *via* a double Pechmann condensation with isolated umbelliferone derivative intermediate and direct synthesis without isolation of the intermediate.

Having acquired benzodipyrandione **197a**, our attention was devoted to the synthesis of furanocoumarin **198**. As divulged in Scheme 65 below, **196a** was alkylated with bromoacetaldehyde diethyl acetal **200** in the presence of K_2CO_3. The reaction did not give the desired product when THF was used as solvent. This could be due to poor solubility of the starting **196a** in THF. A yield of 67% of the desired product was obtained when using DMF as solvent. Using anhydrous DMF as solvent increased the yield to 92%. Pure **201** was attained as a yellow solid after silica gel column chromatographic separation in EtAOc/cyclohaxane (4:1). In addition to the known proton shifts for umbelliferone derivative **196a**, chemical shifts resonating at 4.91 (t), 4.12 (d), 3.82 (dq) and 3.68 (dq) ppm, corresponding to the acetaldehyde diethyl acetal fragment were observed on the ^{1}H NMR spectrum of the sample, heralding the success of the operation. The mass of 489.3576 a.u. was found for the sample, correlating well with the calculated mass ($[M + H]^+$ 489.3580) for **201**. Intermediate **201** is suited to participate in an acid-mediated intramolecular condensation forming a furan ring, in a fashion reminiscent of the Barker synthesis of benzofurans (see Scheme 56 above). As such, intermediate **201** was treated with PPA in refluxing toluene for 2.5 h. A

precipitate formed and was separated by filtration. Subsequent recrystallization with pure EtOAc gave a white solid. The ^{1}H NMR spectrum (Figure 14) of the solid uncovered a mixture of psoralen-type and angelicin-type furanocoumarins in approximately 70:30 ratio (from the integration of the proton NMR spectrum). The ratio of linear and angular furanocoumarins arising from the cyclization of alkylated umbelliferones similar to **201** are skewed in favour of angelicin. This observation bears testament to the hindering nature of the C15 chain.

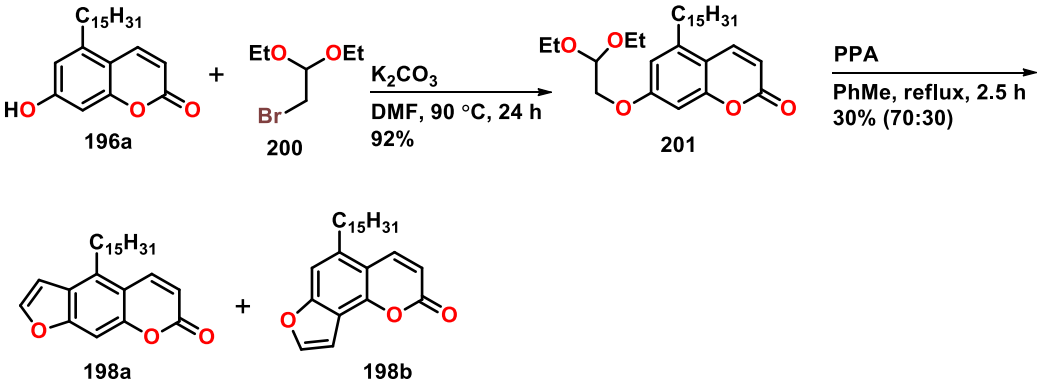

Scheme 65. Synthesis of furanocoumarin from umbelliferone derivative **196a**.

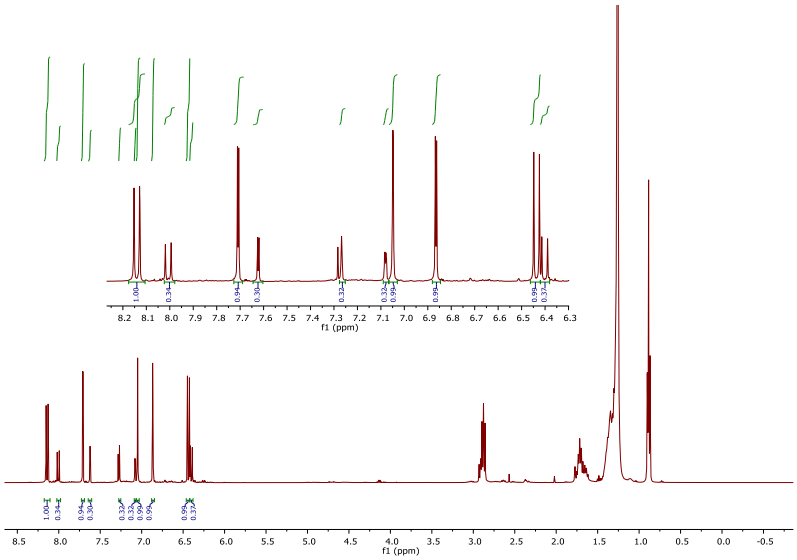

Fig 14. The ^{1}H NMR spectrum of the mixture of linear and angular furanocoumarins **198a** and **198b**.

All the efforts to separate the compounds were unsuccessful, as such no further characterization of the mixture was made. Therefore, the peaks could not be assigned to any specific isomer of the two furanocoumarins. Due to time constraints, the separation problem was left for the future researchers in our labs and so are the photophysical studies of all the cardanol- and cardol-based coumarins and its annulated variants.

4.6 Conclusions

Our efforts to synthesize cardanol- and cardol-based photo-active compounds was met with mixed results. The attempted synthesis of cardol-derived fluorescein proved challenging. The perceived failure to synthesize this compound could be attributed to the steric demand imposed by the C15 side chain of cardol **10**. Due to this insurmountable challenge, this project was terminated, instead shifting our focus to the synthesis of cardanol- and cardol-based synthesis of coumarins and its annulated derivatives.

The synthesis of coumarins was achieved through the known Pechmann condensation of either cardanol **9a** or cardol **10a**, smoothly unveiling the anticipated coumarin **195** and umbelliferone derivative **196a**. A second Pechmann condensation of **196a** gave angular benzodipyrandione **197a** as a sole product, an observation unprecedented in literature. This provided further proof of the enhanced congestion brought about by the C15 side chain. This exaggerated steric hindrance was also visible in the synthesis of furanocoumarins which gave a mixture of psoralen and angelicin derivatives in lower ratio than previously reported for derivatives not containing the C15 alkyl chain.[166] The separation of the regioisomers proved challenging and the solution may be lying await in the future!

Chapter 5

5.1 Introduction

In keeping up with our program directed towards the synthesis of UV-absorbing oxa-heterocyclic compounds derived from cardanol **9** and cardol **10**, we were drawn to the synthesis of cardol-based Δ^9–*trans*–tetrahydrocannabinol (Δ^9–*trans*–THC, it will simply be referred to as THC from here onwards). THC bears a chroman motif that closely resembles the chromen-2-one nucleus of coumarins. Indeed, the THC skeleton has been synthesized from the tricyclic coumarin **202** through a double Grignard reaction with MeMgX, furnishing triol **203** that underwent a ring closure upon treatment with an acid leading to **204** (Scheme 66).[167-168] Coumarin **202** was in turn obtained from Pechmann condensation of olivetol with an appropriate keto ester[167] or by other means.[169] Also, Lydon and co-workers observed that THC concentration increased upon irradiation of cannabis plants with UV-B light, suggesting that cannabinoids play some role in UV protection[170-171]

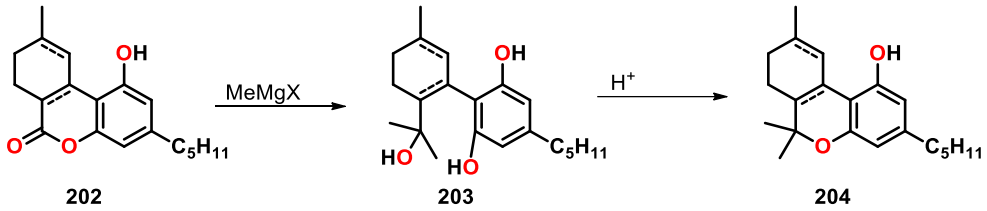

Scheme 66. Synthesis of THC and its derivatives from coumarin derivatives.

THC is the major and the psychoactive component isolated from the female cannabis (*Cannabis sativa* L.; Cannabaceae), one of the most abused drug in many countries for ages. However, cannabis has been used for more than 5000 years to treat diverse ailments.[172] Notwithstanding the continued use of cannabis over the centuries, the scientific evidence of its supposed medicinal benefits remained largely a black-box.

Research in this area was thwarted largely by the use of cannabis as a recreational drug, leading to its use for any purpose being outlawed by many governments across the globe. It is only recently that scientists have taken an interest in systematic investigation of alleged medicinal benefits of cannabis, prompting many countries to implement legislation and systems for medical access and sometimes even recreational use.[173]

So far, research on cannabis has focused on its medicinal properties. The pioneering studies of the biological effects of cannabinoids (terpenophenolic metabolites found in cannabis) were undertaken by the group of Raphael Mechoulam in Israel. Mechoulam and Shvo re-isolated and elucidated the structure of cannabidiol (CBD),[174] the main non-psychoactive component of cannabis which was initially isolated by the groups of Roger Adams[175] and Lord Alexander Todd,[176] but whose structure was only partially known.[177] Mechoulam and co-workers later demonstrated that CBD is a potent anti-inflammatory agent, reduces the production of tumour necrosis factor (TNF)-α,[178] lowers the symptoms of rheumatoid arthritis in a mouse,[178] and was shown to be an effective anti-epileptic agent in clinical trials,[179] as well as many other biological activities.[173, 180-181]

Arguably, the most important contribution by Mechoulam and colleagues was the isolation and structural elucidation of THC and its identification as the psychoactive constituent of cannabis.[182] Following its structural elucidation, THC was shown to be responsible for most of the medicinal properties of cannabis. Currently, THC is used for the treatment of various conditions which include spasticity,[183] anorexia,[183-184] neuropathic pain,[172] and as an anti-nauseant for chemotherapy patients[185] and many more. Pharmacological investigations revealed that THC activates two types of previously unknown G-protein-coupled receptors that were named CB1 present in the central nervous system, also found in other peripheral tissues together with CB2.[186] Recent evidence suggests THC and other cannabinoids act on CB1- and CB2-independent receptors, pointing to cannabinoid activation of other receptors.[187-189]

Despite the progress made in understanding the biological effects of THC and other cannabinoids, little attention has been paid to studying THC as a potential UV

protecting agent. To remedy this situation, we set out to synthesize cardol-derived THC as a potential UV protecting compound.

5.2 Structural features of THC

THC is characterized by an angular tricyclic ring architecture that habours a dimethylchroman nucleus and a cyclohexenyl ring fused to the pyran structural unit in a *trans* fashion (Figure 15). This tricyclic architecture features a hydroxyl group at C–1, an alkyl chain at C–3 and an endo olefin functionality at C–9. Natural and synthetic THC-derivatives with structural variations at the C–3 alkyl chain, position of the alkene functional group and stereochemistry at C–6a and C–10a have been synthesized. Sulfur congeners of THC have also been described.

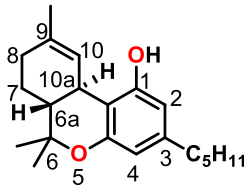

Fig. 15. Chemical structure of Δ^9– *trans*–THC and the popular numbering system.

5.3 Biosynthesis of THC

The hydroxyl group at C–1, *n*-pentyl at C–3 and ether at C–4a indicates that THC **205** biosynthetically arises from olevitol derivatives. Indeed, the accepted paradigm points to the olevitolic acid **206** as the biosynthetic precursor of THC **205**, which in turn is furnished through polyketide synthase mediated cyclization of tetraketide-CoA **207** (Scheme 65). The monoterpinoid fragment is biogenetically derived from farnesyl pyrophosphate **208**. Aromatic prenyltransferase facilitates the union between olevitolic acid **206** and farnesyl pyrophosphate **208** producing cannabigerolic acid (CBGA) **209**, which cyclizes to Δ^9-tetrahydrocannabinolic acid (THCA) **210** in the presence of THCA Synthase. A non-enzymatic decarboxylation of THCA **210** yields THC **205**.

Details on the enzymes and intermediates in the biosynthesis of THC and other cannabinoids is the subject of a recent review.[190]

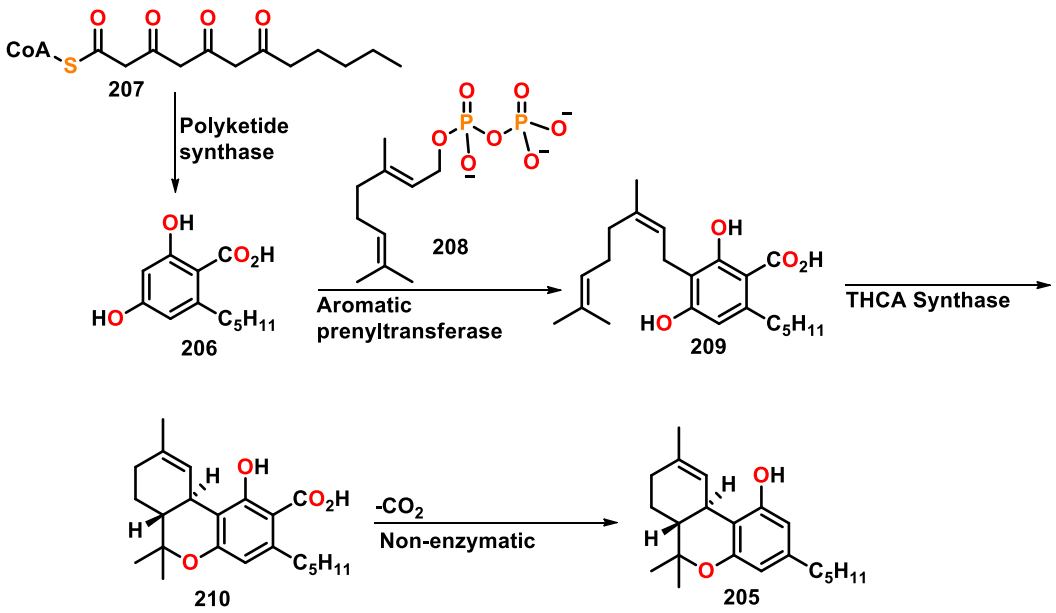

Scheme 65. Summary of the biosynthesis of THC.

5.4 Total syntheses of THC

The majority of synthetic campaigns towards the synthesis of THC **205** rely on the construction of the central pyran ring from CBD or other cyclohexylbenzene intermediates through O5–C6 bond formation, securing the THC backbone (Scheme 66). Facile functional group manipulations may be necessary to get to THC **205** depending on the identity of the monoterpene used. Disparities in the synthesis of THC **205** arise in the construction of the cyclohexylbenzene intermediates **211**. Strategies to cyclohexylbenzene intermediates **211** can be divided into two. Firstly, **211** could arise from the condensation of olivetol **212** or its derivatives and acyclic polyene monoterpenoid fragments, followed by the formation of the cyclohexyl ring through ring-closing methods such as olefin metathesis, biomimetic electrocyclic ring closure or Diels-Alder reaction. Chiral auxiliaries are usually employed to obtain enantiopure THC **205** when employing this route. This is known in the literature as the 'concerted'

approach.[191] A second approach involves coupling olivetol **212** with optically active monocyclic or bicyclic monoterpenoid units. This is termed the "terpenoid chiral pool approach". Most of the cyclic monoterpenoids used are usually natural products, which are available in copious amounts, thus the second strategy for the synthesis of **205** is advantageous as the routes are shorter and eliminate the use of chiral auxiliaries.

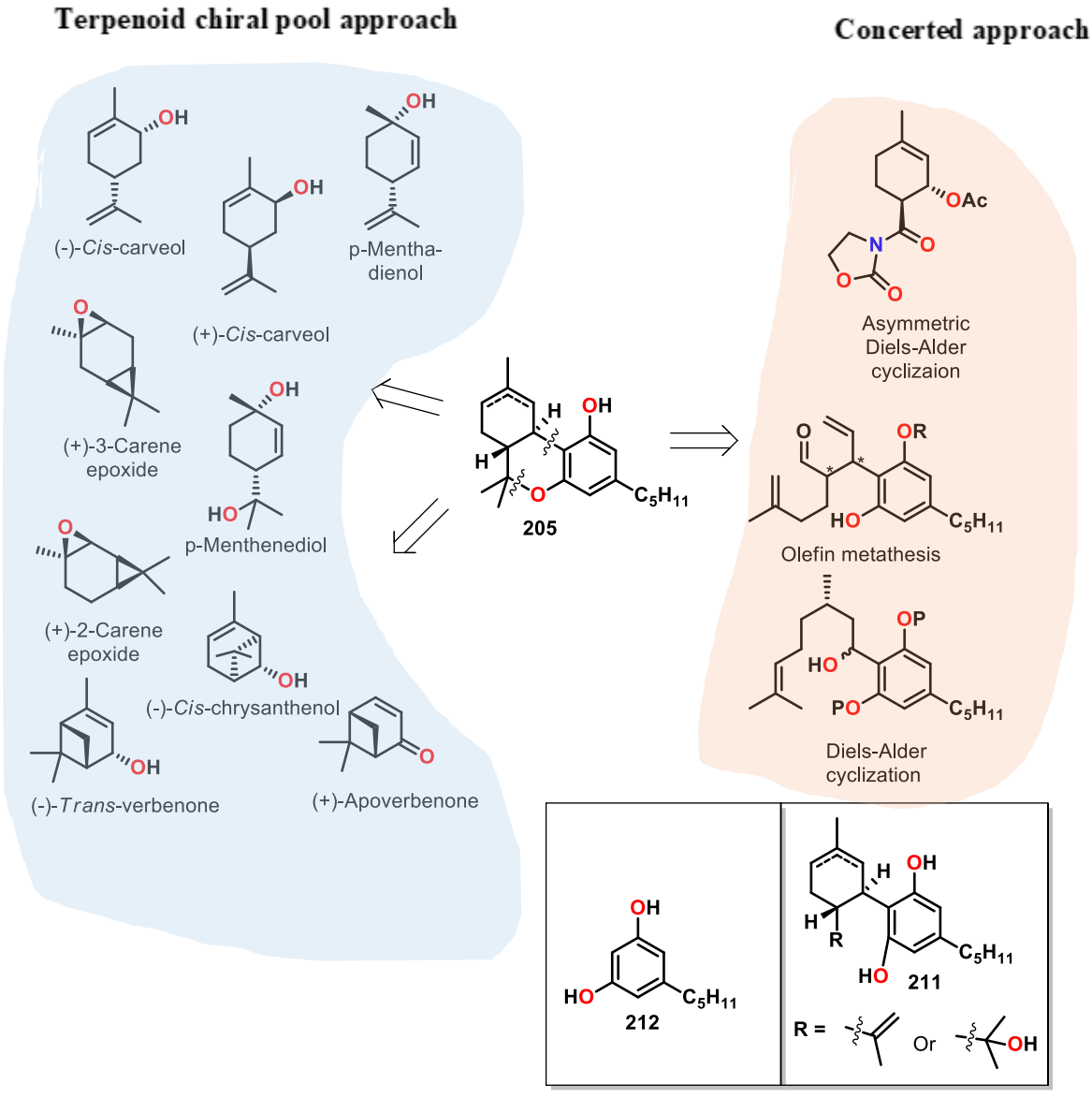

Scheme 66. Summary of the approaches used to access THC.

Total syntheses of THC **205** have been extensively reviewed starting with the book chapter by Razdan, covering literature from the first total synthesis of THC **205** by Mechoulam and Gaoni in 1965 to the Razdan synthesis of 1979.[167] The primary focus of the chapter was the strategies used and nature of the terpenoid motif used with emphasis on the stereochemistry of the resulting THC **205**. A recent overview on the total syntheses of THC **205** from 1965 to 2019 was published by Rutjes and colleagues[191] which follows the same structure as the Razdan book chapter. The reader is directed to these reviews for further reading.

5.5 Aims and objectives

The main aim of this section was to synthesize cardol **10a** derived THC **213**, taking special care to obtain all the atoms from bio-renewable starting materials. To achieve this we hoped to leverage existing protocols that could allow condensation of cardol **10** with a naturally occurring monoterpinoid fragment to give THC **213** in short order.

5.6 Results and discussion

5.6.1 Retrosynthetic analysis of cardol derived THC

Due to our commitment to construct useful compounds with carbons coming from bio-renewable starting materials, we were attracted to the terpinoid chiral pool approach as THC **213** could be accessed in few steps without the need for chiral auxiliaries (Scheme 67). We found the Mechoulam (1967)[192-193] Δ^9–*trans*–THC synthesis particularly attractive due to the use of readily available starting materials. The projected synthesis of cardol **10** derived Δ^9–*trans*–THC **213** is shown in Scheme 67. This method involves acid-catalyzed cyclization of 4-(2-cardoyl)pinene **214** that could arise from the condensation of cardol **10** with the naturally occurring verbenol **215** that was purchased from Sigma-Aldrich. The caveat of this reaction is that the cyclization leads to Δ^8–*trans*–THC **216** that requires isomerization to the desired Δ^9–*trans*–THC **213** through HCl addition, giving **217**. Elimination of HCl would give the desired isomer **213**. However, we found comfort from the realization that this method remains a route of

choice in the syntheses of many other THC derivatives and it is also used in industrial scale syntheses of related compounds – after all these years![167]

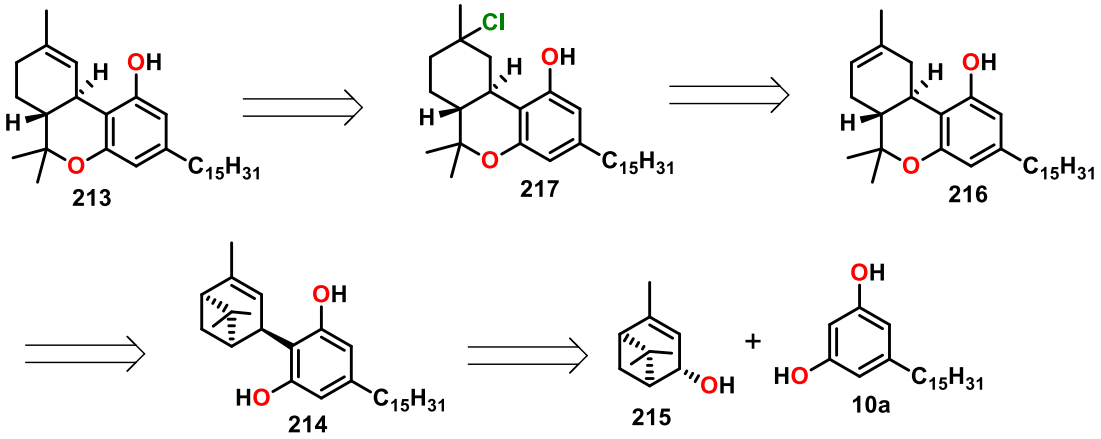

Scheme 67. Retrosynthetic analysis of the synthesis of cardol based THC.

5.6.2 Attempted condensation between cardol and verbenol

As such, cardol **10a** was reacted with verbenol **215** in dichloromethane in the presence of catalytic amounts of methanesulfonic acid (MsOH) (Scheme 68). The TLC analysis showed a single spot having the same R_f value as cardol **10a**, but verbanol **215** was consumed. Column chromatographic purification and the subsequent ^{1}H NMR spectroscopic analysis revealed that cardol **10a** was indeed not consumed. However, analysis of the ^{1}H NMR spectrum of the other spot immediately betrayed its identity as the undesired doubly alkylated 2,4-bis(pinene)cardol **218** as shown by the single aromatic proton signal at 6.24 ppm, accompanied by two alkene protons that overlap, giving the multiplet at 5.74 – 5.67 ppm and the two methine protons at 3.92 and 3.71 ppm. This view is further supported by the two signals at 1.86 and 1.83 ppm, each integrating for three protons, corresponding to the two allylic methyl groups. The ^{13}C NMR spectrum also shows ten signals in the downfield region of the spectrum between 155.1 and 109.7 ppm, which can be accounted for by the proposed structure

corresponding to the six aromatic carbons and the four alkene carbons. The ^{1}H NMR spectrum also shows that 2,4-bis(pinene)cardol **218** was produced as a single diastereomer. This result is in agreement with literature and the stereochemistry around C–3 was confirmed from NMR spectroscopic analysis, therefore we propose that **218** bears the same stereochemistry. The ^{13}C NMR spectrum shows slight racemization, probably induced by the acidic $CDCl_3$ solvent while the sample was left to run overnight. Definitive evidence for dialkylation was obtained from HRMS analysis which gave 589.4985, corresponding to $M+H^+$ in agreement with the calculated mass for **218**. This further strengthens our assigning of the product as **218**. It must be pointed out that 2,4-bis(pinene)cardol **218** was anticipated, albeit, as a minor side product as pointed by Mechoulam in their synthesis of the naturally occurring THC **205**. It is not clear why cardol **10** preferred dialkylation with verbenol **215** under these conditions.

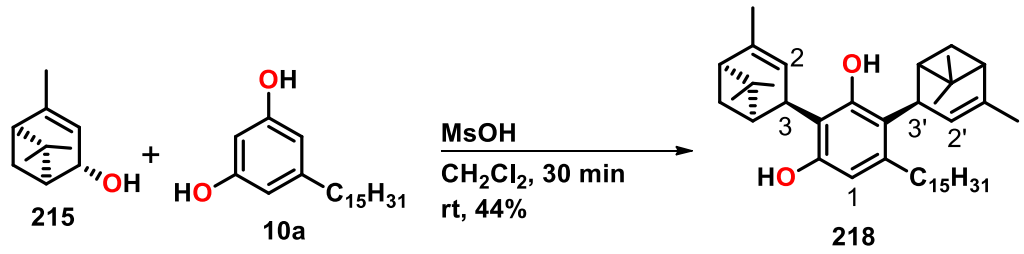

Scheme 68. Attempted synthesis of cardol derived THC using (-)-*cis*-verbenol as the coupling partner.

5.6.3 Condensation of cardol and (+)-*cis*-chrysanthenol

Disappointed, we went back to the literature and searched for an alternative method, guided by our ambition of acquiring all the carbon atoms in our target compound from bio-renewable starting materials. We found our answer in the protocol developed by Razdan (1975) in which THC **205** was synthesized using (+)-*cis*-chrysanthenol **219** as the monoterpenoid fragment.[194] We were particularly excited about this method since it promises to deliver Δ^9–*trans*–THC **213** in a single synthetic operation! Alcohol **219** is not itself a naturally occurring terpene, however, it can be obtained from (-)-*cis*-verbenone **220**, an naturally occurring bicyclic monoterpenoid extracted from pine trees.[195]

Therefore, the first part of our synthesis directed towards THC **213** involved making (+)-*cis*-chrysanthenol **219** from verbenone **220** as disclosed in Scheme 69. Following a procedure developed by Erman,[196] verbenone **220** was irradiated with a 450 W medium pressure Hg lamp in glacial acetic acid under argon for 18 h, affording (-)-*cis*-chrysanthenone **221** in 43% yield. Purification of chrysanthenone **221** was achieved through short-path distillation under reduced pressure. The NMR spectra were in agreement with literature. This photo-induced conversion of (-)-*cis*-verbenone **220** to (-)-*cis*-chrysanthenone **221** involves a 1,3-alkyl shift and is possible due to the α,β-unsaturation on **220**. The detailed mechanistic analysis of this transformation was disclosed by Erman and colleagues.[196] Lithium aluminum hydride reduction of chrysanthenone **221** in ether afforded the requisite (+)-*cis*-chrysanthenol **219** which was used in the subsequent reaction without further purification.

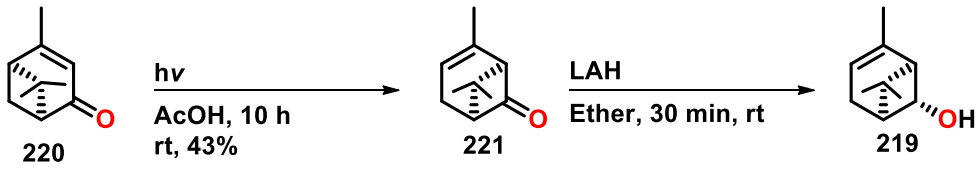

Scheme 69. Synthesis of (+)-*cis*-chrysanthenol

Having secured the terpenoid structural motif, the remaining challenge was the condensation of (+)-*cis*-chrysanthenol **219** with cardol **10a** to produce the coveted THC **213**. As such, cardol **10** and alcohol **219** were advanced to THC **213** by treatment with catalytic amounts of boron trifluoride etherate in methylene chloride at 0 °C (Scheme 70). We noticed that for the reaction to go to completion, we needed to stir the mixture for an hour as opposed to 30 minutes as was the case when the protocol was applied to olivetol. Careful column chromatography on silica gel with 2% EtOAc/hexane and thin layer chromatography in the same solvent system gave pure Δ^9–*trans*–THC **213**, closely resembling the natural THC **205**, with the obvious difference in the alkane region of the ^{1}H NMR and ^{13}C NMR spectra as would be expected. The reaction is believed to go *via* 4-(2-cardoyl)pinene **222** which then suffers nucleophilic attack by one of the hydroxyl groups on the carbon bearing the geminal methyl groups.[194] This

reaction is possible due to ring strain on the cyclobutane motif of **219**. No 2,4-bis(pinene)cardol **218** was obtained.

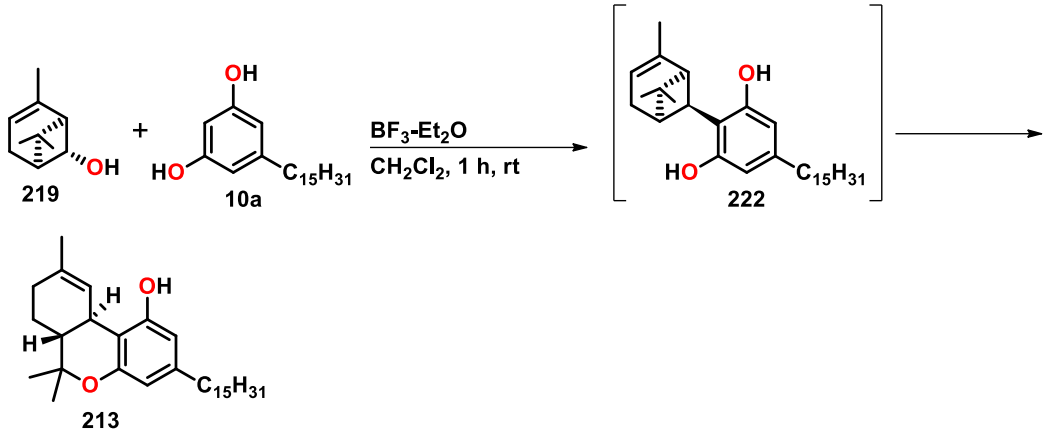

Scheme 70. Synthesis of cardol based THC using (+)-*cis*-chrysanthenol as the monoterpenoid fragment.

This synthesis allows the construction of the C-15 THC derivative **213** in a single step from chrysanthenol **219** and cardol **10a** in a moderate unoptimized yield of 43%. However, it still gives better yields than the most reliable multistep THC synthesis which involves use of gaseous HCl in one of the steps and gives meagre overall yields in the range of 19%. The efficiency (in terms of reaction steps) of this protocol is still not matched by the contemporary methods towards THC **205** syntheses which rely heavily on exotic reagents and require multiple steps.

5.7 Conclusions

We set out to synthesize cardol **10a** derived THC **213** with all its carbon atoms secured from bio-renewable resources. This goal was achieved with astounding success as not only the carbons but all the atoms came from bio-renewable starting materials. The product was obtained in a moderate yield of 43%, but it is still above average when compared with other syntheses. Pivotal to this success was the use of chrysanthenol **219** as a condensation partner to cardol **10a**. Chrysanthenol **219** was in turn derived from verbenone **220** which was converted to chrysanthenone **221** through photochemical means, echoing the theme of chapters 2 and 3 of this theses.

Chapter 6

General conclusions and future outlook

6.1 Synthesis of phenanthridines

The first part of this work was concerned with the application of photo-induced cyclization of phenanthridines from biaryl oxime esters **143a-f** intermediates endowed with at least one methoxy group on one of the benzene groups and the oxime ester on the other benzene ring (accepting ring), both groups positioned *ortho* to the biaryl axis. With the specific focus on the scope and limitations of the method, it was found that this reaction requires an electron-rich accepting ring. The reaction is also sensitive to steric congestion and the position of the additional methoxy groups on the accepting ring is important, preferring *ortho*- and *para*-substituted substrates. The *meta*-substituted substrate **143c** exclusively gave a nitrile **141c**, a decomposition product, which was produced in all substrates in varying degrees. This points to the resonance stabilization of the radical intermediate formed upon photo-irradiations of the substrates.

Table 1. Photo-induced cyclization of biaryl oxime esters

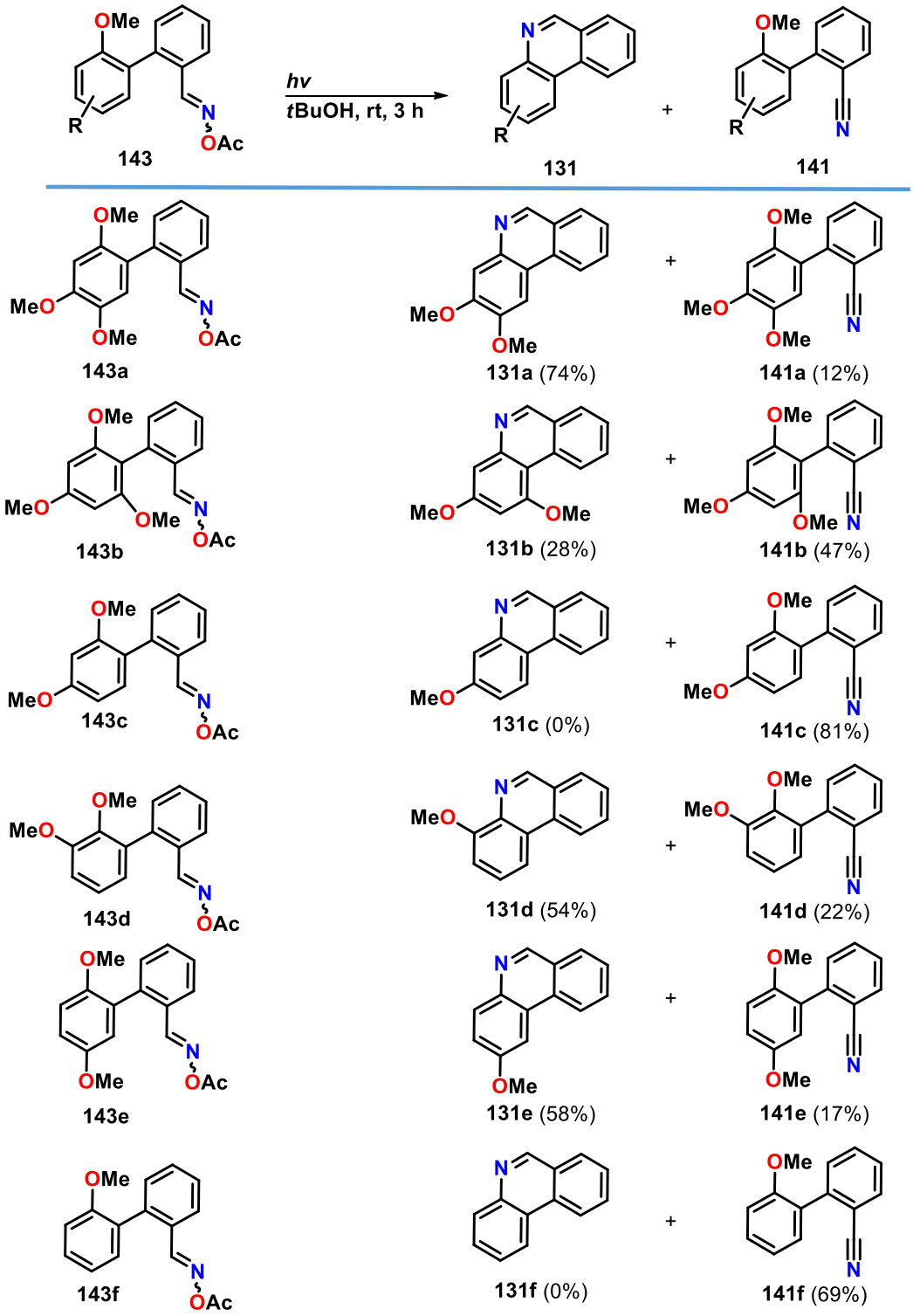

The method was successfully applied in the total synthesis of the naturally occurring trisphaeridine **77**, with the phenanthridine structural motif embedded in its backbone. The synthesis took advantage of palladium-catalyzed Suzuki coupling as a key step to assemble biaryl aldehydes which were used to prepare the key biaryl oxime ester intermediates, followed by the photochemical cyclization. The use of catalysis and UV light in a synthetic route points to the relevance of this work on the current topic of green chemistry and sustainability which seeks to make everyday chemicals in an environmentally safe way.

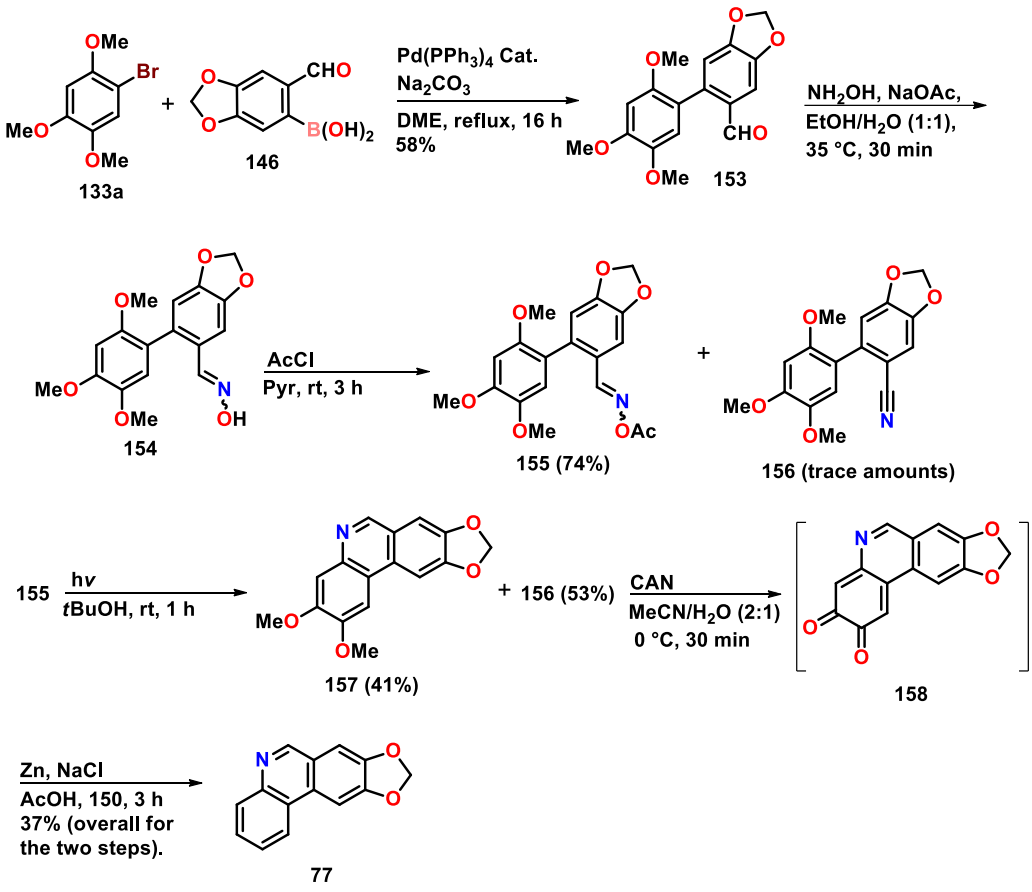

Scheme 47. Total synthesis of trisphaeridine.

6.1.1 Future work

The reaction could, for example, possibly be expanded to the synthesis of other biologically relevant *N*-heterocyclic frameworks like tetrahydroquinolines **223** starting

from appropriately substituted oxime esters such as **224** (Scheme 71). Oxidation of tetrahydroquinolines **223** (where n = 2) could also lead to quinolones, another important family of *N*-heterocyclic compounds found in may important medicines and materials. Another direction this work could take is replacing the UV lamp with LED sources. When used in conjunction with flow chemistry, this could allow the large scale synthesis of phenanthridines, an area of active research that is driving progress in photochemistry.

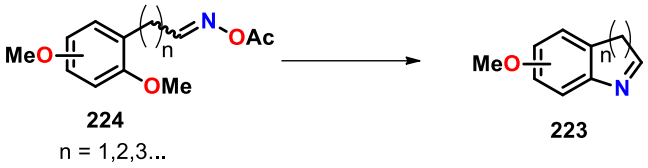

Scheme 71. Proposed photo-induced synthesis of other N-heterocyclic compounds using our photochemical cyclization method.

6.2 Synthesis of coumarins and annellated coumarin derivatives

In keeping with the green and sustainable chemistry theme, we synthesized cardanol **9a** and cardol **10a** based coumarin derivatives that could be used as photosensitizers with possible application as photo-insecticides (Figure 16). The most interesting feature of this part was that all the atoms of the final products could be derived from bio-renewable resources such as malic acid **199**, cardanol **9** and cardol **10a**. Therefore, this work paves the way towards the synthesis of value-added chemicals completely from bio-renewable resources. Most importantly, the feasibility of using CNSL as a source of phenolic starting material is demonstrated.

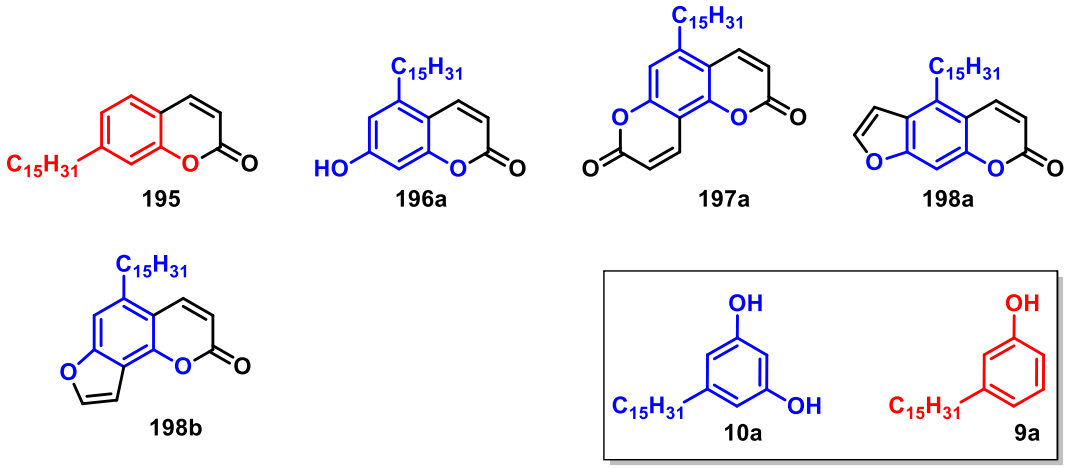

Fig. 16. Cardanol **9a** and cardol **10a** based coumarin derivatives that were synthesized

6.2.1 Future work

Separation of furanocoumarins **198a** and **198b** is of urgent concern as this would allow in depth photo-physical studies of the compounds in collaboration with researchers from physics. If the compounds show favourable photo-physical properties such as high quantum yields then their cytotoxicity would have to be investigated. Subsequent evaluation against crop-damaging insects, possibly in collaboration with researchers from the fields of entomology and agriculture, would be undertaken.

6.3 Synthesis of cardol derived Δ^9– *trans*–tetrahydrocannabinol

Still under the theme of the synthesis of oxa-heterocyclic compounds from completely bio-renewable starting materials, we set out to synthesize THC derivative **213** from cardol **10** and a monoterpenoid condensation partner that could be made from bio-renewable starting material. The aim was to synthesize THC **213** in a concise manner. Attempted synthesis of THC **213** from the MsOH-mediated union of cardol **10** and verbenol **215** led exclusively to dialkylation, giving **218**. However, success was found in reacting cardol **10** with (+)-*cis*-chrysanthenol **219** in the presence of BF_3-Et_2O (Scheme 72). (+)-*cis*-Chrysanthenol was made from photo-induced rearrangement of the naturally-occurring verbenone **220**.

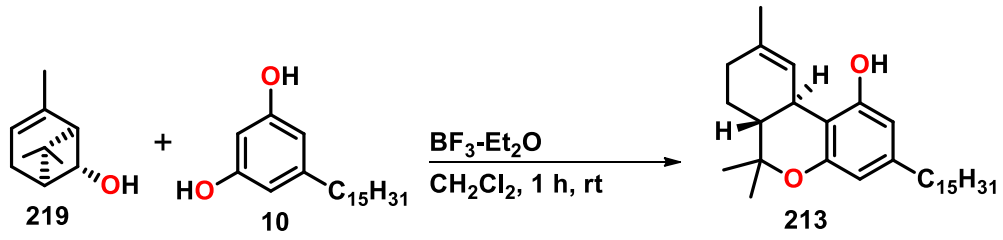

Scheme 72. Synthesis of cardol derived THC

6.3.1 Future work

The work described for the synthesis of THC **213** proved indeed that this compound could be obtained from bio-renewable starting materials. However, the study has some limitations as far as green chemistry is concerned, i.e "non-green" solvents like dichloromethane and diethyl ether were used in the protocol. Future research will be directed towards addressing this limitation by replacing these undesirable solvents with greener alternatives. 2-Methyltetrahydrofuran and cyclopentyl methyl ether will be considered as possible green replacements for dichloromethane and diethyl ether.

On the application side, THC **213** will also be subjected to photo-physical studies to establish whether it is an effective UV absorbing compounds as suggested by its high production in cannabis under UV stress. These photo-physical studies would answer the biosynthetic basis for the naturally occurring THC **205** and could lead to novel applications.

THC **213** will also be tested against a variety of cancer cell lines. Due to the long lipophilic chain, THC **213** is expected to act on CB2 that is found on the periphery and not cross the blood-brain-barrier, thus it will not be psychoactive. In this context, cardol-based THC **213,** differing in stereochemistry with the naturally occurring THC at C–6a and C–10a (Figure 17), could be synthesized using the robust protocol invented by Carreira[197] or other protocols that exist in the literature to access these compounds.

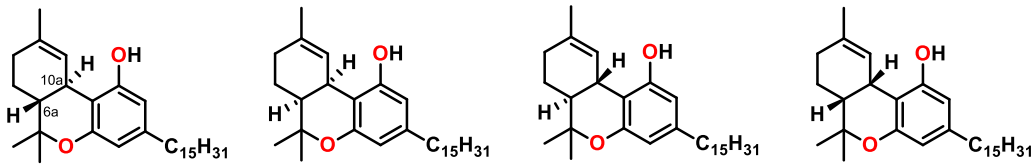

Fig. 17. Possible diastereomers of cardol-derived THC that could be synthesized and tested for biological activity.

Experimental

7.1 General experimental procedures

The reagents were purchased from ACE Chemicals or Sigma-Aldrich and were used without further purification unless otherwise specified. All solvents used (except 1,2-dichlorothane (DME)) were distilled under nitrogen atmosphere prior to use. Dichloromethane (DCM) was distilled over calcium hydride, tetrahydrofuran (THF) was distilled over sodium wire and benzophenone. Purification of reaction products was accomplished by flash chromatography on EM Reagent silica gel 60 (230-400 mesh). Thin layer chromatography was carried out on EM Reagent 0.25 mm silica gel 60-F plates. Visualization was achieved with UV light and Dinitrophenylhydrazine (DNP). Infrared spectra were recorded on a Bruker Tensor 27 Spectrophotometer. NMR spectra were recorded on a Bruker Advance-500 and Bruker Advance-300 and were measured at 500 or 300 MHz for ^{1}H NMR and 125 MHz or 75.47 MHz for ^{13}C NMR. Spectra were recoded using $CDCl_3$, d_4-MeOD or d_6-DMSO as solvents and were reported in ppm using tetramethylsilane (TMS) as an internal standard (0.00 ppm).

7.2 Synthesis of the Phenanthridines

7.2.1 Preparation of halogenated methoxybenzenes

Bromo-2,4,5-trimethoxybenzene 133a

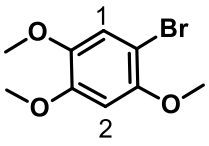

To a cooled (0 ºC) solution of 1,2,4-trimethoxybenzene (5.04 g, 30.0 mmol, 1.0 equiv.) in dichloromethane (50 mL, 0.6 M) was added bromine (1.80 mL, 32.9 mmol, 1.1 equiv.) dropwise via a dropping funnel over 15 min. The reaction mixture was stirred for further 5 min maintaining the same temperature. The resulting mixture was transferred into a separating funnel and was washed with a concentrated aqueous solution of $Na_2S_2O_3$ (50 mL portions) until the aqueous layer gave a clear colour. Removal of the solvent under reduced pressure gave bromo-2,4,5-trimethoxybenzene (18.9 g, 87%) as a white solid. **^{1}H NMR** (400 MHz, $CDCl_3$) δ 7.03 (s, 1H, H-1), 6.56 (s, 1H, H-2), 3.88 (s, 3H, OMe), 3.85 (s, 3H, OMe), 3.82 (s, 3H, OMe). **^{13}C NMR** (101 MHz, $CDCl_3$) δ 150.3, 149.1, 143.8, 116.5, 101.1, 98.9, 57.2, 56.6, 56.3.[20]

2-Bromo-1,3,5-trimethoxybenzene 133b

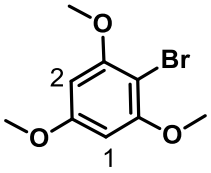

To a solution of 1,3,5-trimethoxybenzene (5.13 g, 30.5 mmol, 1.0 equiv.) in dichloromethane (50 mL, 0.6 M) was added NBS (10.58 g, 33.2 mmol, 1.1 equiv.) in one portion, and the reaction mixture was refluxed gently for 3 h. After cooling, the reaction mixture was filtered, and concentration of the filtrate under vacuum followed by silica gel column chromatographic purification of the residue using 20% EtOAc/hexane gave 2-bromo-1,3,5-trimethoxybenzene (14.6 g, ~100%) as a white solid. **^{1}H NMR** (400 MHz, $CDCl_3$) δ 6.13 (d, *J* = 1.8, 2H, H-1 & H-2), 3.83 (s,

6H, OMe), 3.78 (s, 3H, OMe). **^{13}C NMR** (101 MHz, $CDCl_3$) δ 160.45, 157.4, 91.8, 91.6, 56.3, 55.5.[198]

1-Bromo-2,4-dimethoxybenzene 133c

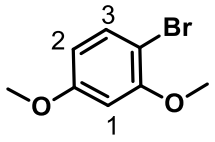

A round-bottom flask equipped with a magnetic stirrer was charged with 1,3-dimethoxybenzene (2.14 g, 15.5 mmol, 2.0 mL, 1.0 equiv.) and acetonitrile (15 mL, 1 M). Then a dropping funnel was placed on the flask and the reaction mixture was cooled to 0 °C through the use of an ice-bath. After this a solution of NBS (2.74 g, 15.5 mmol, 1.0 equiv.) in CH_3CN (15 mL) was added dropwise. The ice-bath was removed and the solution was allowed warm to room temperature. The contents of the flask were stirred for an hour. Upon completion (this was determined with TLC), the reaction quenched with H_2O (15 mL). The volatiles were removed in the rotary and the resulting aqueous solution was extracted with EtOAc (3 × 10 mL). The organic layers were combined, dried over $MgSO_4$ and the solvent was removed under reduced pressure. The crude compound was purified with column chromatography on silica (20% EtOAc/hexane). The title compound was obtained as clear oil.

^{1}H NMR (400 MHz, $CDCl_3$) δ 7.39 (d, *J* = 8.6, 1H, H-3), 6.48 (d, *J* = 2.5, 1H, H-1), 6.39 (dd, *J* = 8.7, 2.7, 1H, H-2), 3.86 (s, 3H, OMe), 3.79 (s, 3H, OMe). **^{13}C NMR** (101 MHz, $CDCl_3$) δ 160.3, 156.6, 133.1, 105.9, 102.5, 100.0, 56.1, 55.6.[199]

1-Iodo-2,3-dimethoxybenzene 133d

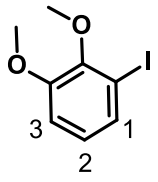

A solution of veratrol (2.07 g, 1.9 mL, 14.5 mmol, 1.0 equiv.) in THF (15 mL, 1 M) was brought to 0 °C by immersion in an ice bath for about 15 min. After this a solution of *n*Buli (1.5 M in *n*-hexane, 14.6 mL, 21.8 mmol, 1.40 g, 1.5 equiv.) was added, and the resulting mixture was allowed to warm to room temperature and stirred for 2 h. The solution was then cooled to -45 °C through liquid nitrogen-chlorobenzene

slush bath and a solution of iodine (4.40 g, 17.4 mmol, 1.1 equiv.) in THF (20 mL). The bath was removed and the reaction mixture was allowed to warm to room temperature and was left to stir for another additional 2 h. The volatiles were removed under reduced pressure and the resulting slurry was dissolved in dichloromethane (50 mL). The solution was washed sequentially with saturated solutions of $NaHSO_3$, $NaHCO_3$, and NaCl. The organic was then dried with $MgSO_4$. The crude product was purified with the aid of column chromatography on silica gel (10% EtOAc/hexane). The title compound was isolated as a yellow oil (3.1 g, yield 83 %).

^{1}H NMR (400 MHz, $CDCl_3$) δ 7.34 (dd, *J* = 8.0, 1.5, 1H, H-3), 6.88 (dd, *J* = 8.2, 1.7, 1H, H-1), 6.79 (td, *J* = 8.1, 1.2, 1H, H-2), 3.85 (s, 3H, OMe), 3.83 (s, 3H, OMe). **^{13}C NMR** (101 MHz, $CDCl_3$) δ 152.9, 149.0, 130.6, 125.9, 112.8, 92.6, 60.4, 56.0.[119]

2-Bromo-4-methoxyphenol 137

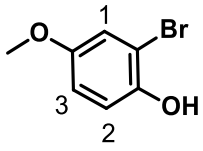

To a solution of 4-methoxyphenol (4.97 g, 40.0 mmol, 1.0 equiv.) in CH_2Cl_2 (0.20 M, 200 mL) at 0 ºC was added bromine (6.84 g, 42.8 mmol, 1.1 equiv.) drop wise. The reaction was allowed to stir for an additional 15 min while maintaining temperature at 0 ºC after which the temperature was increased to RT and continued stirring till the consumption of the starting material (75 min). Upon completion, the reaction mixture was transferred into a separating funnel and the organic layer was washed successively with a saturated solution of sodium thiosulfate ($Na_2S_2O_3$) (40 mL portions) until the aqueous layer gave a clear colour. The organic layer was dried over $MgSO_4$ and the solvent was removed under reduced pressure to yield the product as a yellow solid (8.18 g, quant.). **^{1}H NMR** (400 MHz, $CDCl_3$) δ 7.00 (d, *J* = 3.1, 1H, H-1), 6.95 – 6.89 (m, 1H, H-3), 6.81 – 6.75 (m, 1H, H-2), 5.26 (s, 1H, OH), 3.72 (s, 3H).[200]

2-Bromo-1,4-dimethoxybenzene 133e

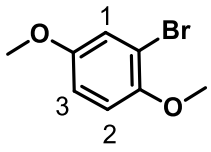

Following literature precedent,[201] To a stirring solution of 2-bromo-4-methoxyphenol (7.00 g, 34.5 mmol, 1.0 equiv.) in acetone (0.30 M, 115 mL) at room temperature was added K_2CO_3 (7.15 g, 58.6 mmol, 1.5 equiv.). After 30 min, dimethyl sulfate (3.92 mL, 41.1 mmol, 1.2 equiv.) was added and the reaction mixture was left to stir at RT for 12 h. The reaction was quenched with water (40 mL) and acetone was evaporated. The resultant mixture was extracted with EtOAc (3 × 40 mL). The combined organic layers were successively washed with water, brine, dried over $MgSO_4$ and concentrated under reduced pressure. The residue was purified by silica gel column chromatography with Hexane/EtOAc(20 %) as eluent to afford the tittle compound. **^{1}H NMR** (500 MHz, $CDCl_3$) δ 7.09 (d, *J* = 2.5, 1H, H-1), 6.81 – 6.74 (m, 2H, H-2 & H-3), 3.78 (s, 3H, OMe), 3.70 (s, 3H, OMe). **^{13}C NMR** (126 MHz, $CDCl_3$) δ 154.0, 150.3, 119.0, 113.6, 112.9, 111.9, 56.8, 55.8.[201]

7.2.2 General Procedure for Suzuki-Miyaura Cross Coupling reactions

To a deoxygenated solution of aryl boronic acid (1.2 equiv.) in DME (0.25 M) stirring under argon was added aryl bromide (1.0 equiv.), $Pd(PPh_3)_4$ (10% mol) and deoxygenated 2 M solution of Na_2CO_3 (4.0 equiv.) in water. The resulting suspension was heated to reflux for 18 h. The resulting solution was allowed to cool to room temperature and was quenched with water (30 mL). The solution was extracted with EtOAc (3 x 50 mL). The combined organic layers were dried over $MgSO_4$. The solvent was removed under reduced pressure and the resulting crude biaryl carbonyls were purified with column chromatography (using EtOAc/hexane mixtures as eluent).

2',4',5'-Trimethoxy-[1,1'-biphenyl]-2-carbaldehyde 132a

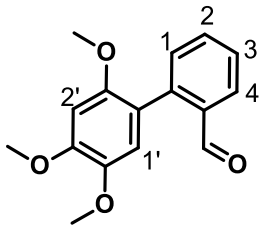

Prepared from 1-bromo-2,4,5-trimethoxybenzene (0.44 g, 1.68 mmol), (2-formylphenyl)boronic acid (0.32 g, 2.02 mmol), tetrakis(triphenylphosphine)palladium(0) (0.20 g, 0.17 mmol) and 2 M aqueous solution of Na_2CO_3 (0.71 g, 3.3 mL, 6.72 mmol). The title compound was obtained as a yellow solid (0.31 g, yield = 68 %). **M.p.** 140–143 °C. **FTIR: ṽ** = 2997.5 (C–H stretch), 1691.1 (C=O), 1596.5 (C=C), 1149.7 (C–O) cm^{-1}. **^{1}H NMR** (300 MHz, $CDCl_3$): δ = 9.80 (s, 1H, ArCO), 7.98 (dd, *J* =7.8, 1.5, 1H, H-4), 7.63 (td, *J* =7.5, 1.5, 1H, H-2), 7.45 (tt, *J* = 7.5, 1.1, 1H, H-3), 7.36 (dd, *J* = 7.7, 1.3, 1H, H-1), 6.84 (s, 1H, H-1'), 6.61 (s, 1H, H-2'), 3.96 (s, 3H, OMe), 3.87 (s, 3H, OMe), 3.69 (s, 3H, OMe). **^{13}C NMR** (75 MHz, $CDCl_3$): δ = 192.8, 150.9, 150.2, 143.5, 141.6, 134.2, 133.6, 131.2, 127.5, 126.7, 118.0, 115.0, 97.4, 56.7, 56.2 ppm. **HRMS** (ESI^+): calcd. for $C_{16}H_{17}O_4$ $[M + H]^+$ 273.1127; found $[M + H]^+$ 273.1123; *m/z* (%) = 273.1127 (100) $[M + H]^+$, 257.1174 (20), 249.0865 (50).

2',4',6'-Trimethoxy-[1,1'-biphenyl]-2-carbaldehyde 132b

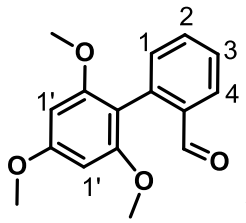

Prepared from 1-bromo-2,4,5-trimethoxybenzene (0.41 g, 1.68 mmol), (2-formylphenyl)boronic acid (0.34 g, 2.02 mmol), tetrakis(triphenylphosphine)palladium(0) (0.20 g, 0.17 mmol) and 2 M aqueous solution of Na_2CO_3 (0.71 g, 3.3 mL, 6.72 mmol). The title compound was obtained as

a yellow solid (0.17 g, yield = 39 %). **M.p.** 132–134 °C. **FTIR: ṽ** = 2935.0 (C–H stretch), 1681.1 (C=O), 1508.4 (C=C), 1026.3 (C–O) cm^{-1}. **^{1}H NMR** (300 MHz, $CDCl_3$): δ = 9.74 (d, *J* = 0.9, 1H, ArCO), 7.98 (ddd, *J* = 7.8, 1.6, 0.5, 1H, H-4), 7.60 (td, *J* = 7.5, 1.5, 1H, H-2), 7.42 (tt, *J* = 7.5, 1.1, 1H, H-3), 7.32 (ddd, *J* = 7.7, 1.3, 0.6, 1H, H-1), 6.23 (s, 2H, H-1'), 3.88 (s, 3H, OMe), 3.69 (s, 6H, OMe). **^{13}C NMR** (75 MHz, $CDCl_3$) δ = 193.1, 161.7, 158.5, 138.1, 134.6, 133.2, 132.8, 127.3, 126.5, 107.5, 90.7, 55.7, 55.4 ppm. **HRMS** (ESI^+): calcd. for $C_{16}H_{17}O_4$ $[M + H]^+$ 273.1127; found $[M + H]^+$ 273.1123; *m/z* (%) = 295.0938 (30), 273.1127 (100) $[M + H]^+$.

2',4'-Dimethoxy-[1,1'-biphenyl]-2-carbaldehyde 132c

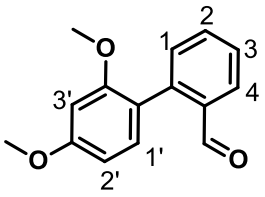

Prepared from 1-bromo-2,4-dimethoxybenzene (0.83 g, 3.84 mmol), (2-formylphenyl)boronic acid (0.69 g, 4.61 mmol), tetrakis(triphenylphosphine)palladium(0) (0.44 g, 0.38 mmol) and 2 M aqueous solution of Na_2CO_3 (1.63 g, 4.62 mL, 15.4 mmol). Yellow oil (0.59 g, yield = 64 %). **^{1}H NMR** (500 MHz, $CDCl_3$): δ = 9.78 (s, 1H, ArCO), 7.95 (d, *J* = 10, 1H, H-4), 7.56 (t, *J* = 10, 1H, H-2), 7.39 (t, *J* = 7.4, 1H, H-3), 7.30 (d, *J* = 7.5, 1H, H-1), 7.16 (d, *J* = 8.3, 1H, H-1'), 6.58 (dd, *J* = 8.2, 2.4, 1H, H-2'), 6.53 (d, *J* = 2.4, 1H, H-3'), 3.81 (s, 3H, OMe), 3.66 (s, 3H, OMe). **^{13}C NMR** (126 MHz, $CDCl_3$): δ = 192.7, 161.4, 157.6, 141.7, 134.2, 133.6, 132.0, 131.4, 127.4, 126.6, 119.4, 105.0, 98.5, 55.4, 55.4 ppm.[202]

2',3'-Dimethoxy-[1,1'-biphenyl]-2-carbaldehyde 132d

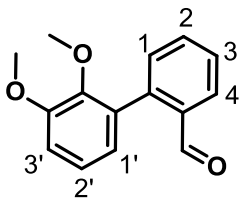

Prepared from 1-iodo-2,3-dimethoxybenzene (0.31 g, 1.13 mmol), (2-formylphenyl)boronic acid (0.26 g, 1.36 mmol), tetrakis(triphenylphosphine)palladium(0) (0.20 g, 0.17 mmol) and 2 M aqueous

solution of Na_2CO_3 (0.71 g, 3.3 mL, 6.72 mmol). Yellow solid (0.22 g, yield = 62 %). **^{1}H NMR** (500 MHz, $CDCl_3$): δ = 9.77 (s, 1H, ArCO), 7.94 (dd, *J* = 7.8, 1.5, 1H, H-4), 7.55 (td, *J* = 7.5, 1.5, 1H, H-2), 7.41 (tt, *J* = 7.6, 1.1, 1H, H-3), 7.32 (dd, *J* = 7.6, 1.3, 1H, H-1), 7.07 (t, *J* = 7.9, 1H, H-2'), 6.93 (dd, *J* = 8.2, 1.5, 1H, H-3'), 6.81 (dd, *J* = 7.7, 1.5, 1H, H-1'), 3.83 (s, 3H, OMe), 3.39 (s, 3H, OMe). **^{13}C NMR** (126 MHz, $CDCl_3$): δ = 192.2, 152.7, 146.5, 141.4, 133.8, 133.4, 132.2, 131.1, 127.9, 126.9, 124.3, 123.1, 112.7, 60.4, 56.0 ppm.[203]

2',5'-Dimethoxy-[1,1'-biphenyl]-2-carbaldehyde 132e

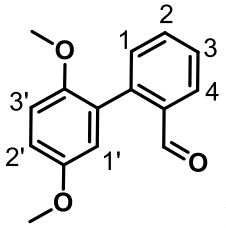

Prepared from 2-bromo-1,4-dimethoxybenzene (0.34 g, 1.51 mmol), (2-formylphenyl)boronic acid (0.28 g, 1.82 mmol), tetrakis(triphenylphosphine)palladium(0) (0.17 g, 0.15 mmol) and 2 M aqueous solution of Na_2CO_3 (0.64 g, 2.8 mL, 6.04 mmol).The title compound was obtained as a white solid (0.22 g, yield = 61 %). **FTIR: $\tilde{\nu}$** = 2909.0 (C–H stretch), 1690.5 (C=O), 1593.9 (C=C), 1052.7 (C–O) cm^{-1}. **^{1}H NMR** (500 MHz, $CDCl_3$) δ 9.69 (s, 1H, ArCO), 7.87 (dd, *J* = 7.8, 1.5, 1H, H-4), 7.51 (td, *J* = 7.5, 1.5, 1H, H-2), 7.35 (tt, *J* = 7.6, 1.1, 1H, H-3), 7.24 (dd, *J* = 7.7, 1.2, 1H, H-1), 6.82 (dd, *J* = 8.9, 3.0, 1H, H-2'), 6.78 (s, 1H, H-1'), 6.76 (d, *J* = 3.1 Hz, 1H, H-3'), 3.68 (s, 3H, OMe), 3.54 (s, 3H, OMe). **^{13}C NMR** (126 MHz, $CDCl_3$): δ = 192.5, 153.8, 150.7, 141.6, 134.0, 133.7, 131.1, 127.9, 127.7, 126.6, 117.3, 114.4, 111.8, 55.9, 55.8 ppm.[204]

2'-Methoxy-[1,1'-biphenyl]-2-carbaldehyde 132f

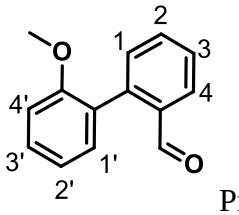

Prepared from 1-bromo-2-methoxybenzene (0.28 g, 1.51 mmol), (2-formylphenyl)boronic acid (0.25 g, 1.82 mmol),

tetrakis(triphenylphosphine)palladium(0) (0.17 g, 0.15 mmol) and 2 M aqueous solution of Na_2CO_3 (0.64 g, 2.8 mL, 6.04 mmol). The title compound was obtained a slightly yellow solid (0.24 g, yield = 64 %).**^{1}H NMR** (400 MHz, $CDCl_3$) δ 9.79 (s, 1H, ArCO), 7.98 (dd, *J* = 7.8, 1.5, 1H, H-4), 7.61 (td, *J* = 7.5, 1.4, 1H, H-2), 7.49 – 7.43 (m, 1H, H-3), 7.40 (td, *J* = 7.9, 1.7, 1H, H-1'), 7.36 – 7.31 (m, 1H, H-3'), 7.27 (dd, *J* = 7.5, 1.8, 1H, H-1), 7.10 – 7.03 (m, 1H, H-2'), 6.96 (d, *J* = 8.3, 1H, H-4'), 3.71 (s, 3H, OMe). **^{13}C NMR** (101 MHz, $CDCl_3$) δ 192.6, 156.5, 141.8, 134.1, 133.7, 131.4, 131.2, 130.0, 127.7, 126.9, 126.6, 121.0, 110.7, 55.4 ppm.[204]

6-(2,5-Dimethoxyphenyl)benzo[*d*][1,3]dioxole-5-carbaldehyde 147

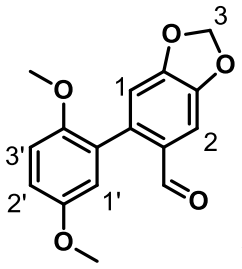

Prepared from 2-bromo-1,4-dimethoxybenzene (3.0 g, 13.2 mmol), (6-formylbenzo[*d*][1,3]dioxol-5-yl)boronic acid (2.38g, 15.8mmol) tetrakis(triphenylphosphine)palladium(0) (1.5 g, 1.32 mmol) and 2 M aqueous solution of Na_2CO_3 (5.6 g, 26.4 mL, 52.8 mmol). The title compound was obtained as a white solid (2.26 g, yield = 60 %). **FTIR: ṽ** = 2960.2, 2898.4 (C–H stretch), 1615.1 (C=O), 1505.9 (C=C), 1050.3 (C–O) cm^{-1}. **^{1}H NMR** (500 MHz, $CDCl_3$): δ = 9.58 (s, 1H, ArCO), 7.44 (s, 1H, H-2), 6.92 (dd, *J* = 8.9, 3.0, 1H, H-2'), 6.88 (d, *J* = 9.0, 1H, H-3'), 6.80 (d, *J* = 2.9, 1H, H-1'), 6.78 (s, 1H, H-1), 6.06 (d, *J* = 6.7, 2H, H-3), 3.79 (s, 3H, OMe), 3.69 (s, 3H, OMe). **^{13}C NMR** (126 MHz, $CDCl_3$): δ = 190.9, 153.6, 152.2, 150.9, 147.9, 138.9, 129.02, 127.3, 117.5, 114.4, 111.9, 110.8, 105.8, 102.0, 56.0, 55.8 ppm.

5-Chloro-2',4',5'-trimethoxy-[1,1'-biphenyl]-2-carbaldehyde 149a

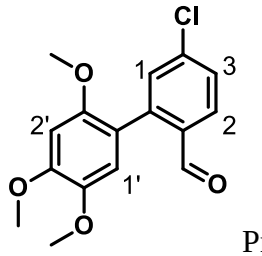

Prepared from 1-bromo-2,4,5-trimethoxybenzene (0.52 g, 5.02 mmol), (5-chloro-2-formylphenyl)boronic acid (1.11 g, 6.02 mmol) tetrakis(triphenylphosphine)palladium(0) (0.58 g, 0.50 mmol) and 2 M aqueous solution of Na_2CO_3 (2.13 g, 10.0 mL, 20.1 mmol). The pure product was obtained as a light brown solid (0.97 g, yield = 63 %). **M.p.** 160–162 °C. **FTIR: $\tilde{\nu}$** = 2999.8 (C–H stretch), 1681.1 (C=O), 1608.4 (C=C), 1044.0 (C–O) cm^{-1}. **^{1}H NMR** (400 MHz, $CDCl_3$) δ 9.73 (s, 1H, ArCO), 7.95 – 7.87 (m, 1H, H-1), 7.42 (dd, *J* = 8.3, 2.2, 1H, H-3), 7.36 (s, 1H, H-1'), 6.82 (d, *J* = 2.0, 1H, H-1), 6.60 (s, 1H, H-2'), 3.97 (s, 3H, OMe), 3.88 (s, 3H, OMe), 3.71 (s, 3H, OMe). **^{13}C NMR** (101 MHz, $CDCl_3$) δ 191.5, 150.9, 150.6, 143.5, 143.1, 139.8, 132.6, 131.1, 128.2, 127.8, 116.4, 114.6, 97.2, 56.7, 56.2, 56.2 ppm.

6-(2,4,5-Trimethoxyphenyl)benzo[*d*][1,3]dioxole-5-carbaldehyde 153

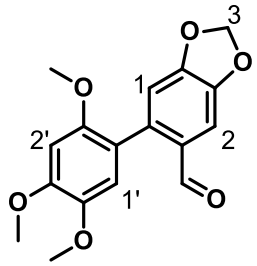

The title compound **21** was prepared from 1-bromo-2,4,5-trimethoxybenzene (1.14 g, 4.66 mmol), (6-formylbenzo[*d*][1,3]dioxol-5-yl)boronic acid (2.51 g, 5.59 mmol, 1.2 equiv.), tetrakis(triphenylphosphine)palladium(0) (0.54 g, 0.47 mmol) and an aqueous 2M aqueous solution of Na_2CO_3 (1.97 g, 9.2 mL, 18.6 mmol). The product was obtained as a cream solid (1.1 g, yield = 58 %). **M.p.** 89-90 °C. **FTIR: $\tilde{\nu}$** = 2843.5 (C–H stretch), 1691.7 (C=O), 1604.9 (C=C), 1050.7 (C–O) cm^{-1}. **^{1}H NMR** (300 MHz, $CDCl_3$): δ = 9.61 (s, 1H, ArCO), 7.44 (s, 1H, H-1), 6.80 (s, 1H, H-2), 6.79 (s, 1H, H-1'), 6.61 (s, 1H, H-2'), 6.08 (d, *J* = 3.4, 2H, H-3), 3.97 (s, 3H, OMe), 3.87 (s, 3H, OMe), 3.73 (s, 3H, OMe). **^{13}C NMR** (101 MHz, $CDCl_3$) δ 191.1,

152.2, 151.0, 150.0, 147.5, 143.1, 139.0, 129.1, 117.5, 115.0, 110.9, 105.8, 102.0, 97.2, 56.6, 56.3, 56.2. **HRMS** (ESI^+): calcd. for $C_{17}H_{17}O_6$ $[M + H]^+$ 317.1025; found $[M + H]^+$ 317.1013; *m/z* (%) = 339.0830 (23), 317.1013 (100) $[M + H]^+$, 289.1062 (18).

7.2.3 Attempted synthesis of oxime ethers

2',4',5'-Trimethoxy-[1,1'-biphenyl]-2-carbaldehyde *O*-phenyl oxime 130a

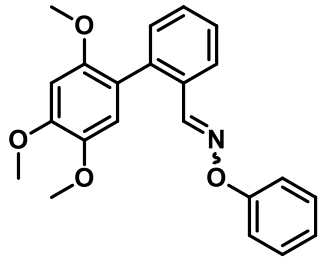

Method A

To a solution of *O*-phenylhydroxyamine hydrochloride (55.4 mg, 0.38 mmol, 1.0 equiv.) in anhydrous pyridine (10 mL) was added 2',4',5'-trimethoxy-[1,1'-biphenyl]-2-carbaldehyde (0.103 g, 0.38 mmol, 1.0 equiv.) in one portion. The reaction was allowed to stir for 18 h at room temperature under Argon. Upon completion, the reaction was quenched with H_2O (30 mL) and was extracted with EtOAc (3 × 20 mL). The organic layer was combined and washed with aq. $CuSO_4$ (3 × 30 mL), and then with brine. The organic phase was dried over $MgSO_4$, and the solvent was removed under reduced pressure. The crude product was purified by short column chromatography (silica gel; 20% EtOAc/hexane). The product was fomed as a white solid and was identified to be 2',4',5'-trimethoxy-[1,1'-biphenyl]-2-carbonitrile (94.9 mg, yield = 93%)

Method B

To a solution of *O*-phenylhydroxylamine hydrochloride (74.6 mg, 0.51 mmol, 1.0 equiv.) in 1,4-dioxane (5.0 mL) was added 2',4',5'-trimethoxy-[1,1'-biphenyl]-2-carbaldehyde (0.14 g, 0.51 mmol, 1.0 equiv.) and a single drop of 0.5 N HCl and the

solution was allowed to stir for 18 h at room temperature. A white precipitate that formed was filtered and re-desolved in EtOAc. The resulting solution was successively washed with water and brine and dried over $MgSO_4$. The solvent was removed on the rotary evaporator and the sample was submitted for NMR analyses. Unfortunately, the oxime ether was not obtained, instead 2',4',5'-trimethoxy-[1,1'-biphenyl]-2-carbonitrile was formed (the NMR spectroscopic data is presented below) in quantitative yield.

2',4'-Dimethoxy-[1,1'-biphenyl]-2-carbaldehyde O-phenyl oxime 141c

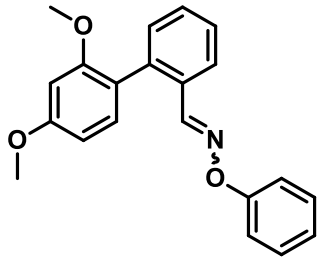

Was attempted using *Method A* from *O*-phenylhydroxyamine hydrochloride (72.5 mg, 0.50 mmol, 1.0 equiv.) and 2',4'-dimethoxy-[1,1'-biphenyl]-2-carbaldehyde (0.121 g, 0.50 mmol, 1.0 equiv.) in anhydrous pyridine (10 mL). The corresponding nitrile (spectroscopic data shown below) was obtained as a pale yellow solid quantitatively. Purification was effected with column chromatography (eluent; 20% EtOAc/hexane).

2',4'-Dimethoxy-[1,1'-biphenyl]-2-carbaldehyde O-phenyl oxime 141e

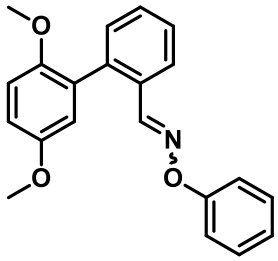

Was attempted following *Method A* from *O*-phenylhydroxyamine hydrochloride (68.9 mg, 0.48 mmol, 1.0 equiv.) and 2',5'-dimethoxy-[1,1'-biphenyl]-2-carbaldehyde (0.115 g, 0.48 mmol, 1.0 equiv.) in anhydrous pyridine (10 mL). The corresponding nitrile (spectroscopic data shown below) was obtained as a pale yellow solid quantitatively after column chromatographic purification using 10% EtOAc/hexane as eluent.

7.2.4 Oxime formation general procedure

To a solution of biaryl carbonyl (1.0 equiv.) in EtOH (0.1 M) was added hydroxylamine hydrochloride (2.0 equiv.) and sodium acetate (2.0 equiv.). The resulting suspension was stirred under reflux for 18 h. The contents of the flask were allowed to cool to room temperature upon which a precipitate formed. The solvent was filtered and the resulting white solid was dissolved in EtOAc and washed successively with water and brine. The organic layer was dried over $MgSO_4$ and the volatiles were removed under reduced pressure. The resulting biaryl oximes were used without further purification.

A two-necked flask equipped with a magnetic bar and a dropping funnel was charged with a biaryl oxime (1.0 equiv.), dry CH_2Cl_2 and trimethylamine (2.0 equiv.). The solution was cooled to 0º C in ice bath and a solution of acetyl chloride (2.0 equiv.) in dry CH_2Cl_2 (2.75 M) was added dropwise for 15 min. The ice bath was removed and resulting solution was allowed to slowly warm to room temperature. The reaction mixture was stirred overnight. Water (30 mL) was added and the layers were separated. The aqueous layer was extracted with CH_2Cl_2 (3 x 30 mL). The combined organic layer was washed with saturated aqueous $NaHCO_3$ solution (10 mL) and brine (10 mL). The solution was dried over $MgSO_4$ and the solvent was evaporated under reduced pressure. The resulting crude oxime esters were purified with column chromatography.

2',4',5'-Trimethoxy-[1,1'-biphenyl]-2-carbaldehyde O-acetyl oxime 143a

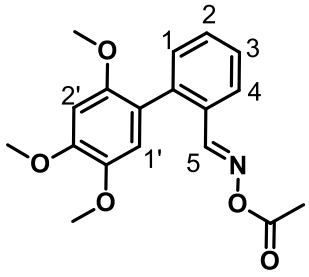

Prepared from 2',4',5'-trimethoxy-[1,1'-biphenyl]-2-carbaldehyde (0.25 g, 0.98 mmol, 1.0 equiv.), hydroxylamine hydrochloride (0.13 g, 1.84 mmol, 2.0 equiv.), sodium acetate (0.17 g, 1.84 mmol, 2.0 equiv.), trimethylamine (0.27 g, 0.37 mL, 1.84 mmol, 2.0 equiv.) and acetyl chloride (0.21 g, 1.4 mL, 1.84 mmol, 2.0 equiv.). The title compound was obtained as a white solid (0.32 g, yield =

76 %). **M.p.** 68-71 °C. **FTIR: ṽ** = 2990.5 (C–H stretch), 1610.6 (C=O), 1510.1 (C=C), 1439.8, 1348.0 (N–O stretch), 1203.8 (C–O), 755.7 cm^{-1}. **^{1}H NMR** (500 MHz, $CDCl_3$) δ 8.15 (s, 1H, H-5), 8.12 (dt, *J* = 7.9, 0.9, 1H, H-4), 7.50 (td, *J* = 7.5, 1.4, 1H, H-2), 7.41 – 7.36 (m, 1H, H-1), 7.32 (dd, *J* = 7.7, 1.2, 1H, H-3), 6.72 (s, 1H, H-1'), 6.62 (s, 1H, H-2'), 3.97 (s, 3H, OMe), 3.84 (s, 3H, OMe), 3.69 (s, 3H, OMe), 2.18 (s, 3H, CO_2Me). **^{13}C NMR** (126 MHz, CDCl3) δ 169.0, 155.7, 150.7, 149.9, 143.3, 139.8, 131.2, 130.9, 128.9, 127.5, 126.4, 119.0, 115.0, 97.8, 56.6, 56.5, 56.2, 19.7.

2',4',6'-Trimethoxy-[1,1'-biphenyl]-2-carbaldehyde O-acetyl oxime 143b

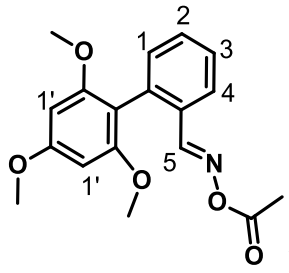

Prepared from 2',4',6'-trimethoxy-[1,1'-biphenyl]-2-carbaldehyde (0.13 g, 0.48 mmol, 1.0 equiv.), hydroxylamine hydrochloride (0.19 mg, 0.96 mmol, 2.0 equiv.), sodium acetate (58 mg, 0.96 mmol, 2.0 equiv.), trimethylamine (97 mg, 133 μL, 0.96 mmol, 2.0 equiv.) and acetyl chloride (75 mg, 69 μL, 0.96 mmol, 2.0 equiv.). The product was obtained as a white solid (83 mg, yield = 53%). **M.p.** 70-72 °C. **FTIR: ṽ** = 2935.6 (C–H stretch), 1604.7 (C=O), 1497.6 (C=C), 1458.2, 1340.5 (N–O stretch), 1255.3 (C–O), 755.7 cm^{-1}. **^{1}H NMR** (500 MHz, $CDCl_3$) δ 8.12 (d, *J* = 7.9, 1H, H-1), 8.06 (s, 1H, H-5), 7.47 (t, *J* = 7.5, 1H, H-4), 7.36 (t, *J* = 7.6, 1H, H-2), 7.27 – 7.23 (m, 1H, H-3), 6.22 (s, 2H, H-1'), 3.88 (s, 3H, OMe), 3.68 (s, 6H, OMe), 2.17 (s, 3H, CO_2Me). **^{13}C NMR** (126 MHz, $CDCl_3$) δ 169.3, 161.6, 158.4, 155.6, 136.1, 132.3, 130.9, 129.5, 127.3, 126.1, 108.5, 90.7, 55.8, 55.4, 19.7 ppm.

2',4'-Dimethoxy-[1,1'-biphenyl]-2-carbaldehyde *O*-acetyl oxime 143c

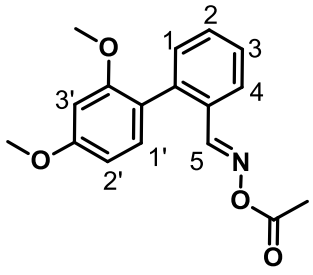

Prepared from 2',4'-dimethoxy-[1,1'-biphenyl]-2-carbaldehyde (0.40 g, 1.72 mmol, 1.0 equiv.), hydroxylamine hydrochloride (0.24 g, 3.44 mmol, 2.0 equiv.), sodium acetate (0.28 g, 3.41 mmol, 2.0 equiv.), trimethylamine (0.34 g, 0.47 mL, 3.41 mmol, 2.0 equiv.) and acetyl chloride (0.27 g, 0.24 mL, 3.41 mmol, 2.0 equiv.). White solid (0.33 g, yield = 65 %). **M.p.** 74-76 °C. **FTIR: ṽ** = 2951.1 (C–H stretch), 1778.8 (C=O), 1581.3 (C=C), 1466.5, 1365.0 (N–O stretch), 1270.1 (C–O), 774.1 cm^{-1}. **^{1}H NMR** (500 MHz, $CDCl_3$) δ 8.13 (d, *J* = 7.7, 2H, H-1 & H-5), 7.51 (td, *J* = 7.5, 1.3, 1H, H-3), 7.43 – 7.38 (m, 1H, H-2), 7.31 (dd, *J* = 7.7, 1.3, 1H, H-4), 6.95 – 6.90 (m, 2H, H-1' & H-2'), 6.76 (d, *J* = 2.7, 1H, H-3'), 3.79 (s, 3H, OMe), 3.68 (s, 3H, OMe), 2.17 (s, 3H, CO_2Me). **^{13}C NMR** (126 MHz, $CDCl_3$) δ 169.1, 161.2, 157.4, 155.8, 140.0, 132.1, 131.2, 131.2, 128.9, 126.4, 120.4, 104.8, 98.7, 55.5, 19.7 ppm. **HRMS** (ESI^+): calcd. for $C_{17}H_{17}NO_4Na$ $[M + Na]^+$ 322.1055; found $[M + Na]^+$ 322.1041; *m/z* (%) = 291.2824 (7), 338.0771 (7), 322.1041 (100) $[M + Na]^+$, 309.2041 (5).

2',3'-Dimethoxy-[1,1'-biphenyl]-2-carbaldehyde O-acetyl oxime 143d

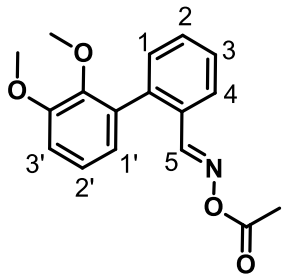

Prepared from 2',3'-dimethoxy-[1,1'-biphenyl]-2-carbaldehyde (0.17 g, 0.63 mmol, 2.0 equiv.), hydroxylamine hydrochloride (0.88 mg, 1.27 mmol, 2.0 equiv.), sodium acetate (0.12 g, 1.27 mmol, 2.0 equiv.), trimethylamine (0.13 g, 0.18 mL, 1.27 mmol, 2.0 equiv.) and acetyl chloride (0.20 g, 1.3 mL, 2.54 mmol, 2.0

equiv.). The title compound was obtained as white solid (0.16 g, yield = 76%). **M.p.** 64-66 °C. **FTIR: ṽ** = 2943.7 (C–H stretch), 1742.0 (C=O), 1531.7 (C=C), 1438.1, 1329.2 (N–O stretch), 1281.6 (C–O) cm^{-1}. **^{1}H NMR** (400 MHz, $CDCl_3$) δ 8.21 (s, 1H, H-5), 8.17 (d, *J* = 7.9, 1H), 7.49 (dd, *J* = 7.4, 1.4, 1H), 7.43 (d, *J* = 8.2, 1H), 7.34 (dd, *J* = 7.7, 1.3, 1H), 7.14 (t, *J* = 7.9, 1H), 7.00 (dd, *J* = 8.3, 1.5, 1H), 6.79 (dd, *J* = 7.6, 1.5, 1H), 3.92 (s, 3H, OMe), 3.48 (s, 3H, OMe), 2.15 (s, 3H, CO_2Me). **^{13}C NMR** (101 MHz, $CDCl_3$) δ 168.8, 155.2, 152.9, 146.3, 139.6, 133.2, 131.0, 130.7, 128.5, 127.8, 126.5, 124.2, 123.2, 112.4, 60.5, 55.9, 19.6 ppm. **HRMS** (ESI^+): calcd. for $C_{17}H_{17}NO_4Na$ [M + Na]$^+$ 322.1055; found [M + Na]$^+$ 322.1161; *m/z* (%) = 322.1161 (20) [M + Na]$^+$, 300.1338 (5), 272.1378 (25), 258.1216 (100), 240.1106 (95), 225.0989 (10).

2',5'-Dimethoxy-[1,1'-biphenyl]-2-carbaldehyde O-acetyl oxime 143e

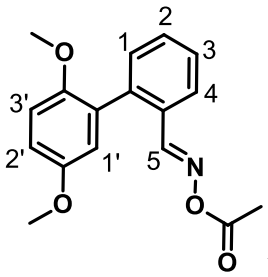

Prepared from 2',5'-dimethoxy-[1,1'-biphenyl]-2-carbaldehyde (0.15 g, 0.62 mmol, 1.0 equiv.), hydroxylamine hydrochloride (86 mg, 1.24, 2.0 equiv. mmol), sodium acetate (0.14 g, 1.23 mmol, 2.0 equiv.), trimethylamine (0.17 g, 0.23 mL, 1.24 mmol, 2.0 equiv.) and acetyl chloride (0.15 g, 0.12 mL, 1.234mmol, 2.0 equiv.). The product was obtained as a white solid (0.14 g, yield = 79%). **M.p.** 67-70 °C. **FTIR: ṽ** = 2997.5, 2937.7 (C–H stretch), 1604.1 (C=O), 1563.9 (C=C), 1438.1, 1312.6 (N–O stretch), 1203.4 (C–O), 772.5 cm^{-1}. **^{1}H NMR** (400 MHz, $CDCl_3$) δ 8.14 (d, *J* = 2.6, 1H, H-1), 8.12 (s, 1H, H-5), 7.51 (t, *J* = 7.5, 1H, H-2), 7.41 (t, *J* = 7.6, 1H, H-3), 7.31 (d, *J* = 7.6, 1H, H-4), 6.93 (d, *J* = 3.1, 2H, H-2' & H-3'), 6.76 (d, *J* = 2.5, 1H, H-1'), 3.80 (s, 3H, OMe), 3.68 (s, 3H, OMe), 2.18 (s, 3H, CO_2Me). **^{13}C NMR** (101 MHz, $CDCl_3$) δ 169.1, 155.4, 153.7, 150.6, 139.8, 131.2, 130.7, 128.7, 127.8, 126.4, 117.2, 114.4, 112.3, 56.1, 55.8, 19.7 ppm. **HRMS** (ESI^+): calcd. for $C_{17}H_{17}NO_4Na$ [M + Na]$^+$ 322.1055; found [M + Na]$^+$ 322.1048; *m/z* (%) = 323.1076 (20), 322.1048 (100)[M + Na]$^+$, 317.1499 (18) 300.1233 (20).

2'-Methoxy-[1,1'-biphenyl]-2-carbaldehyde O-acetyl oxime 143f

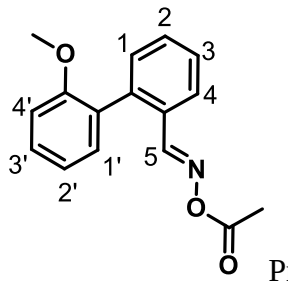

Prepared from 2'-methoxy-[1,1'-biphenyl]-2-carbaldehyde (0.19 g, 0.85 mmol, 1.0 equiv.), hydroxylamine hydrochloride (0.12 g, 1.72 mmol, 2.0 equiv.), sodium acetate (0.14 g, 1.72 mmol, 2.0 equiv.), trimethylamine (0.17 g, 0.25 mL, 1.72 mmol, 2.0 equiv.) and acetyl chloride (0.15 g, 0.18 mL, 1.72 mmol, 2.0 equiv.). The product was obtained as a tan solid (0.14 g, yield = 62%). **M.p.** 92-93 °C. **FTIR: ṽ** = 2939.3 (C–H stretch), 1756.5 (C=O), 1595.6 (C=C), 1430.1, 1364.3 (N–O stretch), 1256.5 (C–O), 746.2 cm^{-1}. **^{1}H NMR** (500 MHz, $CDCl_3$) δ 8.12 (s, 1H, H-5), 7.49 (td, *J* = 7.6, 1.4, 1H, H-1), 7.42 – 7.36 (m, 3H, H-1', H-2 & H-4), 7.30 (dd, *J* = 7.6, 1.3, 1H, H-3), 7.17 (dd, *J* = 7.5, 1.8, 1H, H-3'), 7.04 (td, *J* = 7.5, 1.0, 1H, H-4'), 6.99 – 6.96 (m, 1H, H-2'), 3.73 (s, 3H, OMe), 2.16 (s, 3H, CO_2Me). **^{13}C NMR** (126 MHz, $CDCl_3$) δ 169.1, 156.3, 155.5, 140.0, 131.6, 131.2, 130.9, 129.8, 128.7, 127.8, 127.7, 126.4, 120.9, 111.0, 55.5, 19.7 ppm.

2',4',5,5'-Tetramethoxy-[1,1'-biphenyl]-2-carbaldehyde oxime 152b

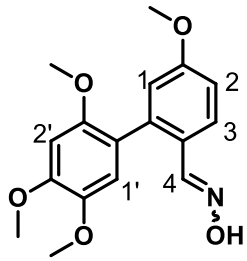

Prepared from 2',4',5,5'-tetramethoxy-[1,1'-biphenyl]-2-carbaldehyde (0.54 g, 1.79 mmol, 1.0 equiv.), hydroxylamine hydrochloride (0.248 g, 3.57 mmol, 2.0 equiv.), sodium acetate (0.292 g, 3.57 mmol, 2.0 equiv.). The product was obtained as a white solid (0.88 g, yield = 95%). **^{1}H NMR** (500 MHz, $CDCl_3$) δ 7.83 (s, 1H, H-4), 7.33 (d, *J* = 2.7, 1H, H-1), 7.09 (d, *J* = 8.5, 1H, H-3), 6.87 (dd, *J* = 8.5, 2.7, 1H, H-2), 6.60 (s, 1H, H-1') 6.49 (s, 1H, H-2'), 3.82 (s, 3H, OMe), 3.71 (s, 6H,

OMe), 3.58 (s, 3H, OMe).**^{13}C NMR** (126 MHz, $CDCl_3$) δ 158.7, 150.9, 149.8, 149.4, 143.1, 132.1, 131.6, 131.3, 119.4, 116.7, 115.4, 109.0, 97.9, 56.6, 56.5, 56.2, 55.4.

5-Chloro-2',4',5'-trimethoxy-[1,1'-biphenyl]-2-carbaldehyde oxime 152a

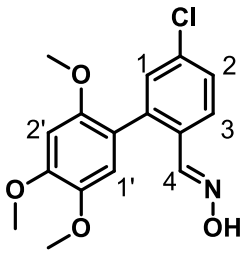

Prepared from 5-chloro-2',4',5'-trimethoxy-[1,1'-biphenyl]-2-carbaldehyde (0.84 g, 2.73 mmol, 1.0 equiv.), hydroxylamine hydrochloride (0.380 g, 5.48 mmol, 2.0 equiv.), sodium acetate (0.483 g, 5.48 mmol, 2.0 equiv.). The product was obtained as a white solid (0.88 g, yield = 100%). **^{1}H NMR** (300 MHz, $CDCl_3$) δ 7.91 (s, 1H, H-4), 7.87 (d, *J* = 8.4, 1H, H-3), 7.35 (ddd, *J* = 8.4, 2.3, 0.7, 1H, H-2), 7.32 – 7.30 (m, 1H, H-1), 6.72 (s, 1H, H-1'), 6.63 (s, 1H, H-2'), 3.99 (s, 3H, OMe), 3.88 (s, 3H, OMe), 3.76 (s, 3H, OMe). **^{13}C NMR** (75 MHz, $CDCl_3$) δ 159.1, 151.3, 150.3, 149.8, 143.4, 132.4, 131.9, 131.7, 119.7, 117.1, 115.7, 109.3, 98.2, 57.0, 56.6, 55.7.

5-Chloro-2',4',5'-trimethoxy-[1,1'-biphenyl]-2-carbaldehyde O-acetyl oxime 151a

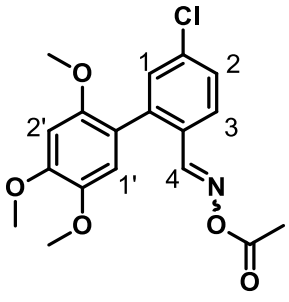

From 5-chloro-2',4',5'-trimethoxy-[1,1'-biphenyl]-2-carbaldehyde oxime (0.75 g, 2.33 mmol, 1.0 equiv.), trimethylamine (0.47 g, 0.42 mL, 4.66 mmol, 2.0 equiv.) and acetyl chloride (0.37 g, 0.35 mL, 4.66 mmol, 2.0 equiv.). The product was obtained as a white solid (0.73 g, yield = 87%). **^{1}H NMR** (300 MHz, $CDCl_3$) δ 8.10 (s, 1H, H-4), 8.07 (d, *J* = 8.4, 1H, 3), 7.40 – 7.35 (m, 1H, H-2), 7.33 (d, *J* = 2.0, 1H, H-1), 6.72 (d, *J* = 1.1, 1H, H-1'), 6.63 (s, 1H, H-2'), 3.98 (s, 3H, OMe), 3.87 (s, 3H, OMe), 3.73 (s, 3H, OMe), 2.19 (s, 3H, CO_2Me). **^{13}C NMR** (126 MHz,

$CDCl_3$) δ 168.8, 154.8, 150.6, 150.3, 143.4, 141.4, 137.1, 130.90, 127.8, 127.5, 117.5, 114.7, 97.6, 56.7, 56.4, 56.2, 19.6.

6-(2,4,5-Trimethoxyphenyl)benzo[*d*][1,3]dioxole-5-carbaldehyde O-acetyl oxime 155

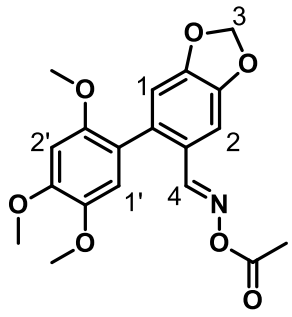

Prepared from 6-(2,4,5-trimethoxyphenyl)benzo[*d*][1,3]dioxole-5-carbaldehyde (0.97 g, 3.07 mmol, 1.0 equiv.), hydroxylamine hydrochloride (0.43 g, 6.14 mmol, 2.0 equiv.), sodium acetate (0.52 g, 2.57 mmol), trimethylamine (0.62 g, 0.85 mL, 6.13 mmol, 2.0 equiv.) and acetyl chloride (0.48 g, 0.44 mL, 6.13 mmol, 2.0 equiv.). The tittle product was furnished as a white solid (0.84 g, yield = 74%). **M.p.** 68-71 °C. **FTIR:** $\tilde{\nu}$ = 2913.7 (C–H stretch), 1681.3 (C=O), 1519.6 (C=C), 1398.0 (N–O stretch), 1254.6 (C–O), 719.0 cm^{-1}. **^{1}H NMR** (400 MHz, $CDCl_3$) δ 8.02 (s, 1H, H-4), 7.59 (s, 1H, H-2), 6.76 (s, 1H, H-1), 6.66 (s, 1H), 6.61 (s, 1H), 6.04 (d, *J* = 2.3, 2H, H-3), 3.97 (s, 3H, OMe), 3.84 (s, 3H, OMe), 3.72 (s, 3H, OMe), 2.17 (s, 3H, CO_2Me). **^{13}C NMR** (101 MHz, $CDCl_3$) δ 169.1, 155.3, 150.7, 150.3, 149.8, 147.4, 143.1, 135.5, 122.5, 118.6, 115.0, 110.7, 105.6, 101.8, 97.7, 56.6, 56.5, 56.2, 19.7. **HRMS** (ESI^+): calcd. for $C_{19}H_{19}NO_7$ $[M + H]^+$ 374.1162; found $[M + H]^+$ 374.1236; *m/z* (%) = 396.1045 (30) $[M + Na]^+$, 374.1236 (15) $[M + H]^+$, 314.1018 (100).

7.2.5 UV cyclisation of oxime ester derivatives general procedure

A quartz UV reactor was charged with oxime ester or oxime ether and *tert*-butyl alcohol (5 mL) and the solution was degassed for 30 min. The solution was then subjected to UV light irradiation (450 W medium pressure Hg lamp) for 3 h. The crude residue was purified with column chromatography using mixtures of EtOAc/hexane as eluent.

2,3-Dimethoxyphenanthridine 131a

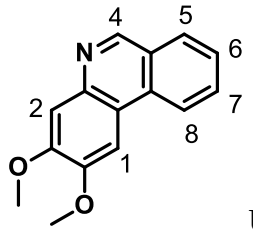

UV irradiation of 2',4',5'-trimethoxy-[1,1'-biphenyl]-2-carbaldehyde *O*-acetyl oxime (93 mg, 0.28 mmol, 1.0 equiv.) afforded the desired product as an oil (50.1 mg, yield = 74%) after column chromatography (10 to 30% EtOAc/hexane). **^{1}H NMR** (300 MHz, $CDCl_3$) δ = 9.46–9.31 (m, 1H, ArH), 9.22 (s, 1H, ArH), 8.08–7.97 (m, 1H, ArH), 7.81 (ddd, *J* = 8.6, 7.0, 1.6, 1H, ArH), 7.62 (ddd, *J* = 8.0, 7.0, 1.1, 1H, ArH), 7.29 (d, *J* = 2.5, 1H, ArH), 6.81 (d, *J* = 2.5, 1H, ArH), 4.12 (s, 3H, OMe), 3.99 (s, 3H, OMe).[205]

2',4',5'-Trimethoxy-[1,1'-biphenyl]-2-carbonitrile 141a

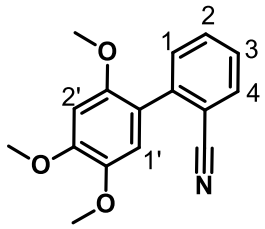

Also obtained from irradiation of 2',4',5'-trimethoxy-[1,1'-biphenyl]-2-carbaldehyde *O*-acetyl oxime as a white solid (11.2 mg, yield = 12%). **M.p.** 143-144 °C. **FTIR: ṽ** = 2936.0 (C–H stretch), 2225.4 (C≡N), 1499.1 (C=C), 1458.2, 1051.0 (C–O), 831.6 cm^{-1}. **^{1}H NMR** (300 MHz, $CDCl_3$) δ 7.88 (d, *J* = 0.6, 1H, H-4), 7.82 (d, *J* = 8.4, 1H, 1H-1), 7.32 (ddd, *J* = 8.4, 2.3, 0.6, 1H, H-2), 7.29 – 7.27 (m, 1H, H-3), 6.69 (s, 1H, H-1'), 6.60 (s, 1H, H-2'), 3.96 (s, 3H, OMe), 3.85 (s, 3H, OMe), 3.73 (s, 3H, OMe). **^{13}C NMR** (75 MHz, $CDCl_3$) δ 151.0, 150.3, 149.6, 143.5, 140.4, 135.7, 131.1, 129.7, 128.0, 126.9, 118.4, 115.0, 97.9, 57.0, 56.8, 56.6. **HRMS** (ESI^+): calcd. for $C_{16}H_{16}NO_3$ $[M + H]^+$ 270.1130; found $[M + H]^+$ 270.1225; *m/z* (%) = 288.1337 (47), 279.1037 (100), 270.1225 (52) $[M + H]^+$, 257.1174 (20), 258.1225 (27), 256.1062 (25).

2,4-Dimethoxyphenanthridine 131b

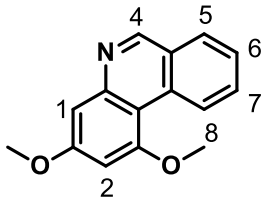

UV irradiation of 2',4',6'-trimethoxy-[1,1'-biphenyl]-2-carbaldehyde *O*-acetyl oxime (77 mg, 0.23 mmol, 1.0 equiv.) afforded the desired product 15b as an oil (16.1 mg, yield = 28%) after column chromatography (5% EtOAc/hexane). **^{1}H NMR** (300 MHz, $CDCl_3$) δ = 9.46–9.31 (m, 1H, ArH), 9.22 (s, 1H, ArH), 8.08–7.97 (m, 1H, ArH), 7.81 (ddd, J = 8.6, 7.0, 1.6, 1H, ArH), 7.62 (ddd, J = 8.0, 7.0, 1.1, 1H, ArH), 7.29 (d, J = 2.5, 1H, ArH), 6.81 (d, J = 2.5, 1H, ArH), 4.12 (s, 3H, OMe), 3.99 (s, 3H, OMe).

2',4',6'-Trimethoxy-[1,1'-biphenyl]-2-carbonitrile 141b

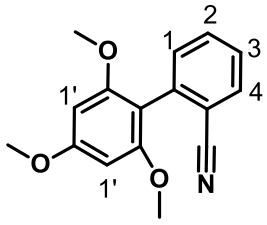

Also obtained from irradiation of 2',4',6'-trimethoxy-[1,1'-biphenyl]-2-carbaldehyde *O*-acetyl oxime as a white solid (33.8 mg, yield = 47%). **M.p.** 139-141 °C. **^{1}H NMR** (300 MHz, $CDCl_3$) δ 7.78 – 7.71 (m, 1H, H-4), 7.62 (td, *J* = 7.7, 1.4, 1H, H-1), 7.44 (dt, *J* = 7.7, 1.1, 1H, H-2), 7.39 (dd, *J* = 7.6, 1.3, 1H, H-3), 6.28 (s, 2H, H-1'), 3.90 (s, 3H, OMe), 3.79 (s, 6H, OMe). **^{13}C NMR** (75 MHz, $CDCl_3$) δ 162.3, 158.7, 139.2, 132.9, 132.8, 132.2, 127.2, 119.3, 115.1, 109.0, 91.3, 56.1, 55.7 ppm.[206]

2',4'-Dimethoxy-[1,1'-biphenyl]-2-carbonitrile 141c

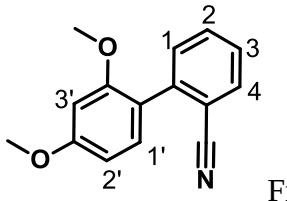

From irradiation of 2',4'-dimethoxy-[1,1'-biphenyl]-2-carbaldehyde O-acetyl oxime (90 mg, 0.33 mmol). The crude product was purified with column chromatography purification (20% EtOAc/hexane as eluent). The pure product was obtained as light yellow solid (67.1 mg, yield = 81%). **M.p.** 166-167 °C. **FTIR: ṽ** = 2964.6 (C–H stretch), 2228.9 (C≡N), 1581.6 (C=C), 1415.7, 1031.1 (C–O), 785.6 cm^{-1}. **^{1}H NMR** (300 MHz, $CDCl_3$) δ 7.74 (ddd, *J* = 7.7, 1.4, 0.6, 1H, H), 7.63 (td, *J* = 7.7, 1.4, 1H, H-), 7.50 – 7.45 (m, 1H, H), 7.42 (td, *J* = 7.6, 1.3, 1H, H), 7.22 – 7.16 (m, 1H, H-1'), 6.66 – 6.59 (m, 2H, H-2' & H-3'), 3.90 (s, 3H, OMe), 3.86 (s, 3H, OMe). **^{13}C NMR** (75 MHz, $CDCl_3$) δ 161.9, 157.9, 142.8, 133.1, 132.7, 131.9, 131.4, 127.3, 120.4, 119.2, 113.8, 105.2, 99.3, 55.8 ppm. **HRMS** (ESI^+): calcd. for $C_{15}H_{14}NO_2$ $[M + H]^+$ 240.1025; found $[M + H]^+$ 240.1018; *m/z* (%) = 258.1126 (10), 240.1018 (15) $[M + H]^+$, 210.0917 (100).[207]

4-Methoxyphenanthridine 131d

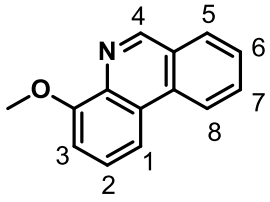

Prepared from UV irradiation of 2',3'-dimethoxy-[1,1'-biphenyl]-2-carbaldehyde *O*-acetyl oxime (97 mg, 0.32 mmol, 1.0 equiv.) affording the desired product the title compound as an a clear oil (36.2 mg, yield = 54%) after column chromatography (10% EtOAc/hexane). **^{1}H NMR** (400 MHz, $CDCl_3$) δ 9.17 (s, 1H, H-4), 8.55 (d, *J* = 8.3, 1H, H-8), 8.12 (d, *J* = 9.0, 1H, H-3), 8.08 – 7.98 (m, 1H, H-5), 7.91 (d, *J* = 2.8, 1H, H-1), 7.85 (ddd, *J* = 8.4, 7.0, 1.4, 1H, H-7), 7.71 (ddd, *J* = 8.0, 7.0, 1.1, 1H, H-6), 7.38 (dd, *J* = 9.0, 2.8, 1H, H-2), 4.03 (s, 3H, OMe). **^{13}C NMR** (101 MHz,

$CDCl_3$) δ 156.4, 149.0, 137.6, 130.0, 129.4, 128.5, 126.7, 125.5, 124.4, 123.0, 119.8, 116.5, 101.0, 53.6.[121]

2',3'-Dimethoxy-[1,1'-biphenyl]-2-carbonitrile 141d

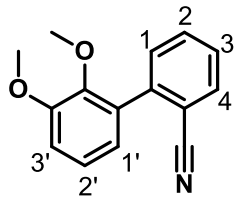

Also obtained from irradiation of 2',3'-dimethoxy-[1,1'-biphenyl]-2-carbaldehyde *O*-acetyl oxime as a white powder (16.8 mg, yield = 22%). **M.p.** 154-155 °C. **FTIR: ṽ** = 2937.0 (C–H stretch), 2217.5 (C≡N), 1586.8 (C=C), 1472.0, 1025.9 (C–O), 846.8 cm^{-1}. **^{1}H NMR** (400 MHz, $CDCl_3$) δ 7.75 (d, *J* = 7.8, 1H, H-), 7.62 (t, *J* = 7.7, 1H), 7.49 (d, *J* = 7.9, 1H), 7.45 (t, *J* = 7.7, 1H), 7.15 (t, *J* = 7.9, 1H), 7.01 (d, *J* = 8.2, 1H), 6.91 (dd, *J* = 7.6, 1.6, 1H), 3.92 (s, 3H), 3.65 (s, 3H). **^{13}C NMR** (101 MHz, $CDCl_3$) δ 152.3, 145.9, 141.7, 132.2, 131.9, 131.5, 130.4, 126.9, 123.4, 121.9, 117.8, 112.6, 112.2, 60.3, 55.3. **HRMS** (ESI^+): calcd. for $C_{15}H_{14}NO_2$ $[M + H]^+$ 240.1025; found $[M + H]^+$ 240.1018; *m/z* (%) = 258.112 (10), 240.1018 (100) $[M + H]^+$, 210.0906 (7).

2-Methoxyphenanthridine 131e

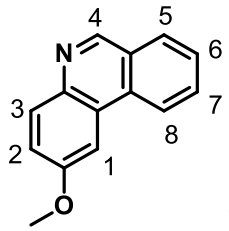

From UV irradiation of 2',5'-dimethoxy-[1,1'-biphenyl]-2-carbaldehyde *O*-acetyl oxime (95 mg, 0.32 mmol, 1.0 equiv.). The product was obtained as an oil (38.5 mg, yield = 58%) after column chromatography (gradient from 5% to 30% EtOAc/hexane). **FTIR: ṽ** = 2973.4 (C–H stretch), 1649.4 (C=C), 1592.7, 1166.7, 1117.0 (C–O) cm^{-1}. **^{1}H NMR** (400 MHz, $CDCl_3$) δ 9.18 (s, 1H, H-4), 8.55 (d, *J* = 8.3, 1H, H-8), 8.12 (d, *J* = 8.9, 1H, H-3), 8.05 (d, *J* = 7.9, 1H, H-5), 7.92 (d, *J* = 2.7, 1H, H-1), 7.86 (t, *J* = 7.7, 1H, H-7), 7.72 (t, *J* = 7.5, 1H, H-6), 7.38 (dd, *J* = 9.0,

2.7, 1H, H-2), 4.03 (s, 3H, OMe). **^{13}C NMR** (101 MHz, $CDCl_3$) δ 158.5, 151.1, 132.1, 131.4, 130.6, 128.8, 127.6, 126.5, 125.2, 121.9, 118.6, 103.1, 55.7 ppm.[111]

2',5'-Dimethoxy-[1,1'-biphenyl]-2-carbonitrile 141e

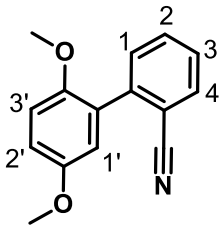

Also from UV irradiation of 2',5'-dimethoxy-[1,1'-biphenyl]-2-carbaldehyde *O*-acetyl oxime (95 mg, 0.32 mmol, 1.0 equiv.). The product was obtained as a white solid (13.0 mg, yield = 17%). **M.p.** 173-176 °C. **FTIR: ṽ** = 2959.8 (C–H stretch), 2226.4 (C≡N), 1598.0 (C=C), 1457.9, 1049.5 (C–O) cm^{-1}. **^{1}H NMR** (400 MHz, $CDCl_3$) δ 7.71 (dd, *J* = 7.7, 1.3, 1H, H-4), 7.61 (td, *J* = 7.7, 1.3, 1H, H-3), 7.45 (d, *J* = 7.8, 1H, H-1), 7.43 – 7.37 (m, 1H, H-2), 6.94 (d, *J* = 1.7, 2H, H2' & H-3'), 6.83 (d, *J* = 1.6, 1H, H-1'), 3.79 (s, 3H, OMe), 3.78 (s, 3H, OMe). **^{13}C NMR** (101 MHz, $CDCl_3$) δ 153.6, 150.7, 142.4, 132.8, 132.4, 130.8, 128.0, 127.5, 118.6, 116.7, 115.0, 113.4, 112.5, 56.0, 55.9 ppm.[208]

2'-Methoxy-[1,1'-biphenyl]-2-carbonitrile 141f

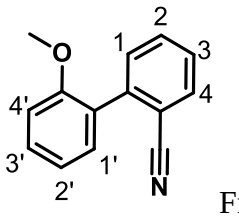

From irradiation of 2'-methoxy-[1,1'-biphenyl]-2-carbaldehyde O-acetyl oxime (89 mg, 0.33 mmol). The pure product (white solid) was obtained after column chromatography purification using 20% EtOAc/hexane as eluent. The product was obtained as a clear oil (62.8 mg, yield = 69%). **FTIR: ṽ** = 2951.1 (C–H stretch), 2224.3 (C≡N), 1567.5 (C=C), 1415.7, 1026.9 (C–O), 712.1 cm^{-1}. **^{1}H NMR** (400 MHz, $CDCl_3$) δ 7.70 (d, *J* = 7.7, 1H, H-4), 7.59 (td, *J* = 7.7, 1.5, 1H, H-2), 7.47 – 7.35 (m, 3H, H-1, H-1', H-3), 7.24 (dd, *J* = 7.5, 1.7, 1H, H-3'), 7.05 (d, *J* = 7.5, 1H, H-2'), 7.01

(d, *J* = 8.4, 1H, H-4'), 3.82 (s, 3H, OMe). **^{13}C NMR** (101 MHz, $CDCl_3$) δ 156.5, 142.6, 132.8, 132.4, 130.9, 130.9, 130.4, 127.3, 120.8, 118.7, 113.5, 111.4, 55.5 ppm.[207]

6-(2,5-Dimethoxyphenyl)benzo[d][1,3]dioxole-5-carbonitrile 148

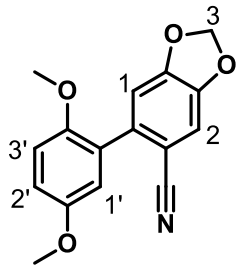

Prepared from 6-(2,5-dimethoxyphenyl)benzo[*d*][1,3]dioxole-5-carbaldehyde (0.74 g, 2.58 mmol, 1.0 equiv.) and *O*-phenylhydroxylamine hydrochloride (0.38g, 2.58 mmol, 1.0 equiv.). The title compound was obtained as a white solid quantitatively. **^{1}H NMR** (500 MHz, $CDCl_3$) δ 7.32 – 7.25 (m, 1H, H-1), 7.12 (d, *J* = 3.2, 1H, H-2), 6.95 (s, 2H, H-3), 6.93 – 6.88 (m, 1H, H-2'), 6.84 (s, 1H, H-1'), 6.15 – 6.06 (m, 1H, H-3'), 3.81 (d, *J* = 3.2, 6H, OMe). **^{13}C NMR** (126 MHz, $CDCl_3$) δ 153.5, 151.2, 150.7, 150.1, 147.2, 146.9, 138.7, 127.7, 116.8, 115.0, 112.5, 111.6, 111.2, 105.6, 102.4, 56.1, 55.8.

2,3-Dimethoxy-[1,3]dioxolo[4,5-*j*]phenanthridine 157

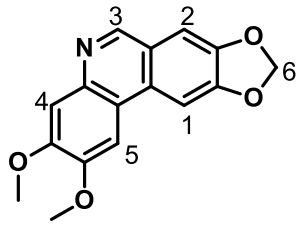

From irradiation of 6-(2,4,5-trimethoxyphenyl)benzo[*d*][1,3]dioxole-5-carbaldehyde *O*-acetyl oxime (95 mg, 0.32 mmol, 1.0 equiv.), the pure product (cream solid) was obtained after column chromatography purification using 50% EtOAc/cyclohexane as eluent. (37.2 mg, yield = 41%). **^{1}H NMR** (400 MHz, Methanol-d_4) δ 8.88 (s, 1H, H-3), 7.97 (s, 1H, H-2), 7.74 (s, 1H, H-1), 7.36 (s, 1H, H-1'), 7.28 (s, 1H, H-2') 6.14 (s, 2H, H-6), 3.97 (s, 3H, OMe), 3.93 (s, 3H, OMe). **^{13}C NMR** (101 MHz, $CDCl_3$) δ 153.6, 151.7, 150.4, 148.5, 146.9, 131.6, 105.4, 105.1, 102.6, 99.5, 55.4, 55.2.[194]

6-(2,4,5-Trimethoxyphenyl)benzo[*d*][1,3]dioxole-5-carbonitrile 156

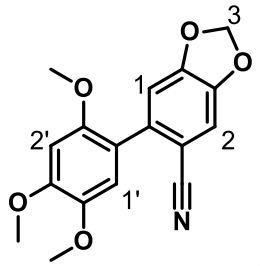

Also obtained from irradiation of 6-(2,4,5-trimethoxyphenyl)benzo[*d*][1,3]dioxole-5-carbaldehyde *O*-acetyl oxime (89 mg, 0.33 mmol). The title was obtained as a white solid (53.3 mg, yield = 53%). **M.p.** 128-129 °C. **FTIR: ṽ** = 2840.7 (C–H stretch), 2211.8 (C≡N), 1483.2 (C=C), 1438.1, 1028.3 (C–O) cm^{-1}). **^{1}H NMR** (400 MHz, $CDCl_3$) δ 7.09 (s, 1H, H-2), 6.89 (s, 1H, H-1), 6.79 (s, 1H, H-1'), 6.62 (s, 1H, H-2'), 6.08 (s, 2H, H-3), 3.95 (s, 3H, OMe), 3.86 (s, 3H, OMe), 3.82 (s, 3H, OMe). **^{13}C NMR** (101 MHz, $CDCl_3$) δ 151.1, 150.9, 150.3, 146.7, 143.0, 138.8, 118.9, 118.1, 114.5, 111.6, 111.4, 105.6, 102.3, 97.6, 56.7, 56.3, 56.1. **HRMS** (ESI^+): calcd. for $C_{17}H_{16}NO_5$ $[M + H]^+$ 314.1028; found $[M + H]^+$ 314.1023; *m/z* (%) = 383.1098 (10), 336.0842 (30), 314.1023 (100) $[M + H]^+$, 102.1279 (80).

Synthesis of Trisphaeridine 77

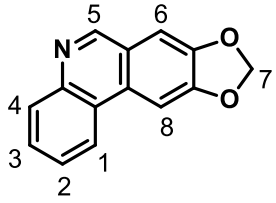

To a solution of 2,3-dimethoxy-[1,3]dioxolo[4,5-*j*]phenanthridine (61 mg, 0.22 mmol) in acetonitrile (3 ml) was slowly added a solution of ceric ammonium nitrate (356 mg, 0.65 mmol) in water (1.5 mL) at 0 °C. The resulting solution was stirred at the same temperature for 30 min and then was quenched with ice-water (1.5 mL). A precipitate formed and was filtered, then washed with water. The solid was then taken up with ethyl acetate, dried over $MgSO_4$ and the volatiles were removed under reduced pressure. [1,3]Dioxolo[4,5-*j*]phenanthridine-2,3-dione was obtained as a black solid (35 mg, yield 63%) and was used in the next step without further purification.

A high-pressure tube equipped with a stirrer bar was charged with [1,3]dioxolo[4,5-*j*]phenanthridine-2,3-dione (35 mg, 0.14 mmol), zinc (37 mg, 0.56 mmol), NaCl (33 mg, 0.55 mmol) and acetic acid (5 ml). The tube was sealed and the mixture was stirred at 150 °C for 3 h. The reaction was neutralized with a saturated aqueous solution of sodium bicarbonate and was extracted with ethyl acetate (3 × 5 ml). The combined organic layer was dried over $MgSO_4$, and the solvent was removed in the rotary evaporator. The crude product was purified with column chromatography (eluent; 5–50% EtOAc/hexane). Trisphaeridine was obtained as a cream solid (19 mg, 59%). **M.p.** 144−146 °C. **^{1}H NMR** (400 MHz, $CDCl_3$) δ 9.08 (s, 1H, H-5), 8.36 (d, *J* = 8.2, 1H, H-1), 8.15 (d, *J* = 8.1, 1H, H-4), 7.89 (s, 1H, H-8), 7.69 (t, *J* = 7.5, 1H, H-3), 7.62 (t, *J* = 7.6, 1H, H-2), 7.32 (s, 1H, H-6), 6.16 (s, 2H, H-7). **^{13}C NMR** (101 MHz, $CDCl_3$) δ 151.7, 151.5, 148.2, 144.0, 130.3, 129.9, 128.0, 126.7, 124.3, 123.0, 122.0, 105.5, 101.9, 99.9 ppm.[209]

7.3 Synthesis of coumarins and annellated coumarin derivatives

Attempted synthesis of 2-(6-hydroxy-3-oxo-1,8-dipentadecyl-3*H*-xanthen-9-yl)benzoic acid 193

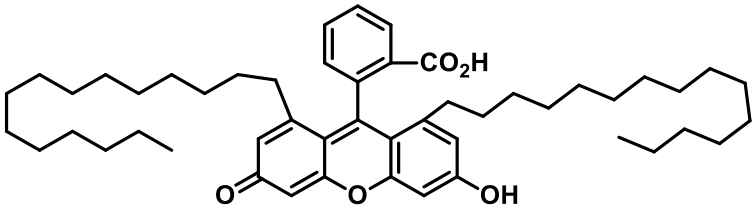

Method A

A 10 mL round-bottom flask equipped with a stirrer bar was charged with cardol **10** (1.13 g, 3.1 mmol, 2.0 equiv.), phthalic anhydride (0.23 g, 1.6 mmol, 1.0 equiv.) and concentrated H_2SO_4 (1 mL). Then resulting slurry was stirred while gradually increasing the temperature to 190 °C, once that temperature was reached the reaction allowed to stir for an additional 30 min. The contents of the flask were poured in crushed ice, forming a precipitate that was recovered through filtration. Separation of the resulting mixture was effected with column chromatography using 80%

EtOAc/cyclohaxane as eluent. Further purification by recrystallization with MeOH and subsequent NMR spectroscopic determination gave an indiscernible spectrum.

Method B

A similar procedure as above was used with the exception that H_2SO_4 was replaced with $ZnCl_2$ (10 mol%). Upon completion, the black resin that resulted was dissolved in CH_2Cl_2 (10 mL) and was successively washed with H_2O (3 × 10 mL) and brine (10 mL). The organic layer was dried over $MgSO_4$, evaporated in the rotary evaporator and was subjected to column chromatography as described in attempt 1 above.

Method C

A high pressure tube was charged with cardol (0.24 g, 0.62 mmol, 1.0 equiv.) and phthalic anhydride (0.18 g, 1.24 mmol, 2.0 equiv.), a drop of H_2SO_4 was also added. DMSO (3 mL) was then added to the tube and was placed in a pre-heated oil bath of 160 °C and was allowed to stir for 30 min. The reaction was quenched with H_2O (50 mL) and was subsequently extracted with CH_2Cl_2 (3 × 15 mL). The combined organic layer was dried over $MgSO_4$. The TLC spots of this reaction were considerably different from the above attempts, as such a crude NMR spectrum was measured and revealed decomposition of the reagents.

7-Pentadecyl-2*H*-chromen-2-one 195

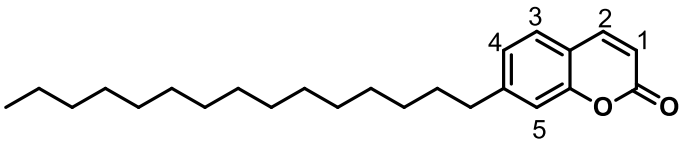

A 100 mL round-bottom flask equipped with a magnetic stirrer was charged with cardanol (1.43 g, 4.68 mmol, 1 equiv.), malic acid (0.75 g, 5.62 mmol, 1.2 equiv.) and H_2SO_4 (5 mL), the resulting suspension was stirred at room temperature for 30 min. Then the temperature was gradually increased to 100 °C and left for further 3 h. Great care needs to be taken to prevent the contents of the flask from overflowing due to the evolution of carbon dioxide from the reaction. After 3 h had elapsed, the contents of the flask were transferred into a beaker containing 200 g crushed ice and stirred for 30 min. The

resulting precipitate was filtered and recrystallized from a cyclohexane/ethyl acetate (1:1) mixture. The pure product was obtained as a white powder (0.94 g, 56%). **M.p**: 72 – 74 °C. **FTIR: ṽ** = 2913.5, 2849.3 (C–H stretch), 1746.7 (C=O), 1621.3 (C=C), 1139.4 (C–O) cm^{-1}. **^{1}H NMR** (400 MHz, $CDCl_3$) δ 7.69 (d, *J* = 9.5, 1H, H-2), 7.39 (d, *J* = 7.8, 1H, H-3), 7.15 (d, *J* = 1.5, 1H, H-5), 7.11 (dd, *J* = 7.9, 1.6, 1H, H-4), 6.37 (d, *J* = 9.5 , 1H, H-1), 2.74 – 2.65 (m, 2H), 1.65 (dd, *J* = 10.5, 4.7, 2H), 1.27 (s, 26H), 0.95 – 0.84 (m, 3H). **^{13}C NMR** (101 MHz, $CDCl_3$) δ 161.1, 154.2, 148.2, 143.4, 127.5, 125.0, 116.7, 116.4, 115.5, 36.0, 31.9, 31.1, 29.7, 29.7, 29.7, 29.6, 29.5, 29.4, 29.4, 22.7. **HRMS** (ESI+): calcd. for $C_{24}H_{37}O_2$ $[M + H]^+$ 357.2794; found $[M + H]^+$ 357.2793; m/z (%) = 357.2793 (100), 569.3807 (8), 735.5309 (40).

7-Pentadecyl-2*H*-chromen-2-one 196b

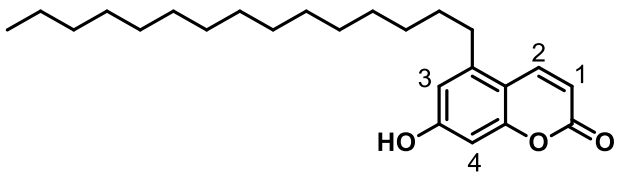

Following the above method, the title compound was obtained from cardol (1.53 g, 4.69 mmol, 1 equiv.), malic acid (0.77 g, 5.64 mmol, 1.2 equiv.) and H_2SO_4 (5 mL). The product was purified by recrystallization from a cyclohexane/ethyl acetate (1:1) mixture. The pure 7-pentadecyl-2*H*-chromen-2-one was obtained as a white powder (0.73 g, yield = 42%). **M.p**: decomposes at 155 °C. **FTIR: ṽ** = 3171.5 (OH), 2915.0, 2848.8 (C–H stretch), 1732.3 (C=O), 1555.5 (C=C), 1139.7 (C–O) cm^{-1}. **^{1}H NMR** (400 MHz, $CDCl_3/D_2O$ (1:2)) δ 9.91 (s, 1H, OH), 8.14 (d, *J* = 9.7, 1H, H-2), 6.83 (s, 1H, H-3), 6.40 (s, 1H, H-4), 6.34 (d, *J* = 9.7, 1H, H-1), 2.65 (t, *J* = 7.7, 2H), 1.61 (q, *J* = 7.4, 3H), 1.27 (s, 32H), 0.89 (t, *J* = 6.7 Hz, 3H). **^{13}C NMR** (101 MHz, $CDCl_3/D_2O$ (1:2)) δ 159.7, 155.9, 145.1, 140.0, 136.8, 116.1, 115.0, 113.4, 113.2, 32.7, 31.9, 31.1, 29.7, 29.7, 29.6, 29.5, 29.4, 22.7, 14.1. **HRMS** (ESI+): calcd. for $C_{24}H_{37}O_3$ $[M + H]^+$ 373.2743; found $[M + H]^+$ 373.2739; m/z (%) = 373.2739 (80), 374.2774 (10), 425.52691 (100).

5-Pentadecylpyrano[2,3-*f*]chromene-2,8-dione 197a

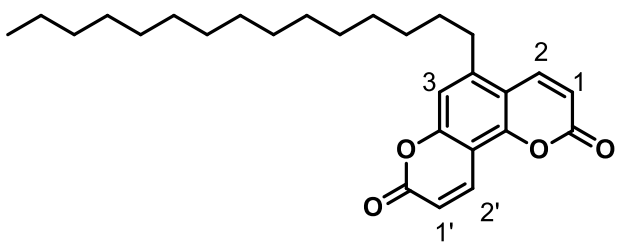

Method A

The title compound was synthesized adopting the method for 7-pentadecyl-2*H*-chromen-2-one with the exception that 2.4 equiv. of malic acid was employed. As such concentrated H_2SO_4 (10 mL) was added in a 100 mL round-bottom flask containing cardol (1.57 g, 4.90 mmol, 1.0 equiv.) and malic acid (1.84, 11.8 mmol, 2.4 equiv). The reaction was worked up as described above but the reaction time was 5 h. The pure product was obtained as a white powder after recrystallization from pure ethyl acetate (1.08 g, yield = 52%).

Method B

Preformed 7-pentadecyl-2*H*-chromen-2-one (0.34 g, 0.81 mmol, 1.0 equiv.) was placed in a 100 mL round bottom flask, and to this was added malic acid (0.31 g, 0.97 mmol, 1.2 equiv.) and H_2SO_4 in succession. The resulting slurry was stirred at room temperature for 30 min and the temperature was gradually increased to 100 °C and maintained at that temperature for 3 h. The reaction mixture was quenched with ice and extracted with ethyl acetate (3 × 50 mL). The organic portions were combined, and washed with H_2O (2 × 50 mL) and brine (50 mL). The crude product was purified as described in method A (0.19 g, yield = 57%). **FTIR: ṽ =** 2916.4, 2885.1 (C–H stretch), 1729.8 (C=O), 1565.0 (C=C), 1130.7 (C–O) cm^{-1}. **^{1}H NMR** (400 MHz, $CDCl_3$) δ 8.29 (d, *J* = 9.7, 1H, H-2'), 7.96 (d, *J* = 9.8, 1H, H-2), 7.09 (s, 1H, H-3), 6.49 (d, *J* = 9.7, 1H, H-1'), 6.47 (d, *J* = 9.7, 1H, H-1), 2.96 – 2.87 (m, 2H), 1.72 – 1.60 (m, 2H), 1.27 (s, 30H), 0.89 (t, *J* = 6.7, 3H). **^{13}C NMR** (101 MHz, $CDCl_3$) δ 159.7, 159.4, 155.9, 151.1, 145.1, 140.0, 136.8, 116.1, 115.0, 113.5, 113.2, 106.8, 32.7, 31.9, 31.1, 29.7, 29.7, 29.6,

29.5, 29.4, 22.7, 14.1. **HRMS** (ESI+): calcd. for $C_{27}H_{37}O_4$ $[M + H]^+$ 425.2692; found $[M + H]^+$ 425.2691; m/z (%) = 357.2795 (45), 397.2742 (76), 398.2778 (20), 425.2691 (100) $[M + H]^+$, 426.2728 (30).

7-(2,2-Diethoxyethoxy)-5-pentadecyl-2*H*-chromen-2-one 201

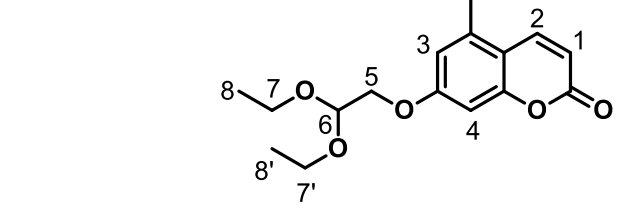

To a stirring solution of 7-pentadecyl-2*H*-chromen-2-one (0.9 g, 2.4 mmol, 1.0 equiv.) in anhydrous DMF (24 mL, 0.1 M) was added K_2CO_3 (0.67 g, 4.8 mmol, 2.0 equiv.) and the resulting mixture was allowed to stir for 30 min. After this, 2-bromoacetaldehyde diethyl acetal (0.71 g, 3.6 mmol, 1.5 equiv.) was added in one portion and the temperature was increased to 90 °C and the reaction was left for 24 h. Upon the completion of the reaction, the mixture was cooled to room temperature, diluted with H_2O (240 mL), and extracted with ethyl acetate (3 × 50 mL). The organic layers were combined and washed successively with H_2O (2× 30 mL) and brine (2 × 30 mL), and then dried over anhydrous $MgSO_4$. The volatiles were evaporated under reduced pressure and the crude product was purified with column chromatography using 15% EtOAc/cyclohexane solvent mixture as eluent. The title compound was obtained as a yellow oil (0.36 g, 92%). **M.p.** 71-73 °C. **FTIR: $\tilde{\nu}$ =** 2927.0, 2867.4 (C–H stretch), 1730.7 (C=O), 1546.5 (C=C), 1129.2 (C–O) cm^{-1}. **^{1}H NMR** (400 MHz, $CDCl_3$) δ 8.05 (d, *J* = 9.7, 1H, H-2), 6.77 (d, *J* = 1.1, 1H, H-3), 6.57 (d, *J* = 1.2, 1H, H-4), 6.29 (d, *J* = 9.7, 1H, H-1), 4.91 (t, *J* = 5.2, 1H, H-6), 4.12 (d, *J* = 5.3, 2H, H-5), 3.82 (dq, *J* = 9.4, 7.1, 2H, H-7 & H-7'), 3.68 (dq, *J* = 9.4, 7.1, 2H, H-7 & H-7'), 2.69 – 2.60 (m, 2H), 1.63 (s, 2H), 1.44 (s, 1H), 1.37 – 1.20 (m, 36H), 0.90 (t, *J* = 6.7 Hz, 3H). **^{13}C NMR** (101 MHz, $CDCl_3$) δ 161.3, 155.1, 154.8, 148.9, 138.5, 113.5, 109.2, 107.8, 106.8, 100.3, 69.1, 62.9, 36.7, 31.9, 31.0, 29.7, 29.6, 29.5, 29.4, 29.2, 26.9, 22.7, 15.4, 14.1. **HRMS** (ESI+): calcd. for $C_{30}H_{49}O_5$ $[M + H]^+$

489.3580; found $[M + H]^+$ 489.3576; m/z (%) = 489.3576 (100), 490.3613 (45), 491.3637 (15).

5-Pentadecyl-2*H*-furo[2,3-*h*]chromen-2-one and **4-Pentadecyl-7*H*-furo[3,2-*g*]chromen-7-one 198a and 198b**

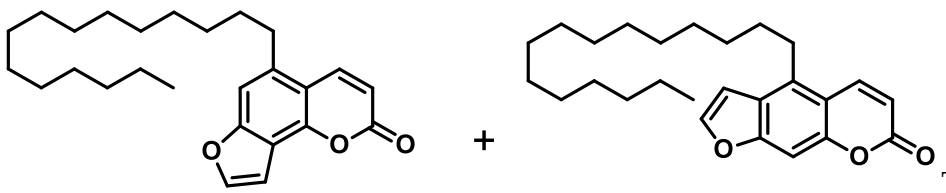

To a solution of 7-(2,2-diethoxyethoxy)-5-pentadecyl-2*H*-chromen-2-one (3.51 g, 7.18 mmol, 1.0 equiv.) in toluene (50 mL) in a 100 ml round bottom flask was added polyphosphoric acid (1.76 g, 18.0 mmol, 2.5 equiv.). The resulting solution was then heated under reflux for 2.5 h after which a white solid precipitated out of solution. This was separated by filtration and recrystallized from pure EtOAc. A mixture of 5-pentadecyl-2H-furo[2,3-*h*]chromen-2-one and 4-pentadecyl-7H-furo[3,2-*g*]chromen-7-one) was formed (0.85 g yield = 30%) **^{1}H NMR** (400 MHz, $CDCl_3$) δ 8.14 (d, *J* = 9.6, 1H), 7.71 (d, *J* = 2.2, 1H), 7.05 (s, 1H), 6.87 (d, *J* = 2.2, 1H), 6.44 (d, *J* = 9.6z, 1H), 2.90 – 2.84 (m, 3H), 1.79 – 1.61 (m, 4H), 1.26 (s, 35H), 0.88 (t, J = 6.8 Hz, 5H). Aromatic protons of the minor product: δ 8.01 (d, *J* = 9.8, 1H), 7.62 (d, *J* = 2.2, 1H), 7.27 (d, *J* = 0.9, 1H), 7.08 (dd, *J* = 2.2, 0.9, 1H), 6.40 (d, *J* = 9.8, 1H).

7.4 Synthesis of cardol derived Δ^9–*trans*–tetrahydrocannabinol

Chrysanthenone 221

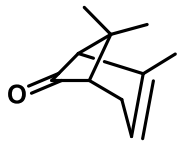

A solution of verbenone (1.20 g, 7.99 mmol, 1.0 equiv.) in 100 ml of glacial acetic acid was degassed by bubbling with argon for 15 min and was subsequently irradiated with a 450 W medium pressure Hg lamp for a period of 10 h. The mixture was then diluted with H_2O (200 mL) and extracted with ether (2 × 200 mL). The combined organic phase was successively washed with H_2O (2 × 100 mL),

saturated potassium carbonate (3 × 100 mL), and brine (100 mL) and dried over $MgSO_4$. Following evaporation of the solvent under reduced pressure, short-path distillation afforded chrysanthenone as a clear oil (43.7 mg yield = 43%). **^{1}H NMR** (400 MHz, $CDCl_3$) δ 5.42 (h, *J* = 1.6, 1H), 2.53 (ddd, *J* = 9.1, 6.7, 4.2, 1H), 2.33 (tt, *J* = 4.6, 2.2, 1H), 2.22 – 2.11 (m, 1H), 1.77 (dd, *J* = 9.2, 3.1, 1H), 1.74 (dd, *J* = 2.7, 1.6, 3H), 1.22 (d, *J* = 2.7, 3H), 0.72 (d, *J* = 2.8 Hz, 3H). **^{13}C NMR** (101 MHz, Chloroform-d) δ 203.7, 170.2, 120.9, 57.4, 53.7, 49.5, 40.6, 26.4, 23.4, 21.8.

5-Pentadecyl-2,4-bis(2,7,7-trimethylbicyclo[3.1.1]hept-2-en-6-yl)benzene-1,3-diol 218

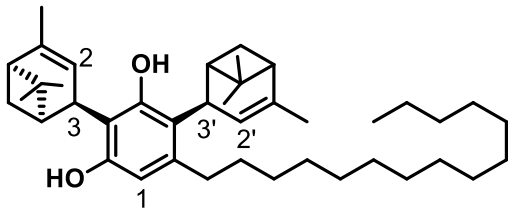

To a solution of cardol (1.07 g, 3.1 mmol, 1.0 equiv.) and methanesulfonic acid (30.4 mg, 0.31 mmol, 0.1 equiv.) in dry CH_2Cl_2 (62 mL) was slowly added a solution of verbenol (0.47 g, 3.1 mmol, 1.0 equiv.) in CH_2Cl_2 (10 mL) over 30 min at 0 °C. The reaction mixture was allowed to warm to room temperature while stirring for a further 30 min. Upon completion of the reaction, the mixture was washed with H_2O (2 × 40 mL) and brine (30 mL). The organic layer was dried over $MgSO_4$ and CH_2Cl_2 was removed in a rotary evaporator and the crude product was purified by column chromatography using 5% EtOAc/hexane as eluent. The title compound was isolated as a yellow oil (0.80 g, 44%). **^{1}H NMR** (500 MHz, $CDCl_3$) δ 7.37 (s, 1H, OH), 7.14 (s, 1H, OH), 6.24 (s, 1H, H-1), 5.74 – 5.67 (m, 2H, H-2 & H-2'), 3.92 (q, *J* = 2.8, 1H, H-3'), 3.71 (q, *J* = 2.8, 1H, H-3), 2.51 – 2.43 (m, 1H), 2.37 – 2.21 (m, 4H), 2.20 – 2.08 (m, 3H), 1.86 (dt, *J* = 4.1, 1.8, 3H), 1.83 (t, *J* = 1.9, 3H), 1.58 (dq, *J* = 30.2, 8.1, 3H), 1.48 (d, *J* = 9.6, 1H), 1.31 (t, *J* = 5.0, 7H), 1.26 (s, 19H), 0.94 (d, *J* = 2.8, 6H), 0.88 (t, *J* = 6.8, 3H). **^{13}C NMR** (126 MHz, $CDCl_3$) δ 155.1, 154.4, 152.4, 151.8, 141.2, 117.3, 117.1, 116.8, 113.3, 109.7, 48.4, 48.0, 47.9, 46.9, 41.0, 40.6, 40.0, 38.3, 33.0 , 32.0, 31.6, 29.9, 29.7, 29.6, 29.5, 29.4, 28.1, 26.0, 23.9, 23.7, 22.7, 20.5, 20.4, 14.2. Minor diastereomer **^{13}C NMR** (126 MHz, $CDCl_3$) δ 155.1,

154.4, 152.3, 151.8, 141.1, 117.4, 113.1, 48.6, 47.9, 46.8, 41.0, 39.9, 38.2, 32.9, 31.3, 30.0, 27.9, 27.4, 23.9, 23.8, 20.5, 20.4. **HRMS** (ESI+): calcd. for $C_{41}H_{65}O_2$ $[M + H]^+$ 589.4985; found $[M + H]^+$ 589.4976; m/z (%) = 589.4976 (100), 549.4672 (30), 509.4359 (15).

(6a*R*,10a*R*)-6,6,9-trimethyl-3-pentadecyl-6a,7,8,10a-tetrahydro-6*H*-benzo[*c*]chromen-1-ol 213

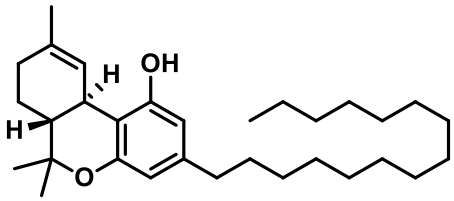

A solution of chrysanthenol (79 mg, 0.52 mmol, 1.0 equiv.) in CH_2Cl_2 (10 mL) was placed in an ice bath and allowed to cool for 15 min, upon which cardol (0.17 g, 0.52 mmol, 1.0 equiv.) and a drop of boron trifluoride etherate were added in succession and the resulting solution was allowed to stir further for 30 min maintaining the temperature at 0 °C. The volatiles were evaporated under reduced pressure and the resin containing crude product was purified by means of column chromatography using 5% EtOAc/hexane as eluent. Further thin layer chromatographic purification was necessary to get a sample of considerable purity as a yellow oil (73.2 mg, yield = 31%). **^{1}H NMR** (400 MHz, $CDCl_3$) δ 8.20 (s, 1H), 7.46 (d, *J* = 45.8 Hz, 1H), 6.38 – 6.18 (m, 2H), 5.20 (s, 1H), 3.20 – 2.94 (m, 1H), 2.53 – 2.25 (m, 2H), 2.20, 2.02 (t, *J* = 15.5, 1H), 1.89 (s, 1H), 1.74 – 1.41 (m, 5H), 1.25 (s, 28H), 1.06 – 0.78 (m, 6H), 0.65 (d, *J* = 24.8 Hz, 1H). **^{13}C NMR** (101 MHz, $CDCl_3$) δ 154. 4, 154.0, 153.3, 143.2, 143.1, 132.4, 119.8, 116.3, 114.3, 110.3, 109.7, 109.4, 77.2, 47.8, 39.6, 36.8, 35.4, 35.3, 34.0, 33.0, 32.0, 31.3, 30.9, 30.0, 29.7, 29.6, 29.5, 29.4, 29.3, 23.4, 23.2, 22.7, 20.7, 14.2 ppm. **HRMS** (ESI+): calcd. for $C_{31}H_{51}O_2$ $[M + H]^+$ 455.3889; found $[M + H]^+$ 455.3865; m/z (%) = 455.3865 (80) $[M + H]^+$, 445.4046 (10), 415.3576 (100), 335.2950 (45).

References

1. Wöhler, F., Poggendorffs Ann. 1828, 12, 253–256.(b) Wöhler, F. *Ann. Chim. Phys* **1828,** *37*, 330-333.

2. Armstrong, R. W.; Beau, J. M.; Cheon, S. H.; Christ, W. J.; Fujioka, H.; Ham, W. H.; Hawkins, L. D.; Jin, H.; Kang, S. H., Total synthesis of palytoxin carboxylic acid and palytoxin amide. *J. Am. Chem. Soc.* **1989,** *111* (19), 7530-7533.

3. Suh, E. M.; Kishi, Y., Synthesis of palytoxin from palytoxin carboxylic acid. *J. Am. Chem. Soc.* **1994,** *116* (24), 11205-11206.

4. Albini, A.; Fagnoni, M., 1908: Giacomo Ciamician and the concept of green chemistry. *ChemSusChem: Chemistry & Sustainability Energy & Materials* **2008,** *1* (1-2), 63-66.

5. Eissen, M.; Metzger, J. O.; Schmidt, E.; Schneidewind, U., 10 years after Rio—concepts on the contribution of chemistry to a sustainable development. *Angew. Chem. Int. Ed.* **2002,** *41* (3), 414-436.

6. Anastas, P. T.; Warner, J. C., Principles of green chemistry. *Green chemistry: Theory and practice* **1998**, 29-56.

7. Trost, B. M., The atom economy--a search for synthetic efficiency. *Science* **1991,** *254* (5037), 1471-1477.

8. Robinson, R., LXIII.—A synthesis of tropinone. *J. Chem. Soc.* **1917,** *111*, 762-768.

9. Trost, B. M., Atom economy—a challenge for organic synthesis: homogeneous catalysis leads the way. *Angew. Chem., Int. Ed. Engl.* **1995,** *34* (3), 259-281.

10. Beletskaya, I. P.; Kustov, L. M., Catalysis as an important tool of green chemistry. *Russ. Chem. Rev.* **2010,** *79* (6), 441.

11. Kühlborn, J.; Groß, J.; Opatz, T., Making natural products from renewable feedstocks: back to the roots? *Nat. Prod. Rep.* **2020**.

12. Smit, W. A.; Bochkov, A. F. E.; Caple, R., *Organic synthesis: The science behind the art*. Royal Society of Chemistry, Cambridge: 2007.

13. Schutyser, W.; Renders, T.; Van den Bosch, S.; Koelewijn, S.-F.; Beckham, G.; Sels, B. F., Chemicals from lignin: an interplay of lignocellulose fractionation, depolymerisation, and upgrading. *Chem. Soc. Rev.* **2018,** *47* (3), 852-908.

14. Anwar, Z.; Gulfraz, M.; Irshad, M., Agro-industrial lignocellulosic biomass a key to unlock the future bio-energy: a brief review. *J. Radiat. Res. Appl. Sci. J RADIAT RES APPL SC* **2014,** *7* (2), 163-173.

15. Den, W.; Sharma, V. K.; Lee, M.; Nadadur, G.; Varma, R. S., Lignocellulosic biomass transformations via greener oxidative pretreatment processes: access to energy and value-added chemicals. *Front. Chem. FRONT CHEM* **2018,** *6*, 141.

16. Luque, R.; Len, C.; Triantafyllidis, K., Nano-(bio) catalysis in lignocellulosic biomass valorization. *Front. Chem. FRONT CHEM* **2018,** *6*, 577.

17. Zhang, Z.; Song, J.; Han, B., Catalytic transformation of lignocellulose into chemicals and fuel products in ionic liquids. *Chem. Rev.* **2017,** *117* (10), 6834-6880.

18. Luterbacher, J.; Alonso, D. M.; Dumesic, J., Targeted chemical upgrading of lignocellulosic biomass to platform molecules. *Green Chem.* **2014,** *16* (12), 4816-4838.

19. Gedam, P.; Sampathkumaran, P., Cashew nut shell liquid: extraction, chemistry and applications. *Prog. Org. Coat.* **1986,** *14* (2), 115-157.

20. Ngwira, K. J.; Kühlborn, J.; Mgani, Q. A.; de Koning, C. B.; Opatz, T., Valorisation of Cashew Nut Shell Liquid Phenolics in the Synthesis of UV Absorbers. *Eur. J. Org. Chem.* **2019,** *2019* (30), 4778-4790.

21. Klessinger, M.; Michl, J., *Excited states and photochemistry of organic molecules*. VCH publishers, New York: 1995.

22. Pfoertner, K. H.; Oppenländer, T., Photochemistry. *Ullmann's encyclopedia of industrial chemistry* **2000**.

23. Kavarnos, G. J.; Turro, N. J., Photosensitization by reversible electron transfer: theories, experimental evidence, and examples. *Chem. Rev.* **1986,** *86* (2), 401-449.

24. Barham, J. P.; König, B., Synthetic photoelectrochemistry. *Angew. Chem. Int. Ed.* **2020,** *59* (29), 11732-11747.

25. Heindel, N. D.; Pfau, M. A., A profitable partnership: Giacomo Ciamician and Paul Silber. *J. Chem. Educ.* **1965,** *42* (7), 383.

26. Albini, A.; Dichiarante, V., The 'belle époque'of photochemistry. *Photochem. Photobiol. Sci* **2009,** *8* (2), 248-254.

27. Ciamician, G.; Silber, P., Chemische lichtwirkungen. *Ber. Dtsch. Chem. Ges.* **1900,** *33* (3), 2911-2913.

28. Ciamician, G.; Silber, P., Chemische Lichtwirkungen. *Ber. Dtsch. Chem. Ges.* **1901,** *34* (2), 1530-1543.

29. Ciamician, G.; Silber, P., Chemische Lichtwirkungen.[XIX. Mitteilung]. *Ber. Dtsch. Chem. Ges.* **1911,** *44* (2), 1280-1289.

30. Sheldon, R. A.; Brady, D.; Bode, M. L., The Hitchhiker's guide to biocatalysis: recent advances in the use of enzymes in organic synthesis. *Chem. Sci.* **2020,** *11* (10), 2587-2605.

31. Ciamician, G.; Silber, P., Chemische Lichtwirkungen. XVIII. *Ber. Dtsch. Chem. Ges.* **1910,** *43* (2), 1536-1541.

32. König, B., *Chemical photocatalysis*. Berlin, Walter de Gruyter GmbH & Co. KG: 2013.

33. Roth, H. D., The beginnings of organic photochemistry. *Angew. Chem., Int. Ed. Engl.* **1989,** *28* (9), 1193-1207.

34. Norrish, R.; Bamford, C., Photodecomposition of aldehydes and ketones. *Nature* **1936,** *138* (3502), 1016-1016.

35. Dainton, F. S.; Thrush, B. A., Ronald George Wreyford Norrish, 9 November 1897-7 June 1978. The Royal Society London: 1981.

36. Yang, N.-C.; Feit, E. D.; Hui, M. H.; Turro, N. J.; Dalton, J. C., Photochemistry of di-tert-butyl ketone and structural effects on the rate and efficiency of intersystem crossing of aliphatic ketones. *J. Am. Chem. Soc.* **1970,** *92* (23), 6974-6976.

37. Abuin, E.; Encina, M.; Lissi, E., The photolysis of 3-pentanone. *Journal of Photochemistry* **1972,** *1* (5), 387-396.

38. Deslongchamps, P.; Cheriyan, U. O.; Lambert, Y.; Mercier, J.-C.; Ruest, L.; Russo, R.; Soucy, P., Synthesis of triquinacene and some of its derivatives. *Can. J. Chem.* **1978,** *56* (12), 1687-1704.

39. Russo, R.; Lambert, Y.; Deslongchamps, P., Synthesis of 2, 3-Dihydrotriquinacen-2-one. *Can. J. Chem.* **1971,** *49* (3), 531-533.

40. Mercier, C.; Soucy, P.; Rosen, W.; Deslongchamps, P., A Convenient Synthesis of Triquinacene. *Synth. Commun.* **1973,** *3* (2), 161-164.

41. Ternansky, R. J.; Balogh, D. W.; Paquette, L. A., Dodecahedrane. *J. Am. Chem. Soc.* **1982,** *104* (16), 4503-4504.

42. Fitjer, L.; Quabeck, U., Pentacyclo [11.3. 0.01, 5.05, 9.09, 13] hexadecan ([4.5] Coronan). *Angew. Chem.* **1987,** *99* (10), 1054-1056.

43. Paquette, L. A.; Sugimura, T., Enantiospecific total synthesis and absolute configurational assignment of (-)-punctatin A (antibiotic M95464). *J. Am. Chem. Soc.* **1986,** *108* (13), 3841-3842.

44. Renata, H.; Zhou, Q.; Baran, P. S., Strategic redox relay enables a scalable synthesis of ouabagenin, a bioactive cardenolide. *Science* **2013,** *339* (6115), 59-63.

45. Matsui, K., Green leaf volatiles: hydroperoxide lyase pathway of oxylipin metabolism. *Curr. Opin. Plant Biol.* **2006,** *9* (3), 274-280.

46. Günther, S. O.; Ziegler, K., Die Synthese des Ascaridols. *Naturwissenschaften32* **1944,** *157*.

47. Johnson, M. A.; Croteau, R., Biosynthesis of ascaridole: iodide peroxidase-catalyzed synthesis of a monoterpene endoperoxide in soluble extracts of Chenopodium ambrosioides fruit. *Arch. Biochem. Biophys.* **1984,** *235* (1), 254-266.

48. Pape, M., Industrial applications of photochemistry. *Pure Appl. Chem.* **1975,** *41* (4), 535-558.

49. Schenck, G. O., Phototrop-isomere Diradikale als reagierende Zwischenstoffe photochemischer Reaktionen. *Z. Naturforsch. B* **1948,** *3* (1-2), 59-60.

50. Schaffner, K., Günther Otto Schenck (1913–2003): A pioneer of radiation chemistry. *Angew. Chem. Int. Ed.* **2003,** *42* (26), 2932-2933.

51. Griesbeck, A. G.; Mattay, J., *Photochemical Key Steps in Organic Synthesis: An Experimental Course Book*. VCH: 1994.

52. Prein, M.; Adam, W., The Schenck ene reaction: diastereoselective oxyfunctionalization with singlet oxygen in synthetic applications. *Angew. Chem., Int. Ed. Engl.* **1996,** *35* (5), 477-494.

53. Westheimer, F. H., Paul Doughty Bartlett (14 August 1907-11 October 1997). JSTOR: 1998.

54. Bartlett, P. D.; Kimura, M.; Nakayama, J.; Watson, W. H., Photochemical oxidation and rearrangement of dibenzobarrelene and dehydrojanusene. *J. Am. Chem. Soc.* **1979,** *101* (21), 6332-6337.

55. Hammond, G. S.; Moore, W. M., The role of a triplet state in the photoreduction of benzophenone. *J. Am. Chem. Soc.* **1959,** *81* (23), 6334-6334.

56. Mulliken, R. S., Electronic Structures of Molecules X. Aldehydes, Ketones and Related Molecules. *J. Chem. Phys* **1935,** *3* (9), 564-573.

57. Arigoni, D.; Bosshard, H.; Bruderer, H.; Büchi, G.; Jeger, O.; Krebaum, L., Photochemische Reaktionen. 2. Mitteilung. Über gegenseitige Beziehungen und Umwandlungen bei Bestrahlungsprodukten des Santonins. *Helv. Chim. Acta* **1957,** *40* (6), 1732-1749.

58. Barton, D.; De Mayo, P.; Shafiq, M., 29. Photochemical transformations. Part II. The constitution of lumisantonin. *J. Chem. Soc* **1958**, 140-145.

59. Zimmerman, H. E.; Schuster, D. I., A new approach to mechanistic organic photochemistry. IV. Photochemical rearrangements of 4, 4-diphenylcyclohexadienone. *J. Am. Chem. Soc.* **1962,** *84* (23), 4527-4540.

60. Schuster, D. I., Howard E. Zimmerman (1926–2012). *Angew. Chem. Int. Ed.* **2012,** *51* (22), 5286-5288.

61. Zimmerman, H. E.; Wilson, J. W., Mechanistic and Exploratory Organic Photochemistry. IX. 1 Phenyl Migration in the Irradiation of 4, 4-Diphenylcyclohexenone2, 3. *J. Am. Chem. Soc.* **1964,** *86* (19), 4036-4042.

62. Büchi, G.; Inman, C. G.; Lipinsky, E., Light-catalyzed organic reactions. I. The reaction of carbonyl compounds with 2-methyl-2-butene in the presence of ultraviolet light. *J. Am. Chem. Soc.* **1954,** *76* (17), 4327-4331.

63. Ramamurthy, V.; Turro, N., Photochemistry: introduction. *Chem. Rev.* **1993,** *93* (1), 1-2.

64. Wender, P.; Howbert, J., Synthetic studies on arene-olefin cycloadditions: total synthesis of (.+-.)-. alpha.-cedrene. *J. Am. Chem. Soc.* **1981,** *103* (3), 688-690.

65. Remy, R.; Bochet, C. G., Arene–alkene cycloaddition. *Chem. Rev.* **2016,** *116* (17), 9816-9849.

66. Ischay, M. A.; Anzovino, M. E.; Du, J.; Yoon, T. P., Efficient visible light photocatalysis of [2+ 2] enone cycloadditions. *J. Am. Chem. Soc.* **2008,** *130* (39), 12886-12887.

67. Nicewicz, D. A.; MacMillan, D. W., Merging photoredox catalysis with organocatalysis: the direct asymmetric alkylation of aldehydes. *Science* **2008,** *322* (5898), 77-80.

68. Romero, N. A.; Nicewicz, D. A., Organic photoredox catalysis. *Chem. Rev.* **2016,** *116* (17), 10075-10166.

69. Beeler, A. B., *Introduction: Photochemistry in organic synthesis. Chem. Rev.* **2016**, 116 (17), 9629–9630.

70. Ihde, A. J., The history of free radicals and Moses Gomberg's contributions. *Pure Appl. Chem.* **1967,** *15* (1), 1-14.

71. Gomberg, M., Triphenylmethyl, ein Fall von dreiwerthigem Kohlenstoff. *Ber. Dtsch. Chem. Ges.* **1900,** *33* (3), 3150-3163.

72. Karkas, M. D., Photochemical generation of nitrogen-centered amidyl, hydrazonyl, and imidyl radicals: methodology developments and catalytic applications. *ACS Catalysis* **2017,** *7* (8), 4999-5022.

73. Corey, E.; Hertler, W. R., A Study of the Formation of Haloamines and Cyclic Amines by the Free Radical Chain Decomposition of N-Haloammonium Ions (Hofmann-Löffler Reaction). *J. Am. Chem. Soc.* **1960,** *82* (7), 1657-1668.

74. Akhtar, M.; Barton, D.; Sammes, P., Some Radical Exchange Reactions during Nitrite Ester Photolysis1. *J. Am. Chem. Soc.* **1965,** *87* (20), 4601-4607.

75. Löffler, K.; Freytag, C., Über eine neue Bildungsweise von N-alkylierten Pyrrolidinen. *Ber. Dtsch. Chem. Ges.* **1909,** *42* (3), 3427-3431.

76. Hernández, R.; Rivera, A.; Salazar, J. A.; Suárez, E., Nitroamine radicals as intermediates in the functionalization of non-activated carbon atoms. *J. Chem. Soc., Chem. Commun.* **1980,** (20), 958-959.

77. Dorta, R. L.; Francisco, C. G.; Suárez, E., Hypervalent organoiodine reagents in the transannular functionalisation of medium-sized lactams: synthesis of 1-azabicyclo compounds. *J. Chem. Soc., Chem. Commun.* **1989,** (16), 1168-1169.

78. Chen, K.; Richter, J. M.; Baran, P. S., 1, 3-diol synthesis via controlled, radical-mediated C− H functionalization. *J. Am. Chem. Soc.* **2008,** *130* (23), 7247-7249.

79. Choi, G. J.; Zhu, Q.; Miller, D. C.; Gu, C. J.; Knowles, R. R., Catalytic alkylation of remote C–H bonds enabled by proton-coupled electron transfer. *Nature* **2016,** *539* (7628), 268-271.

80. Chen, D.-F.; Chu, J. C.; Rovis, T., Directed γ-C (sp3)–H alkylation of carboxylic acid derivatives through visible light photoredox catalysis. *J. Am. Chem. Soc.* **2017,** *139* (42), 14897-14900.

81. Chemler, S. R.; Karyakarte, S. D.; Khoder, Z. M., Stereoselective and regioselective synthesis of heterocycles via copper-catalyzed additions of amine derivatives and alcohols to alkenes. *J. Org. Chem.* **2017,** *82* (21), 11311-11325.

82. McAtee, R. C.; Noten, E. A.; Stephenson, C. R., Arene dearomatization through a catalytic N-centered radical cascade reaction. *Nat. Commun.* **2020,** *11* (1), 1-8.

83. Walton, J. C., Synthetic strategies for 5-and 6-membered ring azaheterocycles facilitated by iminyl radicals. *Molecules* **2016,** *21* (5), 660.

84. Zard, S. Z., Recent progress in the generation and use of nitrogen-centred radicals. *Chem. Soc. Rev.* **2008,** *37* (8), 1603-1618.

85. Walton, J. C., Functionalised oximes: Emergent precursors for carbon-, nitrogen-and oxygen-centred radicals. *Molecules* **2016,** *21* (1), 63.

86. Jackman, M. M.; Cai, Y.; Castle, S. L., Recent advances in iminyl radical cyclizations. *Synthesis* **2017,** *49* (08), 1785-1795.

87. Bisai, V.; Saina Shaheeda, M.; Gupta, A.; Bisai, A., Biosynthetic relationships and total syntheses of naturally occurring benzo [c] phenanthridine alkaloids. *Asian J. Org. Chem.* **2019,** *8* (7), 946-969.

88. Hagel, J. M.; Facchini, P. J., Benzylisoquinoline alkaloid metabolism: a century of discovery and a brave new world. *Plant Cell Physiol.* **2013,** *54* (5), 647-672.

89. Bessi, I.; Bazzicalupi, C.; Richter, C.; Jonker, H. R.; Saxena, K.; Sissi, C.; Chioccioli, M.; Bianco, S.; Bilia, A. R.; Schwalbe, H., Spectroscopic, molecular modeling, and NMR-spectroscopic investigation of the binding mode of the natural alkaloids berberine and sanguinarine to human telomeric G-quadruplex DNA. *ACS Chem. Biol.* **2012,** *7* (6), 1109-1119.

90. Allen, C. F. H., *Six Membered Heterocyclic Nitrogen Compounds with Three Condensed Rings*. John Wiley & Sons: 2009; Vol. 24.

91. Mandadapu, A. K.; Dathi, M. D.; Arigela, R. K.; Kundu, B., Synthesis of 8-aryl substituted benzo [a] phenanthridine derivatives by consecutive three component tandem reaction and 6-endo carbocyclization. *Tetrahedron* **2012,** *68* (39), 8207-8215.

92. Mondal, P.; Thander, L.; Chattopadhyay, S. K., A new entry to the phenanthridine ring system. *Tetrahedron Lett.* **2012,** *53* (11), 1328-1331.

93. Read, M. L.; Gundersen, L.-L., Synthesis of phenanthridine derivatives by microwave-mediated cyclization of o-furyl (allylamino) arenes. *J. Org. Chem.* **2013,** *78* (3), 1311-1316.

94. Li, Y.; Zhu, J.; Zhang, L.; Wu, Y.; Gong, Y., Synthesis of Fluorine-Containing Multisubstituted Phenanthridines by Rhodium-Catalyzed Alkyne [2+ 2+ 2] Cycloaddition and Tandem sp2 C□ H Difluoromethylenation. *Chem. Eur. J.* **2013,** *19* (25), 8294-8299.

95. Pictet, A.; Ankersmit, H., Ueber das phenanthridin. *Justus Liebigs Ann. Chem.* **1891,** *266* (1-2), 138-153.

96. Bhowmik, S.; Pandey, G.; Batra, S., Substituent-Guided Switch between C□ H Activation and Decarboxylative Cross-Coupling during Palladium/Copper-Catalyzed Cascade Reactions of 2-Aminobenzoates with 2-Haloarylaldehydes. *Chem. Eur. J.* **2013,** *19* (32), 10487-10491.

97. Bowman, W. R.; Lyon, J. E.; Pritchard, G. J., Palladium and radical routes to phenanthridines. *ARKIVOC* **2012,** *7*, 210-227.

98. Katritzky, A. R.; Yang, B., Radical mediated synthesis of 6-arylphenanthridines via benzotriazole ring-opening. *J. Heterocycl. Chem.* **1996,** *33* (3), 607-610.

99. Leardini, R.; Tundo, A.; Zanardi, G.; Pedulli, G. F., A new and convenient synthesis of phenanthridines. *Synthesis (Stuttgart)* **1985,** (1), 107-110.

100. Pictet, A.; Hubert, A., Ueber eine neue Synthese der Phenanthridinbasen. *Ber. Dtsch. Chem. Ges.* **1896,** *29* (2), 1182-1189.

101. Morgan, G. T.; Walls, L. P., CCCXXXV.—Researches in the phenanthridine series. Part I. A new synthesis of phenanthridine homologues and derivatives. *J. Chem. Soc* **1931**, 2447-2456.

102. Peytou, V.; Condom, R.; Patino, N.; Guedj, R.; Aubertin, A.-M.; Gelus, N.; Bailly, C.; Terreux, R.; Cabrol-Bass, D., Synthesis and Antiviral Activity of Ethidium− Arginine Conjugates Directed Against the TAR RNA of HIV-1. *J. Med. Chem.* **1999,** *42* (20), 4042-4053.

103. Gilman, H.; Eisch, J., The preparation and dichromate oxidation of certain 6-substituted phenanthridines. *J. Am. Chem. Soc.* **1957,** *79* (16), 4423-4426.

104. Tobisu, M.; Koh, K.; Furukawa, T.; Chatani, N., Modular Synthesis of Phenanthridine Derivatives by Oxidative Cyclization of 2-Isocyanobiphenyls with Organoboron Reagents. *Angew. Chem.* **2012,** *124* (45), 11525-11528.

105. Jiang, H.; Cheng, Y.; Wang, R.; Zheng, M.; Zhang, Y.; Yu, S., Synthesis of 6-alkylated phenanthridine derivatives using photoredox neutral somophilic isocyanide insertion. *Angew. Chem.* **2013,** *125* (50), 13531-13534.

106. Wang, Q.; Dong, X.; Xiao, T.; Zhou, L., PhI (OAc) 2-mediated synthesis of 6-(trifluoromethyl) phenanthridines by oxidative cyclization of 2-isocyanobiphenyls with CF3SiMe3 under metal-free conditions. *Org. Lett.* **2013,** *15* (18), 4846-4849.

107. Zhang, B.; Mück-Lichtenfeld, C.; Daniliuc, C. G.; Studer, A., 6-Trifluoromethyl-Phenanthridines through Radical Trifluoromethylation of Isonitriles. *Angew. Chem. Int. Ed.* **2013,** *52* (41), 10792-10795.

108. Leifert, D.; Daniliuc, C. G.; Studer, A., 6-Aroylated phenanthridines via base promoted homolytic aromatic substitution (BHAS). *Org. Lett.* **2013,** *15* (24), 6286-6289.

109. Zhang, B.; Daniliuc, C. G.; Studer, A., 6-Phosphorylated phenanthridines from 2-isocyanobiphenyls via radical C–P and C–C bond formation. *Org. Lett.* **2014,** *16* (1), 250-253.

110. Watanabe, T.; Miyaura, N.; Suzuki, A., Synthesis of sterically hindered biaryls via the palladium-catalyzed cross-coupling reaction of arylboronic acids or their esters with haloarenes. *Synlett* **1992,** *1992* (03), 207-210.

111. Siddiqui, M.; Snieckus, V., The directed metalation connection to aryl-aryl cross coupling. Regiospecific synthesis of phenanthridines, phenanthridinones and the biphenyl alkaloid ismine. *Tetrahedron Lett.* **1988,** *29* (43), 5463-5466.

112. Li, D.; Zhao, B.; LaVoie, E. J., Nitroarylstannanes as Synthons for the Preparation of Phenanthridine and Benzo [i] phenanthridine Derivatives. *J. Org. Chem.* **2000,** *65* (9), 2802-2805.

113. Lysén, M.; Kristensen, J. L.; Vedsø, P.; Begtrup, M., Convergent synthesis of 6-substituted phenanthridines via anionic ring closure. *Org. Lett.* **2002,** *4* (2), 257-259.

114. Zhang, L.; Ang, G. Y.; Chiba, S., Copper-catalyzed synthesis of phenanthridine derivatives under an oxygen atmosphere starting from biaryl-2-carbonitriles and Grignard reagents. *Org. Lett.* **2010,** *12* (16), 3682-3685.

115. Deb, I.; Yoshikai, N., Phenanthridine synthesis through iron-catalyzed intramolecular N-arylation of O-acetyl oxime. *Org. Lett.* **2013,** *15* (16), 4254-4257.

116. Alonso, R.; Campos, P. J.; Garcia, B.; Rodríguez, M. A., New light-induced iminyl radical cyclization reactions of acyloximes to isoquinolines. *Org. Lett.* **2006,** *8* (16), 3521-3523.

117. Ngwira, K. J.; Rousseau, A. L.; Johnson, M. M.; de Koning, C. B., Reactions of [2-(2-Naphthyl) phenyl] acetylenes and 2-(2-Naphthyl) benzaldehyde O-Phenyloximes: Synthesis of the Angucycline Tetrangulol and 1, 10, 12-Trimethoxy-8-methylbenzo [c] phenanthridine. *Eur. J. Org. Chem.* **2017,** *2017* (11), 1479-1488.

118. Nair, J. J.; Rárová, L.; Strnad, M.; Bastida, J.; van Staden, J., Mechanistic insights to the cytotoxicity of Amaryllidaceae alkaloids. *Natural product communications* **2015,** *10* (1), 1934578X1501000138.

119. Marti, T.; Peterson, B. R.; Fürer, A.; Mordasini-Denti, T.; Zarske, J.; Jaun, B.; Diederich, F.; Gramlich, V., Macrotricyclic Steroid Receptors by Pd°-Catalyzed Cross-Coupling Reactions: Dissolution of cholesterol in aqueous solution and investigations of the principles governing selective molecular recognition of steroidal substrates. *Helv. Chim. Acta* **1998,** *81* (1), 109-144.

120. Johnson, S. M.; Petrassi, H. M.; Palaninathan, S. K.; Mohamedmohaideen, N. N.; Purkey, H. E.; Nichols, C.; Chiang, K. P.; Walkup, T.; Sacchettini, J. C.; Sharpless, K. B., Bisaryloxime ethers as potent inhibitors of transthyretin amyloid fibril formation. *J. Med. Chem.* **2005,** *48* (5), 1576-1587.

121. Jiang, H.; An, X.; Tong, K.; Zheng, T.; Zhang, Y.; Yu, S., Visible-Light-Promoted Iminyl-Radical Formation from Acyl Oximes: A Unified Approach to Pyridines, Quinolines, and Phenanthridines. *Angew. Chem. Int. Ed.* **2015,** *54* (13), 4055-4059.

122. Alvarez-Bercedo, P.; Martin, R., Ni-catalyzed reduction of inert C− O bonds: a new strategy for using aryl ethers as easily removable directing groups. *J. Am. Chem. Soc.* **2010,** *132* (49), 17352-17353.

123. Greer, A., Christopher Foote's discovery of the role of singlet oxygen [1O2 (1Δg)] in photosensitized oxidation reactions. *Acc. Chem. Res.* **2006,** *39* (11), 797-804.

124. Riegler, M., Insect threats to food security. *Science* **2018,** *361* (6405), 846-846.

125. Hassaan, M. A.; El Nemr, A., Pesticides pollution: Classifications, human health impact, extraction and treatment techniques. *Egypt. J. Aquat. Res.* **2020**.

126. Berenbaum, M., *Charge of the light brigade: phototoxicity as a defense against insects*, Vol. 339; ACS Symposium Series, 1987, pp 206-216.

127. Amor, T. B.; Jori, G., Sunlight-activated insecticides: historical background and mechanisms of phototoxic activity. *Insect Biochem. Mol. Biol.* **2000,** *30* (10), 915-925.

128. Nivsarkar, M.; Cherian, B.; Padh, H., Alpha-terthienyl: A plant-derived new generation insecticide. *Curr. Sci.* **2001**, 667-672.

129. Humphrey, A. J.; O'hagan, D., Tropane alkaloid biosynthesis. A century old problem unresolved. *Nat. Prod. Rep.* **2001,** *18* (5), 494-502.

130. Saraeian, A.; Aui, A.; Gao, Y.; Wright, M. M.; Foston, M.; Shanks, B. H., Evaluating lignin valorization via pyrolysis and vapor-phase hydrodeoxygenation for production of aromatics and alkenes. *Green Chem.* **2020,** *22* (8), 2513-2525.

131. Xu, Z.; Lei, P.; Zhai, R.; Wen, Z.; Jin, M., Recent advances in lignin valorization with bacterial cultures: microorganisms, metabolic pathways, and bio-products. *Biotechnol biofuels* **2019,** *12* (1), 1-19.

132. Calò, E.; Maffezzoli, A.; Mele, G.; Martina, F.; Mazzetto, S. E.; Tarzia, A.; Stifani, C., Synthesis of a novel cardanol-based benzoxazine monomer and environmentally sustainable production of polymers and bio-composites. *Green Chem.* **2007,** *9* (7), 754-759.

133. Deutsch, J.; Köckritz, A., Synthesis of novel chemicals from cardanol as a product of cashew nutshell processing. *Food Sci. Nutr.* **2020,** *8* (7), 3081-3088.

134. Mgaya, J. E.; Mubofu, E. B.; Mgani, Q. A.; Cordes, D. B.; Slawin, A. M.; Cole-Hamilton, D. J., Isomerization of anacardic acid: A possible route to the synthesis of an unsaturated benzolactone and a kairomone. *Eur. J. Lipid Sci. Technol.* **2015,** *117* (2), 190-199.

135. Puchot, L. *Cardanol: a bio-based building block for new sustainable and functional materials.* Ph.D Thesis, De l'Université de Cergy-Pontoise, Paris, France, 2016.

136. Mele, G.; Vasapollo, G., Fine chemicals and new hybrid materials from cardanol. *Mini. Rev. Org. Chem.* **2008,** *5* (3), 243-253.

137. Vasapollo, G.; Mele, G.; Del Sole, R., Cardanol-based materials as natural precursors for olefin metathesis. *Molecules* **2011,** *16* (8), 6871-6882.

138. Manda, B. R.; Prasad, A. N.; Thatikonda, N. R.; Lacerda Jr, V.; Barbosa, L. R.; Santos, H.; Romão, W.; Pavan, F. R.; Ribeiro, C. M.; Santos, E. A. d., Synthesis, antibacterial and antitubercular evaluation of cardanol and glycerol-based β-amino alcohol derivatives. *J. Braz. Chem. Soc.* **2018,** *29* (3), 639-648.

139. Suresh, K. I.; Kishanprasad, V. S., Synthesis, structure, and properties of novel polyols from cardanol and developed polyurethanes. *Ind. Eng. Chem. Res.* **2005,** *44* (13), 4504-4512.

140. Mmongoyo, J. A.; Mgani, Q. A.; Mdachi, S. J.; Pogorzelec, P. J.; Cole-Hamilton, D. J., Synthesis of a kairomone and other chemicals from cardanol, a renewable resource. *Eur. J. Lipid Sci. Technol.* **2012,** *114* (10), 1183-1192.

141. Baader, S.; Podsiadly, P.; Cole-Hamilton, D.; Goossen, L., Synthesis of tsetse fly attractants from a cashew nut shell extract by isomerising metathesis. *Green Chem.* **2014,** *16* (12), 4885-4890.

142. Shi, Y.; Kamer, P. C.; Cole-Hamilton, D. J., Synthesis of pharmaceutical drugs from cardanol derived from cashew nut shell liquid. *Green Chem.* **2019,** *21* (5), 1043-1053.

143. Pollini, J.; Bragoni, V.; Gooßen, L. J., Synthesis of a tyrosinase inhibitor by consecutive ethenolysis and cross-metathesis of crude cashew nutshell liquid. *Beilstein J. Org. Chem.* **2018,** *14* (1), 2737-2744.

144. Attanasi, O. A.; Buratti, S.; Filippone, P., Regioselective bromination of cardanol derivatives. *Org. Prep. Proced. Int.* **1995,** *27* (6), 645-650.

145. Yohana, M.; Ndoile, M.; Mgani, Q., Cost effective strategy for the synthesis of azo dyes by using cashew nut shell liquid (CNSL). *Tanz. J. Sci.* **2018,** *44* (2), 141-153.

146. Amorati, R.; Attanasi, O. A.; El Ali, B.; Filippone, P.; Mele, G.; Spadavecchia, J.; Vasapollo, G., Synthesis of new cardanol and cardol derivatives by allylation and regioselective cyclocarbonylation reactions. *Synthesis* **2002,** *2002* (18), 2749-2755.

147. Attanasi, O. A.; Berretta, S.; Fiani, C.; Filippone, P.; Mele, G.; Saladino, R., Synthesis and reactions of nitro derivatives of hydrogenated cardanol. *Tetrahedron* **2006,** *62* (25), 6113-6120.

148. Arcadi, A.; Attanasi, O. A.; Berretta, S.; Bianchi, G.; Filippone, P., Synthesis of new cardanol derivatives through combined iodination/palladium-catalysed cross-coupling reactions. *Synthesis* **2006,** *2006* (15), 2523-2530.

149. Bernini, R.; Cacchi, S.; De Salve, I.; Fabrizi, G., Palladium-catalyzed synthesis of lipophilic benzo [b] furans from cardanol. *Synthesis* **2007,** *2007* (06), 873-882.

150. Barker, P.; Finke, P.; Thompson, K., Preparation and cyclization of aryloxyacetaldehyde acetals; a general synthesis of 2, 3-unsubstituted benzofurans. *Synth. Commun.* **1989,** *19* (1-2), 257-265.

151. Amorati, R.; Attanasi, O. A.; Favi, G.; Menichetti, S.; Pedulli, G. F.; Viglianisi, C., Amphiphilic antioxidants from "cashew nut shell liquid"(CNSL) waste. *Org. Biomol. Chem.* **2011,** *9* (5), 1352-1355.

152. Capozzi, G.; Falciani, C.; Menichetti, S.; Nativi, C., Phthalimidesulfenyl Chloride. 1 11. Generation, General Reactivity, and Synthetic Applications of o-Thioquinones. *J. Org. Chem.* **1997,** *62* (8), 2611-2615.

153. Behalo, M. S.; Bloise, E.; Mele, G.; Salomone, A.; Messa, F.; Carbone, L.; Mazzetto, S. E.; Lomonaco, D., Bio-based benzoxazines synthesized in a deep eutectic solvent: A greener approach toward vesicular nanosystems. *J. Heterocycl. Chem.* **2020,** *57* (2), 768-773.

154. Cimarelli, C.; Fratoni, D.; Mazzanti, A.; Palmieri, G., *Betti reaction of cyclic imines with naphthols and phenols–preparation of new derivatives of Betti's bases*. *Eur. J. Org. Chem.* **2011**, 2094–2100.

155. Lalitha, K.; Nagarajan, S., Strongly fluorescent organogels and self-assembled nanostructures from pyrene coupled coumarin derivatives: application in cell imaging. *J. Mater. Chem. B* **2015,** *3* (28), 5690-5701.

156. Thirunavukkarasu, V. S.; Ackermann, L., Ruthenium-catalyzed C–H bond oxygenations with weakly coordinating ketones. *Org. Lett.* **2012,** *14* (24), 6206-6209.

157. Lorz, P. M.; Towae, F. K.; Enke, W.; Jäckh, R.; Bhargava, N.; Hillesheim, W., Phthalic acid and derivatives. *Ullmann's encyclopedia of industrial chemistry* **2000**.

158. Orndorff, W. R.; Allen, E. R., The orcinolphthaleins, the orcinoltetrachlorophthaleins, and some of their derivatives. *J. Am. Chem. Soc.* **1915,** *37* (5), 1201-1258.

159. Dugrand-Judek, A.; Olry, A.; Hehn, A.; Costantino, G.; Ollitrault, P.; Froelicher, Y.; Bourgaud, F., The distribution of coumarins and furanocoumarins in citrus species closely matches Citrus phylogeny and reflects the organization of biosynthetic pathways. *PLOS one* **2015,** *10* (11), e0142757.

160. Rodrigues, J. L.; Rodrigues, L. R., Biosynthesis and heterologous production of furanocoumarins: perspectives and current challenges. *Nat. Prod. Rep.* **2021**.

161. Molnar, M.; Lončarić, M.; Kovač, M., Green chemistry approaches to the synthesis of coumarin derivatives. *Curr. Org. Chem.* **2020,** *24* (1), 4-43.

162. Yates, P.; Macas, T. S., Tandem Wessely oxidation and intramolecular Diels–Alder reactions. III. Synthesis of isotwistanes. *Can. J. Chem.* **1988,** *66* (1), 1-10.

163. Bhunia, S. C.; Patra, G. C.; Pal, S. C., Reimer–Tiemann Reaction of Coumarins. *Synth. Commun.* **2011,** *41* (24), 3678-3682.

164. Osborne, A., Orientation effects in the pechmann reaction: Synthesis of 5, 6-dimethylcoumarin and an examination of ortho-proximity effects in 13C NMR spectroscopy. *Tetrahedron* **1981,** *37* (10), 2021-2025.

165. Worden, L. R.; Kaufman, K. D.; Smith, P. J.; Widiger, G. N., Synthesis of 4, 6-dihydroxyisophthalaldehyde and the 5-methyl and 5-methoxy-derivatives. *J. Chem. Soc. C Org.* **1970,** (2), 227-230.

166. Chimichi, S.; Boccalini, M.; Cosimelli, B.; Viola, G.; Vedaldi, D.; Dall'Acqua, F., A convenient synthesis of psoralens. *Tetrahedron* **2002,** *58* (24), 4859-4863.

167. Razdan, R. K., The total synthesis of cannabinoids. In: Apsimon J., editor. T*otal Synthesis Natural Products*. Vol. 4. Wiley; New York, NY, USA: 1981. pp. 185–262.

168. Fahrenholtz, K. E.; Lurie, M.; Kierstead, R. W., Total synthesis of (.+-.)-. DELTA. 9-tetrahydrocannabinol and four of its isomers. *J. Am. Chem. Soc.* **1967,** *89* (23), 5934-5941.

169. Pearson, E. L.; Kanizaj, N.; Willis, A. C.; Paddon-Row, M. N.; Sherburn, M. S., Experimental and Computational Studies into an ATPH-Promoted exo-Selective IMDA Reaction: A Short Total Synthesis of Δ9-THC. *Chem. Eur. J.* **2010,** *16* (28), 8280-8284.

170. Lydon, J.; Teramura, A. H.; Coffman, C. B., UV-B radiation effects on photosynthesis, growth and cannabinoid production of two Cannabis sativa chemotypes. *Photochem. Photobiol.* **1987,** *46* (2), 201-206.

171. Eichhorn Bilodeau, S.; Wu, B.-S.; Rufyikiri, A.-S.; MacPherson, S.; Lefsrud, M., An update on plant photobiology and implications for cannabis production. *Front. Plant Sci.* **2019,** *10*, 296.

172. Tramèr, M. R.; Carroll, D.; Campbell, F. A.; Reynolds, D. J. M.; Moore, R. A.; McQuay, H. J., Cannabinoids for control of chemotherapy induced nausea and vomiting: quantitative systematic review. *Bmj* **2001,** *323* (7303), 16.

173. Murillo-Rodríguez, E.; Millán-Aldaco, D.; Palomero-Rivero, M.; Mechoulam, R.; Drucker-Colín, R., Cannabidiol, a constituent of Cannabis sativa, modulates sleep in rats. *FEBS Lett.* **2006,** *580* (18), 4337-4345.

174. Mechoulam, R.; Shvo, Y., Hashish—I: the structure of cannabidiol. *Tetrahedron* **1963,** *19* (12), 2073-2078.

175. Adams, R.; Hunt, M.; Clark, J., Structure of cannabidiol, a product isolated from the marihuana extract of Minnesota wild hemp. I. *J. Am. Chem. Soc.* **1940,** *62* (1), 196-200.

176. Jacob, A.; Todd, A., 119. Cannabis indica. Part II. Isolation of cannabidiol from Egyptian hashish. Observations on the structure of cannabinol. *J. Chem. Soc* **1940**, 649-653.

177. Mechoulam, R., Conversation with Raphael Mechoulam. *Addiction (Abingdon, England)* **2007,** *102* (6), 887-893.

178. Malfait, A.; Gallily, R.; Sumariwalla, P.; Malik, A.; Andreakos, E.; Mechoulam, R.; Feldmann, M., The nonpsychoactive cannabis constituent cannabidiol is an oral anti-arthritic therapeutic in murine collagen-induced arthritis. *PNAS* **2000,** *97* (17), 9561-9566.

179. Cunha, J. M.; Carlini, E.; Pereira, A. E.; Ramos, O. L.; Pimentel, C.; Gagliardi, R.; Sanvito, W.; Lander, N.; Mechoulam, R., Chronic administration of cannabidiol to healthy volunteers and epileptic patients. *Pharmacology* **1980,** *21* (3), 175-185.

180. Bryant, D. N.; Sheldahl, L. C.; Marriott, L. K.; Shapiro, R. A.; Dorsa, D. M., Multiple pathways transmit neuroprotective effects of gonadal steroids. *Endocrine* **2006,** *29* (2), 199-207.

181. Weiss, L.; Zeira, M.; Reich, S.; Har-Noy, M.; Mechoulam, R.; Slavin, S.; Gallily, R., Cannabidiol lowers incidence of diabetes in non-obese diabetic mice. *Autoimmunity* **2006,** *39* (2), 143-151.

182. Gaoni, Y.; Mechoulam, R., Isolation, structure, and partial synthesis of an active constituent of hashish. *J. Am. Chem. Soc.* **1964,** *86* (8), 1646-1647.

183. Verty, A. N.; Evetts, M. J.; Crouch, G. J.; McGregor, I. S.; Stefanidis, A.; Oldfield, B. J., The cannabinoid receptor agonist THC attenuates weight loss in a rodent model of activity-based anorexia. *Neuropsychopharmacology* **2011,** *36* (7), 1349-1358.

184. Andries, A.; Frystyk, J.; Flyvbjerg, A.; Støving, R. K., Dronabinol in severe, enduring anorexia nervosa: a randomized controlled trial. *IJED* **2014,** *47* (1), 18-23.

185. Ware, M. A.; Daeninck, P.; Maida, V., A review of nabilone in the treatment of chemotherapy-induced nausea and vomiting. *Ther Clin Risk Manag.* **2008,** *4* (1), 99.

186. Pertwee, R. G., Pharmacology of cannabinoid CB1 and CB2 receptors. *Pharmacol. Ther.* **1997,** *74* (2), 129-180.

187. Xiong, W.; Cheng, K.; Cui, T.; Godlewski, G.; Rice, K. C.; Xu, Y.; Zhang, L., Cannabinoid potentiation of glycine receptors contributes to cannabis-induced analgesia. *Nature chemical biology* **2011,** *7* (5), 296-303.

188. Zhang, L.; Xiong, W., Modulation of the Cys-Loop Ligand-Gated Ion Channels by Fatty Acid and Cannabinoids. *Vitamins & Hormones* **2009,** *81*, 315-335.

189. Oz, M., Receptor-independent actions of cannabinoids on cell membranes: focus on endocannabinoids. *Pharmacol. Ther.* **2006,** *111* (1), 114-144.

190. Gülck, T.; Møller, B. L., Phytocannabinoids: origins and biosynthesis. *Trends in Plant Science* **2020**.

191. Bloemendal, V. R.; van Hest, J. C.; Rutjes, F. P., Synthetic pathways to tetrahydrocannabinol (THC): an overview. *Org. Biomol. Chem.* **2020,** *18* (17), 3203-3215.

192. Mechoulam, R.; Braun, P.; Gaoni, Y., Stereospecific synthesis of (-)-. DELTA. 1-and (-)-. DELTA. 1 (6)-tetrahydrocannabinols. *J. Am. Chem. Soc.* **1967,** *89* (17), 4552-4554.

193. Mechoulam, R.; Braun, P.; Gaoni, Y., Syntheses of. DELTA. 1-tetrahydrocannabinol and related cannabinoids. *J. Am. Chem. Soc.* **1972,** *94* (17), 6159-6165.

194. Razdan, R.; Handrick, G.; Dalzell, H., A one-step synthesis of (-)-Δ 1-Tetrahydrocannabinol from chrysanthenol. *Experientia* **1975,** *31* (1), 16-17.

195. Liazid, A.; Barbero, G. F.; Palma, M.; Brigui, J.; Barroso, C. G., Optimization of a new extraction technique for analysis of verbenone and cis-verbenol in pine seeds. *Chromatographia* **2007,** *66* (7), 571-575.

196. Erman, W. F., Photochemical transformations of unsaturated bicyclic ketones. Verbenone and its photodynamic products of ultraviolet irradiation. *J. Am. Chem. Soc.* **1967,** *89* (15), 3828-3841.

197. Schafroth, M. A.; Zuccarello, G.; Krautwald, S.; Sarlah, D.; Carreira, E. M., Stereodivergent Total Synthesis of Δ9-Tetrahydrocannabinols. *Angew. Chem.* **2014,** *126* (50), 14118-14121.

198. Fischer, O.; Hubert, A.; Heinrich, M. R., Shifted selectivity in protonation enables the mild deuteration of arenes through catalytic amounts of Bronsted acids in deuterated methanol. *J. Org. Chem.* **2020,** *85* (18), 11856-11866.

199. Petzold, D.; Koenig, B., Photocatalytic Oxidative Bromination of Electron-Rich Arenes and Heteroarenes by Anthraquinone. *Adv. Synth. Catal.* **2018,** *360* (4), 626-630.

200. Kerr, D. J.; Willis, A. C.; Flynn, B. L., Multicomponent coupling approach to (±)-Frondosin B and a ring-expanded analogue. *Org. Lett.* **2004,** *6* (4), 457-460.

201. Zhang, Q.; Dong, J.; Huang, G.; Li, S., An Efficient Synthesis of 1-Hydroxy-5, 8-dimethoxy-2-naphthaldehyde. *Heterocycles: an international journal for reviews and communications in heterocyclic chemistry* **2018,** *96* (2), 334-338.

202. Schaarschmidt, M.; Höfner, G.; Wanner, K. T., Synthesis and Biological Evaluation of Nipecotic Acid and Guvacine Derived 1, 3-Disubstituted Allenes as Inhibitors of Murine GABA Transporter mGAT1. *ChemMedChem* **2019,** *14* (12), 1135-1151.

203. Tummatorn, J.; Krajangsri, S.; Norseeda, K.; Thongsornkleeb, C.; Ruchirawat, S., A new synthetic approach to 6-unsubstituted phenanthridine and phenanthridine-like compounds under mild and metal-free conditions. *Org. Biomol. Chem.* **2014,** *12* (28), 5077-5081.

204. Pradeep, P.; Ngwira, K. J.; Reynolds, C.; Rousseau, A. L.; Lemmerer, A.; Fernandes, M. A.; Johnson, M. M.; de Koning, C. B., Novel methodology for the synthesis of the benzo [b] phenanthridine and 6H-dibenzo [c, h] chromen-6-one skeletons. Reactions of 2-naphthylbenzylamines and 2-naphthylbenzyl alcohols. *Tetrahedron* **2016,** *72* (51), 8417-8427.

205. Dhara, S.; Ghosh, M.; Ray, J. K., Synthesis of Phenanthridines and Analogues via Suzuki coupling and condensation. *Synlett* **2013,** *24* (17), 2263-2265.

206. Ghosh, I.; Shaikh, R. S.; König, B., Sensitization-Initiated Electron Transfer for Photoredox Catalysis. *Angew. Chem. Int. Ed.* **2017,** *56* (29), 8544-8549.

207. Urawa, Y.; Naka, H.; Miyazawa, M.; Souda, S.; Ogura, K., Investigations into the Suzuki–Miyaura coupling aiming at multikilogram synthesis of E2040 using (o-cyanophenyl) boronic esters. *J. Organomet. Chem.* **2002,** *653* (1-2), 269-278.

208. Wan, J.-C.; Huang, J.-M.; Jhan, Y.-H.; Hsieh, J.-C., Novel syntheses of fluorenones via nitrile-directed palladium-catalyzed C–H and dual C–H bond activation. *Org. Lett.* **2013,** *15* (11), 2742-2745.

209. Portela-Cubillo, F.; Scott, J. S.; Walton, J. C., Microwave-assisted syntheses of N-heterocycles using alkenone-, alkynone-and aryl-carbonyl O-phenyl oximes: Formal synthesis of neocryptolepine. *J. Org. Chem.* **2008,** *73* (14), 5558-5565.

Appendices

Synthesis of the Phenanthridines

Compound 133a

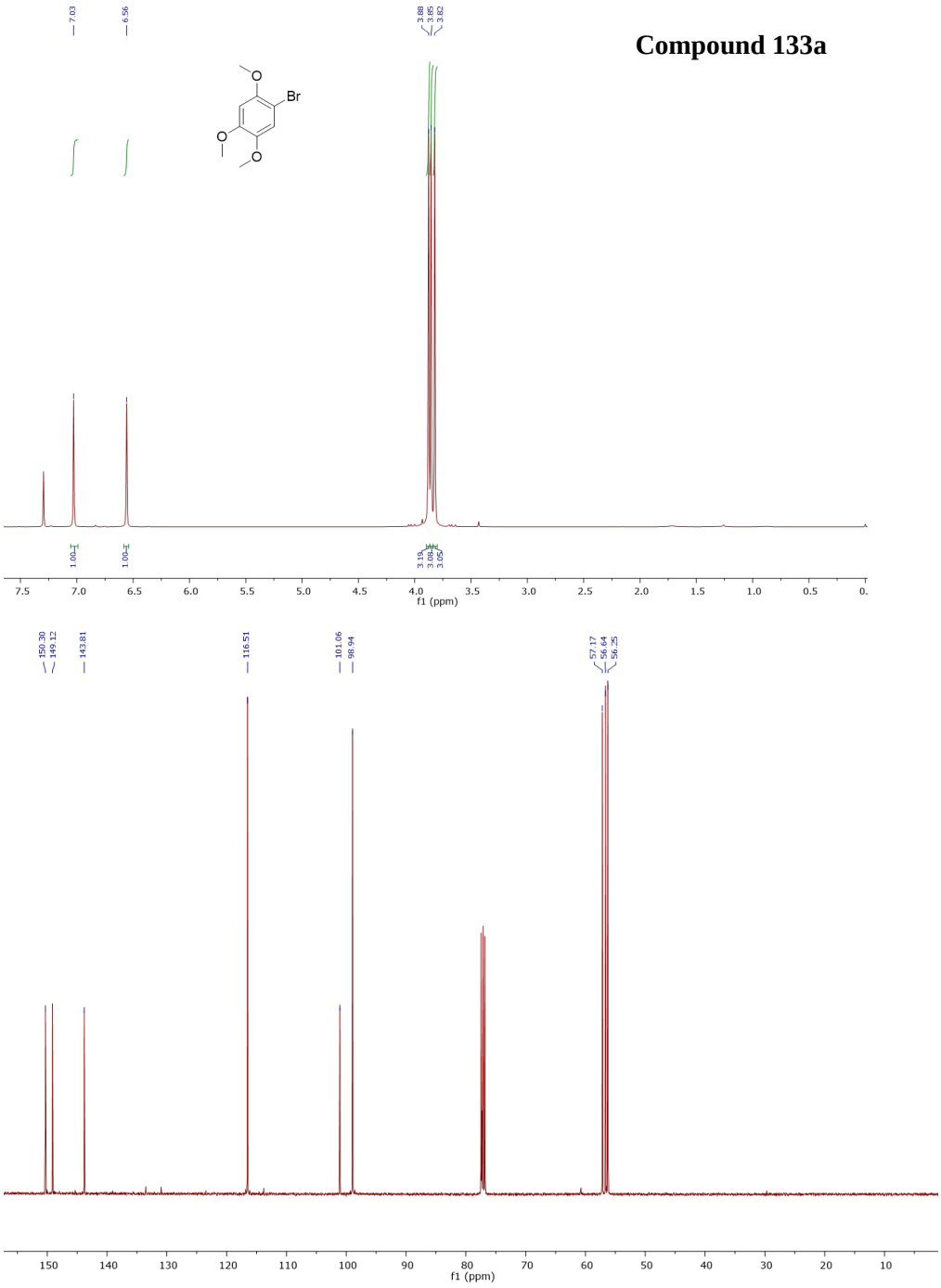

Compound 133b

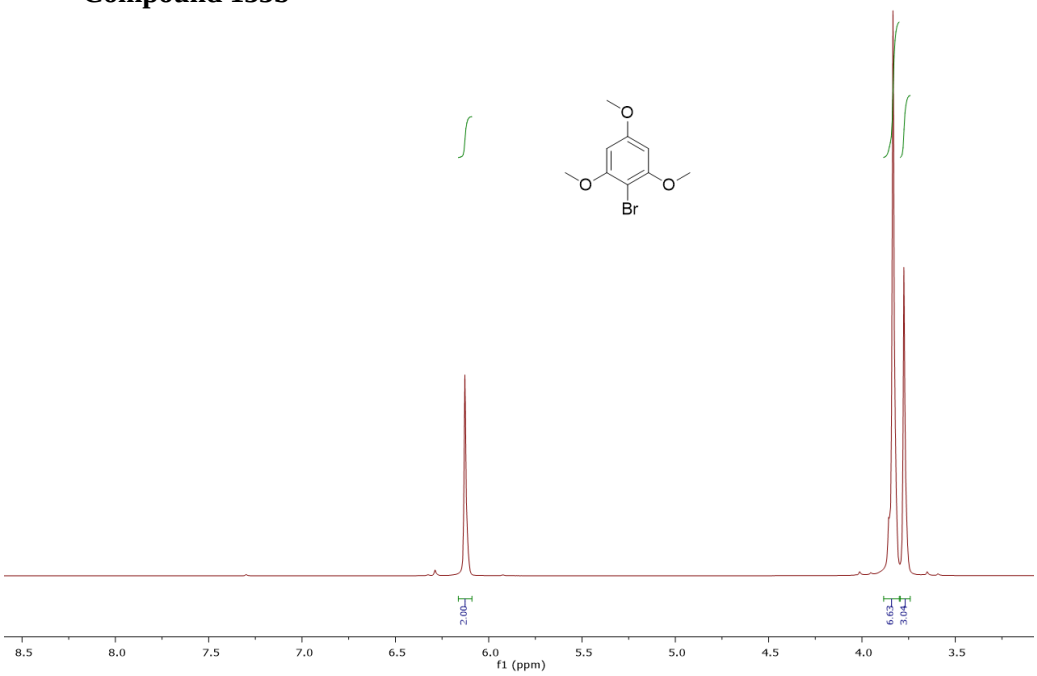

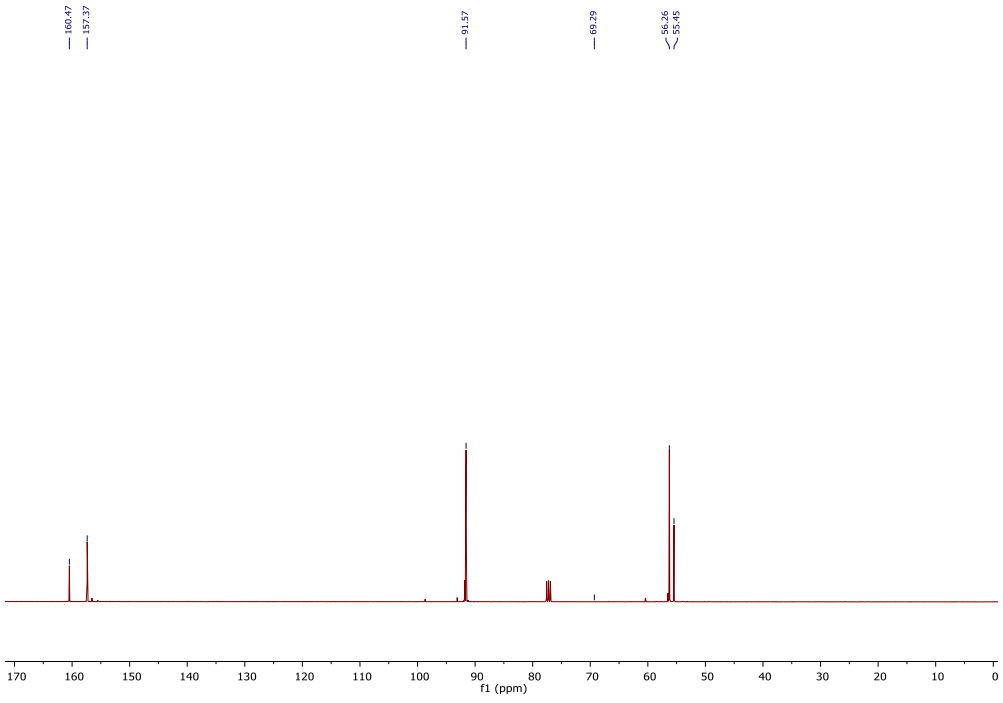

Compound 133c

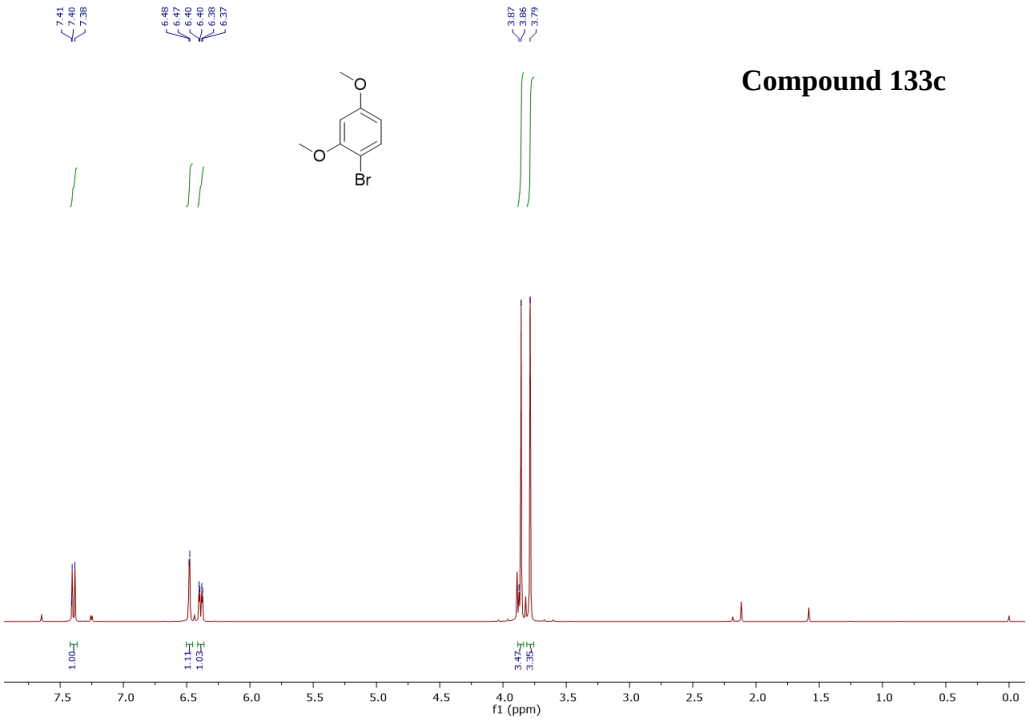

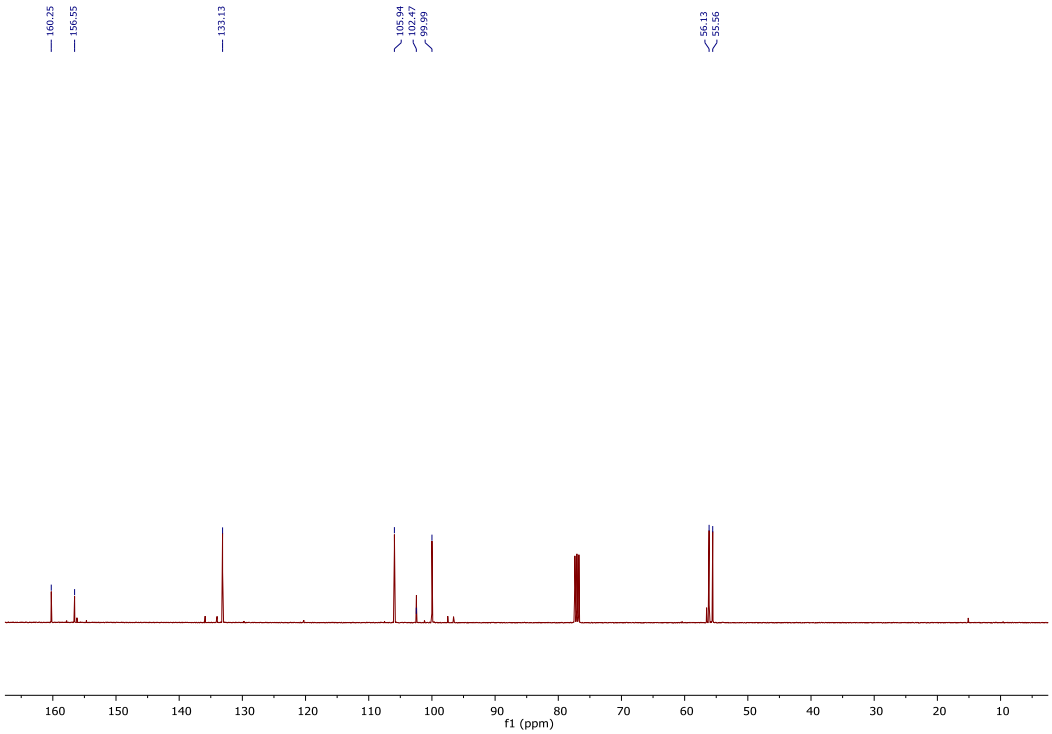

Compound 133d

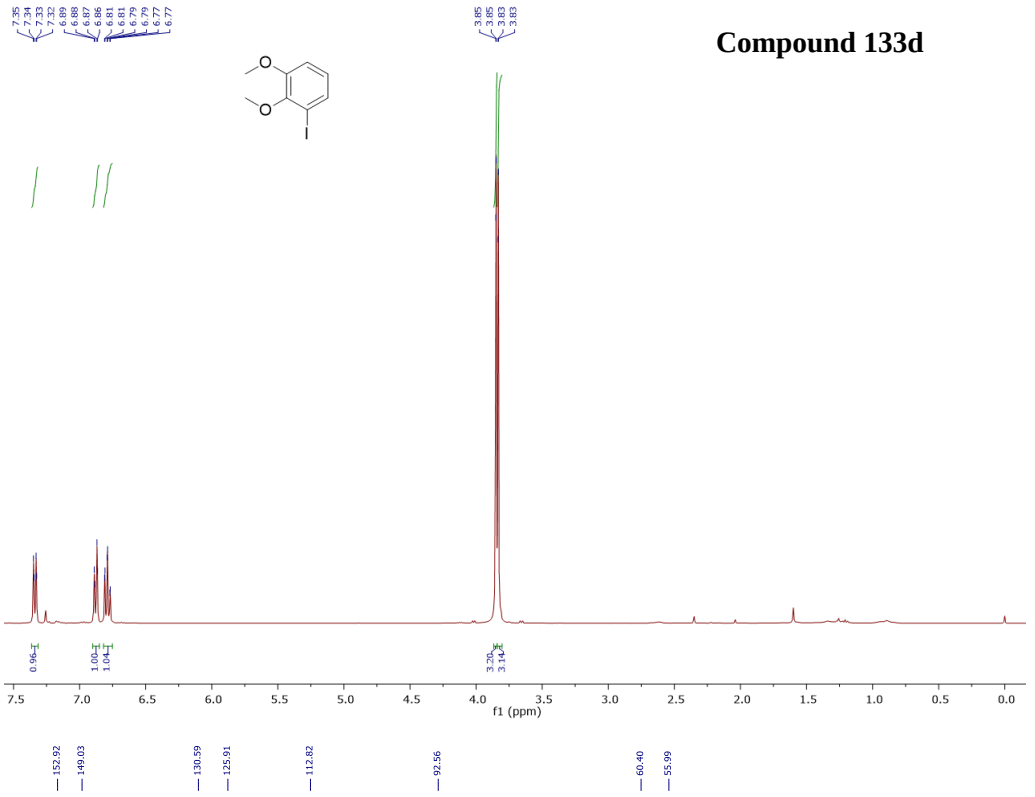

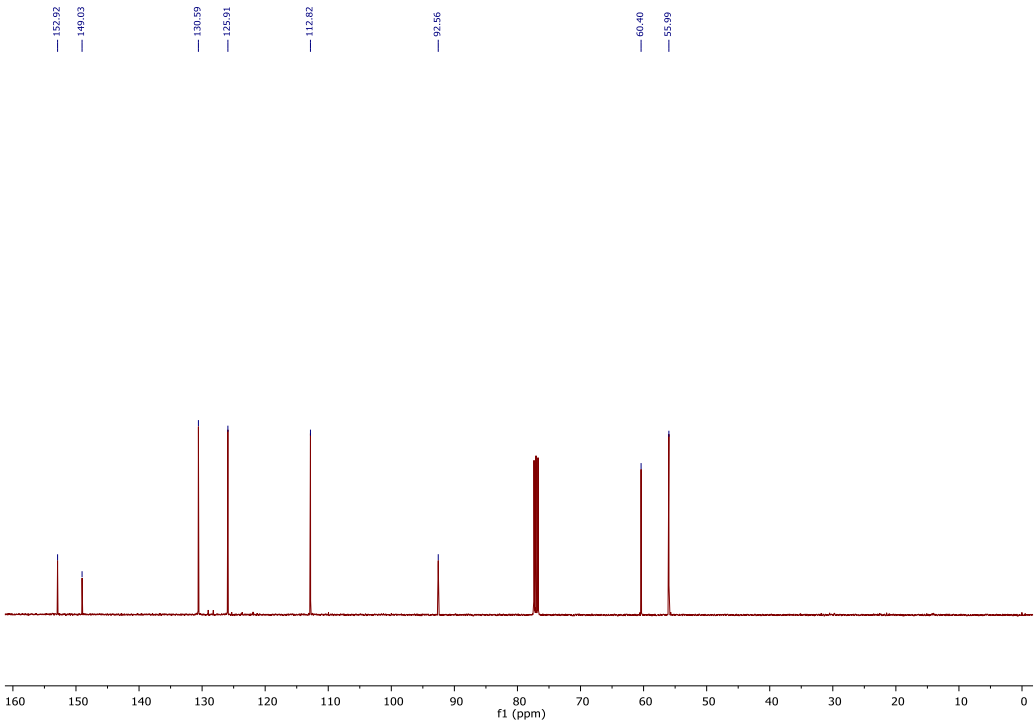

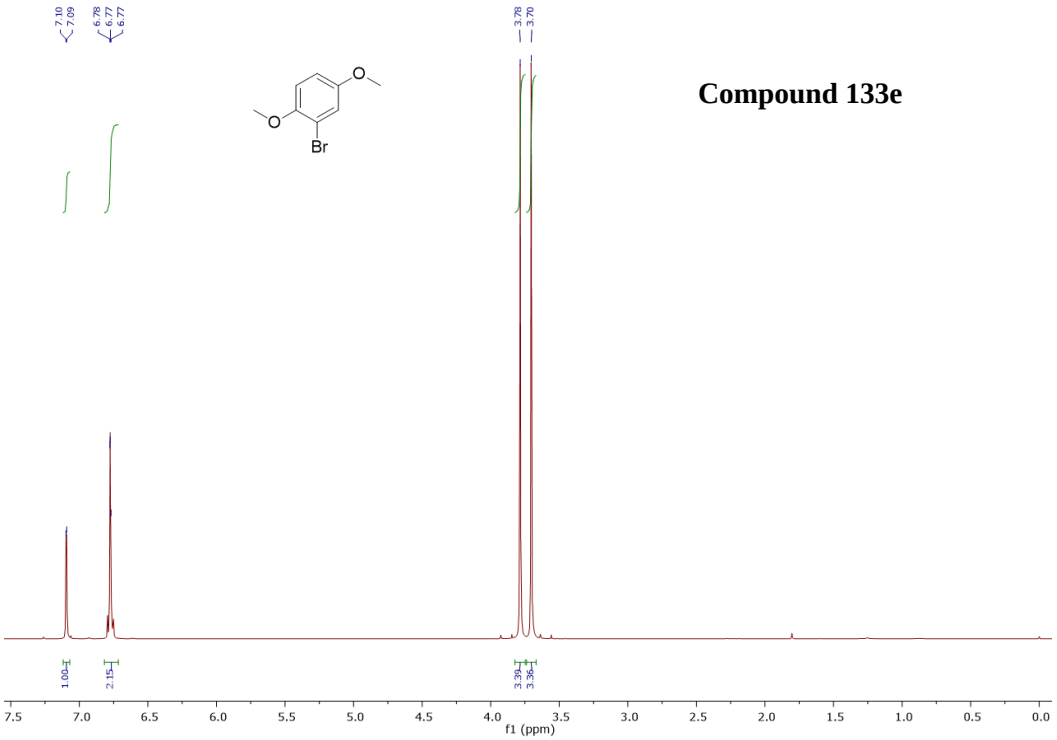

Compound 133e

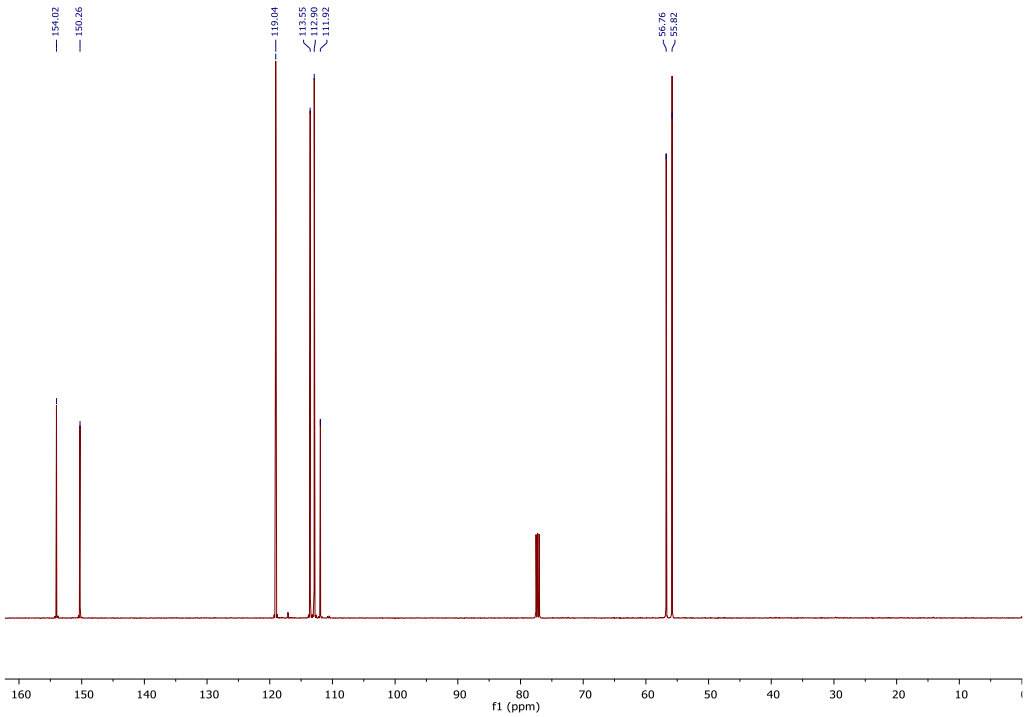

Compound 132a

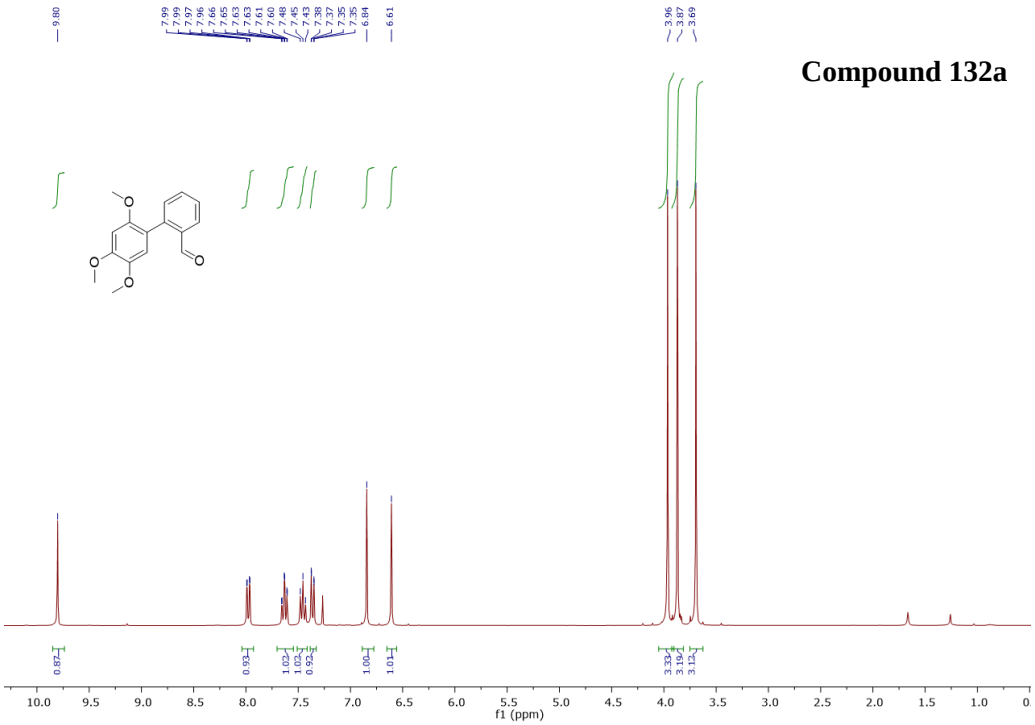

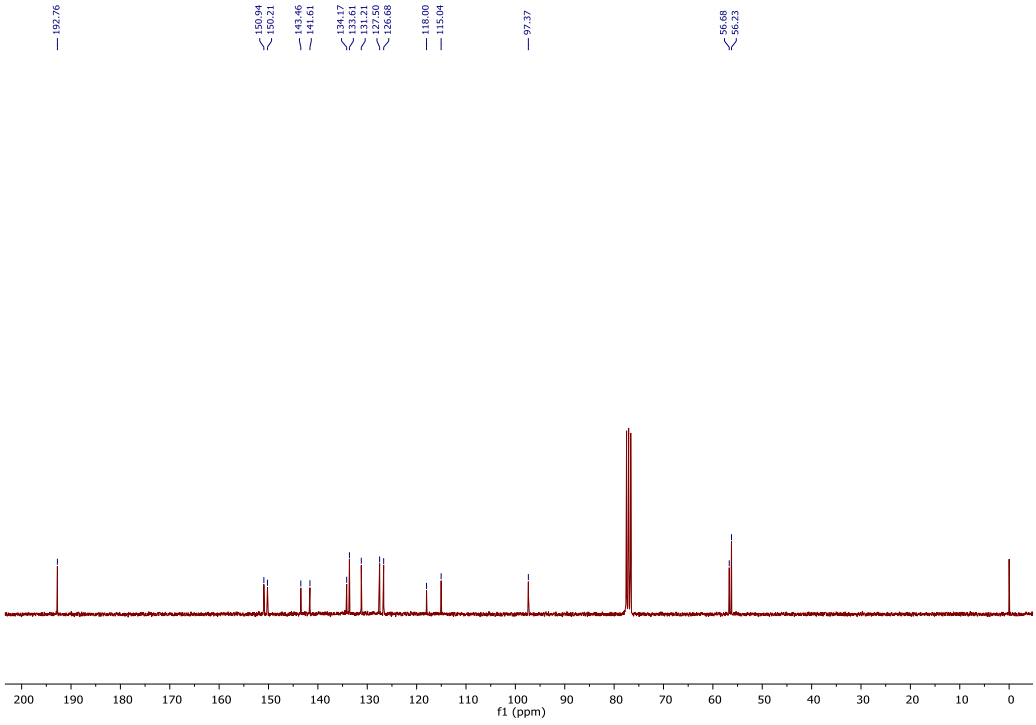

Compound 132b

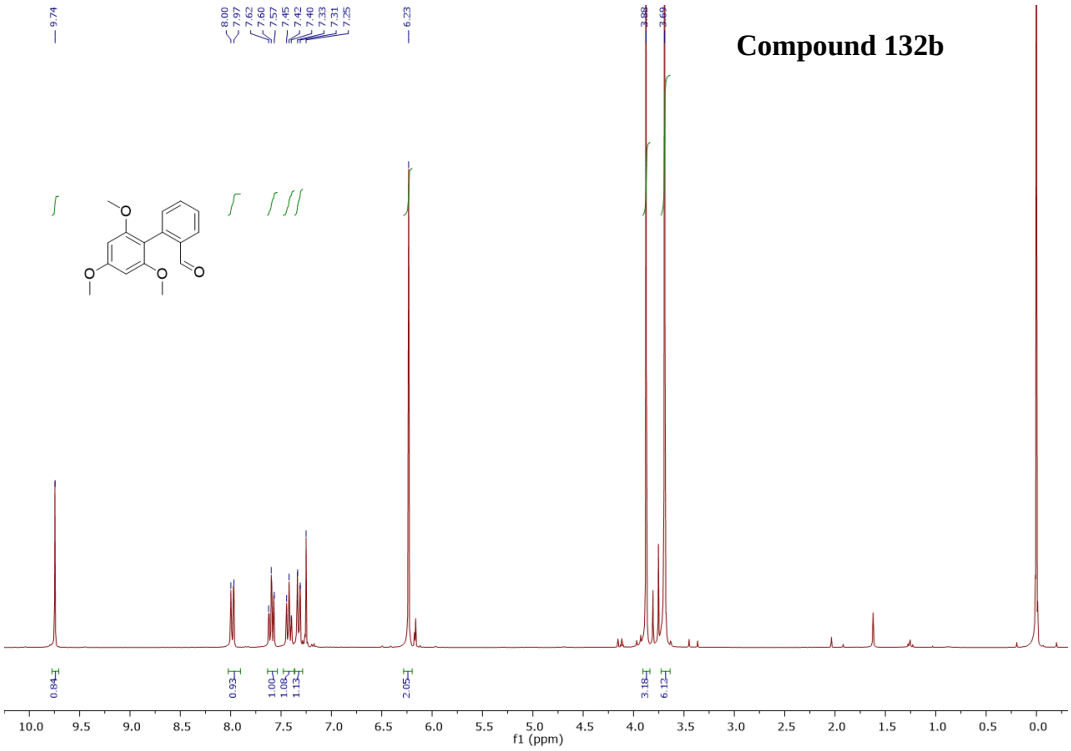

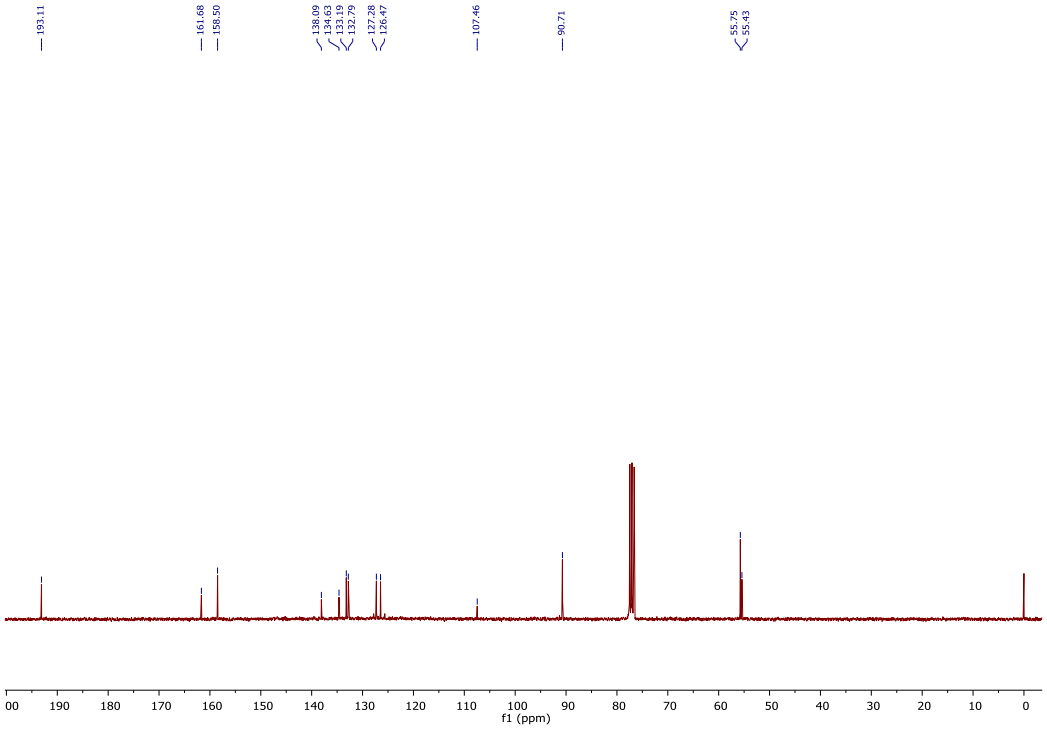

Compound 132e

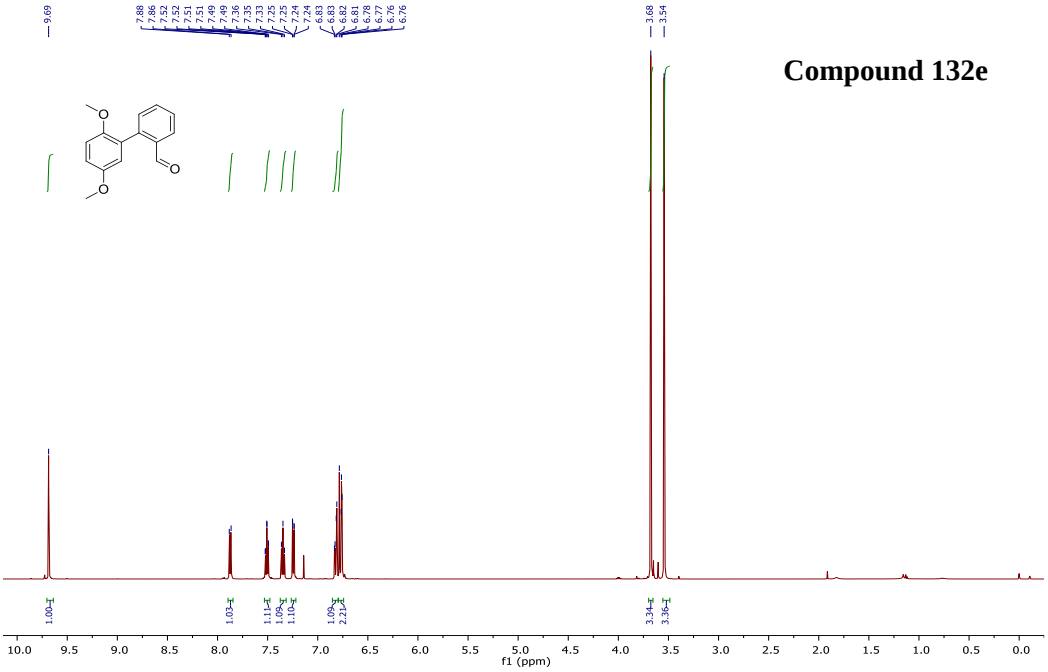

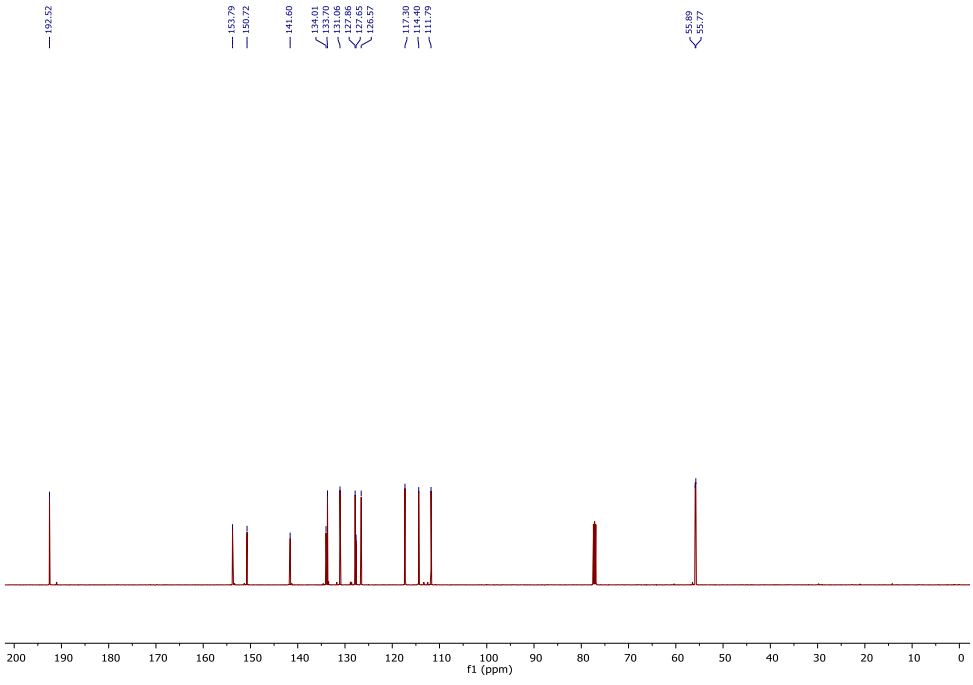

Compound 132d

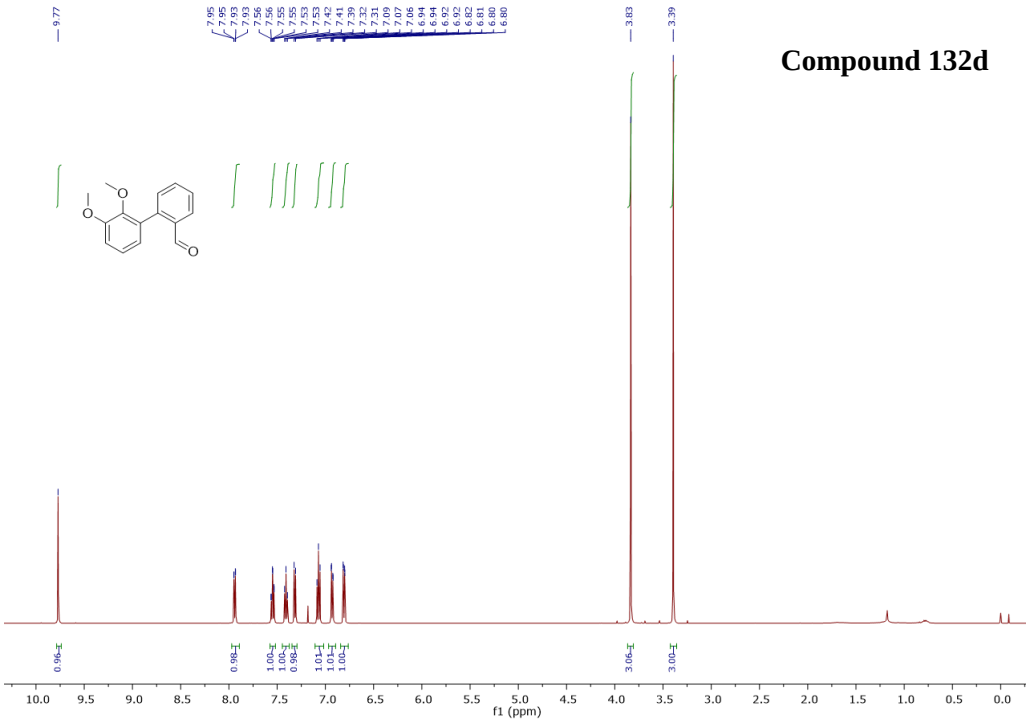

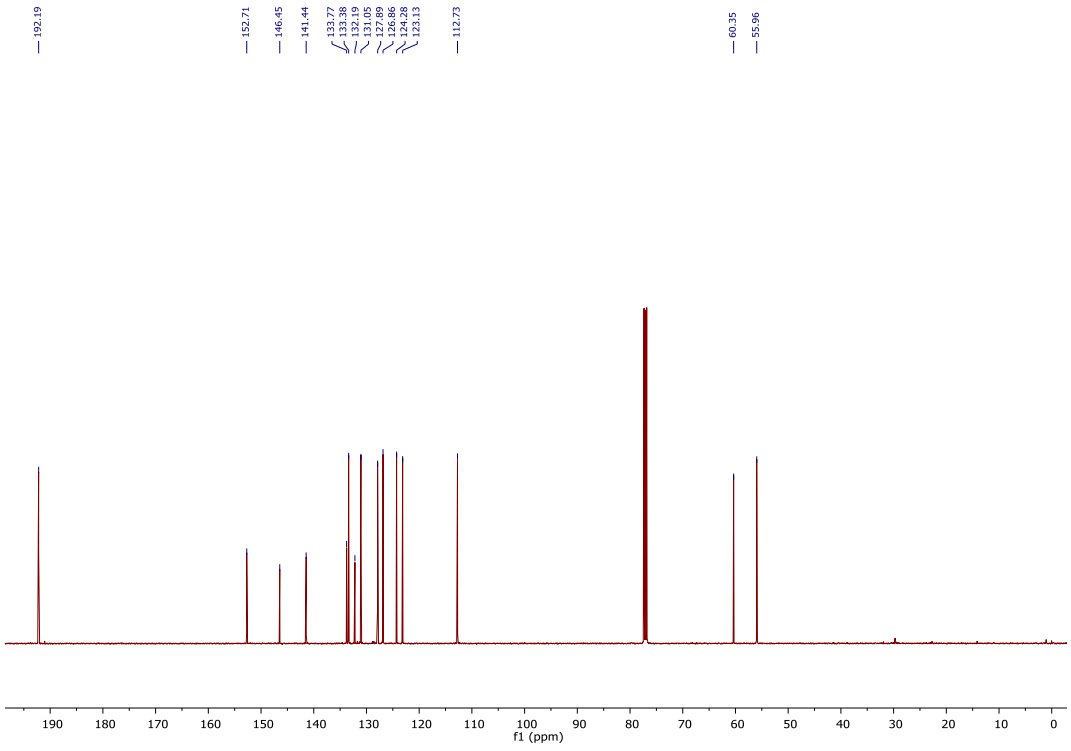

Compound 132c

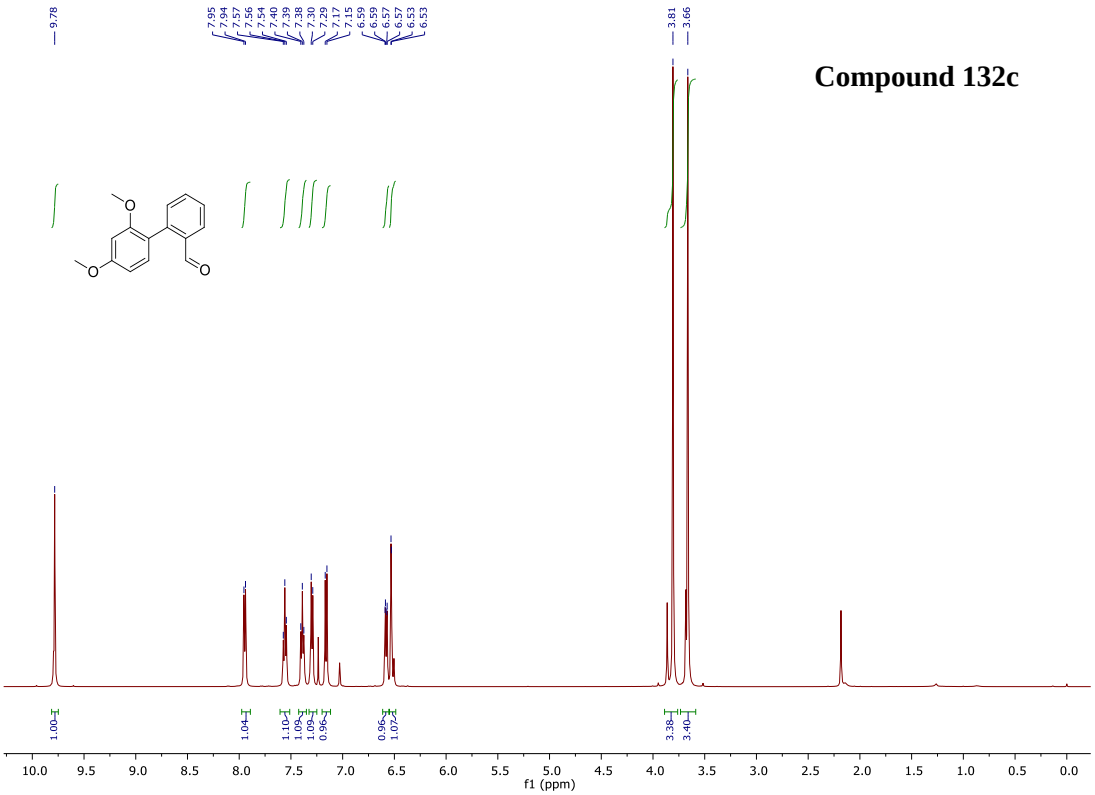

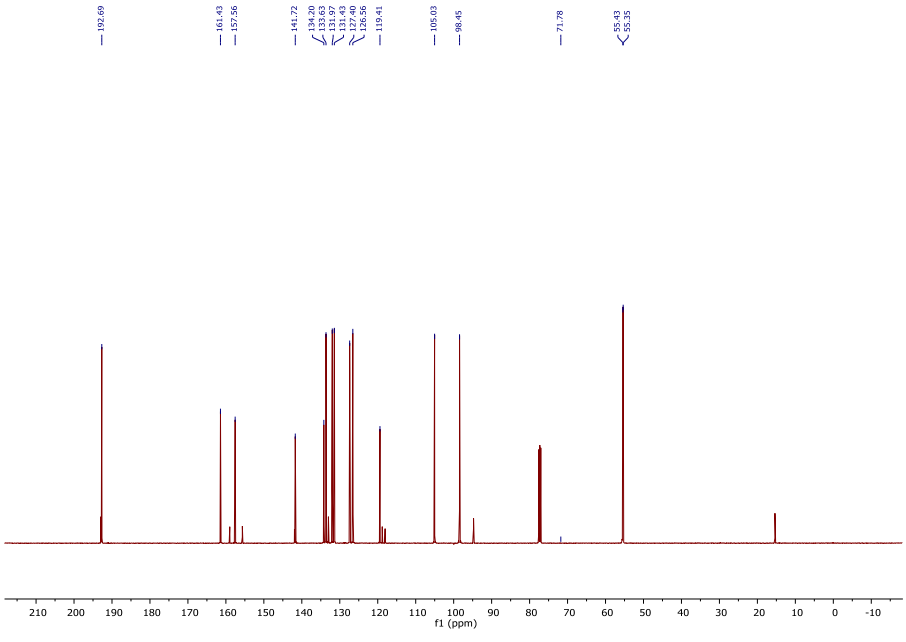

Compound 132f

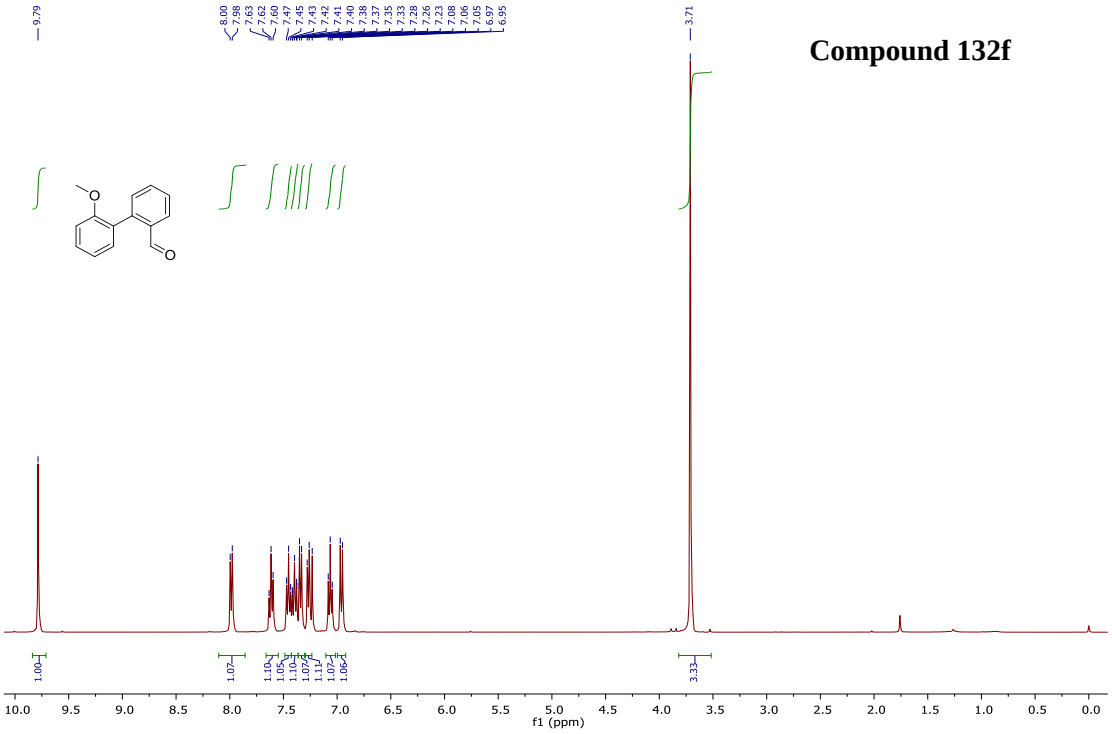

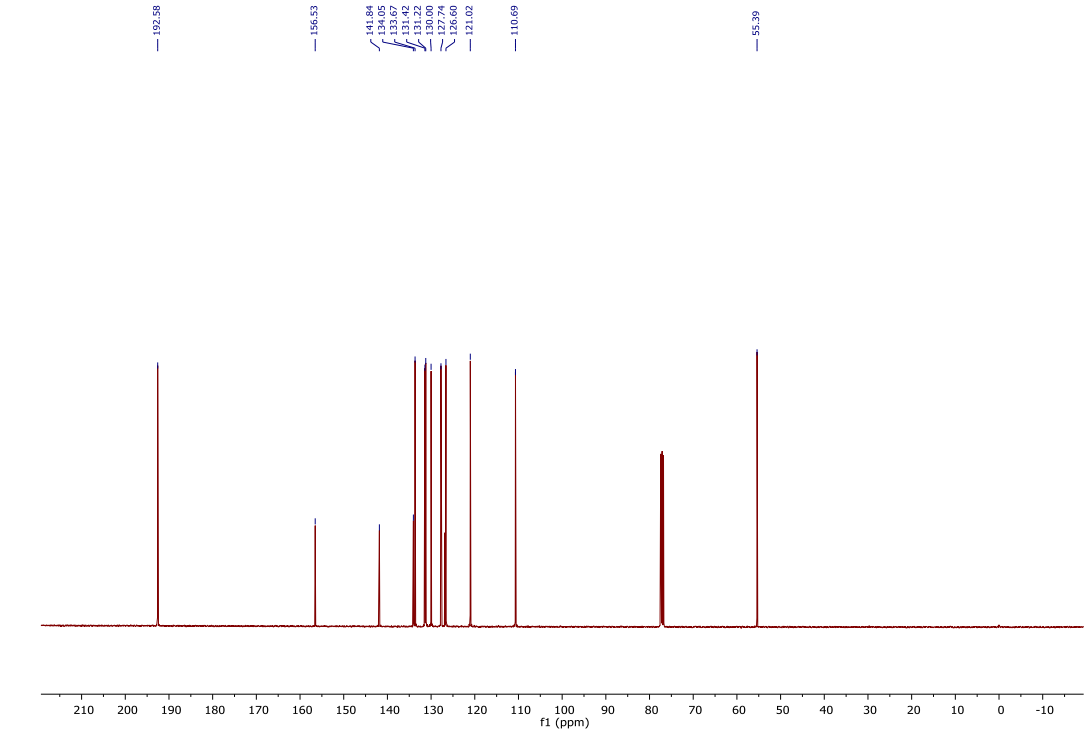

Compound 147

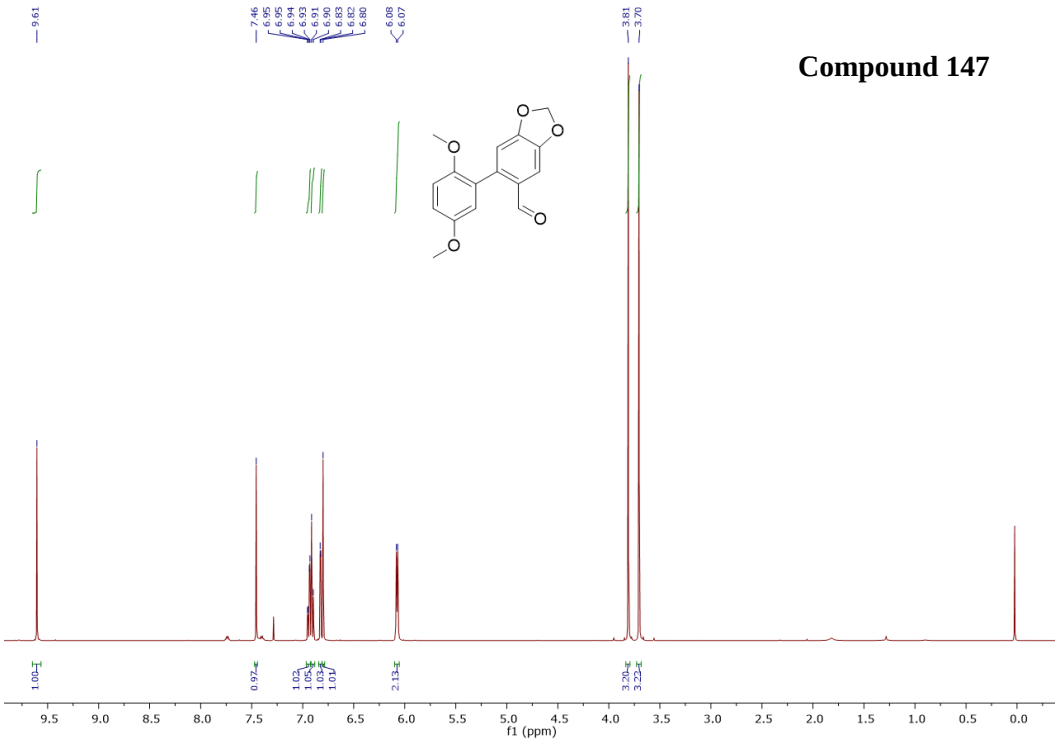

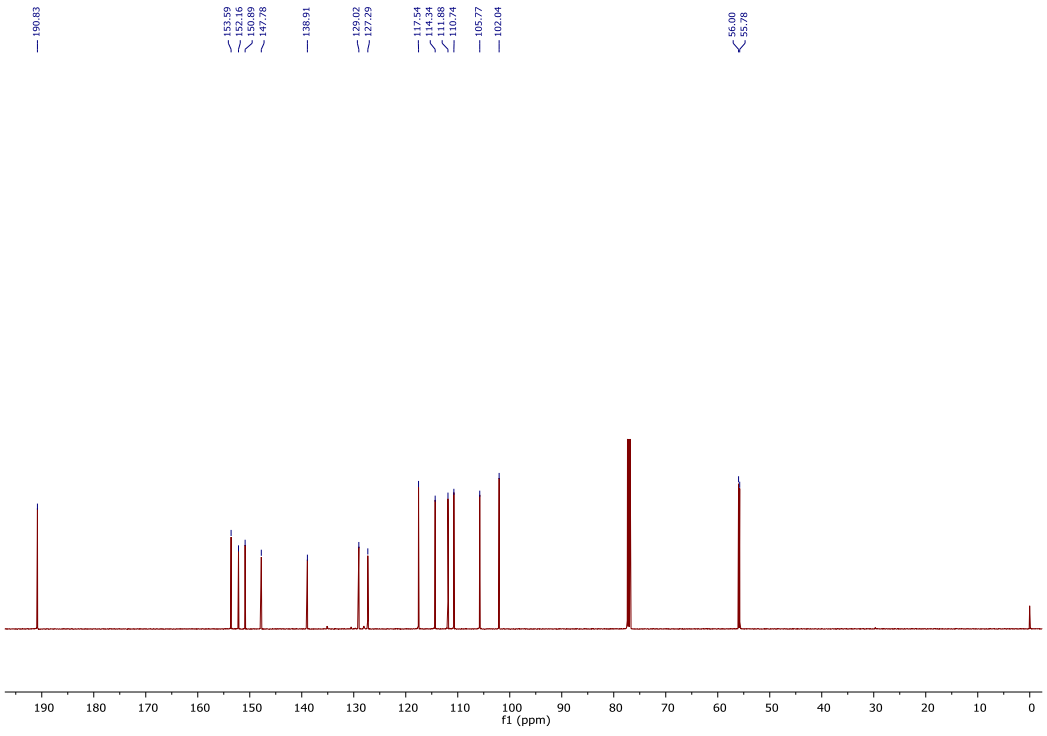

Compound 149a

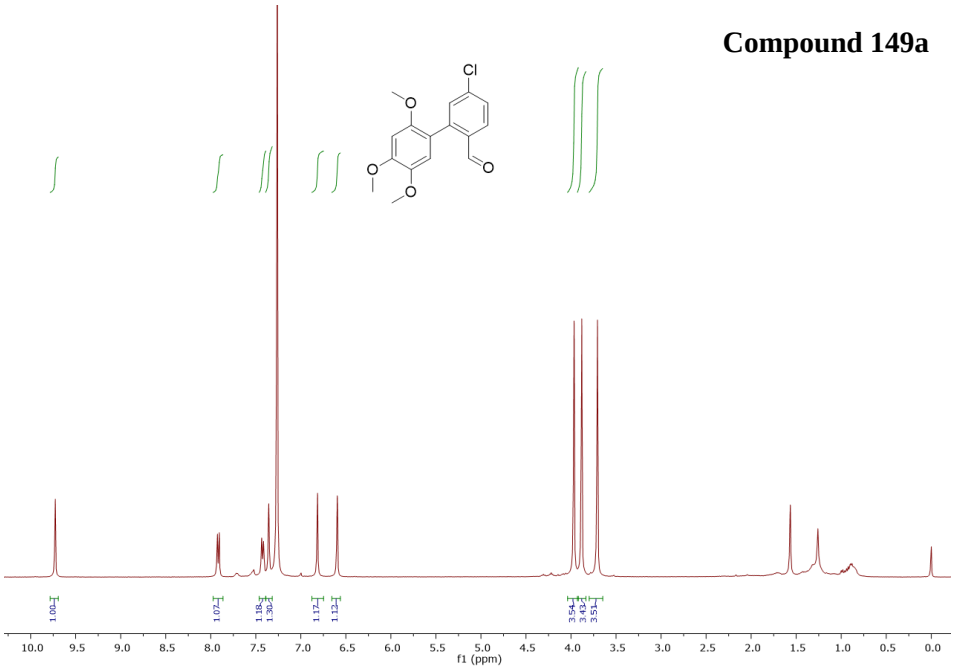

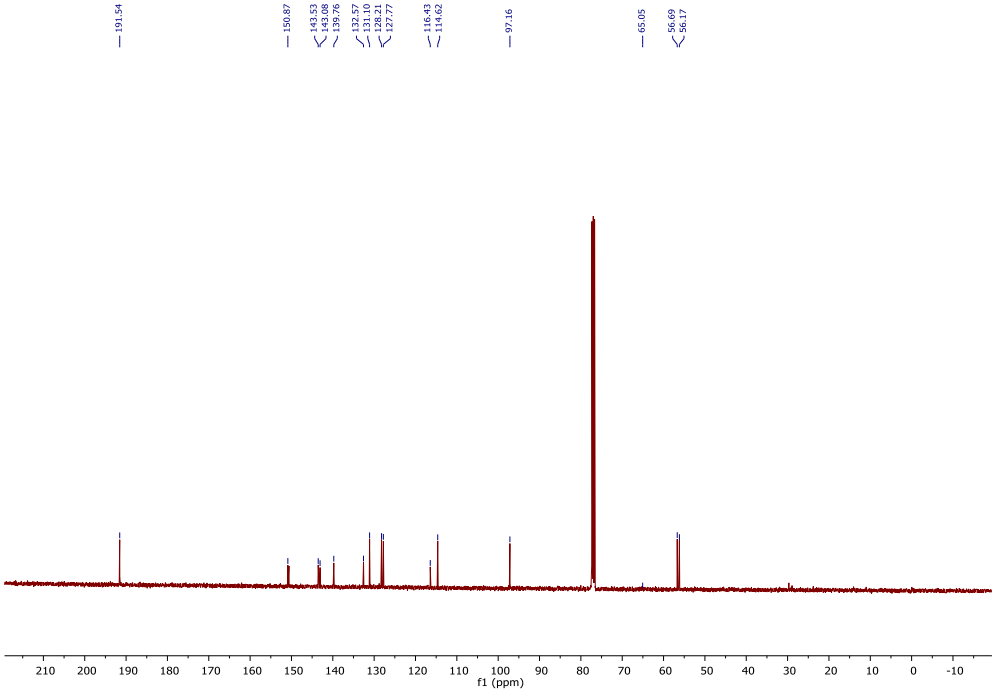

Compound 153

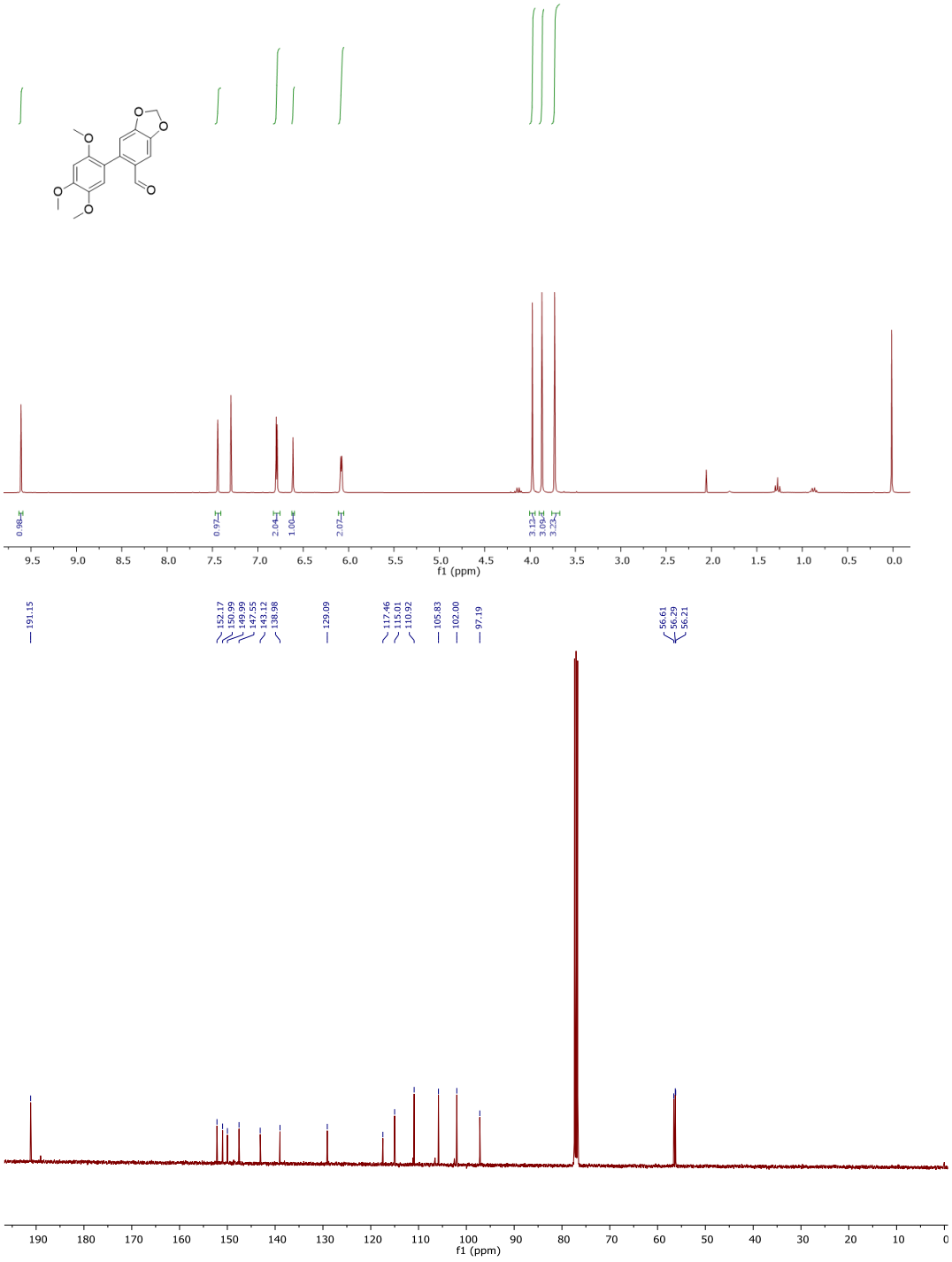

Compound 143a

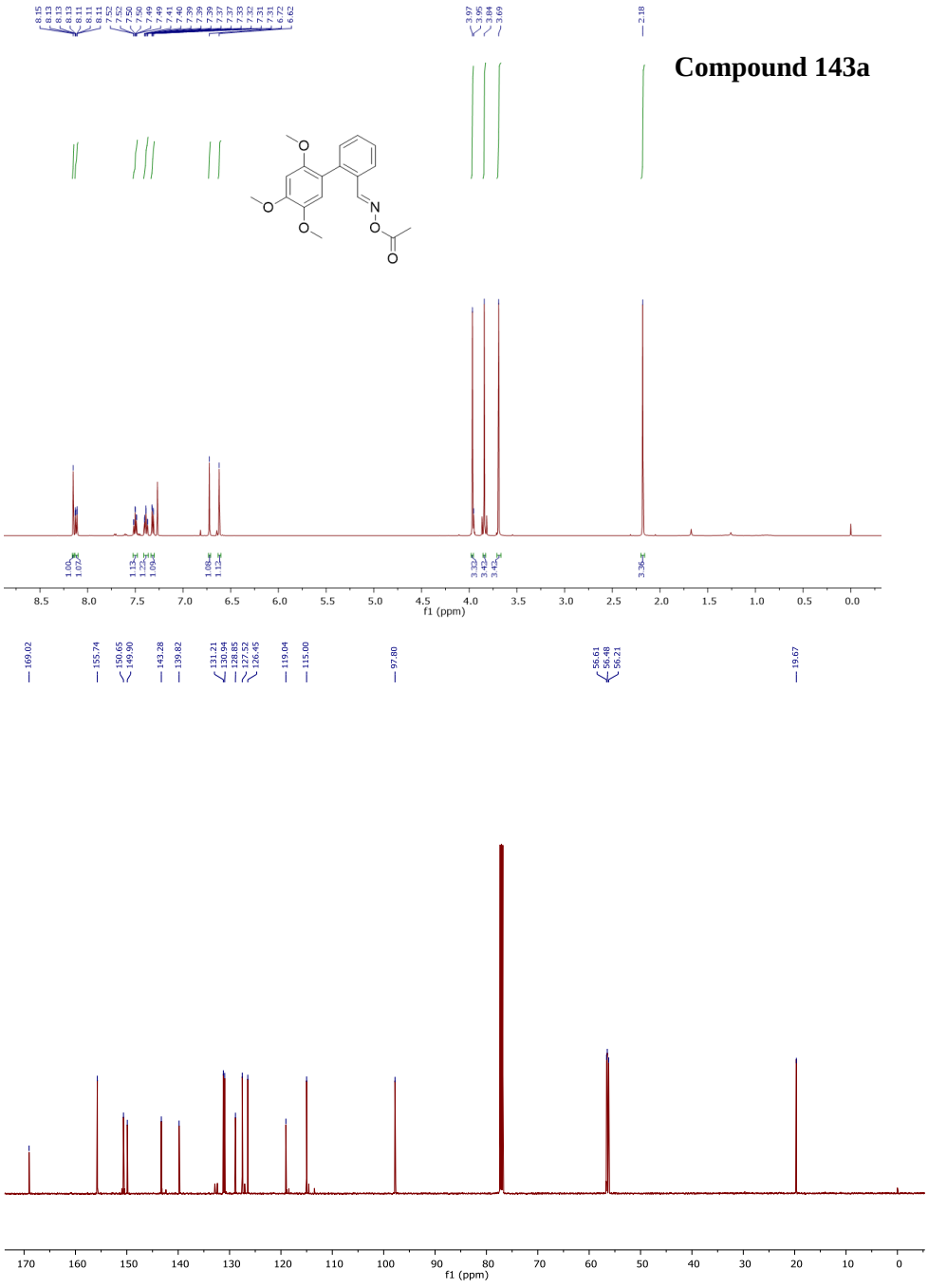

Compound 143b

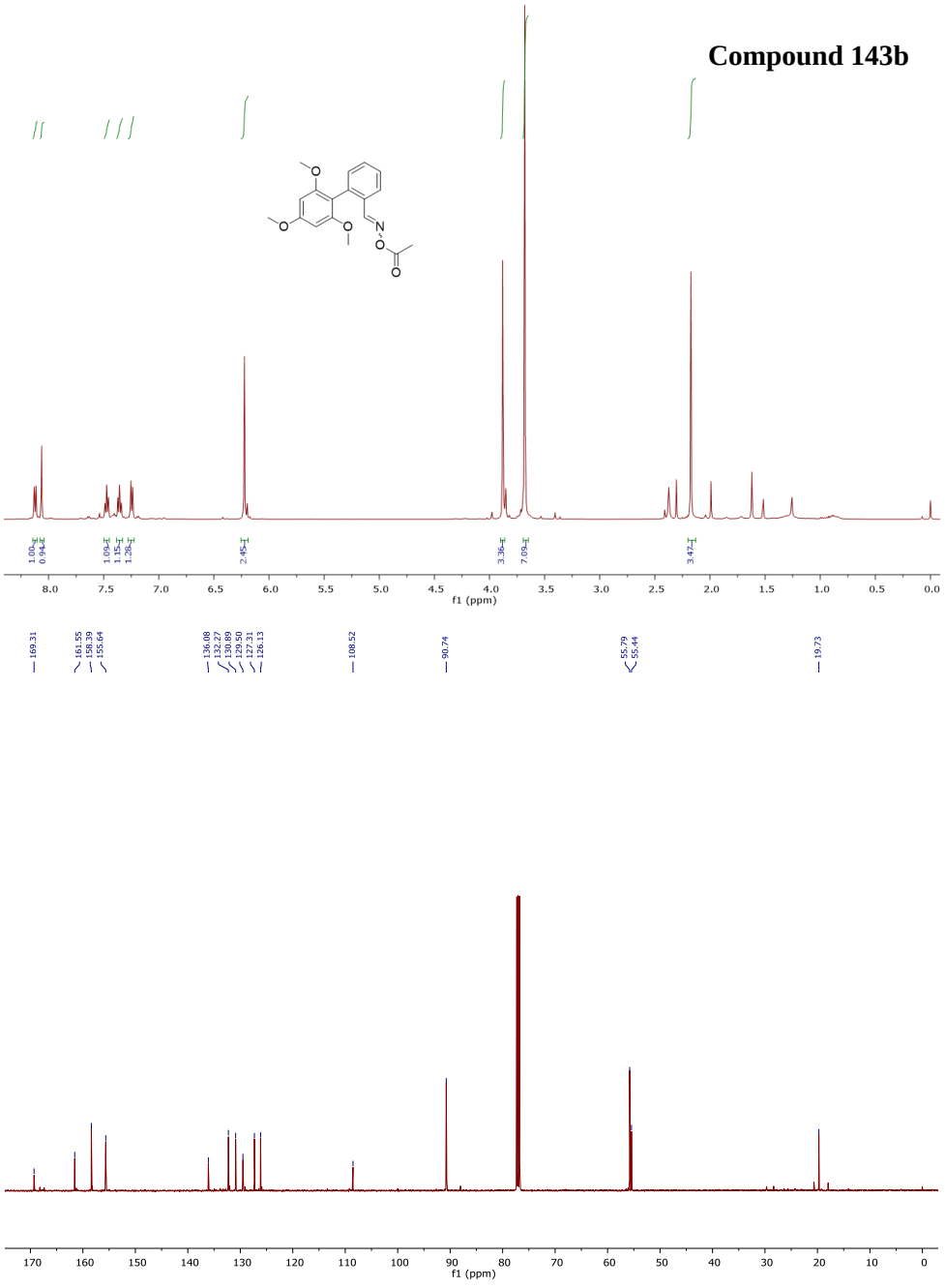

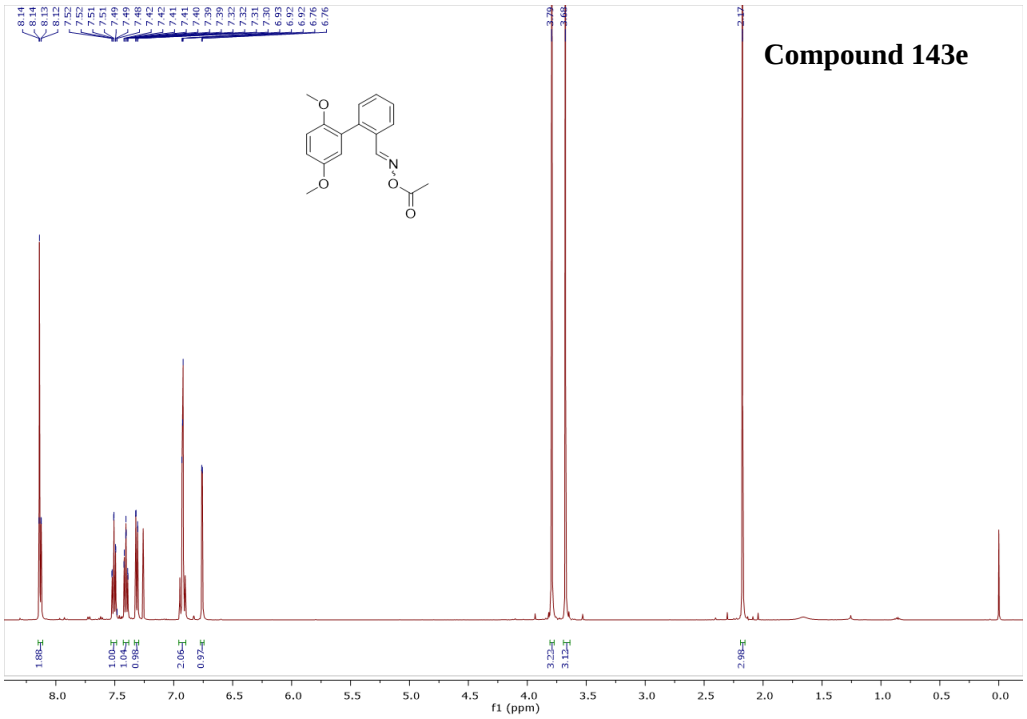
Compound 143e
f1 (ppm)

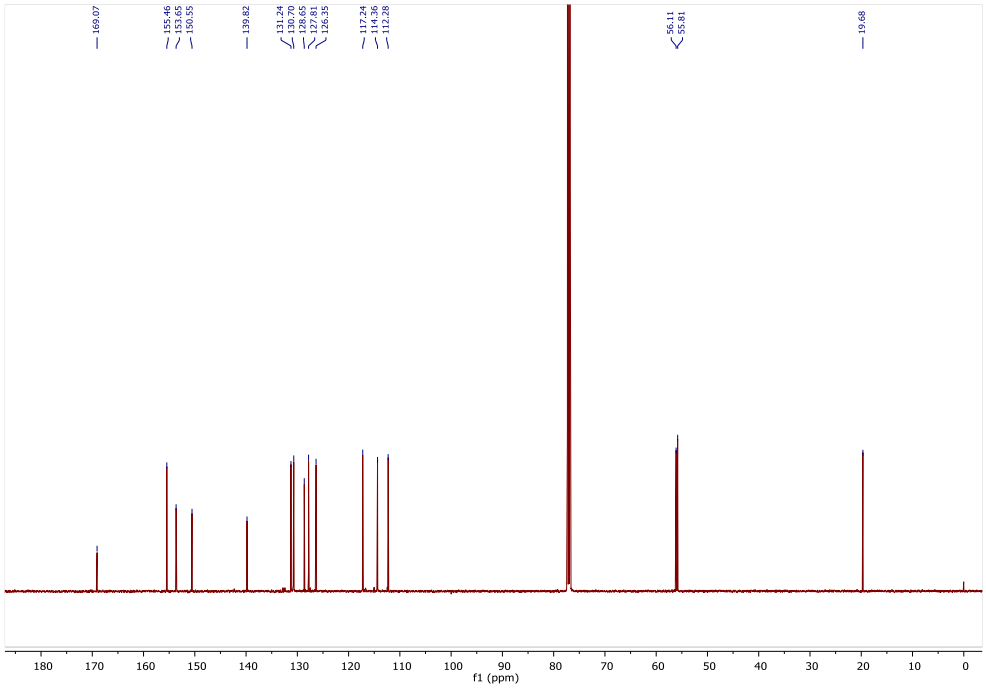
f1 (ppm)

Compound 143c

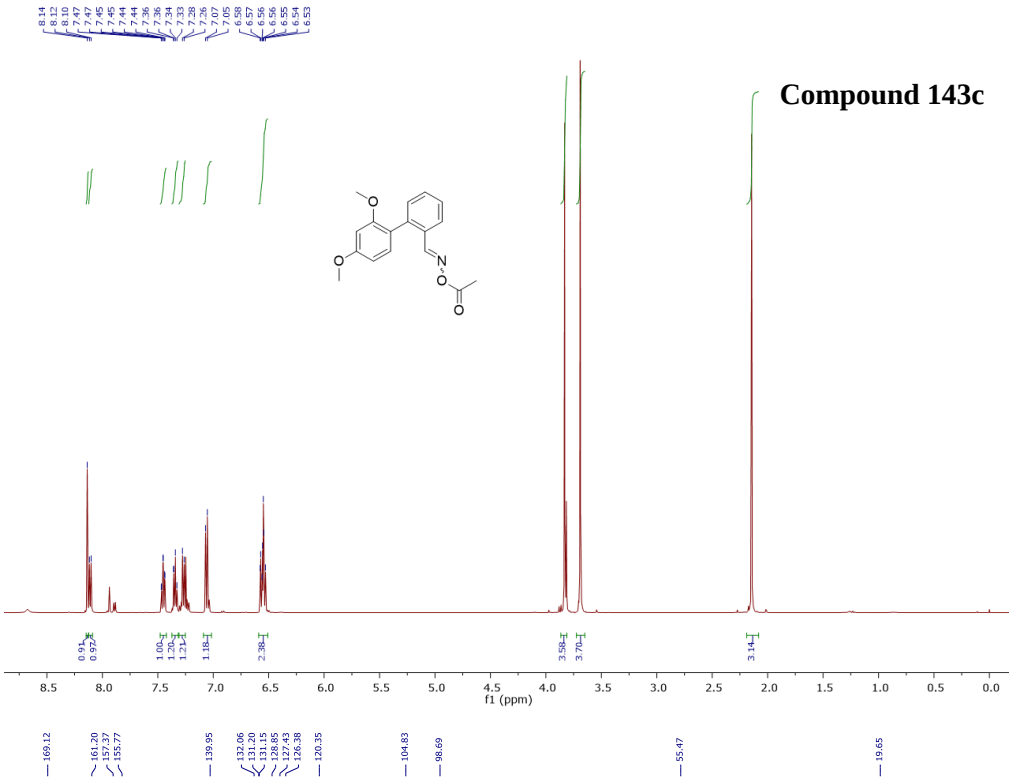

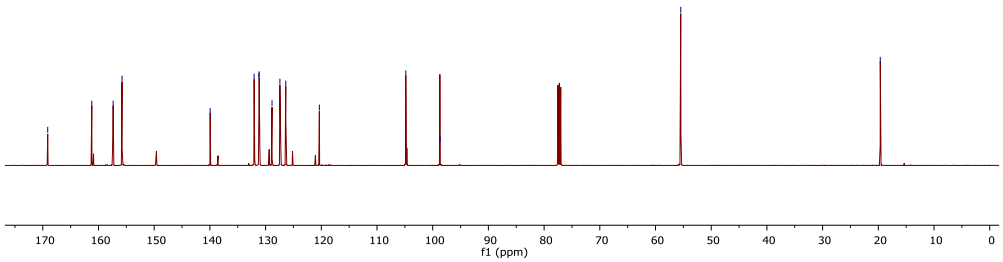

Compound 143d

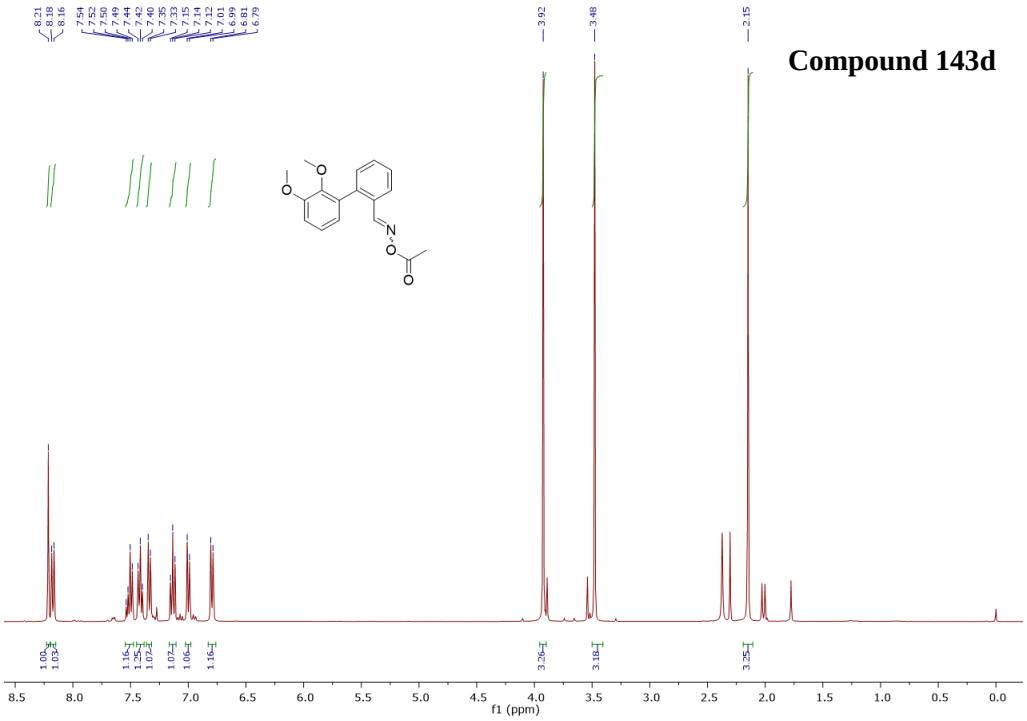

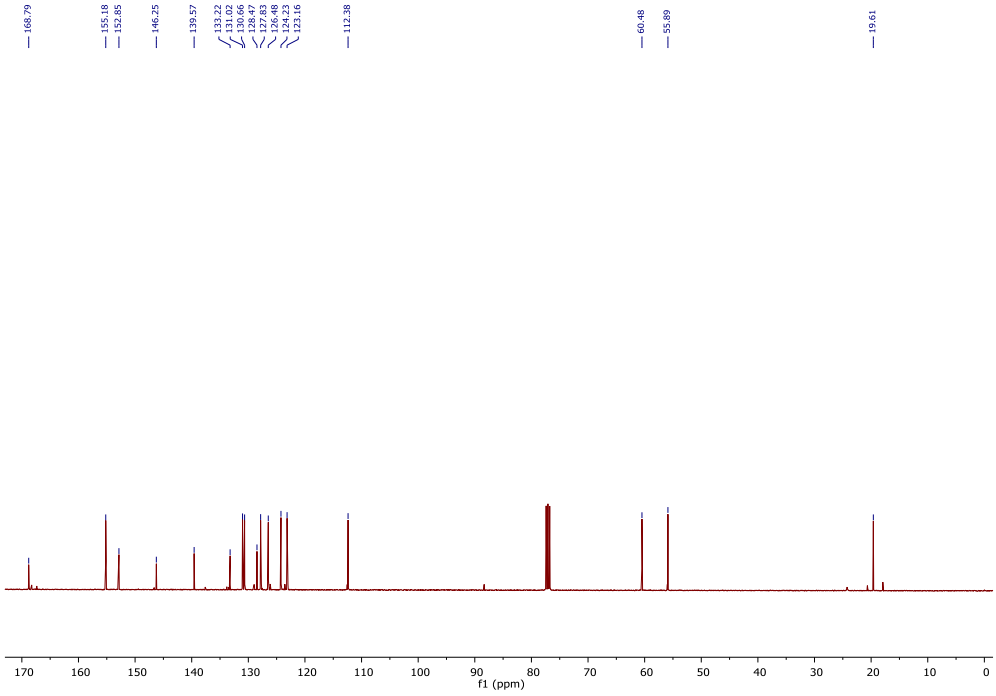

Compound 143f

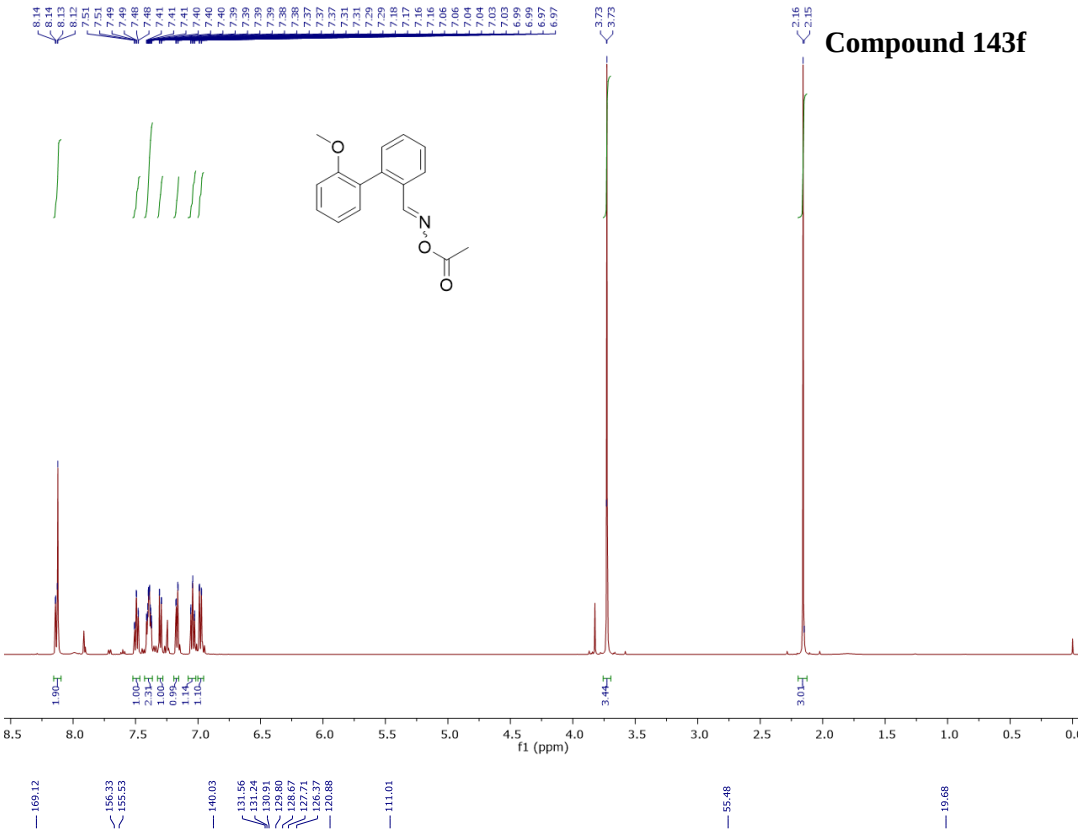

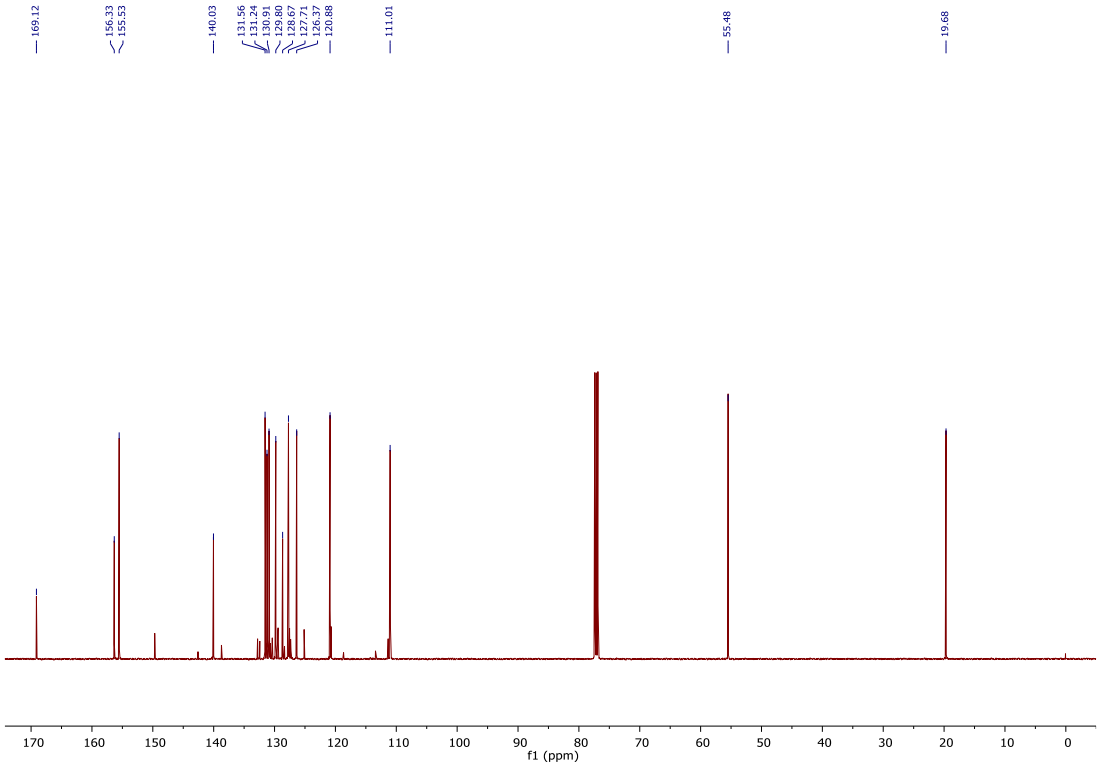

Compound 152b

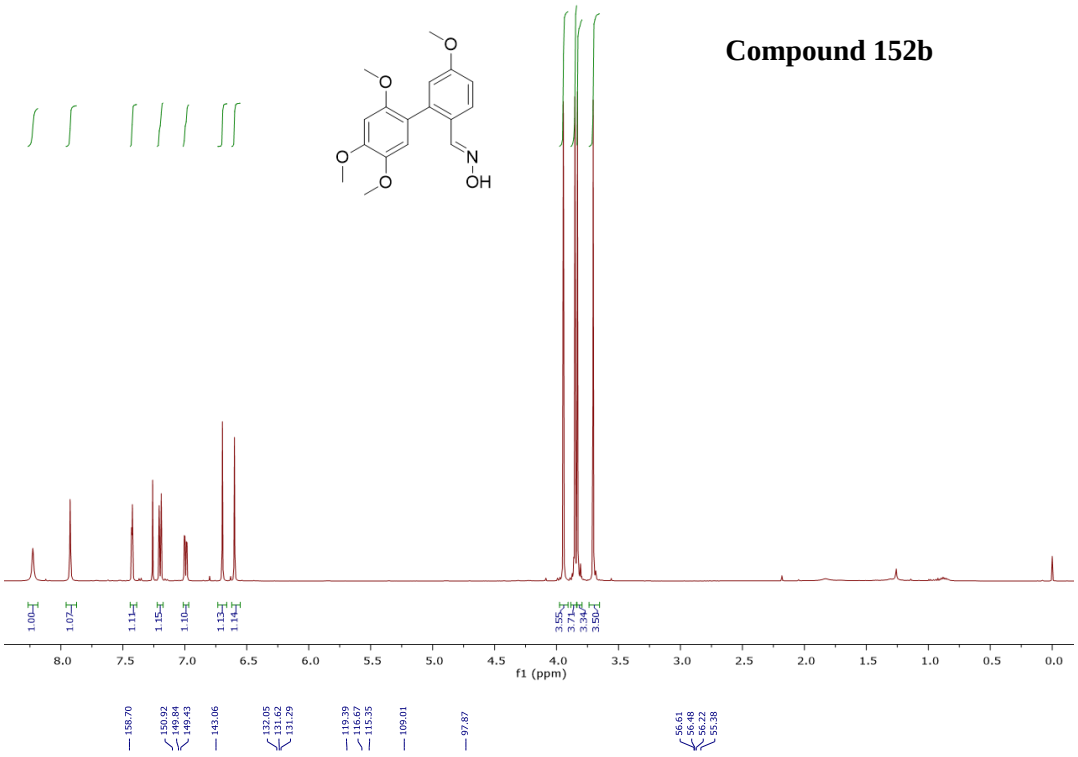

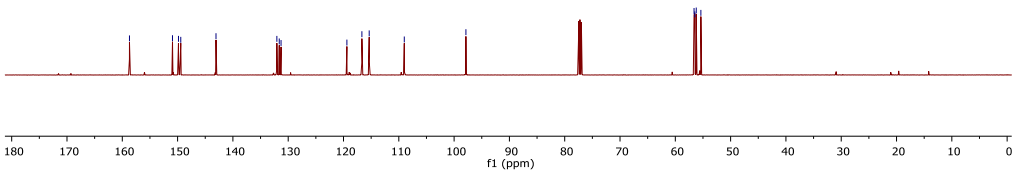

Compound 152a

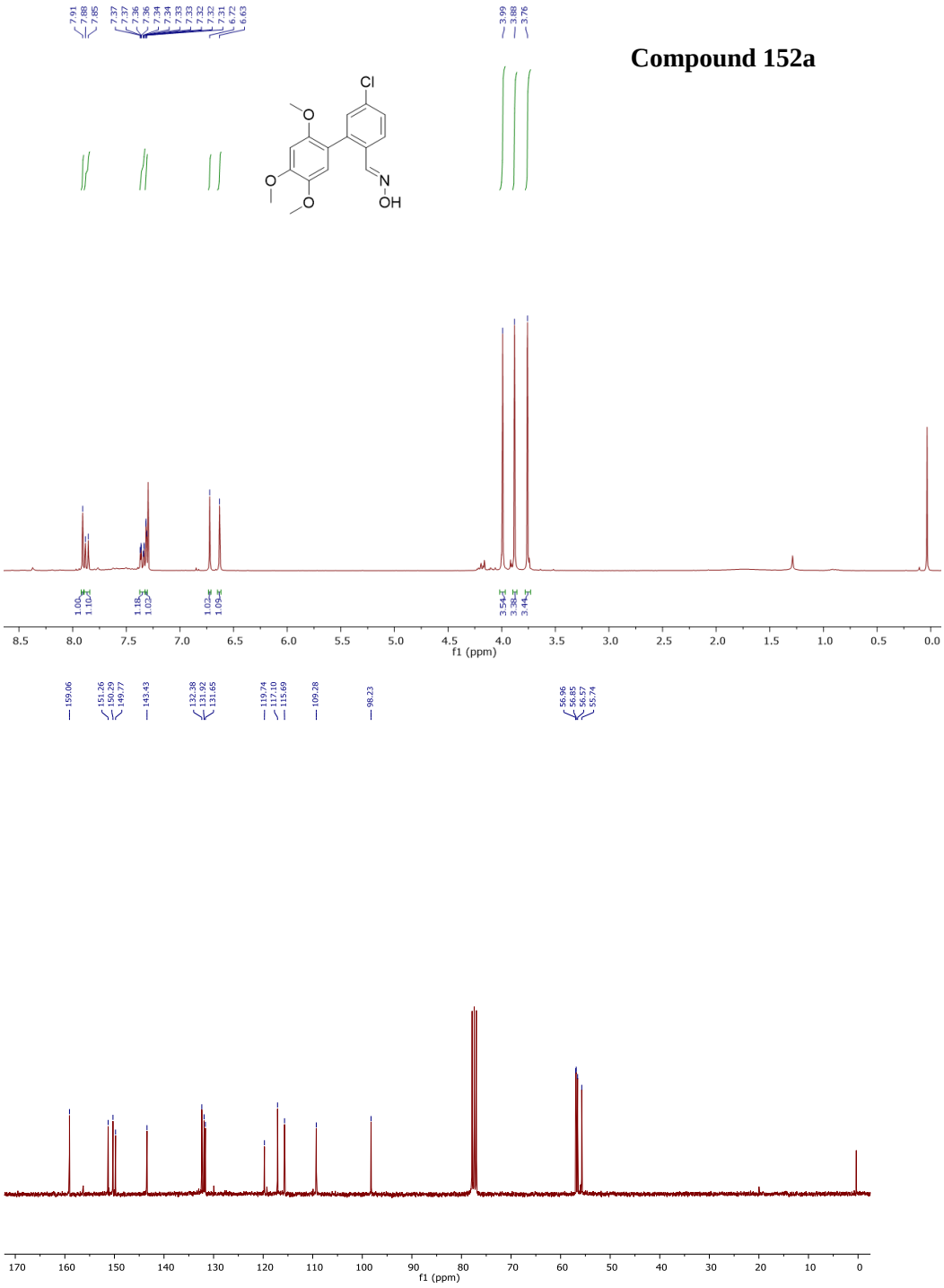

Compound 151a

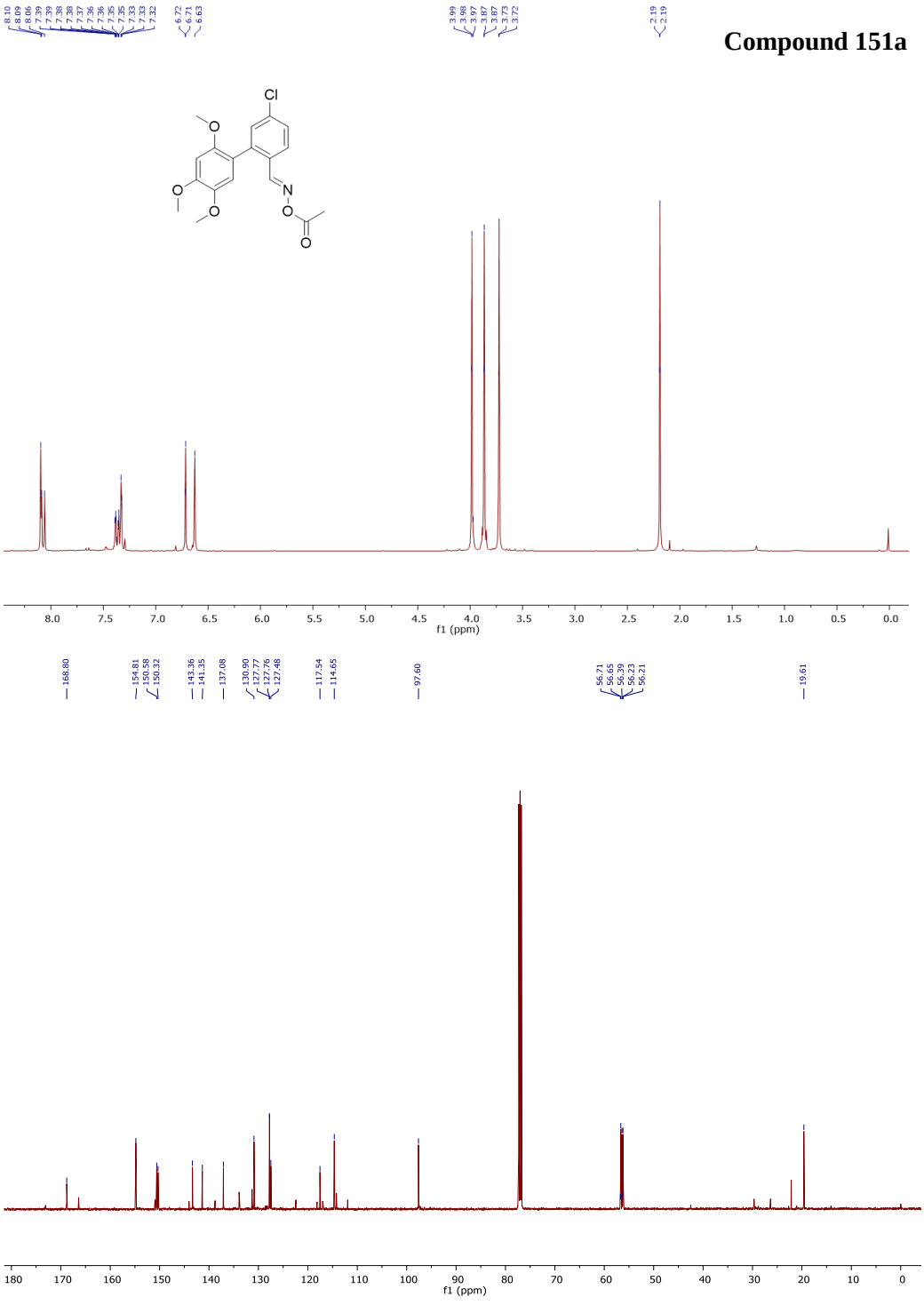

Compound 155

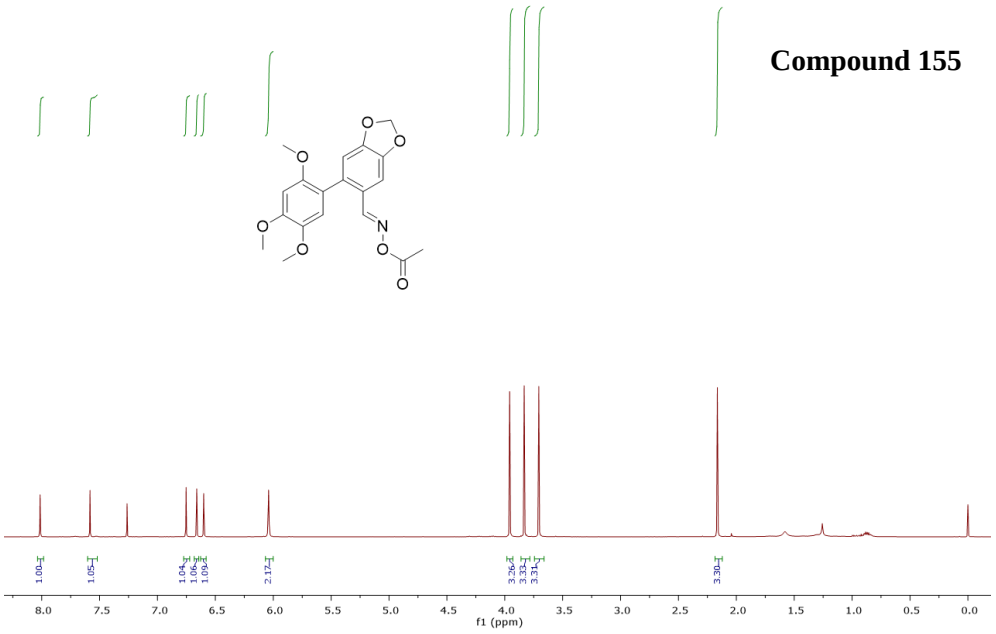

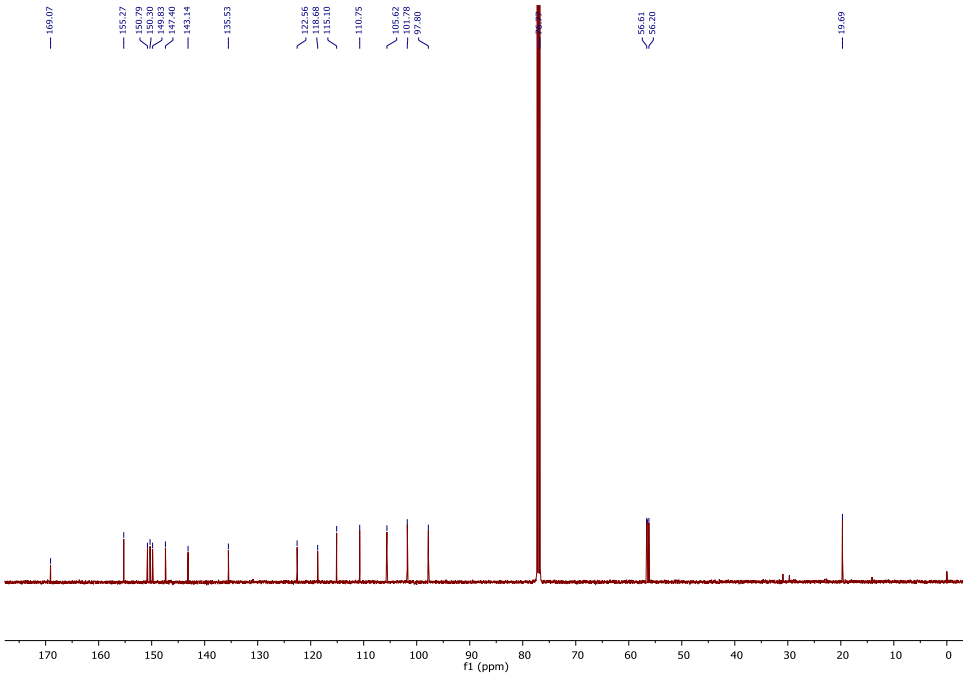

Compound 141a

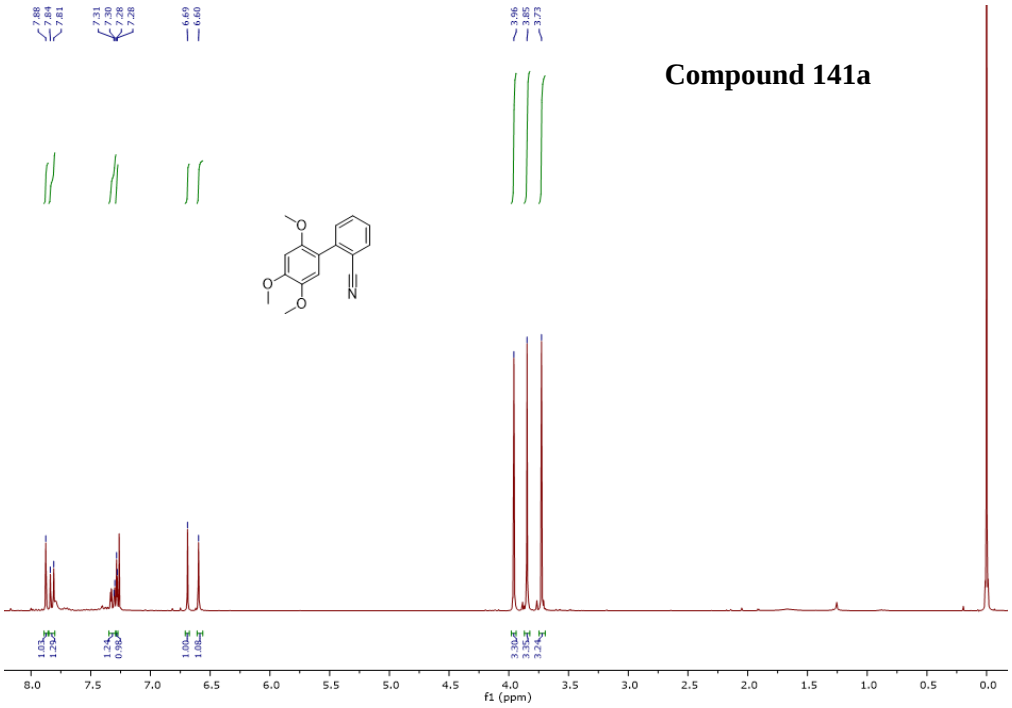

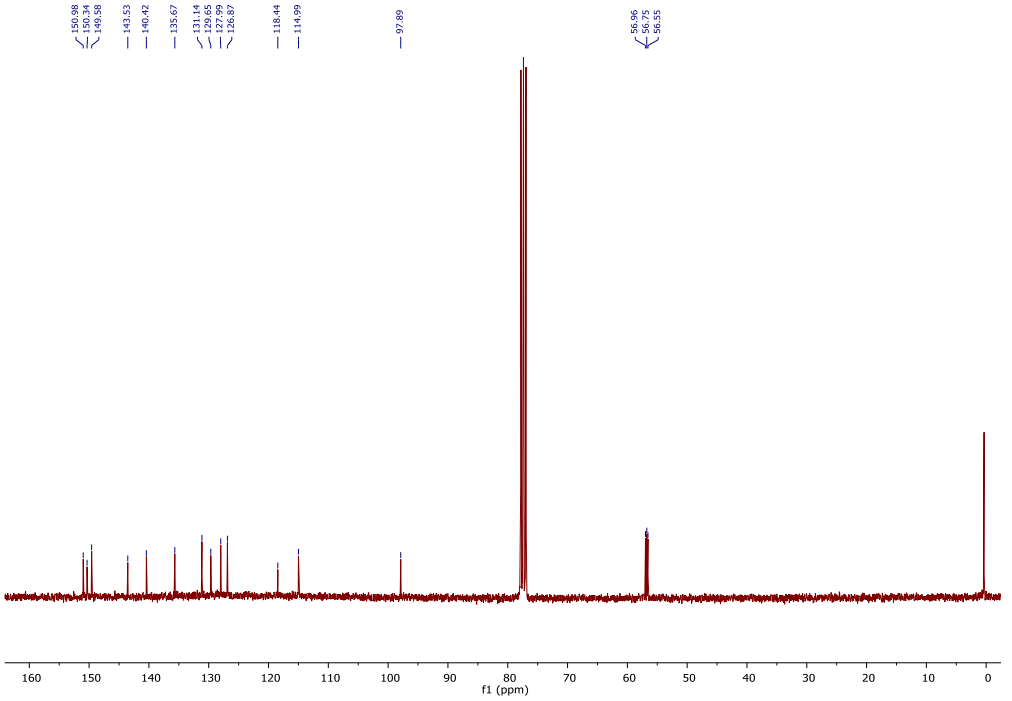

Compound 141b

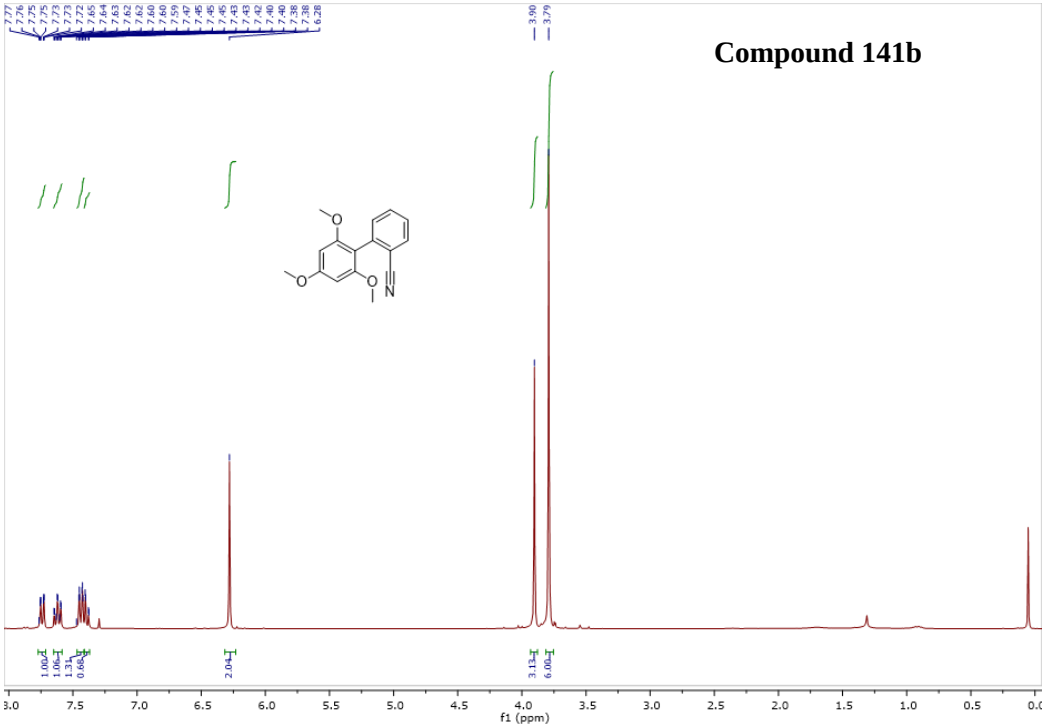

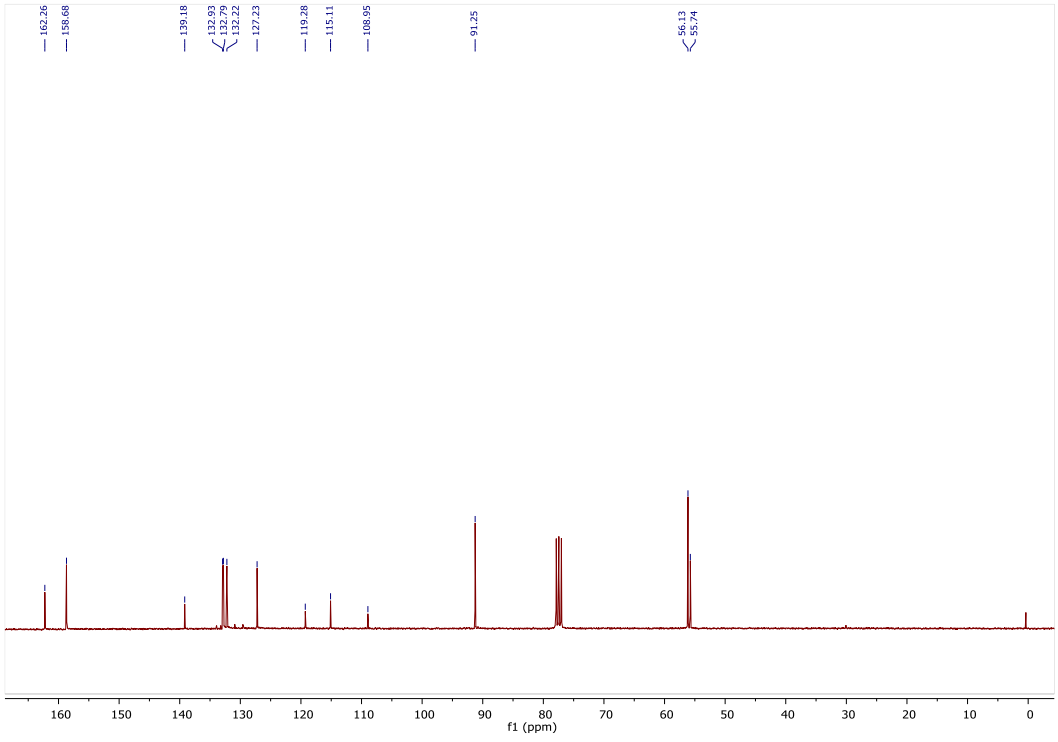

Compound 131e

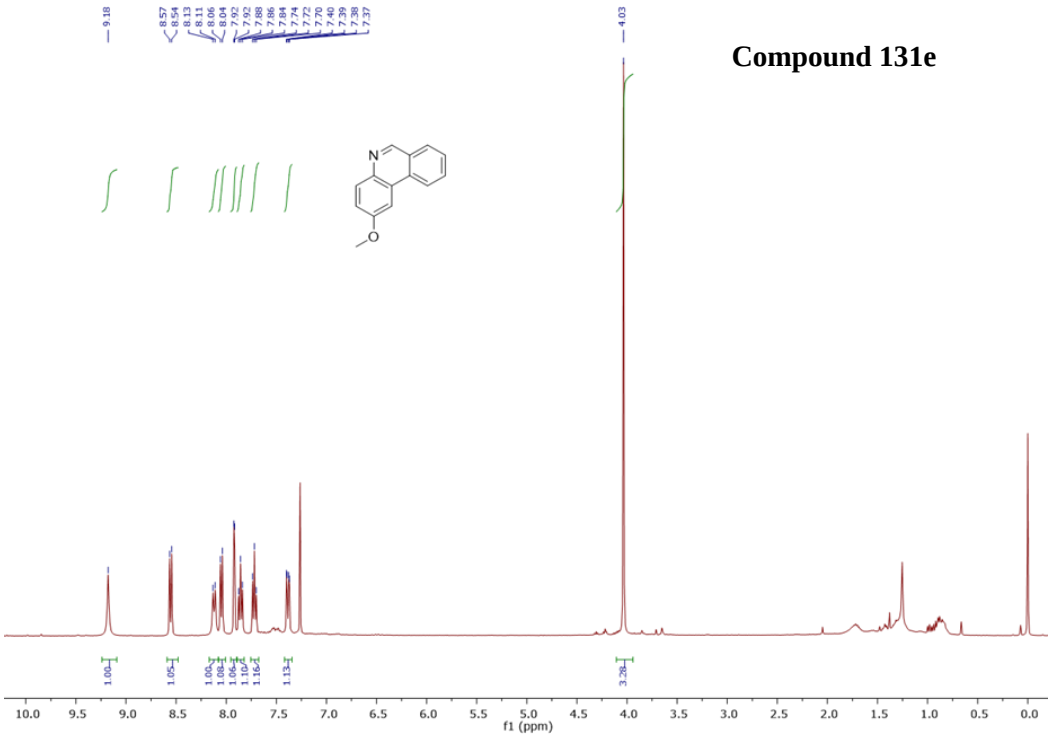

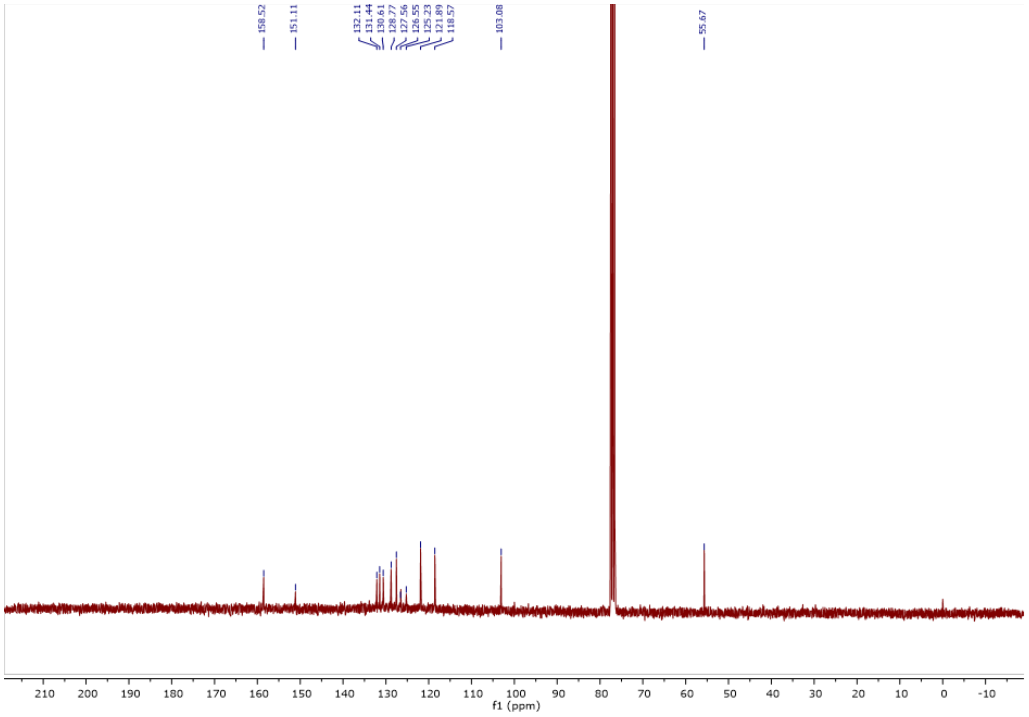

Compound 141e

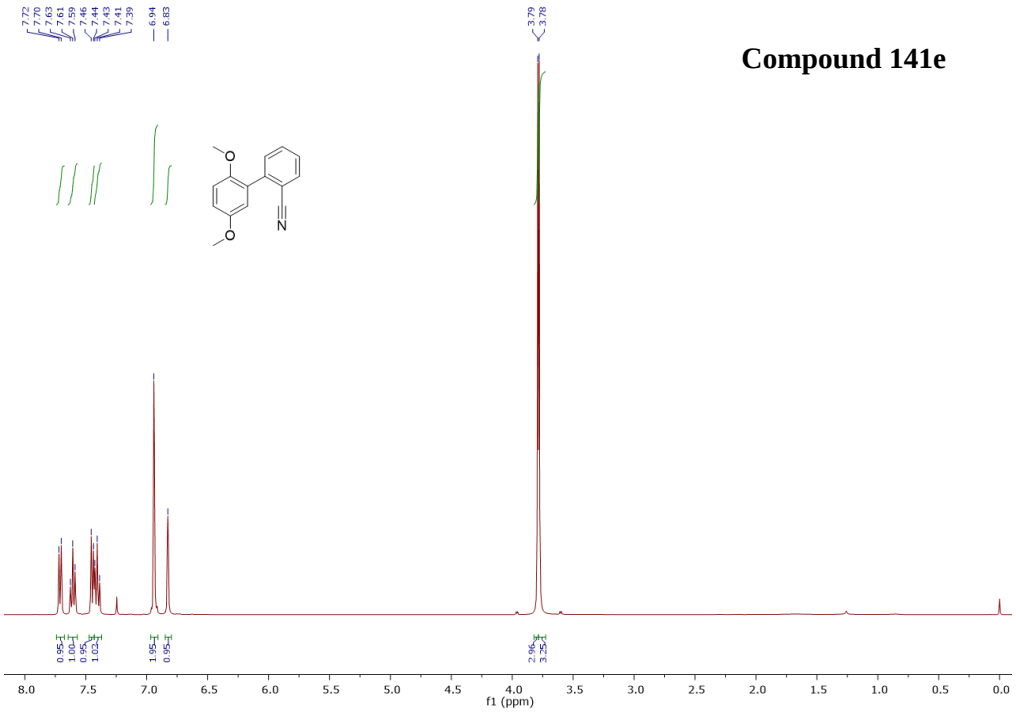

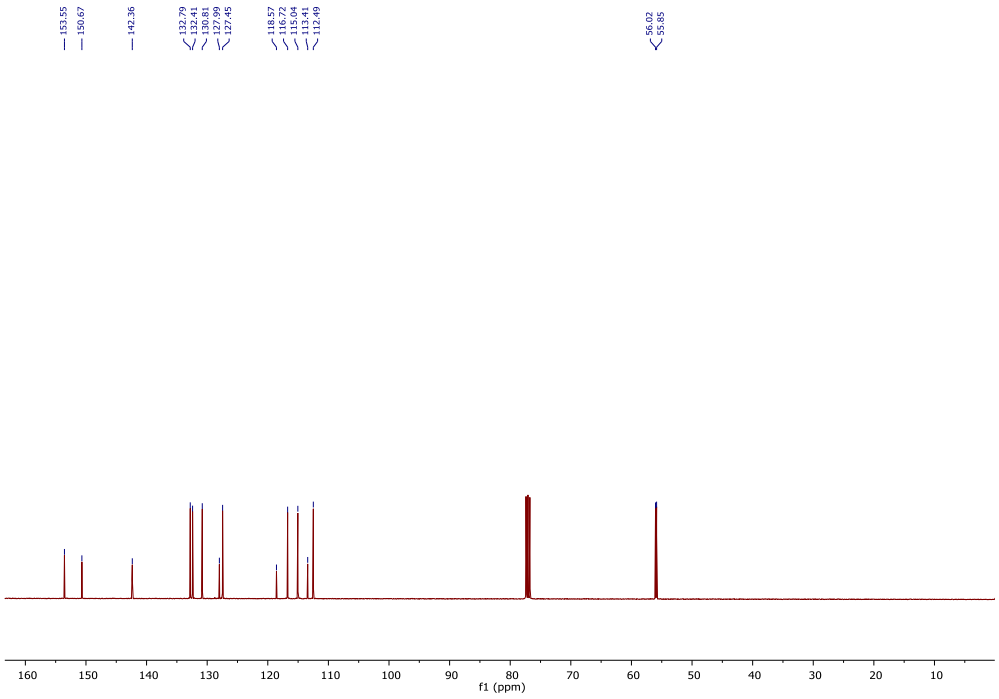

Compound 131d

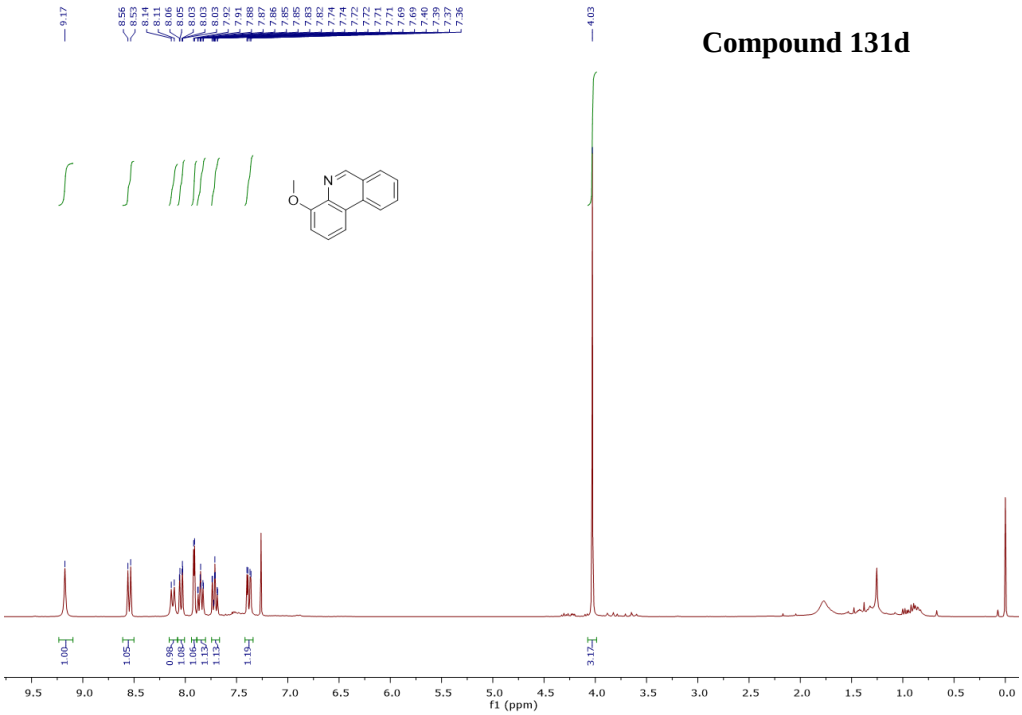

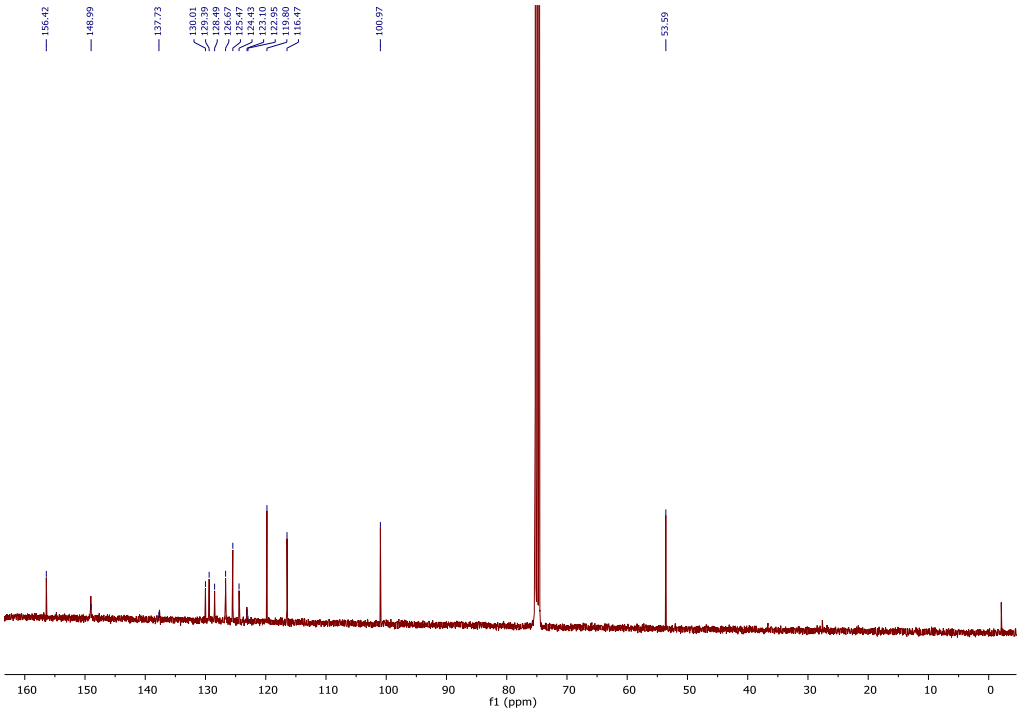

Compound 141d

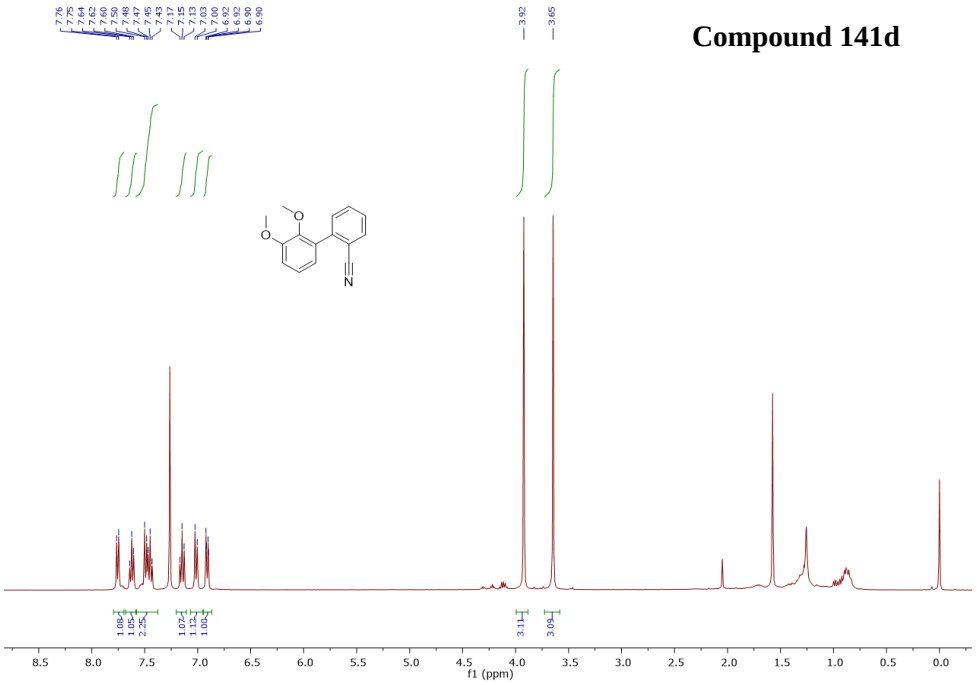

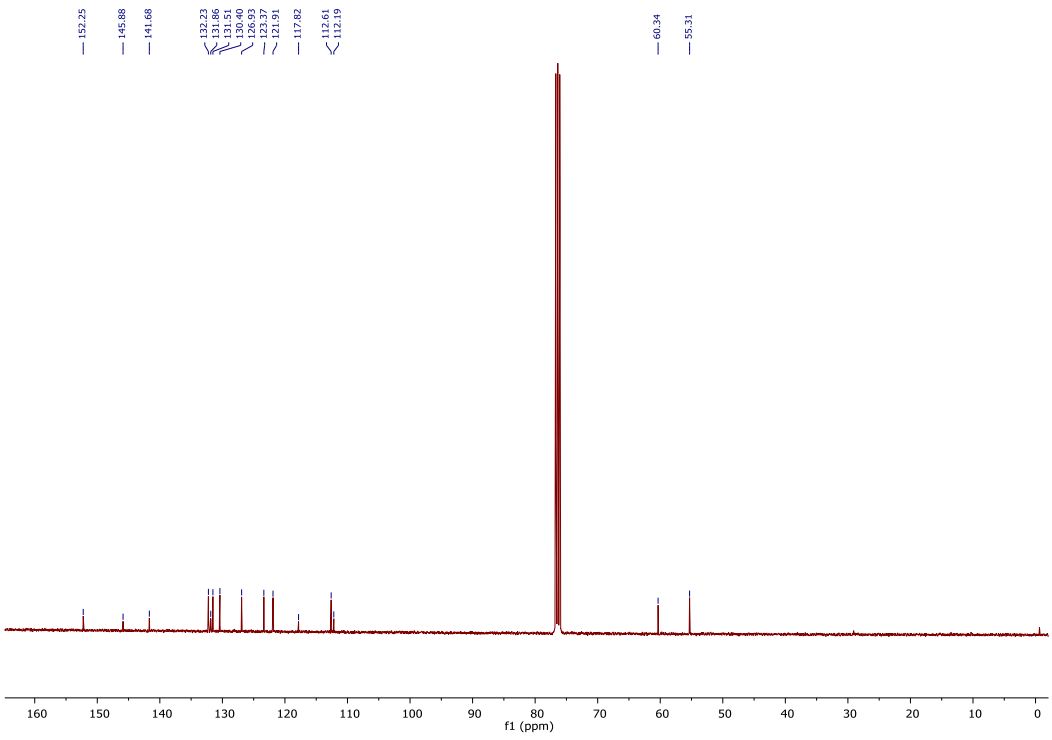

Compound 141c

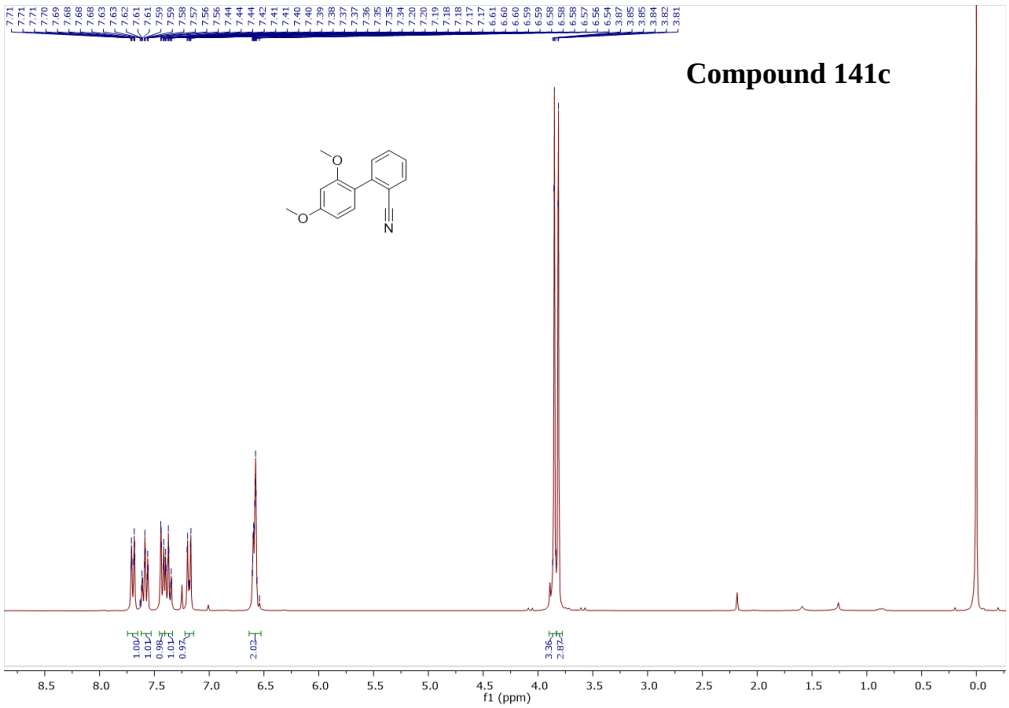

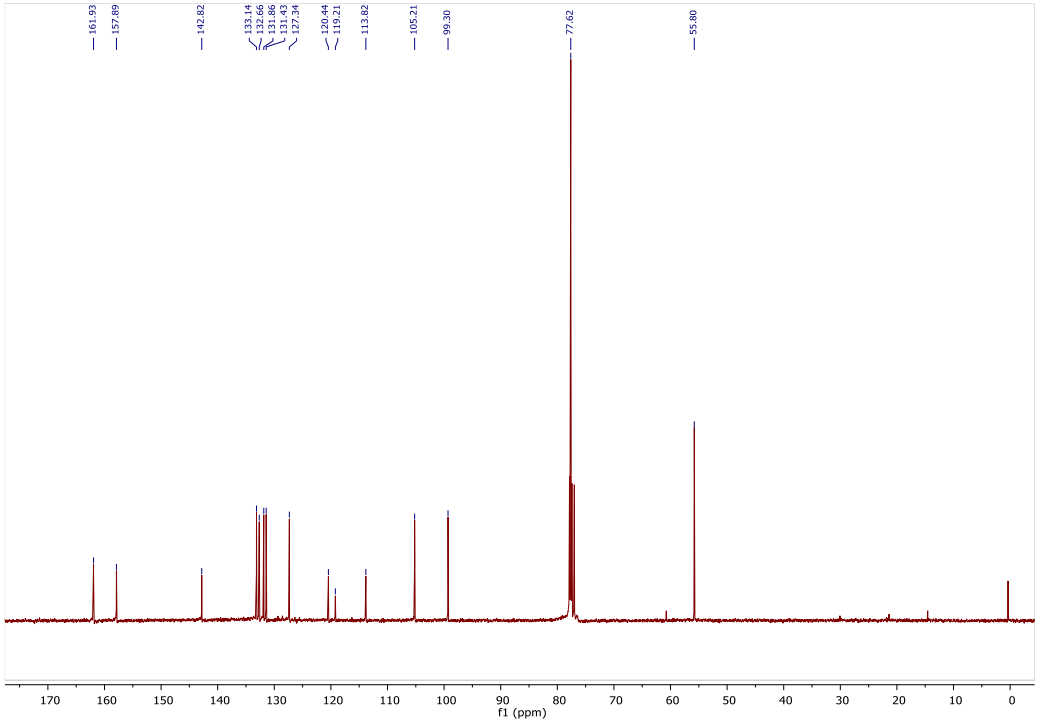

Compound 141f

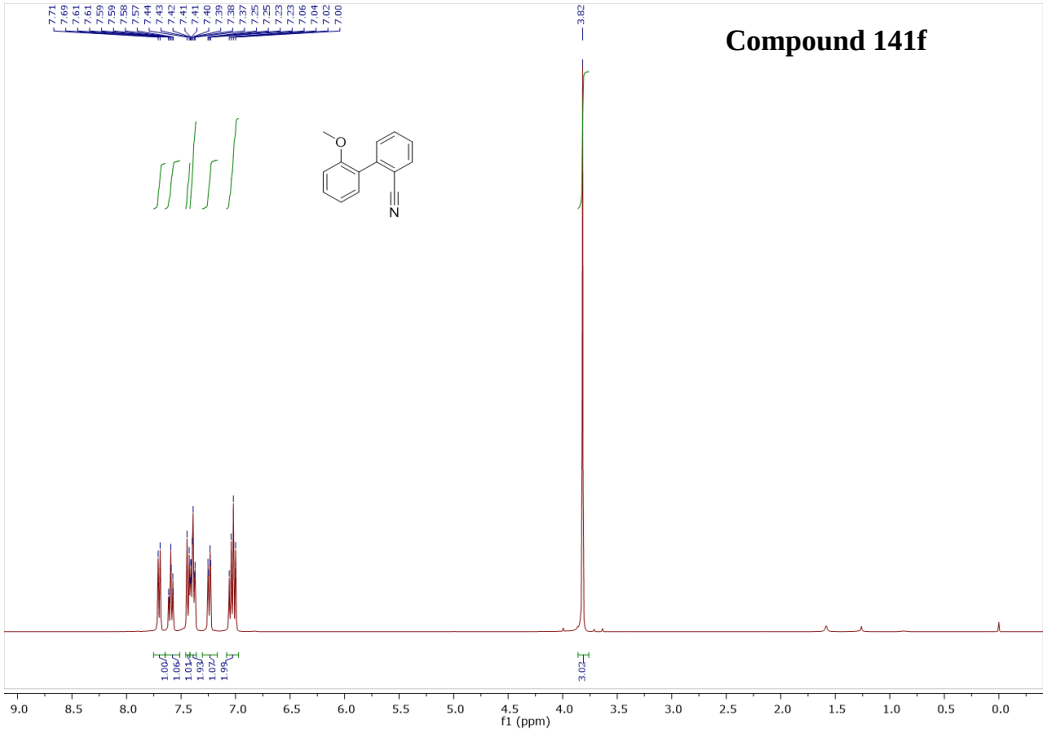

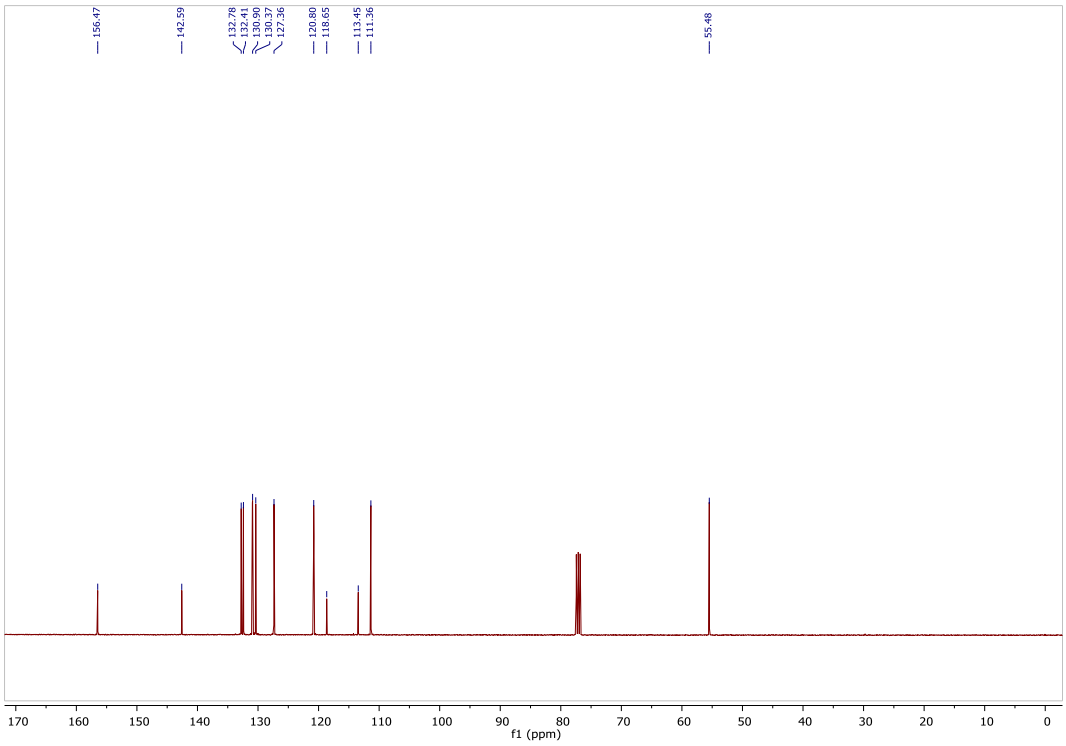

Compound 148

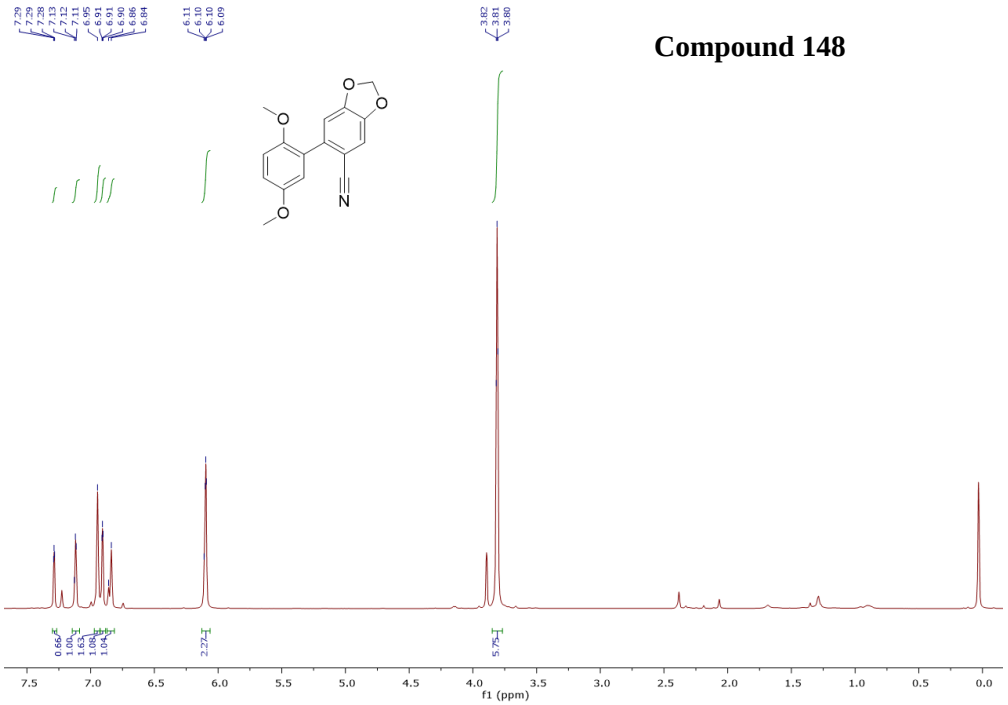

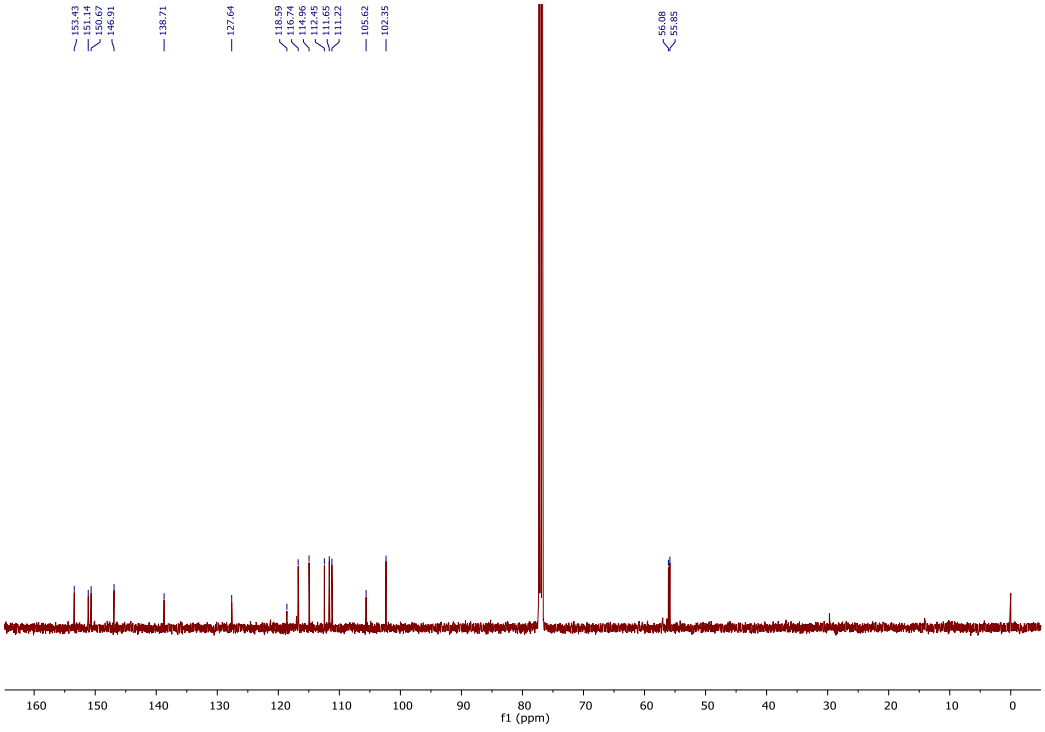

Compound 156

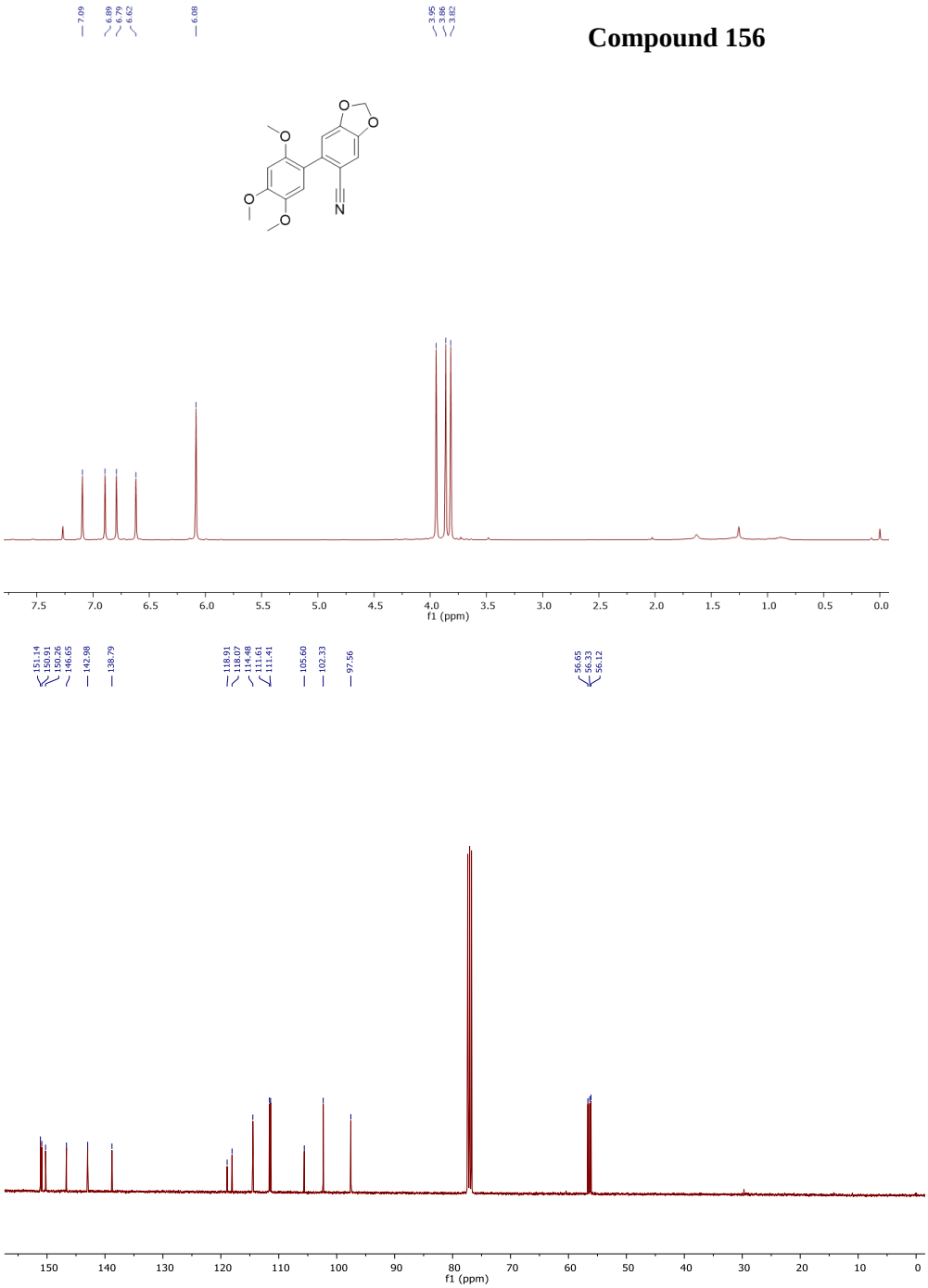

Compound 157

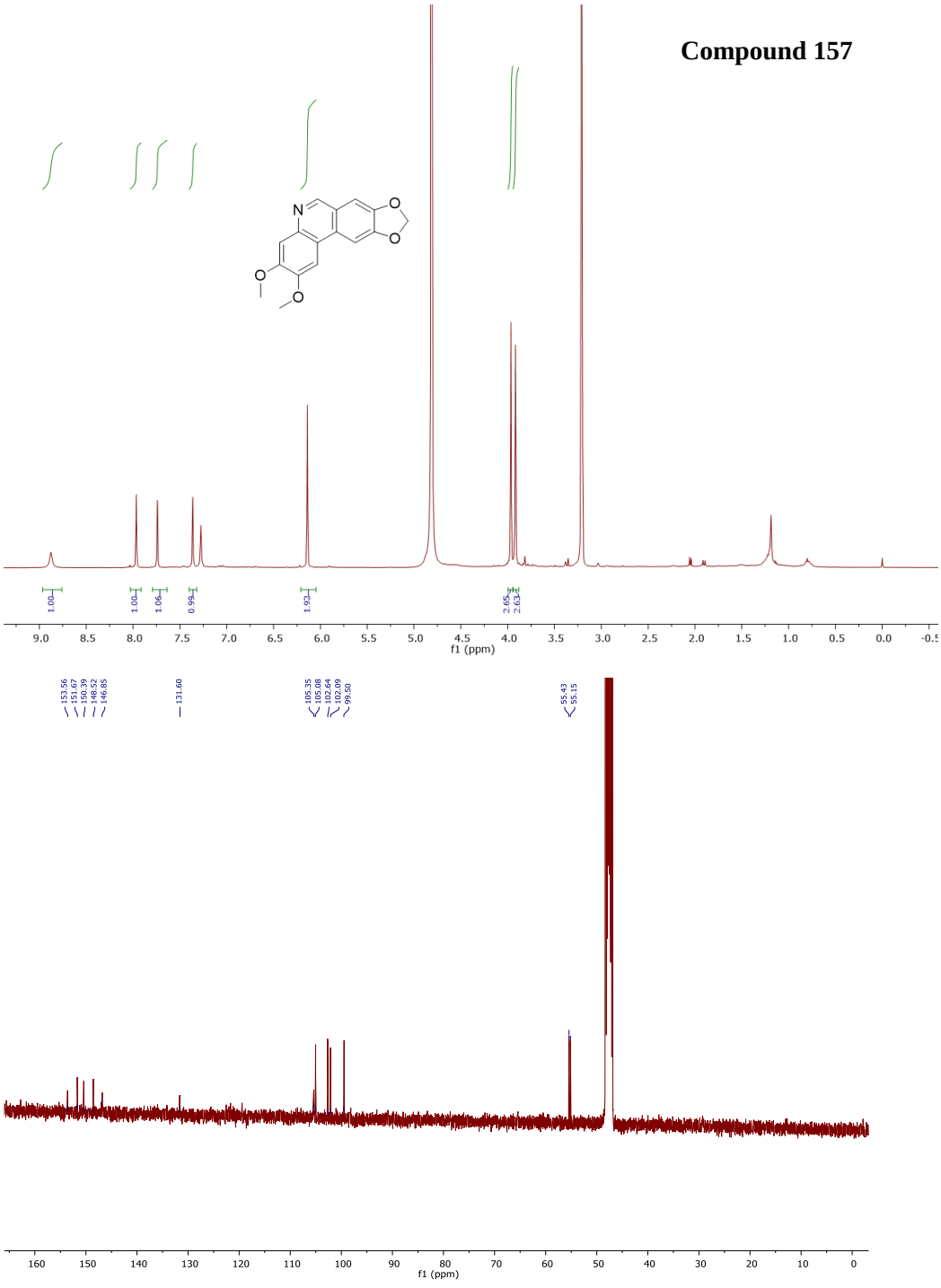

Compound 77

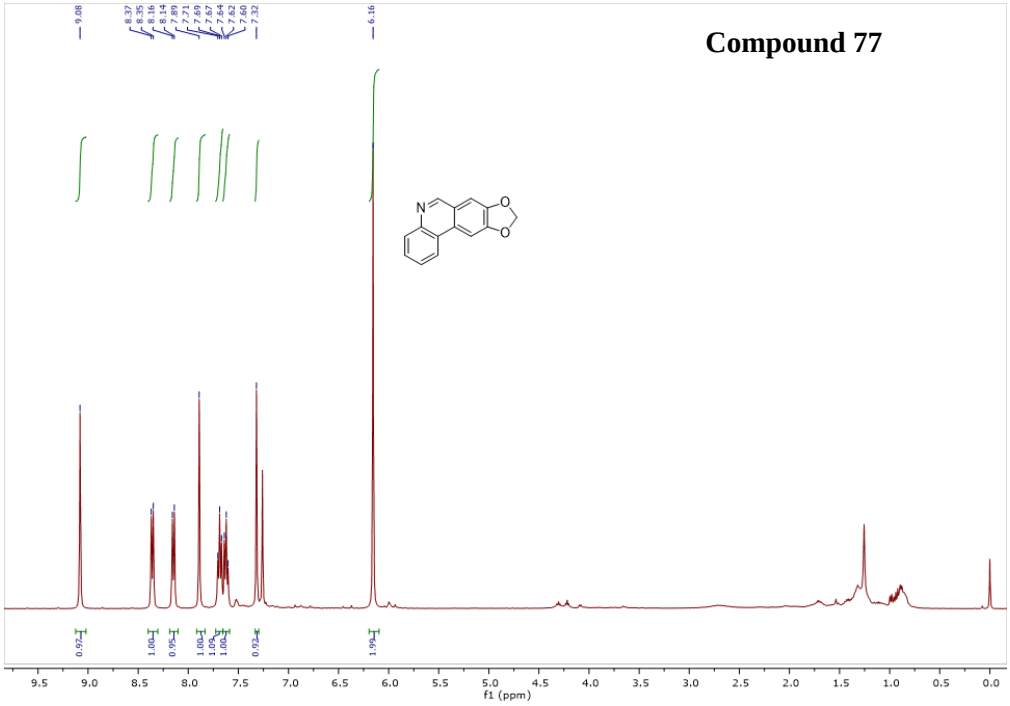
9.08
8.37
8.35
8.16
8.14
7.89
7.71
7.69
7.67
7.64
7.62
7.60
7.32
6.16
N
O
O
f1 (ppm)

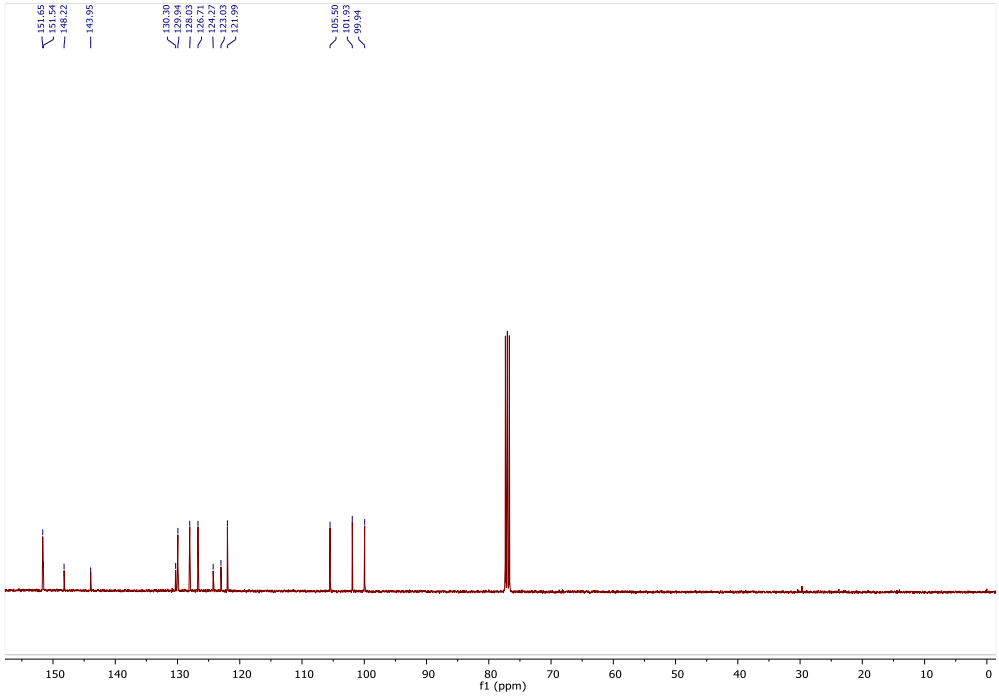
151.65
151.54
148.22
143.95
130.30
130.04
128.03
126.71
124.27
123.03
121.99
105.50
101.83
99.94
f1 (ppm)

Compound 131b

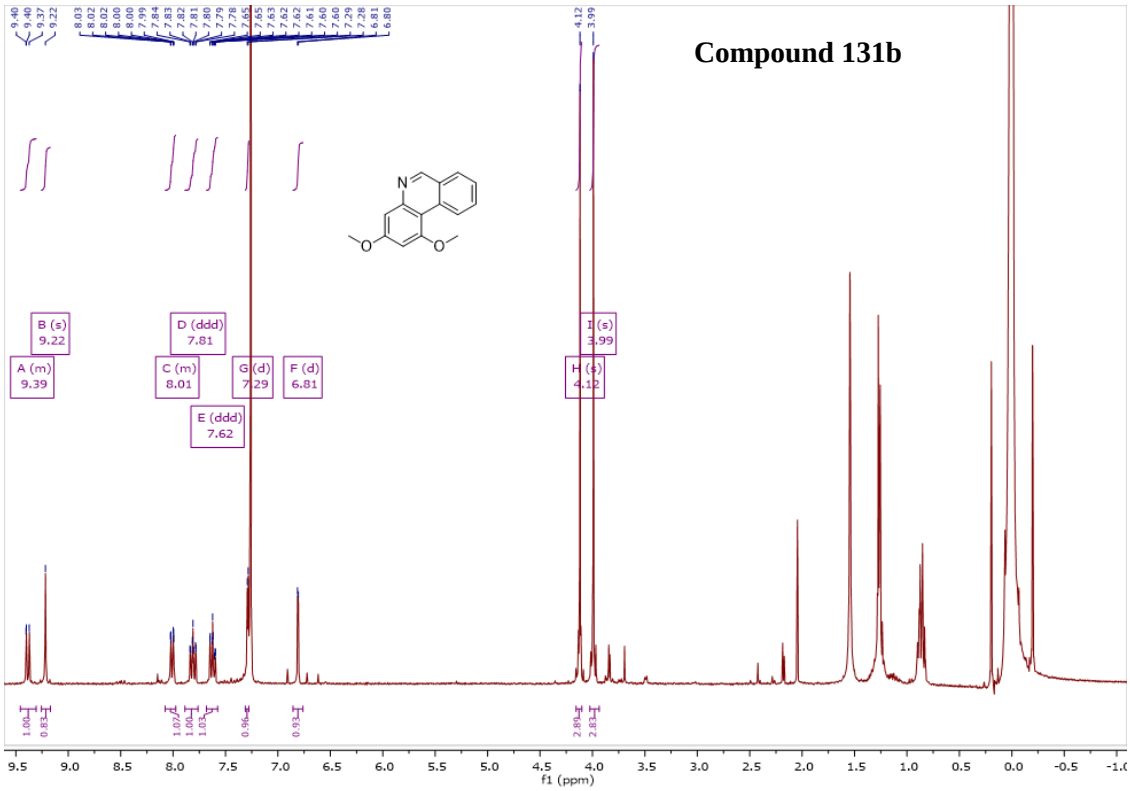

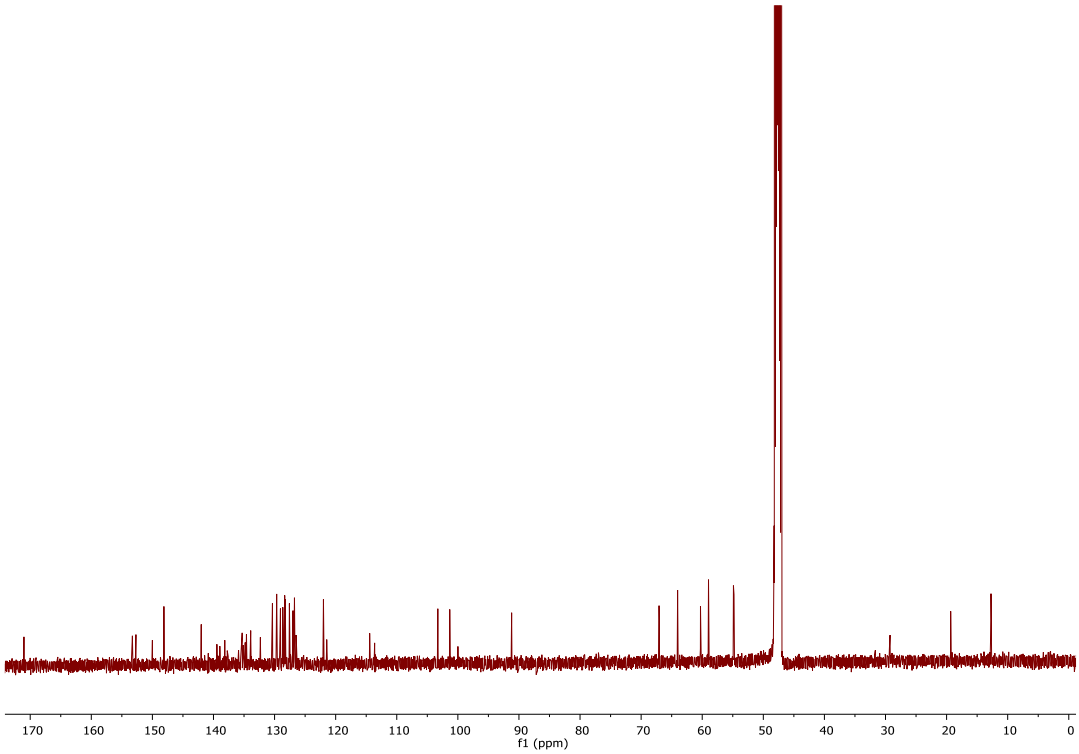

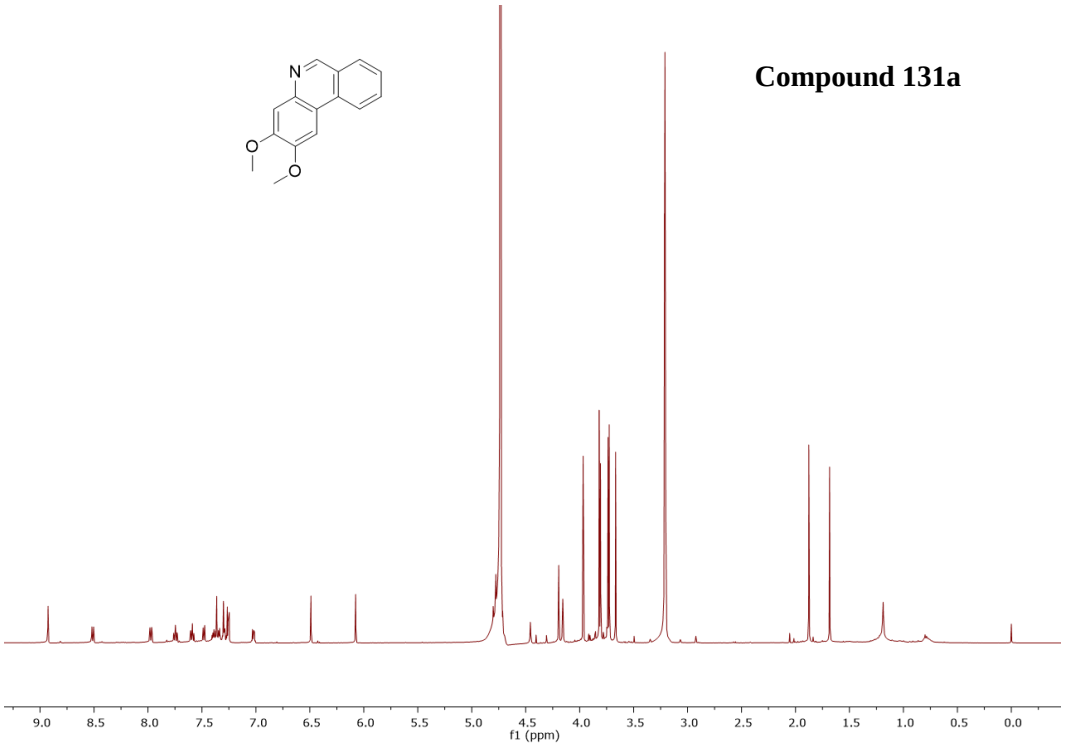

Compound 131a

Appendices

The Synthesis of UV Absorbing *O*-Heterocyclic Compounds from Cashew Nut Shell Liquid

Compound 195

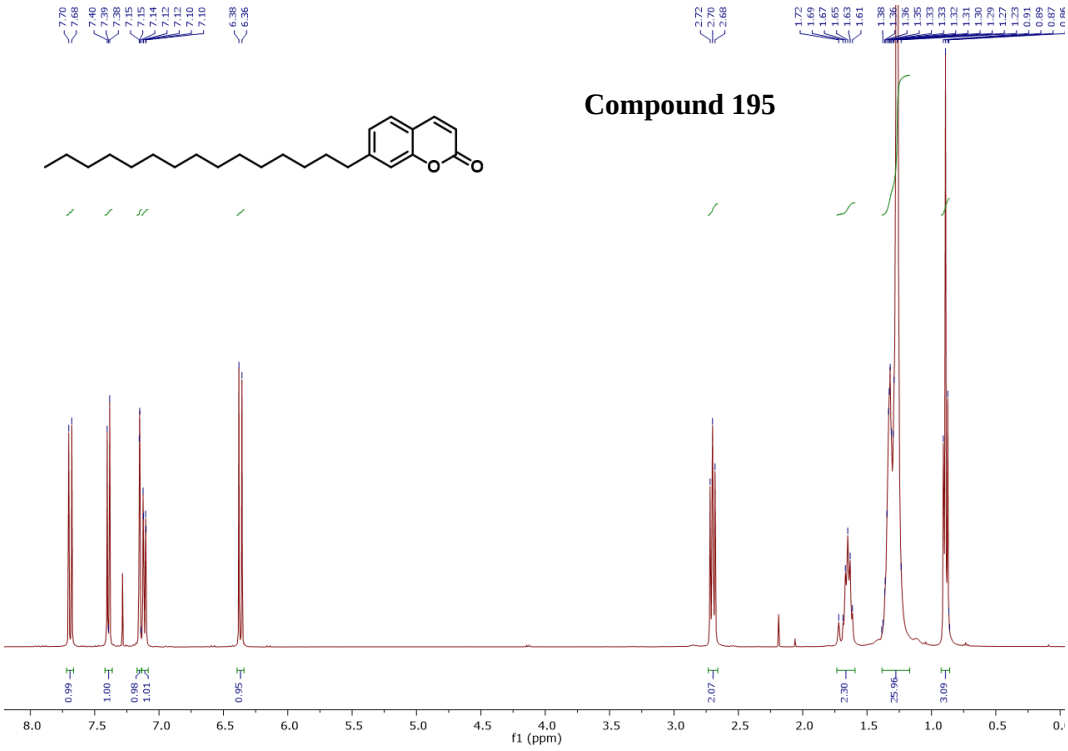

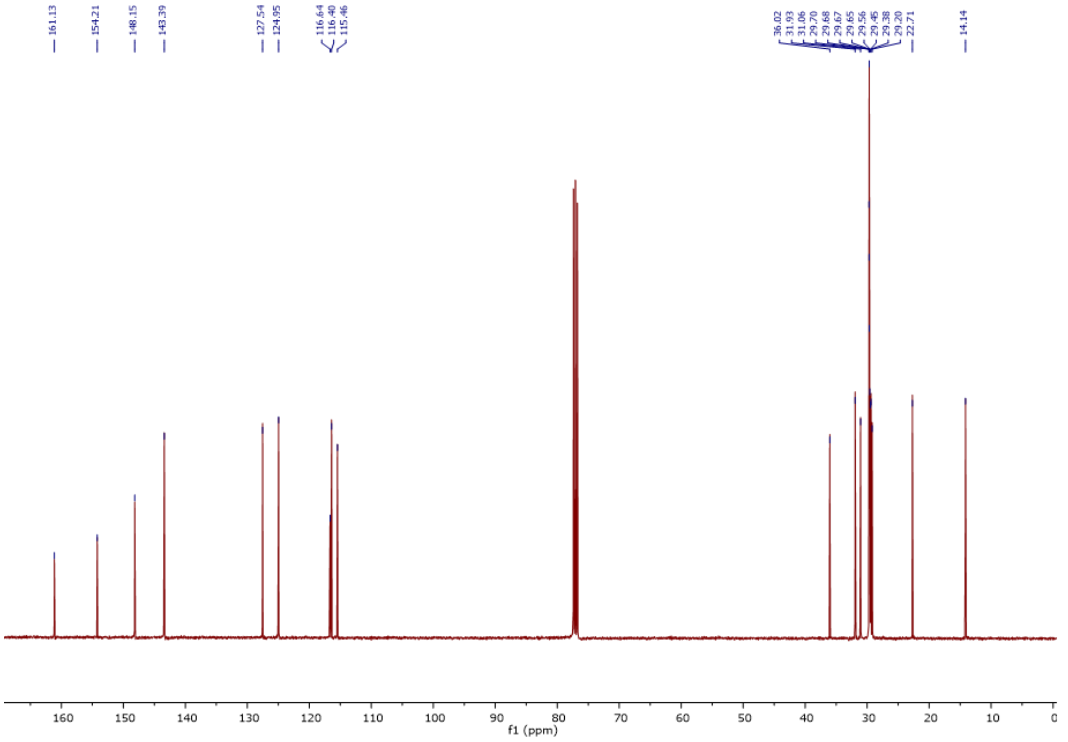

Compound 196b

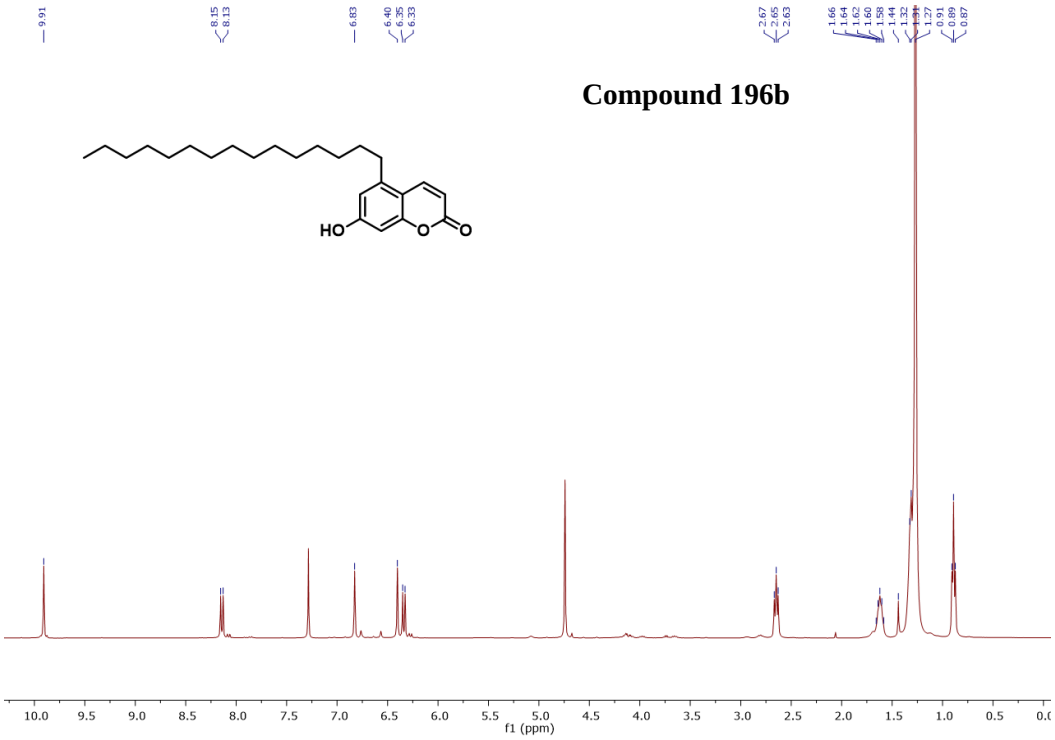

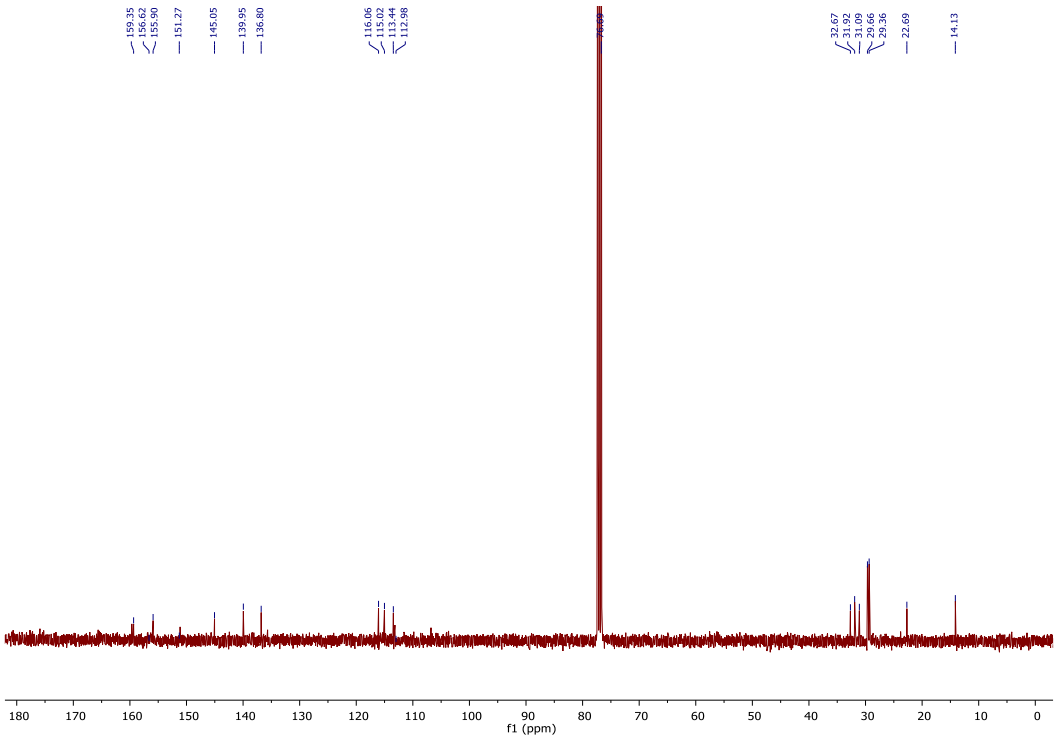

Compound 197a

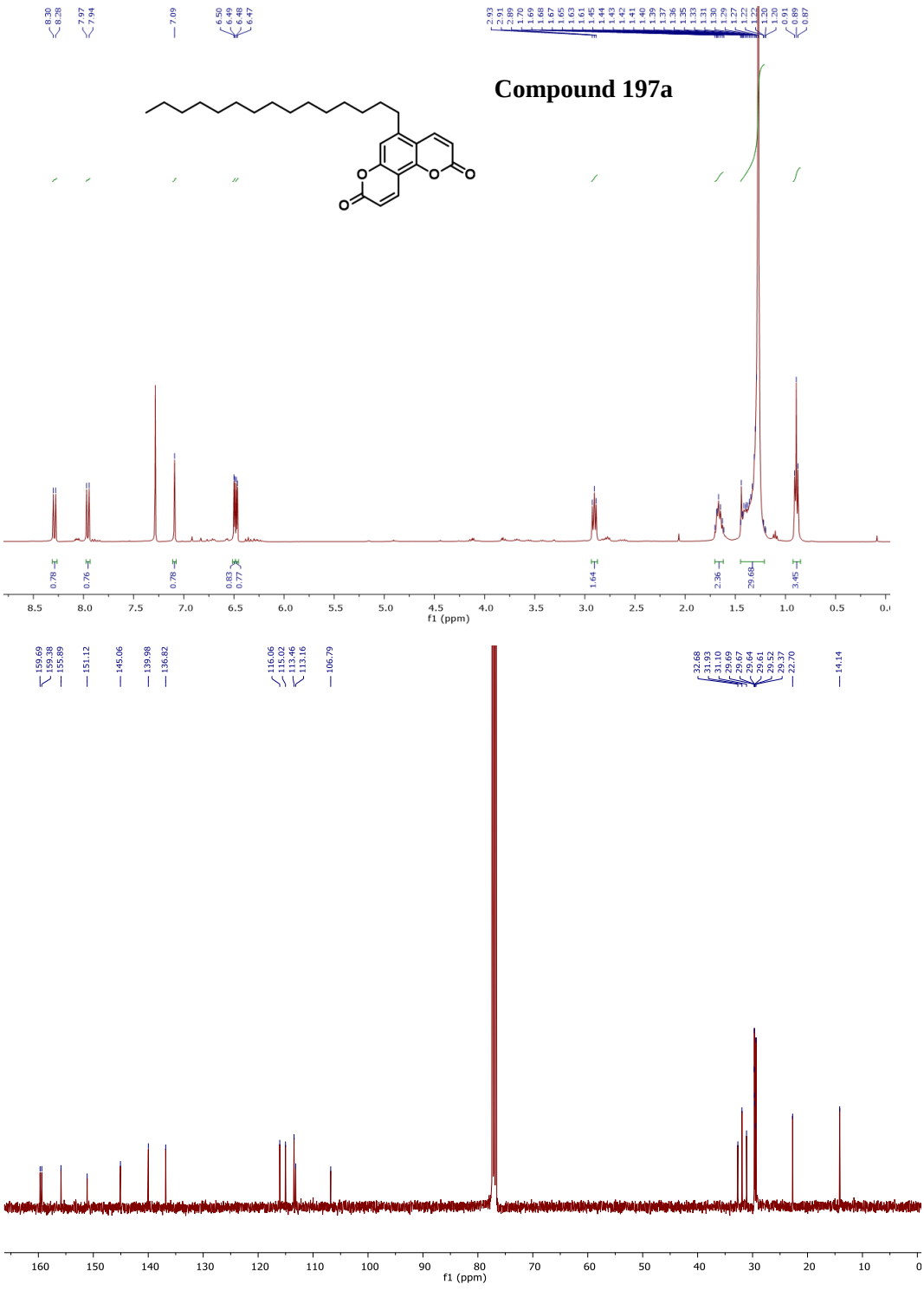

Compound 201

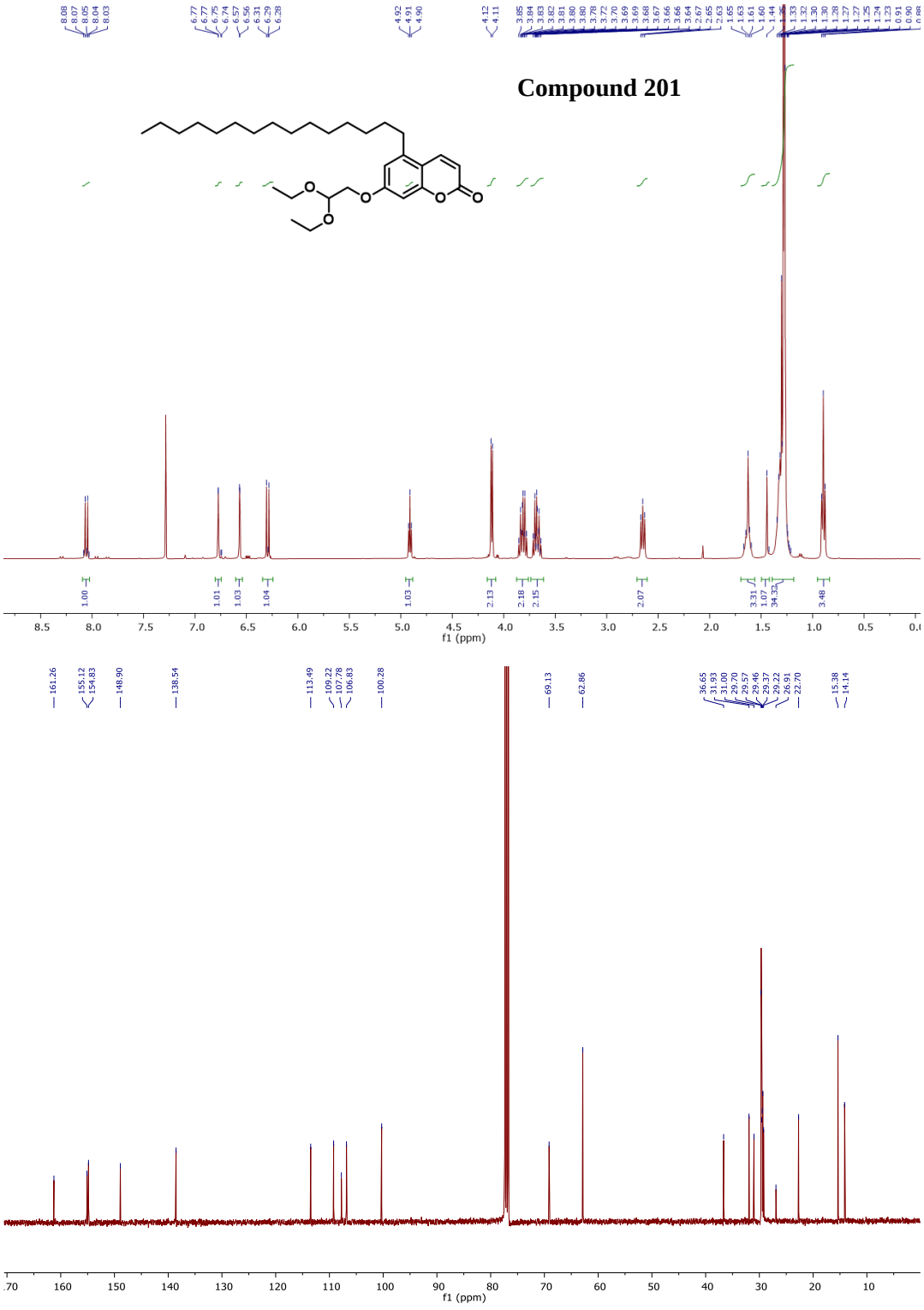

Compound 198a and 198b